Instituto de Neurociencias
Universidad Miguel Hernández-CSIC

The cold-activated TRPM8 channel: agonism by macrolide immunosuppressants and modulation by Gq protein-coupled receptors signaling pathways

Memoria de Tesis Doctoral

Jose Miguel Arcas Santos

Director de Tesis:
Dr. Félix Viana de la Iglesia

Co-directora de Tesis:
Dra. Ana Gomis García

Sant Joan d'Alacant, 2019
Programa de Doctorado en Neurociencias

UNIVERSITAS
Miguel
Hernández

San Juan de Alicante, th of January 2019

DOCTORAL THESIS BY COMPENDIUM OF PUBLICATIONS

To whom it may concern:

The doctoral thesis developed by me, Jose Miguel Arcas Santos, with title: **"The cold-activated TRPM8 channel: agonism by macrolide immunosuppressants and modulation by Gq protein-coupled receptors signaling pathways"**, is a compendium of publications and includes the following publication in which I am the first author:

The immunosuppressant macrolide tacrolimus activates cold-sensing TRPM8 channels

José Miguel Arcas, Alejandro González, Katharina Gers-Barlag, Omar Gonzalez-Gonzalez, Federico Bech, Lusine Demirkhanyan, Eleonora Zakharian, Carlos Belmonte, Ana Gomis, and Felix Viana. Journal of Neuroscience, 2018. https://doi.org/10.1523/JNEUROSCI.1726-18.2018

I declare that this publication will not be used in any other thesis.

UNIVERSITAS
Miguel
Hernández

INFORME DE LA COMISION ACADEMICA DEL PROGRAMA DE DOCTORADO EN NEUROCIENCIAS

A quien corresponda:

Por la presente, la Comisión Académica del Programa de Doctorado en Neurociencias:

Informa FAVORABLEMENTE el depósito de la Tesis presentada por D. Jose Miguel Arcas Santos,

Realizada bajo la dirección del Dr. Félix Viana de la Iglesia y la co-dirección de la Dra. Ana Gomis García,

Titulada: **"The cold-activated TRPM8 channel: agonism by macrolide immunosuppressants and modulation by Gq protein-coupled receptors signaling pathways"**.

Presentada por compendio de publicaciones.

San Juan de Alicante, a de de 2019

Dr. Miguel Valdeolmillos

Coordinador del programa de Doctorado en Neurociencias

UNIVERSITAS
Miguel
Hernández

El Dr. Félix Viana de la Iglesia, Investigador Científico del Consejo Superior de Investigaciones Científicas (CSIC), y la Dra. Ana Gomis García, Científico Titular del Consejo Superior de Investigaciones Científicas (CSIC),

Autorizan la presentación de la Tesis Doctoral titulada **"The cold-activated TRPM8 channel: agonism by macrolide immunosuppressants and modulation by Gq protein-coupled receptors signaling pathways"**, realizada por D. Jose Miguel Arcas Santos (DNI 48620411K) bajo su inmediata dirección y supervisión en el Instituto de Neurociencias de Alicante, centro mixto CSIC-UMH, y que presenta para la obtención del grado de Doctor por la Universidad Miguel Hernández.

Y para que así conste, y a los efectos oportunos, expiden y firman el presente certificado en

San Juan de Alicante, a de de 2019.

Fdo.: Félix Viana de la Iglesia

Fdo.: Ana Gomis García

UNIVERSITAS
Miguel
Hernández

AKNOWLEDGEMENTS

Después de 5 años de aprendizaje diario, esfuerzo, sacrificio, buenos y menos buenos momentos, quiero dar las gracias a todas las personas que han hecho posible que este trabajo llegue a buen puerto;

A mis directores de tesis, Félix y Ana, por su confianza y por haberme enseñado algunos de los secretos de la ciencia. Muchas gracias por todo.

A todos/as los/as grandes científicos/as y las grandes personas que me han rodeado durante estos años y de las que he tenido la oportunidad de aprender; Carlos Belmonte, Laura Almaraz, Elvira de la Peña, Víctor Messeguer, Rodolfo Madrid, María Pertusa, Mireille, Ana Miralles, Eva Quintero, Víctor Rodríguez, Giovanna, Mayte, Salvador Sala, Sergi Soriano, Juan Martínez-Pinna, Armando…

A todos los/as veteranos/as que estaban por el laboratorio cuando llegué y que hicieron el principio del camino más fácil; Enoch, Rebeca, Danny, Carlos y, sobre todo, a Jan-Albert, que guió mis primeros pasos y me enseñó lo básico.

A todos los amigos/as que me he encontrado por los pasillos del INA y que han hecho de esta etapa algo especial; Javi Alegre, Bartoll y demás compañeros de máster, Jordi, Arturo, Fran, David, Alfonso, Peter y un largo etc.

En especial, a todos mis compañeros/as y amigos/as que han pasado por el laboratorio o que se han unido a nuestra pequeña familia, porque por muy mal que vaya el día siempre llega la hora de comer o la hora del mate. Muchas gracias por llenar de grandes momentos, conversaciones y risas todos estos años; Aitana, Ana, Aida, Kat, Jorge, Álex, Pablo, Baptiste, Silvia, Agnese, Puri, Fede, Sempere…

A mi hermana y a mis abuelas y, sobre todo, a mis padres, por confiar en mí y facilitarme mucho el camino. Gracias a vosotros he llegado hasta aquí.

A mis colegas.

Y por supuesto, a Alejandra, por tu apoyo fundamental, porque has hecho que me sienta siempre a tu lado y, porque ahora, volaremos más juntos que nunca.

UNIVERSITAS
Miguel
Hernández

Index

Abstract/Resumen 1

Abstract 3

Resumen 5

1. Introduction 7

1.1 The peripheral sensory system and the somatosensory system 9

1.2 The TRP ion channel family and thermotransduction 11

1.2.1 ThermoTRPs 13

1.3 TRPM8 15

1.3.1 TRPM8 identification 15

1.3.2 TRPM8 structure 17

1.3.3 TRPM8 biophysical properties 19

1.3.4 TRPM8 pharmacology 22

1.3.4.1 TRPM8 agonists 23

1.3.4.2 TRPM8 antagonists 26

1.3.5 Modulation of TRPM8 28

1.3.5.1 PI(4,5)P2 and Gq protein-coupled receptors modulation 28

1.3.5.2 Post-translational modulation of TRPM8 channels 33

1.3.5.3 Other modulatory mechanisms 34

1.3.6 TRPM8 expression pattern 34

1.3.7 Functional characteristics of TRPM8-expressing neurons 36

1.3.8 Physiological role of TRPM8 39

1.3.8.1 Cold sensing 39

1.3.8.2 Ocular physiology 42

1.3.8.3 Temperature regulation and energy homeostasis 43

1.3.8.4 Cooling and menthol mediated analgesia 44

1.3.8.5 Other physiological roles 45

1.3.9 Pathophysiological role of TRPM8 46

1.3.9.1 TRPM8 and cancer 46

1.3.9.2 Migraine 46

1.3.9.3 Role in cold hypersensitivity 47

1.3.9.4 Dry eye disease 49

1.4 The immunosuppressant macrolides tacrolimus and rapamycin 50

2. Objectives 55

General summary

3. Materials and methods 59

3.1 Animals 61

3.2 Culture and transfection of HEK293 cells 61

3.3 Point mutagenesis 63

3.4 Dorsal root ganglia primary sensory neurons culture 63

3.5 Fluorescence calcium imaging 64

3.6 Electrophysiological patch clamp recordings in cultured cells 65

3.7 Perfusion system, temperature stimulation and light stimulation 67

3.8 Confocal imaging of PH-GFP 68

3.9 Behavioral assessment of blinking 68

3.10 Data analysis 69

3.10.1 Calcium measurements 69

3.10.2 Electrophysiological recordings 69

3.10.3 Software and statistics 70

3.11 Chemicals 71

4. Results 73

4.1 The immunosuppressant macrolide tacrolimus activates cold-sensing TRPM8 channels 75

4.1.1 Tacrolimus activates recombinant TRPM8 channels 75

4.1.2 TAC activates TRPM8 currents 77

4.1.3 Biophysical characterization of TAC effects on TRPM8 gating 79

4.1.4 Tacrolimus activates TRPM8 current in membrane delimited inside-out patches 81

4.1.5 Tacrolimus effect is independent of menthol and icilin binding sites and is reduced in cTRPM8 82

4.1.6 Effects of tacrolimus on other thermoTRP channels 85

4.1.7 Tacrolimus activates TRPM8-expressing cold-sensitive neurons and potentiates their cold response 86

4.1.8 TRPM8 mediates tacrolimus responses in DRG neurons 89

4.1.9 Tacrolimus activates inward currents and elicits action potential firing in cold thermoreceptors 93

4.1.10 Tacrolimus triggers tearing and blinking 94

4.2 The immunosuppressant macrolide rapamycin activates TRPM8 channels 96

4.2.1 Rapamycin activates recombinant TRPM8 channels 96

4.2.2 Rapamycin activates TRPM8 currents 98
4.2.3 Rapamycin activates TRPM8-expressing cold-sensitive neurons in a TRPM8-dependent manner and potentiates their cold response 100
4.2.4 Rapamycin responses are almost absent in TRPM8 KO mice 102
4.2.5 Rapamycin activates inward currents and elicits AP firing in cold thermoreceptors 104
4.3 TRPM8 modulation by GqPCR 105
4.3.1. GqPCR-mediated inhibition of TRPM8 105
4.3.2 Dr-VSP-mediated inhibition of TRPM8 109
4.3.3 Melanopsin activation does not increase Dr-VSP evoked TRPM8 inhibition 112
4.3.4 Exploring receptor- and Dr-VSP-mediated inhibition of KCNQ2/3 and Kir2.1 channels 113
4.3.5 PI(4,5)P2 depletion and TRPM8 current decay after M1R activation follow similar kinetics 116
4.3.6 The PLC inhibitor edelfosine prevents M1R-mediated TRPM8 inhibition 117
4.3.7 GqPCR activation on DRG cold-sensitive neurons have modest effects on cold-evoked responses 121
5. Discussion 127
5.1 Agonism of macrolide immunosuppressants 129
5.1.1 Biophysical and molecular aspects of tacrolimus and rapamycin agonism on TRPM8 129
5.1.2 Specificity of tacrolimus and rapamycin effects 130
5.1.3 Therapeutic implications and clinical relevance 132
5.2 TRPM8 modulation by GqPCRs 134
5.2.1 TRPM8 modulation by GqPCR in an heterologous expression system 134
5.2.2 TRPM8 modulation by GqPCR in cold-sensitive DRG neurons 138
6. Conclusions 141
7. Bibliography 145
8. Annex: publication 175

UNIVERSITAS
Miguel
Hernández

Abstract/Resumen

UNIVERSITAS
Miguel
Hernández

Abstract

TRPM8 is a polymodal, non-selective cation channel activated by cold temperature and cooling compounds (i.e. menthol) which is mainly expressed in a small subpopulation of cold-sensitive peripheral sensory neurons. TRPM8 is the principal physiological sensor of environmental cold temperatures and is also involved in different pathophysiological conditions such as cold allodynia or dye eye disease. At the same time, activation of TRPM8-expressing fibers, for example by cold or menthol, has analgesic and antipruritic effects. The dual role of TRPM8 in pain transmission has led to a strong interest in the pursuit of novel modulators of TRPM8 channels.

In this thesis, different aspects of TRPM8 channel modulation have been studied. First, I show that TRPM8 is a pharmacological target of two natural macrolide molecules; tacrolimus (FK506), a calcineurin inhibitor, and rapamycin (Sirolimus), an mTOR inhibitor. These two molecules share immunosuppressant properties and are widely used in the clinic, mainly for the treatment of organ rejection following transplants. Additionally, tacrolimus is also used in topical formulations for the treatment of atopic dermatitis and dry eye disease, and its use is often accompanied by adverse sensory side effects such as burning pain. I demonstrate by calcium imaging and patch clamp experiments that tacrolimus and rapamycin activate heterologously expressed TRPM8 channels in different species, including humans, and sensitize their response to cold temperatures by inducing a leftward shift in the voltage-dependent activation curve. The effect of tacrolimus on TRPM8 channels is direct and independent of the already known binding sites for other TRPM8 agonists (e.g. menthol or icilin). In cultured mouse DRG neurons, tacrolimus and rapamycin activate almost exclusively TRPM8-expressing cold-sensitive neurons, and these responses were drastically blunted in TRPM8 KO mice or after the application of TRPM8 antagonists. Patch-clamp recordings of cold-sensitive neurons confirm that both compounds activate inward currents and strongly potentiate the inward current evoked by cold. Behavioral experiments demonstrated that tacrolimus triggers eye blinking although this effect remains in TRPM8 KO mice, suggesting additional molecular targets.

Second, the mechanisms involved in TRPM8 modulation by Gq Protein-Coupled Receptors (GqPCR) have been studied. This modulation could be important in the context of inflammation, considering that some GqPCRs for pro-inflammatory mediators (e.g. bradykinin type 2 or histamine H1 receptors) can modulate the excitability of peripheral sensory nerve terminals. TRPM8 channels are inhibited by GqPCRs activation; however, the molecular mechanisms underlying TRPM8 modulation remain unclear. Some studies support the modulation through the canonical signaling pathway, involving PLC activation and reduction in PI(4,5)P2 levels or PKC-mediated phosphorylation of the channel, while others point to a direct interaction of TRPM8 with the Gαq subunit. I studied the GqPCR-mediated inhibition of TRPM8 in heterologous expression systems and the mechanisms underlying this effect. Activation of GqPCRs modulates TRPM8 menthol- and cold-evoked currents in a fast and reversible manner, an effect that is dependent on temperature and voltage. By different strategies I confirmed that PI(4,5)P2 depletion is necessary for TRPM8 modulation by GqPCR. The selective depletion of PI(4,5)P2 by activation

of a voltage sensitive lipid 5 phosphatase (Dr-VSP) is enough to recapitulate the effect of GqPCR activation on TRPM8 inward currents. Moreover, I demonstrated that PI(4,5)P2 hydrolysis shows precise temporal correlation with TRPM8 current inhibition in simultaneous patch-clamp and fluorescence-based PI(4,5)P2 level measurements. Importantly, pharmacological blockade of PLC and therefore PI(4,5)P2 hydrolysis prevents the inhibitory effect of GqPCRs activation on TRPM8 channels. In DRG cold-sensitive neurons, cold-evoked responses were not significantly affected by activation of GqPCRs.

Altogether, these results identify TRPM8 channels in sensory neurons as molecular targets of the immunosuppressants tacrolimus and rapamycin, two clinically approved drugs. In addition, these findings contribute to the characterization of TRPM8 modulation by GqPCRs, and demonstrate that PLC-mediated PI(4,5)P2 depletion is a necessary event and underlies TRPM8 inhibition evoked by GqPCR activation.

Resumen

TRPM8 es un canal catiónico no selectivo, polimodal, activado por bajas temperaturas y compuestos refrescantes (p.e. mentol) y que se expresa principalmente en una pequeña subpoblación de neuronas sensoriales periféricas sensibles al frio. TRPM8 es el principal sensor de frio ambiental y también participa en diferentes patologías como la alodinia al frio o en la enfermedad del ojo seco. A su vez, la activación de las fibras que expresan TRPM8, por ejemplo, por frio o mentol, tiene efectos analgésicos y antipruríticos. El papel dual de TRPM8 en la transmisión del dolor ha promovido el interés en la búsqueda de nuevos moduladores específicos de este canal.

En esta tesis he estudiado diferentes aspectos de la modulación del canal TRPM8. En primer lugar, demuestro que TRPM8 es una diana farmacológica de dos macrólidos naturales: tacrolimus (FK506), un inhibidor de la calcineurina, y rapamicina (Sirolimus), un inhibidor de mTOR. Estas dos moléculas comparten propiedades inmunosupresoras y son ampliamente utilizadas en la clínica, principalmente para el tratamiento del rechazo de órganos después de trasplantes. Además, tacrolimus también se utiliza en formulaciones de uso tópico para el tratamiento de la dermatitis atópica o para la enfermedad del ojo seco, y su uso va acompañado frecuentemente de efectos secundarios sensoriales adversos, como por ejemplo quemazón en la piel. Aquí demuestro, mediante técnicas de imagen de calcio y electrofisiología, que tacrolimus y rapamicina activan canales TRPM8 de diferentes especies, incluyendo humanos, expresados en sistemas heterólogos, y sensibilizan su respuesta al frio, induciendo un desplazamiento en la curva de voltaje-dependencia hacia la izquierda. El efecto de tacrolimus sobre los canales TRPM8 es directo e independiente de los sitios de unión conocidos hasta ahora para el resto de agonistas de TRPM8 (p.e. mentol o icilina). En neuronas sensoriales en cultivo, provenientes de los ganglios raquídeos, tacrolimus y rapamicina activan casi exclusivamente neuronas sensibles a frio que expresan el canal iónico TRPM8. Además, estas respuestas prácticamente desaparecen en presencia de antagonistas de TRPM8 o en ratones TRPM8 knockout. Registros electrofisiológicos de patch-clamp en neuronas sensibles a frio confirmaron que ambos compuestos activan una corriente de entrada, y a su vez, potencian fuertemente la corriente de entrada generada por el descenso de la temperatura. Experimentos de comportamiento demostraron que tacrolimus aumenta el parpadeo, aunque este efecto permanece en ratones TRPM8 knockout, sugiriendo otras dianas moleculares adicionales.

En segundo lugar, estudié los mecanismos que participan en la modulación de TRPM8 por receptores acoplados a proteínas Gq (RAPGq). Esta modulación podría ser relevante en el contexto de una situación de inflamación, debido a que diversos mediadores pro-inflamatorios que activan RAPGq (p.e. receptores de bradiquinina tipo 2 o receptores H1 de histamina) pueden modular la excitabilidad de las terminaciones nerviosas periféricas. Los canales TRPM8 se inhiben por la activación de RAPGq. Sin embargo, el mecanismo molecular que media este efecto no está definido. Algunos estudios proponen la modulación de TRPM8 a través de la ruta de señalización canónica de los RAPGq, que incluye la activación de la fosfolipasa C (PLC) y la

reducción de los niveles de fosfatidilinositol 4,5-bifosfato (PI(4,5)P2) o la fosforilación del canal mediada por la protein kinasa C, mientras que otros grupos defienden la interacción directa de la subunidad Gαq con el canal. En este trabajo estudié la inhibición de TRPM8 mediada por RAPGq en sistemas de expresión heterólogos y los mecanismos subyacentes a esta modulación. La activación de RAPGq modula las corrientes evocadas por mentol y frio de una manera rápida y reversible, un efecto que es dependiente de la temperatura y el voltaje. Mediante diferentes estrategias confirmé que la eliminación de PI(4,5)P2 es necesaria para la modulación de TRPM8 por RAPGq. La eliminación selectiva de PI(4,5)P2 por una fosfatasa activada por voltaje (Dr-VSP) es suficiente para recapitular el efecto de la activación de RAPGq sobre la corriente de entrada de TRPM8. Además, mediante experimentos simultáneos de registro electrofisiológico de las corrientes TRPM8 y la imagen de un sensor fluorescente de PI(4,5)P2, demostré que la hidrólisis de PI(4,5)P2 y la inhibición de las corrientes TRPM8 siguen un curso temporal idéntico. El bloqueo farmacológico de la PLC y por tanto de la reducción de los niveles de PI(4,5)P2, elimina el efecto de la activación de RAPGq sobre los canales TRPM8. En neuronas sensoriales activadas por frio, la respuesta se vio modestamente afectada por la activación de RAPGq.

En resumen, mis resultados identifican el canal TRPM8 en neuronas sensoriales como una diana molecular de los inmunosupresores tacrolimus y rapamicina, dos fármacos aprobados clínicamente. Además, este estudio contribuye a la caracterización de la modulación de TRPM8 por RAPGq, demostrando que la eliminación de PI(4,5)P2 mediada por PLC es un evento necesario y que subyace a la inhibición de TRPM8 por la activación de RAPGq.

1. Introduction

UNIVERSITAS
Miguel
Hernández

1.1 The peripheral sensory system and the somatosensory system

The Greek philosopher Aristotle defined five senses—vision, hearing, touch, taste, and smell—each linked to specific sense organs in the body: the eyes, the ears, the skin, the tongue, and the nose. This classification was further expanded by the English neurophysiologist Charles Sherrington (Sherrington, 1906), which recognized three additional major sensory functions; the proprioception, which enables us to have conscious awareness of the posture and movement of our own body, the exteroception, which includes the touch but also the sense of pain and thermal senses (cold and heat), and the interoception, which monitors the state of the major organ systems and regulate autonomic functions. This diverse group of sensory functions is included in a broad concept, the somatosensory system, which is governed by the peripheral nervous system (PNS). The somatosensory system is formed by specialized sensory neurons whose terminals are distributed in the periphery and detect internal and external sensory stimuli, providing a constant flow of sensory information to the central nervous system (Fig. 1). The soma of peripheral sensory neurons (PSN) innervating the limbs and trunk are located in dorsal root ganglia (DRG), which are clusters of sensory neuron cell bodies situated just lateral to the vertebral column, at the base of the spinal nerves. Neurons that innervate cranial structures (e.g. the face, the lips, the oral cavity, the conjunctiva and the dura mater) are located in the trigeminal ganglia, which are placed in the base of the skull, and their afferents form part of the trigeminal nerve, the fifth cranial nerve. PSN are a type of bipolar cell, called pseudo-unipolar cells, with axons divided into two branches, one projecting to the periphery (skin, muscle, joints, blood vessels and organs) and the other projecting to the spinal cord or to the trigeminal sensory nucleus (located in the hindbrain), forming the first synapse in the somatosensory pathway. This axon is the primary afferent and serves as a single transmission “cable” with one polarity.

The PSNs perform two major functions: the transduction and encoding of sensory stimuli into electrical signals and the transmission of these electrical signals to the central nervous system (Fig. 1). This neural activity is subsequently processed at different levels of the central nervous system and interpreted finally by the brain as sensations of different perceptual characteristics (i.e. sensory modalities), such as temperature, touch or pain. The transduction of a specific stimulus into an electrical signal is universal to all sensory organs and the difference between the distinct sensory neurons is the type of energy they can transduce. For each sensory modality, a specific form of stimulus energy is transformed into electrical signals by specialized receptors (i.e. light by photoreceptors). As in other sensory systems, the somatosensory system is heterogeneous and employs many specialized receptors which have specific molecular machinery to transduce concrete types of stimuli and generate different modalities of sensations.

Findings supporting the heterogeneity of the PSN were published independently in the early 1880s by Magnus Blix, Alfred Goldscheider, and Henry Donaldson (reviewed in Norrsell et al., 1999). They found that, on the skin surface, it was possible to electrically or physically stimulate

different spots that evoked separate tactile, warm or cold sensations, suggesting the existence of specific receptors. Twenty years later, Max Von Frey extended this concept to the pain modality by describing the existence of discrete pain points in the human skin (reviewed in Pearce, 2006).

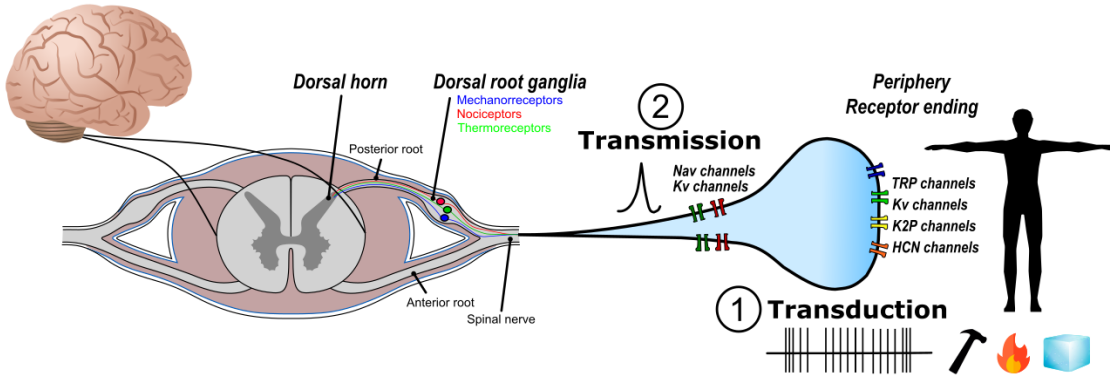

Figure 1. Anatomical and functional organization of the peripheral sensory nervous system. The somas of the peripheral sensory neurons are placed within dorsal root ganglia (DRG). DRG neurons are divided in specialized functional subpopulations known as mechanoreceptors (blue), nociceptors (red) and thermoreceptors (green). These neurons project centrally and synapse with dorsal horn interneurons in the spinal cord, which send the electrical message to the brain, and peripherally to target tissues such as skin, muscle, joints, blood vessels and internal organs. Each subtype of peripheral sensory neuron expresses its own blend of ion channels that determine the transduction of different physical and chemical stimuli into generator potentials and the transmission of the electrical signal to the central nervous system.

With the development of nerve recording techniques in the twentieth century, it was possible to proof experimentally that peripheral sensory receptors encoded the stimulating energy into a discharge of nerve impulses and that cutaneous sensory nerve fibers exhibited a marked degree of functional specialization, transducing a particular form of stimulating energy. Cutaneous fiber endings were subsequently classified into different groups according to their sensory modality. Receptors that responded to heat and/or cold were called thermoreceptors, while receptors that responded to mechanical stimuli such as tension, pressure or vibration were called mechanoreceptors. The receptors that responded selectively to stimuli that can damage tissue were called nociceptors and were subsequently divided into mechanonociceptors, excited only by injurious mechanical forces, and polymodal nociceptors, that respond to a variety of noxious mechanical, thermal, and chemical stimuli (Kandel, 2000).

Until the end of the 1990s, there was no understanding about the molecular mechanism underlying this specialization. This changed with the identification of transducing molecules for different somatosensory stimuli. Starting in 1997, different studies described novel receptors involved in the transduction of specific somatosensory stimuli (summarized in; Lumpkin & Bautista, 2005, Lumpkin & Caterina, 2007 and Murthy et al., 2017) . Overall, the discovery of different thermosensitive channels from the Transient Receptor Potential (TRP) ion channel family extended to a molecular level the concept of response specificity to a particular form of energy. These discoveries suggested that sensory afferent fibers preferentially detect a particular

type of physical or chemical stimulus through the expression of a specific protein in their terminal endings, whose presence would be necessary and sufficient to transduce the particular stimulus into a propagated sensory message and evoke a specific modality of sensation.

1.2 The TRP ion channel family and thermotransduction

The TRP channel tale began in 1969 when Cosens and Manning reported a spontaneously occurring *Drosophila* mutant with an abnormal response to light stimuli. In this mutant fly, the photoreceptor potential showed a transient, rather than sustained, electrical response during prolonged illumination in electroretinogram recordings, a phenotype that was baptized as transient receptor potential (Cosens & Manning, 1969). Twenty years later, this finding led to the discovery of the first TRP ion channel from *Drosophila*. Montell & Rubin (1989) described that the *trp* locus related protein was expressed in the rhabdomeric membranes of the photoreceptor cells, and participated in the phototransduction cascade. The predicted structure of the related protein, with several putative transmembrane segments, and the fact that calcium signals were affected by the mutation, pointed to the possibility that this protein was a Ca^{2+} permeable channel. Afterwards, it was described that this first TRP channel, called TRPL, was gated following the activation of a light-sensitive G protein-coupled receptor (i.e. rhodopsin) resulting in cation influx into the photoreceptor cells (for a review see; Hardie & Raghu, 2001). Nowadays, 30 years after the first TRP channel was cloned, many different TRP-related channels have been discovered in different organisms, including protozoa (i.e. yeast) and metazoa (i.e. fruit flies, worms, zebrafish, mice, and humans) (Palmer et al., 2001; Denis & Cyert, 2002).

TRP proteins form non-selective cation channels which mediate the flow of Ca^{2+} and Na^{+} across the cell membrane (Hardie & Minke, 1992). In multicellular organisms, TRP channels are widely expressed in the nervous system and in non-excitable cells, participating in their excitability and Ca^{2+} signaling upon stimulation (Nilius & Owsianik, 2011). The members of the TRP channel family are very heterogeneous, especially regarding two aspects: their mechanism of activation, including diverse extracellular and intracellular stimuli, and their physiological function, which range from multiple roles in sensory physiology (including hearing, vision, olfaction, touch, pain, thermo- and osmosensation) to male fertility (Nilius & Szallasi, 2014).

The TRP family is divided into groups 1 and 2 based on sequence homology, which themselves are divided into seven subfamilies (Fig. 2A) (Montell et al., 2002). Group 1 consists of five subfamilies, TRPC (Canonical, 7 members), TRPV (Vanilloid, 6 members), TRPM (Melastatin, 8 members), TRPA (Ankyrin, 1 member) and TRPN (NOMP-C, absent in mammals). These 5 subfamilies share several notable sequence elements and domains, including a large region of sequence homology that includes the six transmembrane segments and the pore loop that is situated between the fifth and the sixth transmembrane domain. TRPC, TRPV, TRPM and TRPN channels also contain a highly conserved 25 amino acid segment in the C-terminal domain referred to as the TRP domain. Within the TRP domain, an even more conserved stretch of 6 amino acid residues (EWKFAR) was identified, called the TRP box. Another common element in

the sequence between the members of this subfamily, with the exception of TRPM members, is that they have multiple N-terminal ankyrin repeats (Cohen & Moiseenkova-Bell, 2014) (Fig. 2A).

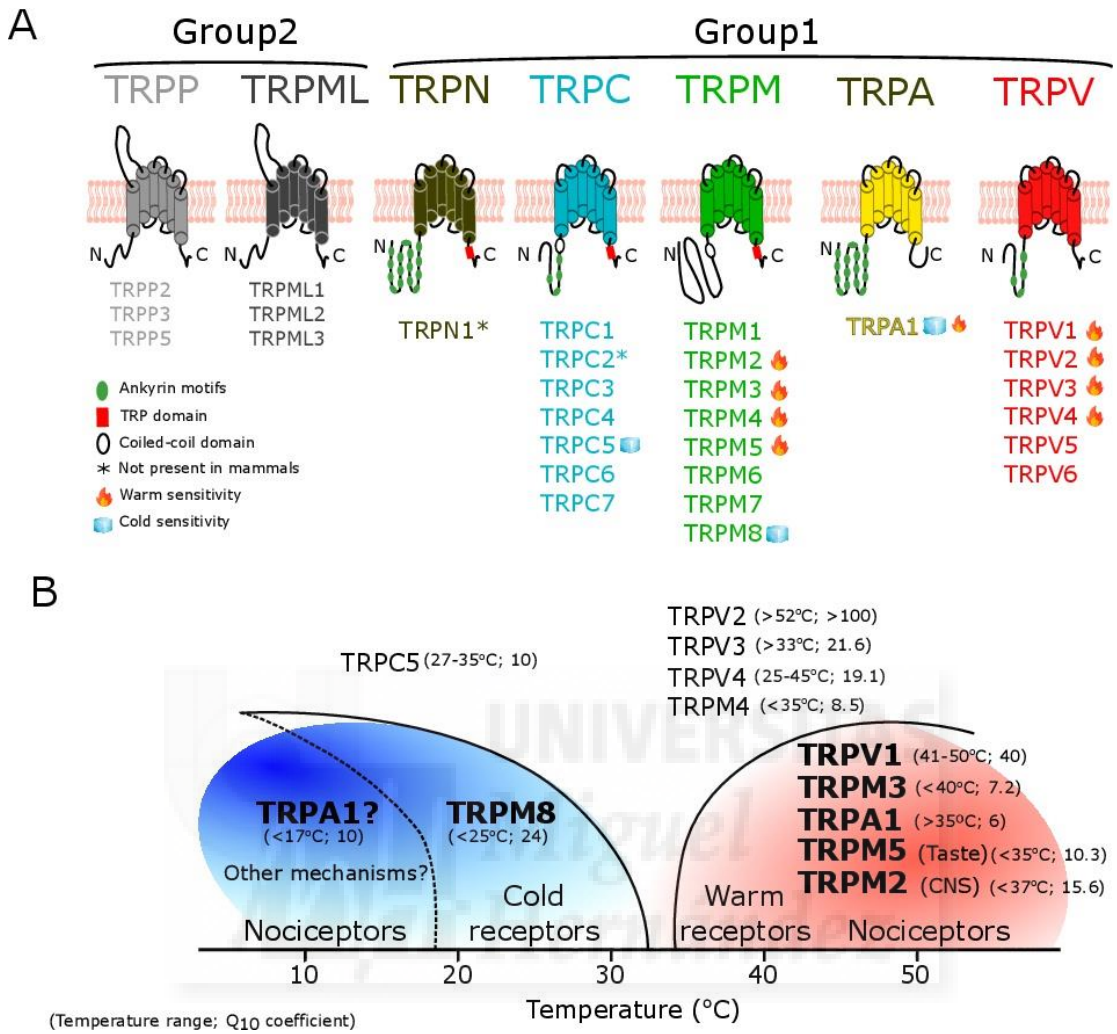

Figure 2. The TRP family and thermoTRPs. *A*, Schematic representation of the representative structure and common structural domains of members from the 7 subfamilies of the TRP channel family. The TRP subfamilies and the members included in each of them are represented in different colors. Thermosensitivity is indicated for the members which show steep temperature dependence. ***B*,** Temperatures ranging from noxious cold to noxious heat activate different members of the TRP family. The sensation evoked depends of the type of fiber which is activated, ranging from innocuous sensations (cold and warm receptors) to painful sensations (nociceptors). Under the colored temperature curves, members whose role as physiological thermosensor is generally accepted are represented. Listed outside the curves are TRPs that show steep temperature dependence but have not been involved as physiological thermosensors. Shown inside the brackets are the temperature range of activation and the Q_{10} coefficient (in heterologous expression system). References: TRPA1, Story et al., 2003, Moparthi et al., 2016; TRPM8, McKemy et al., 2002; TRPC5, Zimmermann et al., 2011; TRPV1, Yao et al., 2010; TRPM3, Vriens et al., 2011; TRPM4 & TRPM5, Talavera et al., 2005; TRPM2, Togashi et al., 2006; TRPV2, Leffler et al., 2007; TRPV3, Peier et al., 2002; TRPV4, Watanabe et al., 2002.

Group 2 comprises two subfamilies, TRPP (Polycystic, 3 members) and TRPML (Mucolipin, 3 members). The members of this group share sequence homology and are distantly related to members of group 1. One of the topological differences that characterize group 2 is a large loop separating the first two transmembrane domains. Members of the TRPP subfamily are extended from yeast to mammals, probably being the most ancient subfamily of TRP channels (Palmer et al., 2005).

Within the different TRP channel subfamilies there is a subset of TRP ion channels that are activated by a wide range of physiological temperatures and are called thermoTRPs (Fig. 2A and 2B). ThermoTRPs are introduced in more detail in the next section.

1.2.1 ThermoTRPs

All chemical and biological reactions are modulated by temperature, including the activity of all ion channels. However, thermoTRPs show and exceptional sensitivity to temperature (Castillo et al., 2018). A way to quantify the temperature sensitivity of a biological or chemical reaction is by measuring the temperature coefficient (Q_{10}), which indicates the change in the rate of activity resulting from a 10 ^{o}C change in temperature. In the case of ion channels, the Q_{10} coefficient can be calculated from the change in the current amplitude at a specific voltage when temperature changes by 10 ^{o}C ($Q_{10}= I_{T+10}/I_T$). That means that the higher Q_{10} the more sensitive to temperature the reaction is, and this parameter is used as the principal characteristic by which a TRP channel is classified as a thermoTRP. However, additional biophysical and functional characteristics have been proposed to identify ion channels with physiological relevance in temperature detection (Voets, 2012). These characteristics are;

- Steep temperature dependence: usually expressed as a Q_{10} value larger than 5 for inward current in a relevant temperature range. This implies that the channel should generate robust depolarizing currents in response to a change in temperature.
- Expression in relevant cell types: in order to have a physiological function as a thermosensor, a thermoTRP channel should be functionally expressed at sites that experience significant changes in temperature, for example sensory nerve endings innervating the skin or keratinocytes.
- Underlying the temperature dependency of a (pato)physiological process. In other words, there must be *in vivo* evidence that the temperature dependence of the channel determines the effects of temperature on a physiological process or pathology.

Up to now, 11 TRP channels have been described that fulfill the first requirement. Activation upon warming has been reported for TRPV1 (Caterina et al., 1997), TRPV2 (Caterina et al., 1999), TRPV3 (Peier et al., 2002), TRPV4 (Watanabe et al., 2002), TRPM2 (Togashi et al., 2006; Song et al., 2016), TRPM3 (Vriens et al., 2011), TRPM4 and TRPM5 (Talavera et al., 2005) (Fig. 2A). The cold-activated channels that have been described are TRPM8 (McKemy et al., 2002; Peier et al., 2002), TRPA1 (Story et al., 2003) and TRPC5 (Zimmermann et al., 2011) (Fig. 2A). However, considering the rest of the requirements listed previously, only some of these channels

merit the title of thermoTRP; TRPV1, TRPM3, TRPM2, TRPM5 and TRPA1 for warming and TRPM8 and TRPA1 for cooling. Recently, human TRPA1 channel has been described as U-shaped thermosensitive channel, responding to both cool and heat temperatures (Moparthi et al., 2016).

Heat-evoked currents in nociceptive neurons were first described by Cesare and McNaughton in 1996 and, soon after, the heat-sensitive channel TRPV1 was cloned, becoming the first mammalian TRP channel identified (Caterina et al., 1997). TRPV1 is activated by heat (≥43 ºC), with a Q_{10} greater than 20 and also by diverse chemical compounds such as the vanilloid compound capsaicin, which gives spicy foods their characteristic hot taste (Caterina et al., 1997). TRPV1 is expressed by many nociceptive neurons and it was soon established as an important molecular entity in the pain pathway (Caterina et al., 1997; Michael & Priestley, 1999). TRPV1 is upregulated in conditions accompanying inflammation, such as low pH, and by inflammatory mediators and is essential for thermal hypersensitivity induced by inflammatory conditions (Tominaga et al., 1998; Caterina et al., 2000; Davis et al., 2000; Bhave et al., 2003; Viana, 2018). Although TRPV1 expressing-neurons are activated in a wide range of noxious temperatures (39 –51 °C) (Caterina et al., 1997), genetic deletion of TRPV1 in mice only reduces noxious heat sensitivity partially in behavioral assays, suggesting that additional mechanisms participate in noxious heat sensitivity (Caterina et al., 2000; Davis et al., 2000; Woodbury et al., 2004). Recently, it has been shown that, at least in mice, two additional TRP channels participate in heat-evoked pain responses in sensory nerve endings, forming together with TRPV1 a redundant trio that operates in concert to avoid burn injury. These two additional channels are TRPM3 and TRPA1; only triple knockout mice ($TKO^{V1/A1/M3}$) totally lacked heat-evoked pain responses, whereas double knockout mice ($DKO^{M3/V1}$ and $DKO^{V1/A1}$) exhibited vigorous withdrawal responses to noxious heat (Vandewauw et al., 2018). TRPM2 has also been described as an important thermosensor of non-noxious warm in the periphery (Tan & McNaughton, 2016) and additionally, it has been shown to be expressed in a subpopulation of warm-sensitive hypothalamic neurons where it is responsible for detecting increased corporal temperatures (e.g. during fever) in order prevent overheating by promoting heat loss (Song et al., 2016). The other TRP channel involved in physiological heat thermoreception is TRPM5, which confers thermal sensitivity to sweet taste in taste buds (Talavera et al., 2005).

TRPM8 is well-established as the main molecular sensor of cool and cold temperatures (Dhaka et al., 2007; Colburn et al., 2007; Bautista et al., 2007) however, other mechanisms have been proposed to participate in cold thermotransduction, as for example TRPA1 channels.

TRPV2, TRPV3, TRPV4, TRPM4, and TRPC5 also show step temperature dependence however, the role of some of these channels as physiological temperature sensors is not clear, and according to the previous requirements they cannot be classified (yet) as a thermoTRP. For example, TRPV2 was described as a channel expressed in peripheral sensory neurons and activated by high temperatures, with a threshold of ~52 °C (Caterina et al., 1999). Despite that, its role in detecting temperature was contradicted by the characterization of TRPV2 knock-out

mice, which showed normal behavioral responses to noxious heat over a broad range of temperatures, refuting the proposal that TRPV2 plays a role for heat nociception in adult mice (Park et al., 2011; Vandewauw et al., 2018). Aside from its thermosensitivity, TRPV2 was described to sense changes in osmolarity and membrane stretch (Muraki et al., 2003). In relation to this mechanosensitivity, TRPV2 has recently gained importance in various physiological functions, for example in the heart, where it has been described to mediate stretch-dependent responses in cardiomyocytes and to play a role in different cardiopathies (Aguettaz et al., 2017; Koch et al., 2017). Another example is TRPC5, which was shown to be potentiated by cooling below 37 °C, peaking around 25 °C, and its presence was detected in DRG neurons (Zimmerman et al., 2011). Nonetheless, it has not been possible to detect cold-activated currents driven by TRPC5 in sensory neurons and, more importantly, behavioral tests of TRPC5 knock-out mice failed to identify temperature-sensitive behavioral changes (Zimmerman et al., 2011). However, ongoing research in this field may cause the list of thermoTRP to expand further in the future.

In conclusion, the identification of thermally gated TRP channels represented a great advance in our understanding of temperature and pain transduction. Nevertheless, thermotransduction is a complex process, not only carried by one single molecule but implicating the concerted operation of different ion channels which in the end leads to different sensory thresholds and fine-tune the activity of thermosensitive neurons (Belmonte & Viana, 2008). As the main topic of this thesis, TRPM8 and cold-thermotransduction will be introduced in detail in the next pages.

1.3 TRPM8

TRPM8 is a polymodal channel, activated by physical stimuli such as temperature and voltage, and chemical cooling compounds (McKemy et al., 2002; Peier et al., 2002). TRPM8 is expressed in the free nerve endings of a specific subpopulation of PSNs and is the most critical molecular entity responsible for the transduction of innocuous cold temperature (Dhaka et al., 2007; Colburn et al., 2007; Bautista et al., 2007). The structure, expression and functions of TRPM8 channels have been covered in several recent reviews (Liu & Qin, 2011; Almaraz et al., 2014; Madrid & Pertusa, 2014; Pérez De Vega et al., 2016). In the following paragraphs I will summarize these and other publications, focusing on the studies that led to the cloning of TRPM8, its structure, its biophysical properties, its pharmacology and the main physiological roles played by this channel.

1.3.1 TRPM8 identification

As I mentioned before, the firsts evidence for the existence of peripheral sensory structures preferentially activated by temperature changes were published independently in the XIX century by three physiologists, Magnus Blix, Alfred Goldscheider and Henry Donaldson. They described the existence on the skin surface of discrete spots whose electrical or physical (cold or warm) stimulation evoked specific sensations of cold and warm (reviewed in Norrsell et al. 1999). In the next century, extracellular recordings of single sensory fibers evidenced the existence of a population of receptors with a prominent sensitivity to thermal stimuli and possibly responsible for

the detection of non-noxious temperature changes in the skin (Zotterman, 1935, 1936). A few years later Hensel & Zotterman (1951) reported the shift in the threshold of thermal activation towards warmer temperature in the presence of menthol in the lingual nerve of the cat. These experiments provided the first evidence for the existence of a physiological mechanism for cold temperature detection in a specific population of peripheral sensory neurons and its sensitization by menthol. Different hypothesis were postulated to explain this specific cold thermotransduction, including modulation of the Na^+-K^+ ATPase (Pierau et al., 1975), differential temperature sensitivity of Na^+ and K^+ channels (Carpenter, 1981; Spray, 1986) and closure of K^+ channels (Maingret et al., 2000; Reid & Flonta, 2001; Viana et al., 2002). However, other findings started to point towards the existence of an ion channel expressed in a small subset of sensory neurons responsible for cold thermotransduction and menthol sensitivity. In 2000, Okazawa et al. described that menthol induced intracellular Ca^{2+} increases in a subset of cultured sensory neurons. One year later, Reid & Flonta (2001a) described an inward current activated by cooling in a small number of rat sensory neurons, which maintained the same features that were described in extracellular recordings of cold thermoreceptors, such as sensitization by menthol or adaptation upon sustained cooling. This cold-activated current was the first evidence of the opening of a non-selective cation channel in cold-sensitive neurons during cooling.

One year later, the molecular entity that mediates the already described cold currents in sensory neurons was discovered during a screening for upregulated genes in a cDNA library of cancerous prostate cells, although it was not linked with this function. Tsavaler and colleagues (2001) have the credit of being the firsts to identify what at the time was a novel gene that shared high homology with TRP proteins, which was baptized as trp-p8, but soon become TRPM8. Shortly thereafter, in March of 2002, two independent groups, using different strategies, published the cloning and characterization of TRPM8 channels in cold-sensitive sensory neurons and in heterologous expression systems.

The group of David Julius (McKemy et al., 2002) characterized by calcium imaging the response to menthol and cold of a relatively small subset (14.8%) of dissociated rat trigeminal neurons. In order to identify a single cDNA coding for the molecular entity that conferred cold and menthol sensitivity to these neurons, they used a screening strategy based upon calcium imaging. They constructed a cDNA expression library from trigeminal tissue, obtaining pools containing about 10.000 clones, which were transfected individually into HEK293 cells, subsequently loaded with the calcium-sensitive fluorescent dye Fura-2 and examined for changes in intracellular calcium levels under exposure to high menthol concentrations (500 µM) at room-temperature. During this methodic and laborious work, they obtained the well-deserved reward, a single cDNA that, when transfected in heterologous expression systems, was sufficient to confer menthol and cold-sensitivity to them. This cold- and menthol-sensitive receptor cDNA (they named it CMR1) contained an open reading frame of 3.312 base pairs and was predicted to code for a protein of 1.104 amino acids. Database searches revealed significant homology between this sequence and members of the TRP ion channel family, and a further search of the literature showed that CMR1 was 92% identical to the sequence originally published by Tsavaler and colleagues.

In the laboratory of Ardem Patapoutian (Peier et al., 2002) the TRPM8 channel was cloned by a different strategy. They searched in genomic DNA databases proteins with multiple putative exons similar to the transmembrane domains 4 and 6 of the previously cloned heat sensitive TRPV1 channel. They were able to amplify a fragment of one TRP channel by RT-PCR from mouse DRG RNA, and confirmed its activation by cold and menthol when expressed in Chinese Hamster Ovary (CHO) cells.

1.3.2 TRPM8 structure

In humans and rodents, the TRPM8 gene encodes for a 1.104 amino acid protein. TRPM8, as other TRP channels, has an overall topology similar to that of voltage-gated potassium (Kv) channels, with six transmembrane segments and the amino- and carboxy-terminals located intracellularly (Fig. 3A). The putative pore loop is formed by the region between transmembrane segments S5 and S6. TRPM8 subunits tetramerize into functional channels, inferred from experiments using Atomic Force Microscopy (AFM) and by perfluorooctanoic acid polyacrylamide gel electrophoresis (Dragoni et al., 2006; Stewart et al., 2010).

Like other ion channels, TRPM8 has distinct structural and functional modules, in the sense that certain regions confer to the channel sensitivity to its different modulators. Consequently, mutations can selectively ablate the response to a specific agonist without altering the sensitivity to others (Bandell et al., 2006; Latorre et al., 2007).

The N-terminal domain of TRPM8 consists of 693 amino acids, which represents more than half of the entire TRPM8 sequence. This domain contains four regions of amino acids that share some sequence similarity with other members of the TRPM family, called melastatin homology regions (MHR) (Fleig & Penner, 2004). These regions may be involved in stabilization of the tetramer according to a study of the predicted quaternary structure for TRPM8 (Pedretti et al., 2009). Upstream of the first MHR, TRPM8 contains a 116-amino acid sequence whose function was adressed by Phelps and Gaudet in a study published in 2007. They showed that a TRPM8 mutant with a deletion of the first 39 amino acids (ΔN39) displayed wild-type TRPM8 activity, while a mutant with a deletion of the first 86 (ΔN86) amino acids rendered nonfunctional channels unable to travel to the plasma membrane and producing a retention of TRPM8 in the ER and/or Golgi compartments. Pertusa et al. (2014) continued interrogating the N-terminal region of TRPM8 and corroborated the importance of the N-terminus in the generation of a fully functional TRPM8 channel and, together with the coiled-coil domain in the C-terminus, in the proper folding and assembly of TRPM8 channels. Moreover, they showed that a mutant encompassing the deletion of the first 40 amino acids resulted in functional channels with marked enhancement in cold and menthol responses. With further selective deletions, they concluded that the S27P mutation was sufficient to obtain channels with increased sensitivity to cold and menthol (approx. 1.5 times more response). Consequently, region 40–60 plays a primary role in channel biogenesis, whereas the region encompassing the first 40 amino acids are critical for tuning the thermal and chemical sensitivity of this polymodal ion channel. Finally, it has also been predicted that the N-terminal region of TRPM8 has five putative Protein Kinase A(PKA)-phosphorylation sites (Ser9, Thr17,

Thr32, Ser121, and Ser367) (Bavencoffe et al., 2010). Punctual mutations S9D and T17D eliminate the modulatory effect exerted by activating the Gi-coupled α2A-adrenoreceptor, presumably by PKA activation. These results point out that Ser9 and Thr17 are physiologically relevant PKA-phosphorylation sites and participate in the modulation of TRPM8 channels.

The C-terminus, with 120 residues, is shorter than in other members of the TRPM subfamily. An important region within the C-terminus is a conserved coiled-coil motif, a structural element formed by the last 40 residues (Fig. 3A). Some studies suggest that it is involved in tetramerization of TRPM8 (Erler et al., 2006; Tsuruda et al., 2006). In contrast, another study reported that a mutant of TRPM8 lacking the C-terminus is still able to locate to the membrane as a tetramer although the truncation resulted in a non-responsive channel (Phelps & Gaudet, 2007). The C-terminal domain contains the highly conserved intracellular TRP domain (residues 990-1025), important in the energetic coupling of drug binding into channel opening (Bandell et al., 2006; Valente et al., 2008). It also contains critical sites for PI(4,5)P2 regulation (Rohács et al., 2005; Brauchi et al., 2006).

Finally, a structural study using cryo-electron microscopy (Cryo-EM) provided a 3D reconstruction of TRPM8 from the collared flycatcher *Ficedula albicollis* (83% homology with human TRPM8) which was resolved to an overall resolution of ~4.1 Å, with local resolutions ranging from ~3.8 Å at the core to ~8 Å at the periphery (Yin et al., 2018) (Fig. 3B). This study provided new clues about structural organization of the N- and C-terminal regions, transmembrane domains and, in general, about the architecture of TRPM8, and continues the structural revolution which began with the first ever near-atomic resolution (3.4 Å) structure of a TRP channel, that of TRPV1 (Liao et al., 2013). Since then, the structure of different TRP channels has been resolved by cryo-EM techniques including TRPA1 (Paulsen et al., 2015), TRPM4 (Winkler et al., 2017) or TRPV2 (Zubcevic et al., 2016). Joachim Frank, Richard Henderson, and Jacques Dubochet were awarded with the Nobel Prize in Chemistry in 2017 "*for developing cryo-electron microscopy for the high-resolution structure determination of biomolecules in solution*", a technique with particular interest for the study of dynamic proteins such as ion channels (for an excellent review of this technique see Lau et al., 2018).

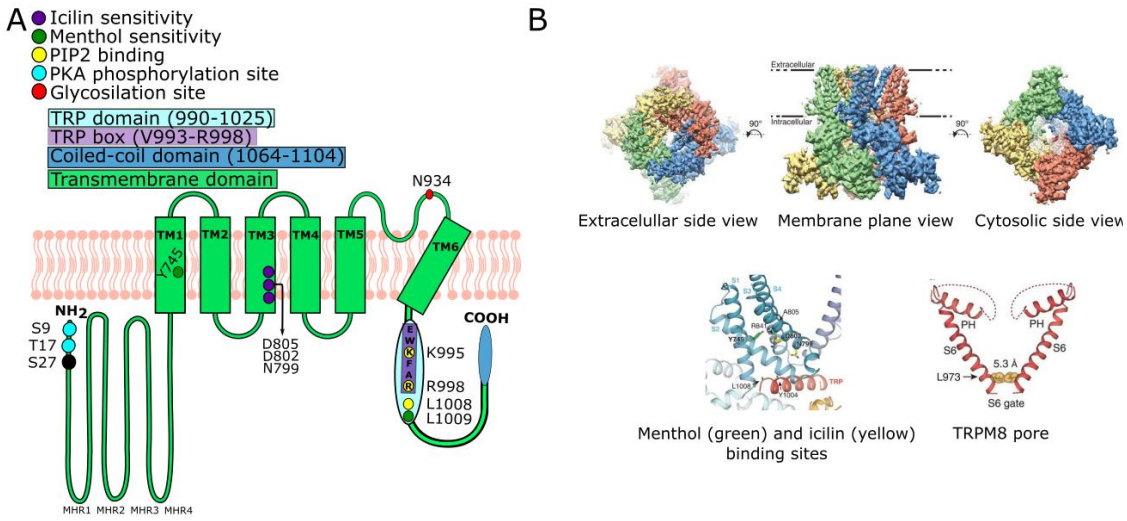

Figure 3. Structure of TRPM8. *A*, Schematic representation of TRPM8 channel subunit topology. Relevant residues for channel gating and modulation of TRPM8 function are highlighted in a color code. ***B,*** On the top, Cryo-EM reconstruction of TRPM8 from different perspectives. On the bottom, detailed view of the residues critical for the sensitivity of TPRM8 to menthol (shown in green) and to icilin sensitivity (yellow stick representation) (left) and a detailed view of the TRPM8 pore showing that the S6 gate in TRPM8 is formed by Leu973 (right) (adapted from Yin et al., 2017).

1.3.3 TRPM8 biophysical properties

TRPM8 channels are gated by physical (i.e. cold temperature), chemical stimuli (e.g. menthol) and by voltage (Fig. 4A) (McKemy et al., 2002; Peier et al., 2002; Voets et al., 2004).

TRPM8 is a voltage-dependent channel, a feature that is clearly evidenced by plotting the current that flows through TRPM8 channels versus the voltage or membrane potential (I-V curve). In such a plot, we can observe the strong outward rectification of the current, as the membrane potential becomes more positive the conductance increases and therefore currents at positive holding potentials are greater than those at negative voltages (Fig. 4A). Rectification could either be an intrinsic property of the pore or reflect a voltage-dependent mechanism that closes the channels at negative potentials. Voets et al. (2004) demonstrated the latter by a classical tail current protocol, based on the activation of TRPM8 by pulses to +120 mV at 15 ^{o}C and subsequent return to hyperpolarized potentials, when TRPM8 rapidly closes (Fig. 4B). The tail current, measured just immediately after returning to negative potentials, when the channel is still open, showed an ohmic current-voltage relation, in contrast with the outward rectification when the current was measured at a steady state point, which demonstrates that outward rectification arises from the rapid and voltage-dependent closure of the channel at negative voltages (Fig. 4B). The exact position of the voltage sensor domain of TRPM8 remains elusive. Neutralization of positive charges in transmembrane domain S4 (R842) and the S4-S5 linker (K856) alter voltage dependence but is not enough to completely abolish voltage-dependent gating (Voets et al., 2007). Interestingly, mutations of these residues also alter the temperature and agonist sensitivity,

suggesting a complex interaction. Later studies suggested that the voltage dependence of TRPM8 depends on an interaction between S3 and S4 (Kühn et al., 2013).

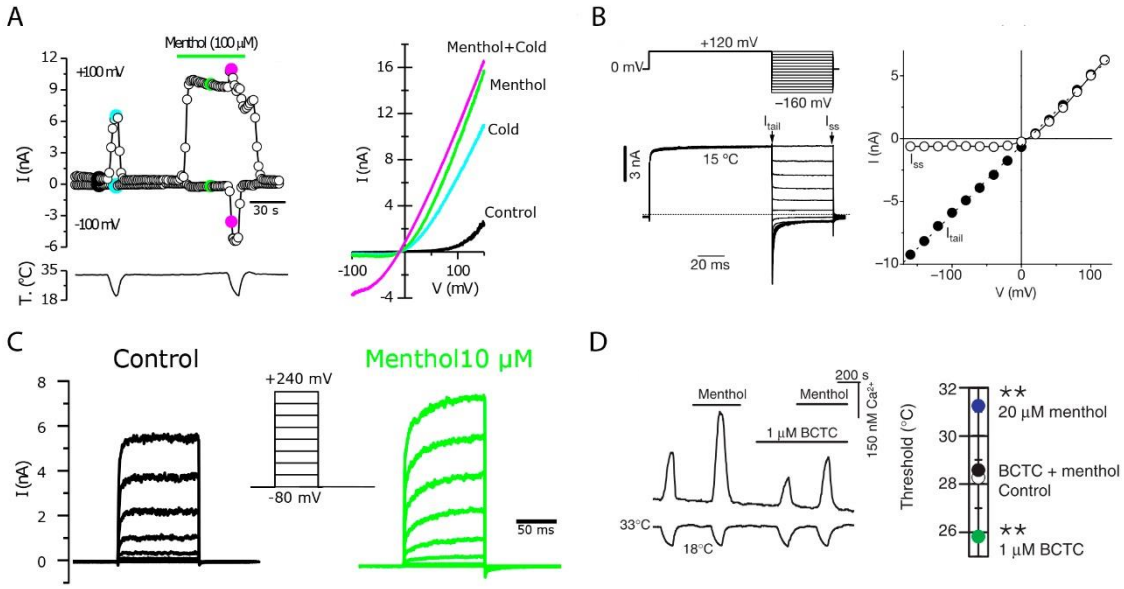

Figure 4. Biophysical characteristics of TRPM8 channels. ***A***, Patch clamp recording in whole-cell configuration from a HEK293 cell transiently transfected with mouse TRPM8 channels. Current at +100 mV and -100 mV is plotted during a protocol in which voltage ramps from -100 to +150 mV were applied. Different stimuli were applied during the protocol, a cold ramp from 33 ºC to 18 ºC, the TRPM8 agonist menthol (100 µM) and a similar cold ramp in the presence of menthol. Current-voltage relationships of colored points are represented at right. Note that voltage in control conditions activates TRPM8 channels, reflecting the intrinsic voltage sensitivity of TRPM8. Cold and menthol activate robust outwardly rectifying currents and cold-evoked currents are potentiated in the presence of menthol. The reversal potential of TRPM8-mediated currents is close to 0 mV. ***B***, Whole-cell TRPM8 currents recorded in HEK293 cells at 15 ºC in response to the indicated voltage protocol. At right, tail (I_{tail}) and steady-state (I_{ss}) currents obtained from the voltage-steps. Adapted from Voets et al., 2004. ***C,*** Voltage steps applied to a HEK293 expressing mouse TRPM8 in control conditions (24 ˚C) and in the presence of menthol (10 µM). Note the strong outward rectification, the slowing of opening kinetics in the presence of menthol and the rapid inactivation of currents just immediately after return to negative potentials. ***D,*** Calcium imaging recording of the effects of 1 µM BCTC plus 20 µM menthol on cold-evoked responses of TRPM8 expressed in HEK293 cells. At right, average response-threshold temperatures in control solution, 20 µM menthol, 1 µM BCTC and 1 µM BCTC + 20 µM menthol. Adapted from Mälkiä et al., 2007.

A defining characteristic of TRPM8, that is also observed in the I-V signature, is the reversal potential of the current: the membrane potential at which there is no net flow of current, or in other words the point at which the I-V curve crosses the X axis. TRPM8 mediated current has a reversal potential close to zero mV in physiological solutions, which is a direct consequence of its permeability to ions (Fig. 4A). TRPM8 is a non-selective cation channel; different cations (Na^+, K^+, Cs^+ and Ca^{2+}) can permeate through TRPM8's pore with little discrimination among

monovalent cations (P_K/P_{Na} =1.1; P_{Cs}/P_K =1.2) but with significantly higher permeability for calcium ions (P_{Ca}/P_{Na} =3.2) (Mckemy et al., 2002).

TRPM8 agonists activate TRPM8 by causing a drastic shift of the voltage dependence activation towards more negative potentials (Fig. 4A), thus increasing the probability of channel openings at physiological membrane potentials (Voets et al., 2004). These authors showed that the midpoint voltage of activation ($V_{1/2}$) at 37 ºC was around +200 mV while cooling to 15 ºC caused a leftward shift of the $V_{1/2}$ of around 150 mV. A similar shift was shown to be induced by menthol and, remarkably, maximal shifts induced by menthol were larger than those induced by cooling to 5 ºC, showing that menthol is a more efficacious TRPM8 agonist than cold temperature. TRPM8 antagonists BCTC, 1,10-phenanthroline and SKF96365 share a common modulatory action that involves marked shifts in the activation curve of TRPM8 towards more positive potentials, the opposite effect exerted by cold and menthol (agonists) (Mälkiä et al., 2007). Mälkiä and colleagues also described that the dynamic voltage-dependent gating was accompanied by a shift in the apparent temperature activation threshold of TRPM8 expressing cells. TRPM8 channels have an apparent threshold temperature of 25 ºC when studied in heterologous expression systems (McKemy et al., 2002; Peier et al., 2002; Andersson et al., 2004). In this work, Mälkiä et al. (2007) reported that the effect of antagonists is a dose-dependent shift in the apparent temperature activation threshold to lower temperatures. Furthermore, the effects induced by menthol and the antagonists appear to counteract each other; they demonstrated it by an elegant approach in which they showed that the response-threshold temperature was shifted to warmer values with 20 µM menthol, was shifted to colder temperatures with 1 µM BCTC and was the same in the presence of both modulators that in control conditions (they cancel each other during joint application of the compounds) (Fig. 4D). Importantly, they showed that the bidirectional modulation of the voltage-dependent activation and the resulting shift in temperature threshold, caused by menthol and antagonists, is also conserved in cold-sensitive trigeminal neurons expressing native TRPM8 channels.

The impact of chemical ligands on TRPM8 gating was studied by Janssens and colleagues (2016). Briefly, they compared the effect of different agonists, including menthol and mustard oil (AITC), on TRPM8 gating by recording whole-cell TRPM8 currents in HEK293 cells during voltage steps from -140 mV to +220 mV. They observed that application of AITC clearly accelerated the gating kinetics upon depolarization to +120 mV, whereas the current relaxation kinetics upon repolarization to -80 mV were not markedly altered compared to control conditions. In contrast, in the presence of menthol, the kinetics of current relaxation were markedly slowed (Fig. 4C). They proposed that menthol prevents the channel from closing (i.e. stabilizes the open state) whereas AITC forces the channel to open faster than it normally would. Based on these differences, they classified agonists as either type I (menthol-like) or type II (AITC-like).

Distinctly, the most relevant functional characteristic of TRPM8 channel is its steep temperature dependence, with Q_{10} values estimated around 30-40 (McKemy et al., 2002; Voets et al., 2004; Brauchi et al., 2004; Zakharian et al., 2010). Temperature-dependent gating of TRPM8 is a

membrane-delimited process, as indicated by experiments showing that TRPM8 can still be activated in cell-free membrane patches (Voets et al., 2004) and even in artificial bilayers (Zakharian et al., 2010), supporting an intrinsic thermal sensitivity of TRPM8. Several studies have tried to identify the structural elements involved in cold (or heat) responses, that means, the structural domain operating as a temperature sensor, in different thermoTRPs (reviewed in Carrasquel-Ursulaez et al., 2015). For TRPM8, it has been suggested that the region of the channel which confers thermosensitivity is in the intracellular C-terminal domain. Brauchi et al. (2006) built chimeras between TRPV1 and TRPM8, exchanging the complete C-terminal intracellular domain. Both constructs, TRPV1 core with TRPM8 C-terminal and vice versa, were functional and showed a switch in temperature sensitivity (the sensitivity of the channel corresponding to the C-terminal) suggesting that most of the key elements necessary for temperature sensing of thermo-TRP channels are self-contained in this cytoplasmic region. However, a recent study investigated the differences between two TRPM8 orthologs with different sensitivity to cold, mouse and chicken TRPM8, and identified the pore loop as a critical structural domain in TRPM8 temperature-dependent responses (Pertusa et al., 2018). Therefore, structural basis of TRPM8 thermosensitivity are still not fully deciphered and the temperature sensor is not yet identified.

1.3.4 TRPM8 pharmacology

An agonist can be defined as a molecule, endogenous or exogenous, that is recognized by the receptor, binds in a specific, reversible and dose-dependent manner and causes its activation. In contrast, an antagonist is a ligand or drug that does not provoke a biological response itself upon binding to the receptor, but blocks or dampens agonist-mediated responses. Both agonist and antagonists modulate receptor activity and this modulation is of special interest for basic research and for the medical treatment of different pathologies in which a receptor is involved. Ideally, an antagonist or an agonist should meet different criteria such as specificity for its receptor, high potency, and high efficacy in order to avoid side effects and the need to use high doses of the drug in a possible clinical setting. However, the most frequently used TRPM8 modulators also display agonistic/antagonistic properties towards other receptors, which justify the search for new, more selective compounds. For example, several TRPM8 agonists and antagonists modulate other TRP channels, as TRPV1 (e.g. BCTC) or TRPA1 (e.g. menthol), despite sharing only 20 percent protein sequence homology. Crossed pharmacology is a common phenomenon in the TRP family (Weil et al., 2005).

Validation of TRPM8 as a therapeutic target in different pathologies such as chronic pain or migraine (reviewed later) has increased the efforts of the pharmacological industry into the search and the design of better TRPM8 modulators. The food and cosmetic industry have also contributed to the identification of new TRPM8 agonists in pursuit of molecules that mimic cooling sensations. The most common strategies for the development of novel modulators consists in the synthesis of new molecules starting from different chemical structural scaffolds known to

modulate TRPM8, high-throughput screening of these molecules and pharmacological characterization of the molecules which show biological activity over TRPM8 channels.

In the last few years, several selective and potent TRPM8 modulators has been described in the scientific and patent literature (for a review see DeFalco et al., 2011; Eid, 2011; Premkumar & Abooj, 2013). Some of these modulators are already undergoing clinical trials (Winchester et al., 2014; Ständer et al., 2017). A list of TRPM8 agonist and antagonist is presented in table 1 and table 2 respectively.

1.3.4.1 TRPM8 agonists

Menthol, the first TRPM8 agonist described, is an organic monoterpene alcohol found in plants belonging to the genus *Mentha.* It has been used since ancient times as analgesic and antipruritic, and synthetic compounds derived from menthol are widely used in the food industry as flavoring chemical compounds and in the cosmetic industry due to its cooling effects. Menthol activates TRPM8 channels with an EC_{50} in the range of micromolar concentration (see table 1) (McKemy et al., 2002). In 2006, during a massive random mutagenesis screen, Bandell and colleagues revealed that the crucial amino acid involved in menthol activation was a tyrosine residue (Y745) located on transmembrane segment 1 according to recent Cryo-EM structural analysis (Yin et al., 2018) (Fig. 3A). The single point mutation of this residue (TRPM8-Y745H) totally abolishes menthol sensitivity, while retaining the responsiveness to cold and voltage exhibited by the wild-type channels. Mälkiä et al., 2009 continued investigating the sensitivity of the TRPM8-Y745H mutant to different antagonists and described that this residue is also essential for the inhibition of cold- and voltage-activated TRPM8 currents mediated by SFK96365, a non-specific blocker of various calcium-permeable channels. In contrast, the inhibition of TRPM8 by another antagonist, BCTC, was unaffected by the mutation and only partially reduced by other inhibitors such as capsazepine, clotrimazole or econazole, suggesting additional binding sites on the TRPM8 channel.

However, menthol is far away from being a specific or selective agonist of TRPM8. Menthol also activates the heat-activated channel TRPV3, although with a much higher EC_{50}, estimated around 20 mM (Macpherson et al., 2006). Additionally, submicromolar to low micromolar concentrations of menthol cause TRPA1 activation, whereas higher concentrations lead to a reversible channel block (Karashima et al., 2007). TRPA1-mediated menthol responses have been described in cultured primary sensory neurons (Karashima et al., 2007; Fajardo et al., 2008; Madrid et al., 2009). However, unlike TRPM8-mediated menthol responses, which are potentiated by cold, the TRPA1-mediated menthol response is inhibited by cooling. Apart from TRP channels, menthol also modulates voltage-gated Na^{2+} and Ca^{2+} channels, and $GABA_A$ receptors (Swandulla et al., 1987; Sidell et al., 1990; Watt et al., 2008; Gaudioso et al., 2012).

Soon after these studies documenting menthol lack of specificity for TRPM8, different menthol derivatives were tested in order to find new and improved TRPM8 agonists as potential drugs. Bödding et al. (2007) studied the effect of different menthol-analog molecules with cooling effects

originally developed in the 1970's by a company called Wilkinson Sword Ltd, and that had been widely used in cosmetics. This leading company in shaving products conducted an extensive research program in which they designed and evaluated about 1200 compounds for their cooling activity, interested in finding cooling compounds without the volatility of menthol which causes side effects such as eye irritation from aftershave lotions (Leffingwell et al., 2014). Several compounds were found to activate TRPM8 channels in a dose-dependent and reversible manner with EC_{50} values in the nM to low µM range. Among them, the carboxamide WS-12 was the most potent in activating TRPM8, with an EC_{50} of 0.19 µM. Further evaluation of WS-12 selectivity profile demonstrated that WS-12 did not activate any of the other thermosensitive TRP channels (Ma et al., 2008). Other synthetic related compounds also behave as TRPM8 agonists such as WS-3, WS-11, WS-148, CPS-113, Frescolat-ML, Frescolat-MAG, PMD-38 and cooling agent 10 (Behrendt et al., 2004; Bödding et al., 2007; Beck et al., 2007).

Icilin, also known as AG-3-5, is another synthetic compound known early on to activate TRPM8 channels (McKemy et al., 2002). This super-cooling agent, synthesized in 1983, has an EC_{50} of 0.36 µM. Icilin acts through a different mechanism of activation than menthol, requiring simultaneous exposure to intracellular calcium ions and binding to different residues (Chuang et al., 2004; Andersson et al., 2004). By comparative studies with the chicken TRPM8, which was found to be insensitive to icilin but maintains cold and menthol sensitivity, three residues located in the cytoplasmatic loop connecting putative transmembrane domains 2 and 3 were shown to be critical for icilin sensitivity (N799, D802, and G805 of rat TRPM8) (Fig. 3A). Moreover, activation of TRPM8 by icilin and cold, but not menthol, is modulated by intracellular pH (Andersson et al., 2004). These data confirm that menthol and icilin have a totally different mechanism of action however, they share the ability to additionally modulate TRPA1 channels (Story et al., 2003).

AITC, also known as mustard oil, activates recombinant TRPM8 channels and excites a subset of cold-sensitive somatosensory neurons at very high concentrations (milimolar range) via direct activation of TRPM8 (Janssens et al., 2016). This irritant compound derived from *Brassica* plants has been extensively used in experimental models to induce pain and inflammation (McMahon & Abel, 1987) and was first described as a potent TRPA1 agonist (Bautista et al., 2006). Later, it was shown by Everaerts and colleague (2011) that mustard oil also activates TRPV1 channels, refuting the view that TRPA1 is the sole nocisensor involved in the mustard oil effect. However, it should be noted that the EC_{50} of AITC for TRPV1 and TRPM8 is in the milimolar range while for TRPA1 is in the micromolar range.

More recently, two different groups reported that TRPM8 is the pharmacological target of a natural compound used in traditional Chinese medicine for the treatment of different ocular diseases and as topical analgesic called borneol, a bicyclic monoterpenoid (Chen et al., 2016; Wang et al., 2017). They demonstrated that borneol activates human TRPM8 currents in a dose- and temperature-dependent manner, in a similar but less effective way than menthol (EC_{50}= 65 µM). In 2017, interested in the search for novel TRPM8 agonists to treat dry eye disease, Yang et al. synthesized a water-soluble TRPM8 agonist called cryosim-3 (C3). C3 has an EC_{50} of 0.9 µM and

activates TRPM8-expressing neurons in primary sensory cultures. They showed that C3 was inactive in cells transfected with TRPV1 and TRPA1 channels, although only low concentrations were tested (10 µM). Recently, it was shown that the anthelmintic drug praziquantel is a selective agonist of TRPM8 channels with an EC_{50} of approximately 25 µM and, as menthol activation, dependent on Y745 residue (Babes et al., 2017).

Other natural agonists of TRPM8 are linalool (6.7 mM), geraniol (5.9 mM), eucalyptol (7.7mM), hydroxylcitronellal (19.6 mM), or camphor (Behrendt et al., 2004). However, it should be noted that many of these agonists are effective only at high concentrations, as for example camphor with an EC_{50} of approximately 4.5 mM (Selescu et al., 2013) (See Table 1).

Compound		EC50	Ortholog	Crossed pharmacology
Menthol		66.7 µM[c] 4.1 µM[a] 10.4 µM[b] 3.6 µM[d] 13 µM[f]	rTRPM8 mTRPM8 hTRPM8 hTRPM8 hTRPM8	TRPV3 (+), TRPA1 (+/-), Na_v^+ channels (-), $GABA_A$ receptors (+), nAChRs(-)
Menthol derivates	**WS-12**	0.19 µM[b] 0.17 µMd[e]	hTRPM8 hTRPM8	
	WS-3	3.7 µM[a]	mTRPM8	
	WS-30	5.6 µM[b]	hTRPM8	
	WS-148	4.1 µM[b]	hTRPM8	
	WS-23	44 µM[a]	mTRPM8	
	CPS-113	1.2 µM[b]	hTRPM8	
	Cps-369	3.6 µM[b]	hTRPM8	
	Frescolat-ML	3.3 µM[a]	mTRPM8	
	Frescolat-MAG	4.8 µM[a]	mTRPM8	
	PMD-38	31 µM[a]	mTRPM8	
	Cooling agent 10	6 µM[a]	mTRPM8	
	Coolact P	66 µM[a]	mTRPM8	
Icilin (AG-3-5)		0.36 µM[c] 1.4 µM[b] 0.2 µM[a]	hTRPM8 mTRPM8	TRPA1 (+)
AITC			hTRPM8	TRPA1 (+), TRPV1(+)
Borneol		65 µM[f]	hTRPM8	TRPA1 (-), TRPV3 (+), $GABA_A$ receptors (+)
Cryosim-3		0.9 µM[d]	hTRPM8	
Praziquantel		25 µM[e]	hTRPM8	
Linalool		6.7 mM[a]	mTRPM8	TRPV1 (+), TRPV3 (+)
Geraniol		5.9 mM[a]	mTRPM8	
Eucalyptol		7.7 mM[a], 0.92 mM[w] 3.4 mM[c], 1.21 mM[w] 145.6 µM[w]	mTRPM8 rTRPM8 hTRPM8	TRPA1(-)
Hydroxylcitronellal		19.6 mM[a]	mTRPM8	
Camphor		4.5 mM[g]	hTRPM8	TRPV1 (+), TRPV3 (+)

Table1. TRPM8 agonists. a, Behrendt et al., 2004; b, Bodding et al., 2007; c, Mckemy et al., 2002; d, Yang et al., 2016; e, Babes et al., 2017; f, Wang et al., 2017; g, Selescu et al., 2013; w, Caceres et al., 2017. In the cross pharmacology column, the symbol (+) means an agonistic effect and (-) an antagonistic effect.

1.3.4.2 TRPM8 antagonists

The number and specificity of TRPM8 antagonists has been growing steadily since the initial reports (Table 2). Early studies identified as TRPM8 antagonists compounds that also modulated several TRP channels, indicating a complex cross pharmacology between different TRP channels.

BCTC (IC_{50}= 0.035 µM), thio-BCTC (IC_{50}= 0.054 µM), and capsazepine (IC_{50}= 0.42 µM) were originally described as potent TRPV1 antagonists (Bevan et al., 1992; Valenzano et al., 2003). In 2004, Behrendt et al., while studying the effect of different compounds on TRPM8 channels using a fluorometric imaging plate reader assay, discovered that these TRPV1 antagonists were also able to block the response of TRPM8 to menthol with relatively low micromolar concentrations (IC_{50}= 0.8 µM for BCTC, IC_{50}= 3.5 µM for thio-BCTC and IC_{50}= 18 µM for capsazepine). In addition to their blocking effect on TRPV1 and TRPM8 channels, BCTC also activates TRPA1 channels (Madrid et al., 2006). A similar case is phenanthroline which was described as a blocker of open TRPV1 channels (Tousova et al., 2004) and later was shown to be a TRPM8 antagonist with an IC_{50} of 180 µM (Mälkiä et al., 2007). Also, the TRPV1 antagonists CTPC, a related piperazinyl urea compound, and SB-452533 were found to inhibit TRPM8 with high potency (IC_{50}= 0.131 µM and 0.57 µM respectively) (Weil et al., 2005).

Hu et al. (2004) described that 2-aminoethoxydiphenyl borate (2-APB) activates TRPV1, TRPV2, and TRPV3 but inhibits the activity of TRPC6 and TRPM8. The IC_{50} value for 2-APB inhibition of menthol-activated currents was 7.7 µM.

Another compound with a promiscuous relationship with different TRP members is clotrimazole. This drug is widely used for the topical treatment of yeast infections in the skin and mucous membranes and common side effects reported include irritation and burning pain, suggesting an effect on peripheral sensory neurons. Indeed, Meseguer and colleagues (2008) described that clinically relevant clotrimazole concentrations activate heterologously expressed TRPV1 and TRPA1 channels, stimulate a subset of capsaicin-sensitive and mustard oil-sensitive trigeminal neurons and evoke nocifensive behavior in mice after intraplantar injection. In addition, they showed that clotrimazole inhibited TRPM8 channels in heterologous expression systems and also in sensory neurons in culture with relative high potency (IC_{50}= 0.2 µM). In 2009, Mälkiä and colleagues, investigated the effect on TRPM8 of two structurally related compounds, imidazole, and econazole. They found that econazole was similarly potent than clotrimazole in antagonizing TRPM8 (IC_{50}= 0.42 µM), while imidazole was ineffective.

SFK96365 is a non-specific blocker of various calcium-permeable channels, including receptor-operated channels, voltage-gated calcium channels and different TRP channels. Reid et al. (2002) described during the earliest descriptions of cold-evoked currents in peripheral sensory neurons that SKF96365 inhibited these currents by almost 70%. Further exploration of SKF96365 effect on TRPM8-transfected HEK293 yields an IC_{50} of approximately 1 µM (Mälkiä et al., 2009). Interestingly, the effect of SKF96365 was almost completely lost in the menthol-insensitive

TRPM8-Y745H mutant channel, demonstrating that the menthol binding site is critical for inhibition mediated by SKF96365.

In 2008, AMTB, a new antagonist of TRPM8 with an IC_{50} of 6.23 µM and relative no effect on TRPV1 and TRPV4 channels was presented (Lashinger et al., 2008). However, more recently AMTB was identified as an inhibitor of voltage-dependent Na^+ channels (Yapa et al., 2018).

PBMC was also described as a highly potent (IC_{50} = 0.6 nM and 0.4 nM at positive and negative voltages respectively), and was demonstrated to have an effect in TRPM8-dependent behavioral responses (Knowlton et al., 2011).

RaQualia company identified in 2014 the compound RQ-00203078, a highly selective, potent (IC_{50}= 4.8 nM for menthol-induced activation of human TRPM8) and orally available TRPM8 antagonist (Ohmi et al., 2014). They explored the *in vivo* activity of RQ-00203078 and demonstrated promising results reducing, in a dose-dependent manner, the TRPM8-dependent icilin-induced wet-dog shakes in rats after oral administration.

Janssen L.T. has published several potent (in the nM range) and selective small molecule antagonists, as for example derivatives of arylglycine (Zhu et al., 2013). Calvo et al. (2012) also developed inylcycloalkyl-substituted benzimidazole derivatives which showed potency in the nanomolar range and *in vivo* efficacy. More recently, de la Torre-Martínez et al. (2017) designed an innovative chemical library based on the β-lactam ring structure. Two potent TRPM8 blockers were identified (Compound 41 and 45) with IC_{50} values in the nanomolar range (IC_{50}= 46 and 83 nM, respectively) and with great selectivity versus other TRP members as well as other ion channels. Naphthyl derivatives have also been described as a novel class of potent and selective TRPM8 inhibitors in the range of nM concentrations (Beccari et al., 2017).

Other TRPM8 antagonist described in the bibliography are ACA (3.9 µM), MAD1d (0.02 µM), MAD2e (0.1 µM), AMG9678 (0.031 µM), AMG2850 (0.156 µM), Compound 496 (12 µM) and M8-An (0.01 µM) (Harteneck et l., 2007; Kraft et al., 2006; Ortar et al., 2010; Gavva et al., 2012; Patel et al., 2014; Lehto et al., 2015).

Compound	EC50	Ortholog	Crossed pharmacology
BCTC	0.8 μM[a] 0.143 μM[i]	mTRPM8	TRPV1 (-), TRPA1 (+)
Thio-BCTC	3.5 μM[a]	mTRPM8	TRPV1 (-)
Capsazepine	18 μM[a]	mTRPM8	TRPV1 (-)
Phenanthroline	180 μM[l]	rTRPM8	TRPV1 (-)
CTPC	0.13 μM[i]	hTRPM8	TRPV1 (-)
SB-452533	0.57 μM[i]	hTRPM8	TRPV1 (-)
2-APB	7.7 μM[j]	mTRPM8	TRPV1 (+), TRPV2 (+), TRPV3 (+), TRPC6 (-), TRPM2 (-)
Clotrimazole	0.200 μM[k]	hTRPM8	TRPV1 (+), TRPA1 (+)
Econazole	0.42 μM[h]	mTRPM8	TRPM3 (-), TRPM2 (-), TRPV5 (-)
SFK-96365	1 μM[l]	rTRPM8	Ca^{2+} permeable channels (-)
AMTB	6.23 μM[m]	hTRPM8	Na_v channels (-)
PBMC	0.4 nM[n]	mTRPM8	
RQ-00203078	8.3 nM[o]	hTRPM8	
Arylglycine derivates	nM range[p]	canine TRPM8	
Benzimidazole derivates	nM range[q]	canine TRPM8	
β-lactam ring derivates	nM range[r]	rTRPM8	
Naphthyl derivatives	nM range[s]	hTRPM8	
ACA[t]	3.9 μM		
MAD1d	0.02 μM		
MAD2e	0.1 μM		
AMG9678	0.031 μM[u]	rTRPM8	TRPA1(-)
AMG2850	0.156 μM[u]	rTRPM8	TRPA1(-)
Compound 496	0.026 μM[u]	rTRPM8	TRPA1 (-)
M8-An	10.9 nM[v]	hTRPM8	

Table 2. TRPM8 antagonists. h, Mälkiä et al., 2009; I, Weil et al., 2005; j, Hu et al., 2004; k, Messeguer et al., 2008; l, Mälkiä et al., 2007; m, Lashinger et al., 2008; n, Knowlton et al., 2011; o, Ohmi et al., 2014; p, Zhu et al., 2013; q, Calvo et al., 2012; r, de la Torre-Martínez et al., 2017; s, Beccari et al., 2017; t, Harteneck et al., 2007; u, Gavva et al., 2012; v, Patel et al., 2014. In the cross pharmacology column, the symbol (+) means an agonistic effect and (-) an antagonistic effect.

1.3.5 Modulation of TRPM8

Apart from agonists and antagonists, TRPM8 function and biophysical properties can be regulated by pH (Anderson et al., 2004), calcium ions (Schäfer et al., 1986, Mahieu et al., 2010) and different signaling cascades and post-translational modifications, which modify trafficking and thermal and chemical sensitivity of the channel.

1.3.5.1 PI(4,5)P2 and Gq protein-coupled receptors modulation

Phosphoinositides (PIs) represent a minor fraction of charged phospholipids found principally in the cytoplasmic leaflet of all eukaryotic cellular membranes where they serve as recognition sites for specific cytoplasmic proteins and act as membrane-delimited second messengers, modulating different physiological processes (Falkenburger et al., 2010). Like other phospholipids, PIs are composed of a glycerol backbone to which two fatty acid chains and a modified phosphate group

are attached. (Fig. 5). The most abundant phosphoinositide is phosphatidylinositol (PI) which comprise around 95% of the total pool of PIs in the cell (Xu et al., 2003). PI can become phosphorylated on the 3, 4 and 5 positions of the inositol ring in every combination forming the seven low-abundance poly-phosphoinositides; PI(3)P, PI(4)P, PI(5)P, PI(3,4)P2, PI(3,5)P2, PI(4,5)2 and PI(3,4,5)P3. The cellular pools of phosphorylated phosphoinositides turn over continuously by the action of different phosphatases and kinases (Fig. 5).

Among the different PIs, PI(4,5)P2, which is a permanent and minor component (<1%) of the plasma membrane, has received major attention since the 1970s for its role as the substrate for cleavage by the enzyme phospholipase C (PLC). Activation of Gq protein-coupled receptors (GqPCRs) and receptor tyrosine kinases activate PLC which cleaves PI(4,5)P2 producing two second messengers, the soluble inositol 1,4,5-trisphosphate (IP3) and diacylglycerol (DAG) which in turn releases calcium from intracellular stores and recruits the activation of protein kinase C (PKC) respectively (Berridge & Irvine, 1984; Kirk et al., 1984; Smrcka et al., 1991). Once the stimulus activating these receptors is terminated, PI(4,5)P2 levels are restored enzymatically (Fig. 5). This is an important and ubiquitous cellular signaling pathway, at least 80 types of PLC-coupled receptors are known and several of them participate in important physiological processes such as transduction of external stimuli, hormone signaling, neurotransmission and pathological processes such as inflammation (Pawson et al., 2014).

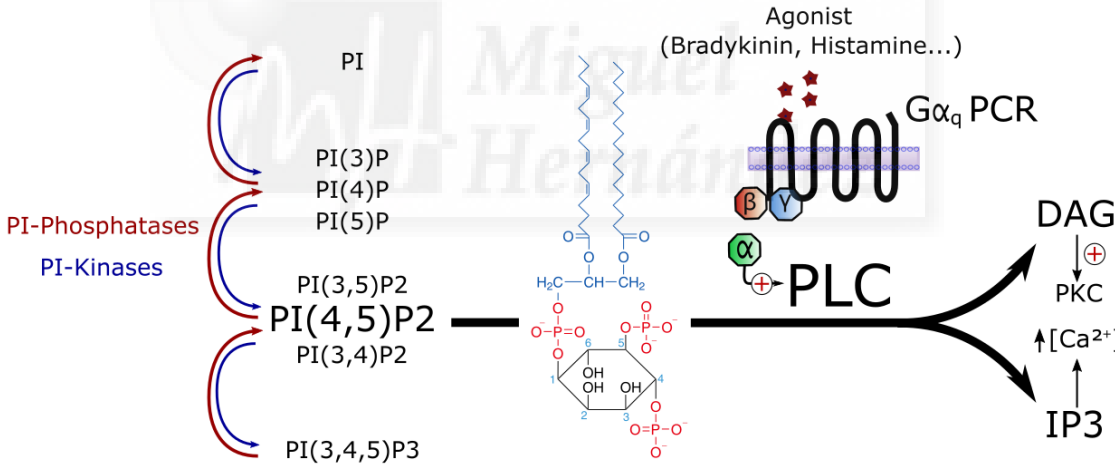

Figure 5. Phosphoinositide turn-over and G-protein coupled receptor effects on PI(4,5)P2. Phosphatidylinositol (PI) is the major component of the cellular phosphoinositide pool. PI-kinases and PI-phosphatases add and remove phosphate groups on the 3, 4 and 5 positions and synthetize the seven low-abundance poly-phosphoinositides. The pools of phosphorylated phosphoinositides turn over continuously. The structure of the phosphoinositides consists on a glycerol backbone esterified by two fatty acid chains (blue chain) and 1 to 3 phosphates attached to a polar head group. PI(4,5)P2 is the substrate for the enzyme phospholipase C (PLC) which is activated by the α subunit of GqPCRs and converts PI(4,5)P2 in inositol 1,4,5-trisphosphate (IP3) and diacylglycerol (DAG).

In the 1990s, a direct signaling role for PI(4,5)P2 itself and other PIs was recognized (Hilgemann & Ball, 1996; Fan & Makielski, 1997). Nowadays it is well established that PIs control many aspects of cellular behavior, including processes such as endocytosis (Cremona & De Camilli,

2001; Posor et al., 2015), actin filament assembly (Saarikangas et al., 2010) or release of synaptic vesicles (Martin, 2015). Additionally, and relevant to our work, PI(4,5)P2 directly regulates the activity of different ion channels (Suh & Hille, 2008). Among the ion channels sensitive to PI(4,5)P2 are members of the voltage-gated potassium channel family (Kv) (Kruse et al., 2012), inward-rectifier potassium channels (Kir) (Huang et al., 1998), voltage-gated calcium channels (Cav) (Suh et al., 2010), two-P domain potassium channels (K2P), cyclic nucleotide-gated channels (CGN) and TRP channels (for a recent review see; Hille et al., 2015).

Two of the channel subunits in which PI(4,5)P2 dependence is better established are KCNQ2/3 channels (Kv7.2/Kv7.3), which generate the M-current in neurons, a potassium current which regulates excitability in a variety of central and peripheral neurons (Wang et al., 1998). It was known that muscarinic 1 receptor (M1R) activation suppressed M-current (Brown & Adams, 1980), enhancing neuronal excitability. However, for many years, little was known about the molecular mechanism responsible for this inhibition. In 2002, Suh & Hille provided the first evidence about the dependence of M-current on the PI(4,5)P2 presence, which was further confirmed by other groups (Zhang et al., 2003; Ford et al., 2004; Winks et al., 2005). These studies established the absolute and exclusive requirement of PI(4,5)P2 for KCNQ2/3 in order to stay in an open state, making these channels a relatively straight-forward model to study PI(4,5)P2 regulation of ion channels.

Different theories about the influence of PI(4,5)P2 on channel activity have been proposed. The effects of PI(4,5)P2 on ion channels fit many features of a ligand or an agonist as it binds to channels in a reversible, specific and dose-dependent manner. It has been proposed to act as a cofactor or as a molecule that facilitates the proper organization of the channel but unable to initiate a change in channel gating state (Hansen, 2015). PI(4,5)P2 has been proposed to serve as a coincidence detector, which would facilitate the transport of inactive channels in the endoplasmic reticulum and in vesicles, until they arrive at the plasma membrane where the abundance of PI(4,5)P2 would allow the activation of the channel (Di Paolo & Camilli, 2006; Zhang et al., 2012) .

As mentioned, PI(4,5)P2 regulation is also important for the activity of the TRP ion channel family, where most, if not all channels, are modulated (positively or negatively) by PI(4,5)P2 levels. Therefore, PI(4,5)P2 is a good candidate to serve as a common modulator of TRP channels inside their exceptional diverse modes of regulation. TRPM channels provide, among all TRP channel subfamilies, the clearest picture of PI(4,5)P2 regulation, which acts as a positive modulator of all members of this subfamily; TRPM1 (Shen et al., 2012), TRPM3 (Badheka et al., 2015; Tóth et al., 2015; Badheka et al., 2017), TRPM4 (Nilius et al., 2006), TRPM5 (Liu & Liman, 2003), TRPM6 (Xie et al., 2011) and TRPM7 (Runnels et al., 2002). Focusing on TRPM8 channels, PI(4,5)P2 is a crucial factor for its activity. The first indication that TRPM8 was PI(4,5)P2-dependent arose with studies in excised membrane patches (e.g. inside-out patch): after excision, channel activity steadily decreased until full inactivation (Liu & Qin, 2005; Rohacs et al., 2005). This phenomenon is known as “rundown” and is observed in PI(4,5)P2-dependent channels due to the lack of the

cytosolic factors necessary to maintain sufficient PI(4,5)P2 levels in the excised patch, which support ion channel function. Adding back a soluble PI(4,5)P2 analog, like diC8PIP2, rescues activity and PI(4,5)P2 scavengers like polylysine or PI(4,5)P2 antibodies, which mask PI(4,5)P2 availability, accelerate rundown (Rohacs et al., 2005; Liu et al., 2005). Phosphatase inhibitors were shown to delay rundown whereas cytosolic application of Mg^{2+} (blockade of PI-kinases) accelerate the process by modifying the activity of the kinases and phosphatases in charge of PI(4,5)P2 synthesis and clearance respectively (Liu et al., 2005).

Rohacs et al. (2005) explored in detail the relation of TRPM8 activity with PI(4,5)P2. They demonstrated that the dependence of TRPM8 is relatively specific to PI(4,5)P2, as PI(3,4)P2, PI(3,4,5)P3 and PI(4)P produced less than 30% of the PI(4,5)P2 effect. Moreover, they determined the EC_{50} values of TRPM8 for PI(4,5)P2, obtaining an "apparent affinity", by performing dose-response measurements of PI(4,5)P2 at various temperatures and in the presence of menthol. Both menthol and cold shifted the EC_{50} of activation by PI(4,5)P2 to lower concentrations. Therefore, cold and menthol strengthen the interaction of TRPM8 channels with PI(4,5)P2 or, in other words, TRPM8 agonists sensitize TRPM8 channels to PI(4,5)P2. Notably, voltage also sensitizes TRPM8 channels to PI(4,5)P2; TRPM8 showed higher sensitivity to PI(4,5)P2 at +100 mV than at –100 mV. By performing point mutations in conserved residues, they found three positively charged residues in the TRP domain (K995, R998 and R1008) important for PIs effects. These mutations render channels with smaller currents in response to agonist and a decrease in their sensitivity to PI(4,5)P2, suggesting that the TRP domain may serve as a PI(4,5)P2-interacting domain.

Studies of reconstituted TRPM8 channels in planar lipid bilayers and its activation by different stimuli corroborated that TRPM8 activation by cooling and cooling agents depend specifically on the presence of PI(4,5)P2 (Zakharian et al., 2010). In accordance with the PI(4,5)P2 dependence of TRPM8 channels, it has been shown that selective depletion of PI(4,5)P2 by using voltage sensitive phosphatases (Yudin et al., 2011) or chemically inducible PIs phosphatases (Varnai et al., 2006; Daniels et al., 2009) is sufficient to inhibit TRPM8 channel activity in heterologous expression systems.

Functional control of TRPM8 activity by PI(4,5)P2 has been shown to play important physiological roles, as for example the desensitization of cold-thermoreceptors. TRPM8 activity shows adaptation or desensitization; its activity decreases during the prolonged presence of an agonist in a manner that is dependent upon the presence of calcium (Reid & Flonta, 2001b; McKemy et al., 2002; Daniels et al., 2009). It is well known that this desensitization is also observed in cold-sensitive nerve fibers, in which exposure to constant cooling temperatures results in diminished activity over time (Hensel & Zotterman, 1951). The molecular mechanism involved in this process is related to the PI(4,5)P2 dependency of TRPM8 channels. Activation of TRPM8 evokes a Ca^{2+} influx which leads to the activation of a Ca^{2+}-sensitive PLC which depletes PI(4,5)P2, resulting in the decrease of the activity or desensitization of TRPM8 channels (Rohacs et al., 2005; Daniels

et al., 2009; Yudin et al., 2011). A similar process has been hypothesized to mediate the control of the temperature threshold in cold-sensitive neurons (Fujita et al., 2013).

PI(4,5)P2-dependent modulation of TRPM8 channels has also been studied in processes involving the activation of GqPCRs. In heterologous expression systems and in cold-sensitive neurons, GqPCRs activation following application of different inflammatory mediators such as bradykinin, prostaglandin E2 or histamine, decreases TRPM8 activity (Liu and Qin, 2005; Rohacs et al., 2005; Premkumar et al., 2005; Linte et al., 2007; Zhang et al., 2012). Although depletion of PI(4,5)P2 is a direct consequence of GqPCRs activation and the dependence of PI(4,5)P2 is important and well-established for several ion channels, when a GqPCRs is activated the picture becomes more complicated. Activation of a GqPCRs trigger secondary signaling cascades and change the levels of additional secondary messengers (Fig. 4). For example, inflammatory mediators released during tissue injury or inflammation activate GqPCRs that promote the phosphorylation of TRPV1 channels by protein kinases, sensitizing the channel and enhancing heat pain sensations (Cesare & McNaughton, 1996; Caterina et al. 2000; Premkumar & Ahern, 2000).

In the case of TRPM8, the mechanisms involved in TRPM8 downregulation after GqPCRs activation are not well defined. Other components of the GqPCRs signaling cascade, beside PLC-mediated hydrolysis of PI(4,5)P2, have been proposed to participate in the modulation of TRPM8 activity. Thus, different studies proposed that PKC-mediated phosphorylation of the channel is responsible for TRPM8 downregulation after GqPCRs activation, in a similar manner than TRPV1 is sensitized (Premkumar et al., 2005; Abe et al., 2006; Linte et al., 2007). Other groups defended the hypothesis that downregulation of TRPM8 is exerted by a direct interaction of TRPM8 with activated Gαq subunits and, therefore, independent of cell signaling pathways downstream of GqPCRs (Zhang et al., 2012; Li & Zhang, 2013). Specifically, their experiments demonstrated that neither depletion of membrane PI(4,5)P2 nor phosphorylation by PKC are crucial for TRPM8 downregulation after GqPCRs activation.

Direct interaction of the GqPCR's Gαq subunit was also described for TASK channels and it was established as the mechanism by which these background potassium channels are robustly inhibited by receptors that signal through GqPCR family proteins (Chen et al., 2006; Lindner et al., 2011). However, a few years later it was proposed that the second messenger diacylglycerol (DAG) is sufficient for TASK channel inhibition and is necessary for downregulation by GqPCRs (Wilke et al., 2014; Bista et al., 2015). At the same time, Gβγ subunit has the ability to modulate ion channels via a membrane-delimited pathway independently of soluble intracellular messengers. The important direct modulatory role for Gβγ was first demonstrated for cardiac G-protein activated K^+ (GIRK) channels by Logothetis et al. (1987) and was posteriorly extended to other channels such as for example N-type and P/Q-type Ca^{2+} channels (Herlitze et al., 1996). More recently, the direct effect of Gβγ subunits has been shown to mediate physiological modulation of different members of the TRPM subfamily, which are also dependent of PIs presence. TRPM1 inhibition mediated by activation of metabotropic glutamate receptor 6 is part

of the transduction cascade of retinal ON bipolar cells and was shown to be dependent on the Gβγ dimer (Shen et al., 2012). In 2017, three independents groups showed that, after activation of Gi/oCPRs, the inhibition of TRPM3 expressed in neurons occurs via a short signaling cascade involving Gβγ proteins (Dembla et al., 2017; Quallo et al., 2017; Badheka et al., 2017).

Different aspects should be taken into account when we study PI(4,5)P2 regulation of ion channels. Several phosphoinositides, especially PI(4,5)P2 and PI(4)P, are found in substantial levels in resting cells, and their concentrations may decrease upon the activation of PLC but are unlikely to vanish under physiological conditions. Therefore, the apparent affinity of a given ion channel for phosphoinositides would be a very important determinant of their regulation; that is, a channel with high affinity for PI(4,5)P2 may not be affected by a moderate PI(4,5)P2 depletion, whereas a channel with low affinity would be affected. PIs are local signaling molecules that are not distributed homogenously in the plasma membrane; rather, it is likely that specific PI(4,5)P2 "microdomains" or "pools" exist, and these signaling microdomains are of critical importance for the induction of selective effects (Yoshida et al., 2017). At the same time, PI(4,5)P2 depletion have an effect on different ion channels, and the global effect in the excitability of a neuron could be an integration of those effects.

In conclusion, GqPCRs-mediated effects in physiological systems are extremely complex and involve several steps and secondary messengers which are difficult to isolate and study separately. Additionally, the effects observed in heterologous expression systems when a GqPCRs is activated should be interpreted carefully and additional studies in native systems should be performed in order to establish the relevance of PI(4,5)P2 modulation in a physiological context.

1.3.5.2 Post-translational modulation of TRPM8 channels

Another important mechanism modulating neuronal excitability is the number of functional channels present at the plasma membrane, which is regulated by endocytosis and exocytosis processes and also influences the current amplitude in response to a given stimulus (Lai & Jan, 2006). A fraction of TRPM8 channels resides on the plasma membrane whereas a different fraction is part of a dynamic pool within intracellular vesicles near the plasma membrane (Veliz et al., 2010; Ghosh et al., 2016). TRPM8-containing vesicles show distinct patterns of movement and their recruitment to the plasma membrane is induced by different processes such as stimulation by agonists or by nerve growth factor (NGF) (Babes et al., 2004; Toro et al., 2015; Kayama et al., 2017). The incorporation of these vesicles into the plasma membrane has been shown to be mediate by VAMP7, the vesicle-associated membrane protein 7 (Ghosh et al., 2016). Incorporation of new channels through exocytosis upon acute activation (e.g. TRPA1) or stimulation by NGF (e.g. TRPV1) have also been reported for other thermoTRP channels (Zhang et al., 2005; Stein et al., 2006; Schmidt et al., 2009). Other mechanisms, such as activation of μ-opioid receptors leads to the internalization of TRPM8 channels, leading to decreased cold-evoked responses (Shapovalov et al., 2013).

Once in the plasma membrane, TRPM8 is mainly located within lipids rafts (Morenilla-Palao et al., 2009). Lipids rafts are plasma membrane microdomains considerably enriched in cholesterol and sphingolipids and constitute an important mechanism of spatial co-localization of different signaling molecules which facilitate the assembly of intracellular signaling cascades (Simons & Ikonen, 1997). Spatial localization of TRPM8 in lipid rafts has been shown to modulate negatively TRPM8 activity: channel activity increased after disruption of lipid rafts with methyl-β -cyclodextrin (Morenilla-Palao et al., 2009). Therefore, the lipid membrane environment modulates the properties of TRPM8 channels.

TRPM8 is N-glycosylated in the pore loop, specifically on the Asn residue at position 934 (Fig. 3A). This post-translational modification, which consists on the covalent addition of a sugar moiety to an asparagine, plays an important role in the association of TRPM8 with lipid rafts (Morenilla-Palao et al. 2009). Non-glycosylated TRPM8 mutant (N934Q) displays marked functional biophysical differences compared with the wild-type channel, including a shift in the threshold of temperature activation and a reduced response to menthol and cold stimuli (Pertusa et al., 2012). Glycosylation facilitates efficient multimerization and transport to the plasma membrane, although is not essential (Erler et al., 2006).

1.3.5.3 Other modulatory mechanisms

Two products generated after activation of phospholipase A2, lysophospholipids (LPLs) and polyunsaturated fatty acids (PUFAs) has been shown to modulate TRPM8 channel activity *in vitro* (Vanden Abeele et al., 2006; Andersson et al., 2007; Bavencoffe et al., 2011) and *in vivo* (Gentry et al., 2010). LPLs act as positive modulators whereas PUFAs inhibit TRPM8 activity, corroborating the idea that the composition of the lipid bilayer have a significant role in TRPM8 modulation.

Pirt, a membrane protein expressed in the PNS, modulates TRPM8 by direct interaction with TRPM8, increasing the sensitivity of TRPM8 to cold and menthol (Tang et al., 2013).

Finally, recent studies point to a possible direct agonistic action of the steroid hormone testosterone on TRPM8 channels (Asuthkar et al., 2015a; Asuthkar et al., 2015b). Biochemical and functional results were supported by behavioral experiments in humans, which showed that acute applications of testosterone on the skin surface elicited a cooling sensation. This discovery can be considered the first, endogenous, physiological activator of TRPM8 channels and suggests a possible role of TRPM8 in diverse biological processes, including reproductive function in males. However, it is still unclear the link between testosterone, TRPM8 and in vivo thermoreception.

1.3.6 TRPM8 expression pattern

The expression pattern of TRPM8 in the PNS, where TRPM8 expression is more abundant and its function is best known, and in other tissues, has been examined with different techniques, as for example immunohistochemistry, in situ hybridization or using TRPM8 reporter mouse lines.

Due to the poor performance of specific antibodies against TRPM8, these reporter mouse lines, in which a fluorescence protein is expressed under the promoter of TRPM8, is one of the best methods to study TRPM8 expression and the distribution of labeled fibers (Takashima et al. 2007; Dhaka et al. 2008; Morenilla-Palao et al., 2014, Alcalde et al., 2018).

Within the PNS, TRPM8 expression is restricted to a specific subpopulation of sensory neurons distributed in the small- to medium-sized range (~18 µm of diameter). They represent about 15% and 10% of all the neurons in the trigeminal and dorsal root ganglia respectively (Mckemy et al., 2002; Peier et al., 2002; Takashima et al., 2007; Dhaka et al., 2008; Morenilla-Palao et al., 2014). The peripheral terminals of these neurons terminate as free nerve endings and innervate the skin, tongue, palate, teeth, cornea, colon and bladder (Takashima et al., 2007; Dhaka et al., 2008; Hayashi et al., 2009; Parra et al., 2010; Harrington et al., 2011; Alcalde et al., 2018). The central projections of TRPM8-positive afferents terminate in the superficial lamina I and the outer region of lamina II of the spinal cord dorsal horn where they synapse on second order neurons (Takashima et al., 2007; Dhaka et al., 2008). This is the typical projection pattern of Aδ and C primary afferent thermoreceptors and nociceptors (Light et al., 1979; Craig & Dostrovsky, 2001).

The neurochemical phenotype of TRPM8-expressing primary sensory neurons has been studied using different techniques (Mckemy et al., 2002; Peier et al., 2002; Takashima et al., 2007; Dhaka et al., 2008). The application of immunohistochemical techniques to transgenic TRPM8-reporter mice showed that TRPM8 is expressed in a heterogeneous subset of peripheral sensory neurons (Takashima et al., 2007; Dhaka et al., 2008). Approximately 20% of TRPM8-expressing neurons are immunoreactive for the intermediate filament NF200, a marker of neurons with myelinated axons while approximately 25% are reactive for peripherin, a marker for unmyelinated C-fibers. This data suggest that TRPM8 is expressed in lightly myelinated fibers and unmyelinated C-fibers. Unmyelinated C fibers can be broadly subdivided into two classes, peptidergic and non-peptidergic. TRPM8 expressing C-fibers are IB4-negative, a characteristic of peptidergic neurons (Peier et al., 2002; Takashima et al., 2007; Dhaka et al., 2008; Morenilla-Palao et al., 2014). TRPM8 neurons show variable expression of various nociceptive markers, including the calcitonin gene-related peptide (CGRP) and TRPV1 channels. About one-third of TRPM8-expressing somatosensory neurons are immunoreactive for CGRP (Takashima et al., 2007). Additionally, a large percentage of TRPM8-expressing neurons also co-express TRPV1 channels. According to Takashima et al. (2007), immunohistochemical results showed that approximately 40% of GFP-expressing neurons in TRPM8 reporter mice also express TRPV1 in trigeminal ganglia, being this co-localization lower in DRG (23.7%). Applying the same technique but on a different transgenic TRPM8 reporter mouse line, Dhaka et al. (2008) claimed that the co-expression of TRPM8 and TRPV1 in DRG was lower (12%) and that inflammation increases the number of TRPM8 neurons expressing TRPV1 (from 12% to 20%). We have to take into account that different studies, such as Takashima et al. (2007) and Dhaka et al. (2008), estimate TRPM8 expression by indirect signals such as GFP expression in transgenic mice generated by different genetic strategies which could explain the differences reported.

The co-expression of TRPV1 and TRPM8 is also obvious in functional studies from cultured sensory neurons which show that around half of the TRPM8-positive neurons co-express TRPV1, as indicated by their response to the TRPM8 agonist menthol and the TRPV1 agonist capsaicin (McKemy et al., 2002; Viana et al., 2002; Xing et al., 2006). However, the expression data derived from cultured neurons may not represent the true representation in intact tissues due to the possible inflammatory or injured state of axotomized neurons in culture.

More recently, different groups have approached the classification of primary sensory neuron subtypes by the use of more powerful strategies, such as for example single-cell RNA sequencing, which allow a more objective classification based on unique transcriptional profiles (Manteniotis et al., 2013; Usoskin et al., 2015; Flegel et al., 2015; Ray et al., 2018). This is the case of Usoskin et al. (2015) who performed RNA-seq on 799 single cells from the mouse lumbar DRGs, among them seventeen neurons showed TRPM8 expression (expression data is available at http://linnarssonlab.org). The data about the different neurochemical markers expression on these neurons bring a similar situation than in previous studies, with TRPM8 neurons being heterogeneous.

In summary, recent molecular data suggest that TRPM8 neurons are heterogeneous and represent at least two distinct functional classes; a group of neurons which do not express TRPV1, CGRP, or IB4, and would represent a non-nociceptive population (involved in innocuous cold-sensation) and another subpopulation that express TRPV1 or/and CGRP, which would represent putative nociceptive neurons (involved in noxious cold-sensation) (Takashima et al., 2007).

Besides the expression of TRPM8 in peripheral sensory neurons, a wider distribution of this channel has also been reported in non-neuronal tissues. Unfortunately, the low-expression of TRPM8 proteins and the lack of trustworthy antibodies makes TRPM8 detection difficult and hard to corroborate in some of these tissues. Despite this, TRPM8 expression has been found in the prostate and testis (Tsavaler et al., 2001), human sperm (De Blas et al., 2009), bladder and the urogenital tract (Stein et al., 2004), lungs (Sabnis et al., 2008), liver (Henshall et al., 2003), odontoblasts (El Karim et al., 2011), corneal endothelial cells (Mergler et al., 2013), salivary glands (Sobhan et al., 2013), vascular smooth muscle (Yang et al., 2006; Johnson et al., 2009), and in brown adipocytes of mice and white adipocytes in human (Ma et al., 2012; Rossato et al., 2014). TRPM8 has also been shown to be expressed in macrophages (Khalil et al., 2016) and in the central nervous system, specifically in the mouse hypothalamus (Kunert-Keil et al., 2006; Mittag et al., 2013; Wang et al., 2017). The physiological role of TRPM8 in tissues that are not exposed to large temperature fluctuations is not fully understood.

1.3.7 Functional characteristics of TRPM8-expressing neurons

Studies using electrophysiological techniques have shown characteristic functional properties of TRPM8-expressing neurons in culture. Cooling the bath solution produces a rapid depolarization of the membrane potential, leading to an initial tonic discharge (Fig. 6A) followed by a strong firing adaptation during sustained cold. In patch-clamp whole-cell recordings, cold-sensitive neurons

show low resting membrane potentials at 32-34 ºC (around -48 mV) and have low rheobase (40 pA, red trace in Fig. 6B) suggesting a high excitability (Viana et al., 2002). Cold-sensitive neurons fire action potentials of shorter duration than those observed in nociceptors (average spike duration= 1.1 ms) (red trace, Fig. 6B) (Viana et al., 2002). When hyperpolarizing pulses are applied in the current-clamp configuration, cold-sensitive neurons show a prominent rectification in response to hyperpolarizing pulses (sag) and rebound firing at the end of the pulse (black trace, Fig. 6B). The sag and the rebound firing is mainly due to expression of a prominent hyperpolarization-activated current (I_h), mainly carried by the hyperpolarization-activated and cyclic nucleotide-gated 1 channels (HCN1) (Viana et al., 2002; Orio et al. 2012). I_h has an important role in tuning the frequency of the spontaneous activity observed in cold-sensitive nerve terminals of the cornea (Orio et al., 2012).

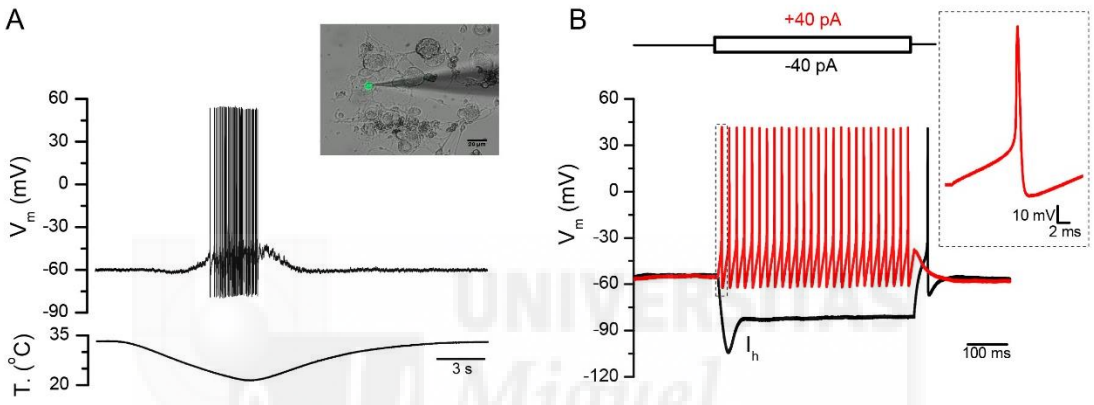

Figure 6. Electrophysiological properties of TRPM8-expressing sensory neurons. ***A,*** Patch-clamp whole-cell recording in the current-clamp configuration of a cultured DRG TRPM8-expressing neuron. Cold produced a rapid depolarization which leads to a tonic discharge of action potentials. Inset shows an image of the recorded neuron, superimposing images taken with transmitted light and GFP fluorescence. The DRG culture was obtained from a transgenic mouse which expresses GFP under the TRPM8 promoter. Note the small size of the recorded neuron compared with the rest of the neurons in the field. ***B,*** Patch-clamp recording in the current-clamp configuration from the same cell as in A during a protocol in which current pulses were injected. Responses to current steps of -40 pA and +40 pA are shown. Note the low rheobase (40 pA), the tonic firing of action potentials during the depolarizing stimuli, the prominent hyperpolarization-activated current (I_h) and the voltage rectification (sag), and the rebound firing after the negative pulse ends.

TRPM8 channels expressed in heterologous expression systems show a cold-activation threshold around 26-28 °C (McKemy et al., 2002). However, the temperature threshold for cold activation of TRPM8-expressing sensory neurons is distributed over a very wide range of temperatures, from 35 to 16 ºC (Madrid et al., 2006). Depending on the temperature threshold of activation, they are often divided into low-threshold and high threshold cold-sensitive neurons (Madrid et al., 2009). This observation led to an important question: how can TRPM8-expressing neurons operate over such a wide range of temperatures?

TRPM8 channels expressed at the sensory nerve terminal initiate the receptor potential upon cooling, driving the membrane potential to the threshold for action potential firing and initiating the transduction mechanism for cold temperatures. However, in the proces of thermotransduction, other ion channels participate, influencing the excitability of the neuron, the temperature threshold for firing and the propagation of the signal (Belmonte et al., 2009). Potassium channels are crucial regulators of neural excitability; because the reversal potential of potassium ions is negative to the resting membrane potential, the opening of potassium channels hyperpolarizes the neuron, acting as brakes (Hille, 2001). Indeed, it is known that the expression of different potassium channels, like shaker-like Kv1.1 channels, KCNQ channels and TASK-3, a two-pore domain leak K^+ channel, determine the excitability and the thermal threshold of activation of mammalian cold-sensitive neurons (Madrid et al., 2009; Vetter et al., 2013; Morenilla-Palao et al., 2014; Teichert et al., 2014; González et al., 2017; Memon et al.,2017). Pharmacological blockade or genetic depletion of these different K^+ channels lead to a very marked increase in the sensitivity of TRPM8-positive neurons to cold. Therefore, variable coexpression of TRPM8 with other ion channels adjusts the thermal sensitivity of individual thermoreceptors. In this line, Madrid et al. (2009) demonstrated that the variable thermal threshold of TRPM8-expressing cold-sensitive neurons is established by a balance between the expression of $K_v1.1$ subunits and TRPM8. Low threshold cold-sensitive neurons (LT-CS) express high levels of TRPM8 and low levels of functional $K_v1.1$ subunits, which results in a neuron that is excited by mild (i.e. innocuous) cold temperatures. The opposite situation occurs in high threshold cold-sensitive (HT-CS) neurons, with low expression of TRPM8 and higher expression of $K_v1.1$ subunits, requiring lower temperatures to reach firing (Fig. 7).

The study by Xing et al. (2006) also supports the idea of two different populations of TRPM8-expressing neurons, a subset of putative non-nociceptive neurons with high expression levels of TRPM8, expression of TTX-sensitive sodium channels and insensitivity to capsaicin, and a subset of nociceptive neurons expressing lower levels of TRPM8, expression of both TTX-sensitive and -insensitive voltage-gated sodium channels and showing capsaicin sensitivity. Again, as in the case of neurochemical markers, functional evidences suggest the separation of TRPM8-expressing neurons into two distinct subpopulations, a subpopulation (LT-CS neurons) which would detect temperatures in the psychophysical range of pleasant cooling and a subpopulation (HT-CS neurons) stimulated by intense cold, codifying a noxious signal and connected centrally with nociceptive pathways (Fig. 7).

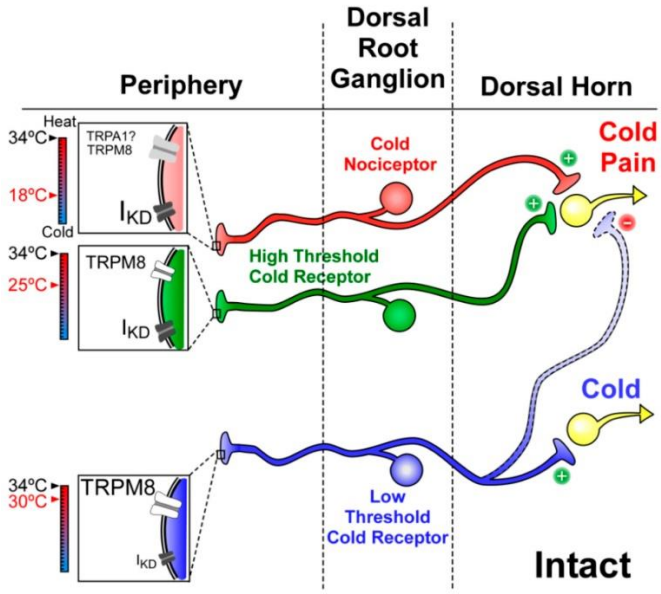

Figure 7. Hypothetical model of cold detection mechanisms in primary sensory neurons. Ion channels involved in the transduction of cold stimuli at the nerve terminal are represented in boxes. The size of labels reflects the relative density of these channels in the different subtypes of neurons. The different blend of ion channel expression determines the temperature range of activation of the different functional subtypes of peripheral sensory neurons. These neurons may have inhibitory (-) or excitatory (+) actions on higher-order neurons of central sensory pathways, leading to distinct cold sensations. The figure was extracted from Gonzalez et al., 2017.

1.3.8 Physiological role of TRPM8

The physiological role of TRPM8 has been inferred primarily from the characterization of transgenic mice lacking TRPM8 channels or following the selective ablation of TRPM8 expressing neurons. The results provide support for multiple physiological roles of TRPM8, which are introduced in the next pages.

1.3.8.1 Cold sensing

The best characterized physiological role of TRPM8 is the transduction of environmental cold temperatures (Fig. 8). From the fist studies of TRPM8, it was established that TRPM8 channels were activated by cold in primary sensory neurons in culture (Mckemy et al., 2002; Peier et al., 2002). A few years later, TRPM8 participation in cold transduction in peripheral nerve terminals in *ex vivo* preparations was also demonstrated (Madrid et al., 2006). However, it was in 2007 when three independent studies, using TRPM8-deficient mice, demonstrated that TRPM8 was the principal molecular entity responsible for innocuous cold detection by peripheral thermoreceptor neurons *in vivo* (Dhaka et al., 2007; Colburn et al., 2007; Bautista et al., 2007). Behavioral studies, using a two-temperature choice assay and surface temperature gradients, showed that, within the innocuous range of temperatures, TRPM8-deficient mice have a specific impairment in sensing cold temperatures, spending more time in cooler zones than wild-type

mice. TRPM8 deficient mice showed clear deficits in their ability to discriminate between cold and warm surfaces. Moreover, the robust behavior of icilin-induced wet-dog shakes was essentially eliminated in TRPM8-deficient mice.

In contrast to the clear deficit in sensing innocuous cold temperatures, the results of TRPM8 deletion were less clear in the noxious temperature range. For example, Dhaka et al. (2007) reported that when animals were placed on a -1 ºC cold plate, both genotypes (WT and TRPM8$^{-/-}$) showed identical nociceptive behaviors with similar latencies. Colburn et al. (2007) showed that when the cold plate was set at 0 ºC, TRPM8-deficient mice still showed noxious behavioral responses, although with higher latencies (5 s for WT and 15 s for TRPM8$^{-/-}$). Bautista et al. (2007) reported equivalent licking, flinching or shivering responses when TRPM8-deficient or wild-type mice were placed on a plate set to 10 ºC, 0 ºC or -5 ºC. Interestingly, they also reported the existence of a notable fraction of cold-sensitive neurons in TRPM8$^{-/-}$ cultured neurons: 45% in the study of Dhaka et al. (2007), 60% in the study of Colburn et al. (2007) and 18% in the study of Bautista et al. (2007), suggesting additional molecular and cellular mechanisms for cold detection. Additionally, other studies have also described cold-evoked responses in sensory neurons independent of TRPM8 channels (Babes et al., 2004, 2006; Munns et al., 2007; Winter et al., 2017).

A different experimental strategy to assess the role of TRPM8-expressing neurons in cold sensing is to ablate TRPM8-expressing neurons. In this approach, the entire population of TRPM8-expressing neurons is ablated, not just the TRPM8 protein like in the previous studies. Mishra et al. (2011) used a molecular genetic approach to generate mice lacking all neurons in the TRPV1 lineage. They observed that TRPV1 is an embryonic marker of many nociceptors, including TRPM8-expressing neurons and, therefore, the generated mice completely lack all TRPV1-expressing neurons and also all TRPM8-expressing neurons. The ablation of TRPM8-expressing neurons was accompanied by a total absence of behavioral reactions during exposure to a cold plate at -5 ºC, suggesting a total lack of cold-sensitivity even at damaging temperatures. Another study corroborated these results by ablating selectively the population of TRPM8-expressing neurons (Knowlton et al., 2013). These authors created a BAC transgenic mouse line in which expression of diphtheria toxin receptor (DTR), fusioned with GFP protein, was driven by the TRPM8 transcriptional promoter. By injection of diphtheria toxin, they were able to selectively ablate TRPM8-expressing neurons at a specific experimental time point. Behavioral tests, exploring the response of these mice to non-noxious cold (acetone test and two-temperature choice assay) confirmed the results of experiments with TRPM8$^{-/-}$ mice; they were impaired in the discrimination of cold temperatures. Importantly, mice depleted of TRPM8 neurons showed no defects in heat sensing or in mechanical responses, suggesting that TRPM8 expressing neurons represent a labeled line solely for cold sensation. However, the most interesting result emerged from the test in which discrimination of noxious temperatures was evaluated. They showed that ablation of TRPM8-expressing neurons leads to more profound deficits in noxious cold behaviors compared with animals in which the TRPM8 gene was rendered inactive embryonically. While TRPM8$^{-/-}$ mice showed robust cool avoidance and warm preference starting at 15 ºC (although

different from control animals), the TRPM8(+) neuron-ablated mice showed very poor capacity to discriminate between 30 ºC and 5 ºC, displaying more activity on the 5 °C surface than control and TRPM8$^{-/-}$ mice, indicating a reduced aversion to this noxious cold stimulus.

These studies indicate that TRPM8 constitutes the primary, if not the sole determinant of thermosensitivity in the cool range. The differences between TRPM8(+) neuron-ablated mice and TRPM8$^{-/-}$ mice suggest that TRPM8 participates in cold sensing in the noxious range of temperatures although other, TRPM8-independent, transduction mechanisms also contribute, supporting noxious-cold sensitivity in the absence of TRPM8 channels.

An important question arises from these data; which molecules or mechanisms could be participating in the residual cold response in TRPM8-null mice?

Before the discovery of TRPM8, different studies suggested that the closure of a background K^+ conductance and a differential ion-channel expression in a subset of cold-sensitive neurons were responsible for the selective excitation of these neurons during temperature reductions (Reid & Flonta 2001b; Viana et al., 2002). As mentioned before, the important role of different K^+ channels in setting the final thermal excitability of TRPM8-expressing cold-sensitive neurons is already well stablished (Madrid et al., 2009; Morenilla-Palao et al., 2014, González et al., 2017), but there is no evidence for a mechanism of cold-sensitivity based exclusively on K^+ channels modulation. However, it should be taking into account that temperature drops affects the excitability of different types of sensory neurons by affecting other types of ion channels like KCNQ2/3 or voltage-gated Na^+ channels (Zimmermann et al., 2007; Sarria et al., 2012; Kanda & Gu, 2017; Vetter et al., 2013).

Despite some conflicting data, TRPA1 channels remain candidates for temperature detection in the noxious cold range (for a review see Kwan & Corey, 2009; Zygmunt & Högestätt, 2014; Chen & Hackos, 2015). In the original description of the TRPA1 channel, Story et al. (2003) presented mouse TRPA1 as a cold-activated channel operating in the range of noxious temperatures (<17 ºC). They described a subset of primary sensory neurons which were cold-sensitive but menthol-insensitive (TRPA1-mediated cold responses) and also demonstrated the cold sensitivity of recombinant TRPA1 channels expressed in a heterologous expression system. The high temperature threshold for cold activation and the fact that these neurons also co-express TRPV1 channels and CGRP guided them to conclude that TRPA1 was expressed in some nociceptors and was responsible for noxious cold temperature sensation. Similar results supporting TRPA1 cold-sensitivity were reported in subsequent studies (Sawada et al., 2007; Fajardo et al. 2008; Karashima et al., 2009; Memon et al., 2017). In contrast, several other studies found that cold did not activate TRPA1 (Jordt et al., 2004; Cordero-Morales et al., 2011). In 2013, Chen et al. published a study in which they systematically analyzed the cold sensitivity of TRPA1 from four mammalian species: mouse, rat, rhesus monkey and human. They showed that cold temperatures activated TRPA1 of the two rodent species but not the two primate species. Interestingly, TRPA1 from several invertebrate and ancestral vertebrate species (for example, fly, mosquito, frog, lizard, and snake) are heat-sensitive instead of being cold-sensitive (Kwon et al.,

2008; Gracheva et al., 2010; Kang et al., 2012). According to these findings, there is a species-dependent divergence in temperature sensitivity of TRPA1 channels. More recently, human TRPA1 has been described as a U-shaped thermoreceptor, responding to bidirectional changes in temperature (cold and warm temperatures), which means that heat-sensitivity would be conserved in mammalian TRPA1 as well (Mopharti et al., 2016).

Behavioral studies using knockout mice were expected to settle the controversy surrounding TRPA1 participation in noxious cold detection. Deletion of TRPA1 demonstrated the functional importance of the TRPA1 protein in chemical nociceptive signaling (Bandell et al., 2004; Bautista et al., 2006; McNamara et al., 2007; Yonemitsu et al., 2013), and even in warm temperature detection (Vandewauw et al., 2018). In contrast, the findings regarding the role of this channel in cold thermotransduction *in vivo* have been less than definitive. Kwan et al. (2006) and Karashima et al. (2009) found that TRPA1-null mice presented deficits in noxious cold sensing, while other studies reported cold-sensitivity in TRPA1-null mice to be indistinguishable from wild-type mice (Bautista et al., 2006; Knowlton et al., 2010). Nevertheless, Fajardo et al. (2008) found that cold sensitivity is present in a large proportion of vagal mouse visceral sensory neurons and that TRPA1 channels are the major contributor to cold sensing in vagal afferent fibers, suggesting a role for visceral TRPA1 channels in non-noxious thermoregulatory reflexes. Thus, a possibility remains that tissue-specific posttranslational modifications or other factors influence the sensitivity of TRPA1 channels to temperature (Fajardo et al., 2008). These results suggest that cold sensing is mediated primarily by TRPM8 in somatic endings while TRPA1 would play a role in cold sensing in vagal visceral endings.

In other species, like for example birds, a mechanism has been described that confers cold-sensitivity to sensory neurons independently of TRPM8; this study showed cold-responses in menthol-insensitive sensory neurons which were mediated via Ca^{2+} release from intracellular stores (Yamamoto et al., 2016).

In summary, although TRPM8 is clearly the most critical molecular entity responsible for cold temperature sensing by peripheral sensory neurons, additional mechanisms have been shown to participate in concert with TRPM8. The molecular nature of some of these additional mechanism is still unclear.

1.3.8.2 Ocular physiology

The cornea is densely innervated by cold thermoreceptors (Gallar et al., 1993; Carr et al., 2003; Alcalde et al., 2018). TRPM8-expressing fibers are the principal sensors for cold temperatures in the corneal surface (Fig. 8) (Parra et al., 2010; Quallo et al., 2015; Kovács et al., 2016; Alcalde et al., 2018). Moreover, these TRPM8-expressing fibers appear to be involved in several important physiological processes in the eye.

Recordings of single nerve terminals innervating the cornea showed characteristic properties of cold thermoreceptors, including their typical ongoing activity at physiological temperatures and high sensitivity to small temperature variations (Gallar et al., 1993). Parra et al. (2010) reported

that TRPM8 knockout mice displayed a profound inhibition of ongoing and cold-evoked activity in corneal cold-sensitive fibers and a reduced basal tear flow, suggesting that the peripheral input at corneal cold-thermoreceptors controls the maintenance of the basal tear secretion. Supporting this hypothesis, different studies demonstrated that TRPM8 agonists increased tear production without evoking nociceptive responses, an effect that was abolished by TRPM8 antagonists or absent in TRPM8 knockout mice (Robbins et al., 2012; Chen et al., 2016).

The activity of corneal cold-thermoreceptors is also increased when the cornea is exposed to high osmolarity solutions or by drying the ocular surface, conditions that are accompanied by tear production (Hirata & Meng, 2010; Quallo et al., 2015). Application of hyperosmotic solutions to the eye surface increases the blink frequency in wild-type animals but not in TRPM8 knock-out mice (Quallo et al., 2015). Moreover, they demonstrated that the number of basal blinks was greatly reduced in TRPM8 knock-out mice, supporting the role of TRPM8 in controlling basal blinking rate, an important process for maintenance of ocular humidity.

Therefore, the data support a model in which corneal TRPM8-expressing cold-thermoreceptors sense tiny changes in temperature and osmolarity produced by the evaporation of the tear film during blinking intervals and increase their firing rate; this peripheral input from the corneal thermoreceptors governs the maintenance of proper ocular wetness by regulating basal tear flow and blinking (Belmonte & Gallar, 2011).

1.3.8.3 Temperature regulation and energy homeostasis

Detection and regulation of body temperature is a fundamental function in homeothermic animals, involving the activity of peripheral, visceral and central thermosensors (for review, see Morrison & Nakamura, 2011). In response to a decrease in external temperature, homoeothermic organisms have the capacity to activate heat-producing mechanisms (e.g. shivering) or heat-saving mechanisms (e.g. cutaneous vasoconstriction). One of the most immediate thermogenic responses to a cold environment is skeletal muscle shivering by which extra heat is produced from the metabolic activity. If cold is sustained, shivering thermogenesis will be replaced by non-shivering thermogenesis of brown adipose tissue (BAT), also referred to as adaptive thermogenesis as it develops over weeks. Other thermogenic behaviors involved in temperature homeostasis are locomotor activity and food intake (Señarís et al., 2018).

TRPM8 activity has been linked to different thermoregulatory processes. Experiments using TRPM8 agonists and antagonists demonstrated that the input from cold-sensitive cutaneous nerve endings affect thermoregulatory processes by triggering thermoregulatory autonomic responses such as behavioral heat-gain responses (i.e. tail-skin vasoconstriction or shivering-like muscle activity) and producing changes in core body temperature (Tajino et al., 2007; Knowlton et al., 2011; Almeida et al., 2012; Gavva et al., 2012). Recently, the influence of TRPM8 on rodent thermoregulation was studied in detail. By housing TRPM8-deficient mice and wild-type littermates at different ambient temperatures, Reimúndez and colleagues (2018) showed that the decrease in body temperature of TRPM8-deficient mice was dependent on ambient temperature,

being the differences higher at 17 °C than at 21 °C or 29 °C. Overall, TRPM8-deficient mice maintain core body temperature within an acceptable physiological range, with an average reduction of approximately 0.7-1.0 °C (Reimúndez et al., 2018). Another study showed that TRPM8 deletion or pharmacological inhibition had no effect on muscle shivering or in core temperature when mice were placed at 10 ºC (Feketa et al., 2013). The modest effect seen in these experiments demonstrate that, in the absence of TRPM8 channels, the core body temperature is maintained within an acceptable range (although less precise) and suggest the existence of TRPM8-independent mechanism participating in heat-generating thermoregulatory effectors.

However, TRPM8 has been shown to participate in other aspects of thermoregulation by regulating known autonomic thermoeffectors. When housed in mild cold conditions (21 °C), TRPM8-deficient mice showed long-term effects in energy homeostasis compared with WT mice, developing late-onset obesity with an altered glucose and lipid metabolism, consistent with daytime hyperphagia observed in these mice (Raimúndez et al., 2018). TRPM8-deficient mice also show defective vasoconstriction in skin blood vessels as a protective response against heat loss (Pan et al., 2018; Raimúndez et al., 2018).

1.3.8.4 Cooling and menthol mediated analgesia

Cold temperatures and menthol have been used as an analgesic since ancient times and still nowadays menthol is a common component of topical medicinal preparations for the relief of pain and itch (Finch & Drummond, 2015). Different studies have quantified the soothing effects of both, menthol and cold, on mechanical and thermal hyperalgesia induced by different models of chronic, chemical and inflammatory pain and revealed a TRPM8-mediated analgesic effect (Proudfoot et al., 2006; Dhaka et al., 2007; Knowlton et al., 2013; Liu et al., 2013). Two studies demonstrated that immersion of paws in water at 17-20 ºC for 5 minutes, or menthol and icilin application, produced significant mechanical analgesia in mice with chronic constriction injury (CCI) in the sciatic nerve (Proudfoot et al. 2006; Knowlton et al. 2013). Moreover, both studies performed parallel experiments in which TRPM8 channels were genetically knockdown and demonstrated that the analgesic effect of cold and TRPM8 agonists on mechanical hyperalgesia in the CCI model was exclusively mediated by TRPM8. Therefore, TRPM8 activation has an analgesic effect in a CCI model of neuropathic pain in mice.

Dhaka et al. (2007) showed that after intraplantar formalin injection, a model of acute pain, mice which were placed in the cold plate at 17 ºC showed less nociceptive responses that mice placed at 24 ºC, an effect which disappears in TRPM8-deficient mice.

A detailed study of the analgesic effect of menthol on mice was performed by Liu et al. (2013). They described that topical menthol almost doubled paw withdrawal latencies in a hot plate set at 55 ºC and that menthol strongly diminished mechanical hyperalgesia in chemical-induced (capsaicin, acrolein, and acetic acid) and inflammatory pain, induced by Complete Freund's Adjuvant (CFA) injection. Importantly, they reproduced the analgesic effect of menthol with the

more specific TRPM8 agonist WS-12 and demonstrated that menthol effect was abolished in TRPM8-deficient mice or in mice pre-treated with AMG2850, a specific TRPM8 inhibitor.

Cooling or mentholated topical formulations are also effective in relieving itch, an effect dependent on TRPM8 channels. Palkar et al. (2018) showed that intraplantar injection of different pruritogens evoked strong licking and biting behaviors on mice placed at 30 ºC, whereas when mice were placed in a cold-plate set at 20 ºC or 17 ºC those behaviors were significantly reduced. Using TRPM8-deficient mice, they observed that pruritogen-evoked behaviors were not attenuated at 20 °C, however, at 17 ºC the behaviors started to be reduced. Additionally, they also studied the behavior of TRPM8(+) neuron-ablated mice and observed a total absence of cooling effects.

All these data suggest that activation of TRPM8-expressing primary afferent fibers can inhibit nociceptive pathways, and account for the analgesic effects of menthol and cold. Actually, different studies have examined the analgesic effect of specific TRPM8 agonists in human patients and reported significant pain and itch relief, opening new therapeutics windows for the treatment of chronic pain and severe pruritus (Wang et al., 2017; Ständer et al., 2017).

However, the precise mechanism of TRPM8-induced analgesia is not well established. It has been proposed that it could be a result of changes in the central processing of nociceptive information (Belmonte et al., 2009). Cold-sensitive fibers could inhibit spinal nociceptive neurons centrally (Fig. 7-8), a similar concept to the most influential circuit model in the spinal cord, the "gate control theory", proposed by Melzack and Wall in 1965 (Melzack & Wall, 1965). It will be valuable to decipher the central mechanisms that cause this analgesia. For this purpose, spinal sensory circuits connected to TRPM8 afferents have to be interrogated.

1.3.8.5 Other physiological roles

As mentioned previously, TRPM8 expression has been confirmed in different non-neural tissues where its function has been examined although, in the majority of cases, its specific role still remains to be elucidated. For example, menthol infusions evoke contractions in the bladder, leading to decreased bladder capacity and voided volume, implicating TRPM8 in these reflexes (Nomoto et al., 2008; Jun et al., 2012; Ito et al., 2016). The presence of TRPM8 in the urogenital tract, prostate, testis, and human sperm are suggestive of a possible role in male fertility. TRPM8 has also been shown to be modulated by the steroid hormone testosterone, suggesting a role of TRPM8 in a wide range of physiological processes (Asuthkar et al., 2015). In colonic afferent neurons, the physiological role of TRPM8 fibers is unknown. However, the anti-nociceptive properties of TRPM8 agonists in different models of colonic pain such as colitis or irritable bowel syndrome suggest a transduction role (Harrington et al., 2011; Ramachandran et al., 2013).

1.3.9 Pathophysiological role of TRPM8

1.3.9.1 TRPM8 and cancer

TRPM8 was originally detected in human prostate cancer cells (Tsavaler et al., 2001) and nowadays it is well established that TRPM8 has an important role in cellular proliferation, survival and invasion of different human cancers (for a review see; Yee, 2015; Grolez & Gkika, 2016).

In prostate cancer, the expression of TRPM8 strongly increases and depends on the stage and androgen-sensitivity of the tumor (Zhang & Barritt, 2004; Gkika et al., 2010). TRPM8 is expressed in the endoplasmic reticulum and plasma membrane of different cell lines derived from prostate cancer tissues, forming functional Ca^{2+} channels that respond to well-characterized agonists of TRPM8 such as cold or menthol although with less sensitivity compared with other tissues (Zhang and Barrit 2004; Valero et al., 2011; Valero et al., 2012). The critical role of TRPM8 in proliferation was demonstrated by different studies which reported that pharmacological blockade and siRNA-mediated silencing of TRPM8 channels reduced the proliferation rates in the different prostate tumor cell lines tested (Valero et al., 2012; Liu et al., 2016). Similar results were shown in pancreatic adenocarcinoma cell lines (Yee et al., 2010).

Pathological analysis of human tissue samples has shown that over-expression of TRPM8 correlates with prostate tumor progression; therefore, by this variation in its expression, TRPM8 mRNA may be considered as a diagnostic/prognostic marker for metastatic prostate cancer detection in body fluids (Bai et al., 2010).

1.3.9.2 Migraine

Migraine is among the most common neurological diseases and one of the most disabling, the latter due mainly to poor treatment efficacy. The clinical symptoms of migraine include severe headache generally accompanied with nausea and/or light and sound sensitivity. A crucial step in migraine pathogenesis is the activation and sensitization of primary sensory afferent neurons in the trigeminovascular system (Strassman et al., 1996). Migraine is associated with a strong genetic component and TRPM8 has been identified in several genome-wide association studies (GWAS) as one of the migraine susceptibility genes in multiple cohorts (Chasman et al., 2011; Esserlind et al., 2013). There are additional data linking TRPM8 to migraine. Cold temperature is known to be a migraine trigger (Prince et al., 2004) and more than 50% of migraine patients exhibit cold allodynia (Burstein et al., 2000). In rats, activation of meningeal TRPM8-expressing fibers causes cutaneous facial and hindpaw allodynia (Burgos-Vega et al., 2016). Conversely, topical application of the TRPM8 agonist menthol offers pain relief in some migraine patients (Borhani Haghighi et al., 2010). Collectively, these studies suggest a potential (although contradictory) role of dural TRPM8 afferents in migraine pathogenesis. The presence of TRPM8-expressing mouse dural afferents has been studied, revealing a sparse and dynamic pattern of innervation (Huang et al., 2012; Ren et al., 2015; Kayama et al., 2018).

The effects of TRPM8 activation after dural application of inflammatory mediators (IM), a well-established preclinical model of headache, has also been studied. Menthol and icilin exert anti-nociceptive effects and reduce IM-induced pain behavior in adult mouse (Ren et al., 2015; Kayama et al., 2018). Kayama et al. (2018) also described that icilin effect was abolished by genetic ablation of TRPM8 and that meningeal inflammation upregulated TRPM8 transcriptional activity, increasing TRPM8/TRPV1 coexpression in TG neurons.

Taken together, the studies listed above strongly suggest a contribution of TRPM8 to the pathophysiology of migraine. A better understanding of the specific role of TRPM8 in migraine may lead to the development of new treatments and drugs based on modulation of TRPM8 activity, an important goal considering the actual lack of efficacious therapeutics for this highly prevalent disorder.

1.3.9.3 Role in cold hypersensitivity

The quality of sensations evoked by the cooling of the body surface is highly variable and ranges from freshness to unpleasant cold or overt pain. Much of the differences depend on the temperature of the stimulus. At temperatures below 15 ºC, the cooling sensations start to become painful, involving aching, burning or princking sensations (Davis, 1998). Perhaps, unpleasant sensations evoked by cold temperature arise from the recruiting of HT-CS neurons, which are connected with nociceptive pathways, producing changes in the perceptual quality of cold sensations established by the activity of LT-CS neurons (Madrid et al., 2009) (Fig. 6). Nonetheless, during different pathological conditions, normally innocuous cold stimuli are detected as painful (cold allodynia) and heightened sensitivity to painful cold stimuli (cold hypersensitivity) appear.

Cold allodynia is a prevalent symptom of neuropathic and inflammatory conditions induced by peripheral nerve damage. It is also a frequent symptom in patients treated with platinum-based anticancer drugs, a serious problem that compromises the patient's quality of life and limits dosage. Logically, TRPM8 is a candidate in mediating painful hypersensitivity to innocuous cold, althouhg the molecular and neural bases of this sensory alteration have not been entirely elucidated (Yin et al., 2015).

The role of TRPM8 in cold allodynia evoked by nerve injury and inflammation has been studied in experimental animals, using the CCI and the CFA models respectively, together with the analysis of TRPM8-deficient mice. With these tools, different groups have reported that TRPM8 channels are indispensable for the development of cold hypersensitivity in these two conditions (Colburn et al., 2007; Knowlton et al. 2011; Knowlton et al., 2013). The general strategy of these experiments was to measure the behavioral responses to acetone application on the hindpaw pre and post CCI or CFA injection in wild-type and in TRPM8-deficient mice. The acetone test is an evaporative cooling assay which consists on application to the hind paw of a small volume of acetone; the acetone quickly evaporates and cools the skin down to temperatures as low as 14-18 ºC (Choi et al., 1994; Vissers & Meert, 2005). Therefore, it is the ideal test to study cold

allodynia because it evokes temperatures near the boundary transition from innocuous cool to cold pain. These studies demonstrated that TRPM8-deficient mice in control conditions showed impaired responses to the acetone test compared with WT animals, as expected, and that CCI or CFA injection increased behavioral responses in wild-type but not in TRPM8-deficient mice, or in mice in which TRPM8 was pharmacologically blocked. These findings suggest that cold-sensitive neurons from CCI or CFA animal models became more sensitive to cold, probably by shifting their threshold to warmer temperatures. In this new situation, high-threshold cold-sensitive neurons which only respond to low noxious temperatures will respond to higher non-noxious temperatures, sending an erroneous painful message when exposed to innocuous temperatures.

Different molecular mechanisms have been proposed to explain the augmented cold sensitivity during these pathological conditions. Several studies support that increased TRPM8 channel expression in sensory neurons provides a mechanism for cold allodynia (Xing et al., 2007; Frederick et al., 2007; Gauchan et al., 2009; Su et al., 2011; Chukyo et al., 2018). However, other studies defend that the pathological increase in cold sensitivity is mediated by the remodeling of the expression levels of different ion channel (not TRPM8) responsible for *finetuning* the excitability of cold thermoreceptors (Descoeur et al., 2011; González et al., 2017; Ling et al., 2018). Descoeur et al. (2011) and González et al. (2017) demonstrated by calcium imaging experiments of cultured L3-L5 DRG neurons from oxaliplatin and CCI treated animals respectively that both, an increase in the proportion of cold-sensitive neurons and a decrease in their cold temperature threshold occurred. Descoeur et al. (2011) studied the expression profile of a set of ion channels in DRGs from oxaliplatin-treated mice and showed that TRPM8 levels were unchanged. In contrast, TRPA1 expression was upregulated. They also showed that the expression of a set of ion channels previously identified as important tuners of cold sensitivity (TREK1, TRAAK, $K_V1.1$, $Na_V1.8$, and HCN1) was misregulated. González et al. (2017) also demonstrated, with electrophysiological techniques, that the I_{KD} current, mediated by $K_v1.1$, was reduced in cold-sensitive neurons from CCI animals, causing a shift in their activation threshold towards warmer temperatures. In addition, TRPM8 current density in CCI animals was indistinguishable from the one observed in neurons from sham-operated animals, suggesting that TRPM8 expression levels were unchanged. These studies support that, mechanistically, oxaliplatin and CCI promote over-excitability by drastically lowering the expression of distinct potassium channels (TREK1, TRAAK, $K_v1.1$) and by increasing the expression of pro-excitatory channels such as the hyperpolarization-activated channels (HCNs), whereas TRPM8 expression remains unaltered.

Both theories, the increase in TRPM8 expression or the increase in excitability by the misregulation of other ion channels, seem to fit with the fact that TRPM8 is essential for the development of cold allodynia. If cold allodynia is due to an increase in TRPM8 expression levels in cold-sensitive neurons or *de novo* expression in nociceptors neurons, TRPM8 depletion by gene inactivation would obviously prevent cold allodynia. If it is due to a remodeling of ion channel expression, which led to an increase in excitation and a shift in the temperature threshold of activation, TRPM8 would be also necessary to start the transduction of cold temperatures. Further

studies are needed to clarify the mechanism of cold allodynia in the different pathological situations.

1.3.9.4 Dry eye disease

The role of TRPM8 in tear production is especially important in the context of dry eye disease (DED). DED is a very common ophthalmological disorder which affects 5-30% of the population (Lin & Polse, 2015; Yu et al., 2011). DED appears when the lacrimal glands are unable to produce enough tears to maintain a healthy coating on the corneal surface which allow proper lubrication and protection and is associated with uncomfortable sensations like sting, burn or itch (Marshall & Roach, 2016). The causes of DED are multiple, related to the dysfunction of lachrymal glands or the decrease of the reflex input from a reduced number of cold receptors (Fig. 8) (Kovacs et al., 2016). In fact, DED often develops with aging, in parallel with a reduction in the density of corneal cold thermoreceptors (Nebbioso et al., 2017; Alcalde et al., 2018). Therefore, TRPM8 agonists have been considered as a possible treatment for DED as they would increase the output of cold-sensitive fibers, a direct stimulator of tear secretion. Until recently, translation of these research findings to therapy of DED has not been clearly defined. However, in 2007 Yang et al. (2017) described a new water-soluble TRPM8 agonist called cryosim-3 (C3) and demonstrated its effectiveness in relieving dry eye related discomfort in human subjects suffering from DED. After a single application of C3 or daily application for 2 weeks, DED symptoms improved and basal tear secretion was increased. This study confirmed the effectiveness and the utility of TRPM8 agonists in the treatment of DED, opening a new therapeutic approach for its treatment.

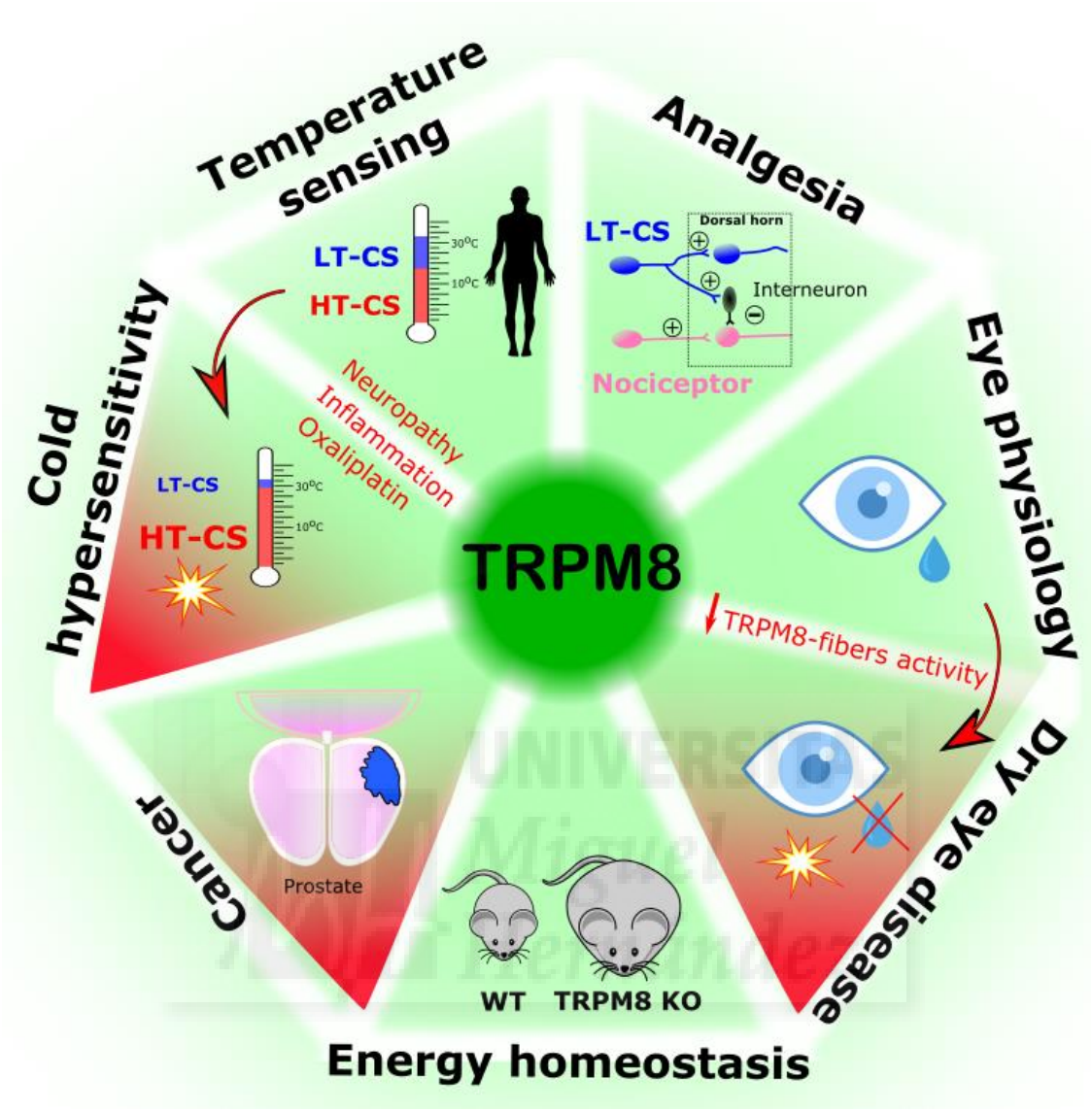

Figure 8. The diverse physiological roles of TRPM8 and its potential implication in different pathologies.

1.4 The immunosuppressant macrolides tacrolimus and rapamycin

Macrolide immunosuppressants are a class of natural compounds sharing a macrolide-like structure and potent immunosuppressive activity *in vitro* and *in vivo* (Fig. 8). Tacrolimus (TAC), also known as FK506, is a 23-member cyclic macrolide lactone and is one of the better characterized drugs in this group. Originally isolated from the bacteria *Streptomyces tsukubaensis,* TAC forms a complex with an immunophilin binding protein, the FK506-binding protein 12 (FKBP12), and this complex acts as a calcineurin inhibitor resulting in the block of T-cell activation and differentiation, and inhibiting the release of inflammatory cytokines (reviewed

by Rusnak & Mertz, 2000). TAC is widely used for the prevention of transplant/graft rejection, currently being the calcineurin inhibitor of choice for the prevention of rejection in renal transplantation. TAC has been shown to confer lower acute rejection rates and better renal allograft survival compared to cyclosporine, a molecule structurally unrelated to TAC but sharing similar inhibitory effects on the calcineurin pathway and similar immunosuppressant activity (Bowman & Brennan, 2008; Kamel et al., 2016). Other clinical applications of TAC include their topical use in several skin disorders, including atopic dermatitis, psoriasis and pruritus (Beck, 2005; Stull et al., 2016), and in ophthalmology for the treatment of various diseases, including Sjögren's syndrome, allergic conjunctivitis, and DED symptoms (Fukushima et al., 2014; Wan & Dimov, 2014). Topical application of TAC is often followed by sensory transient adverse sensations such as burning and itching at the beginning of treatment, being the most common side effect and the most common reason for premature discontinuation of the treatment (Reitamo et al., 2007). Related to these sensory effects, previous studies suggested possible direct effects of TAC on sensory nerve endings. Senba et al. (2004) showed that application of TAC raised intracellular Ca^{2+} levels in a subpopulation of small rat DRG neurons in culture (3.1%), and this population also responded to the application of capsaicin (89.5%). Ständer et al. (2007) described that topical application of pimecrolimus and tacrolimus is followed by an initial release of substance P and calcitonin gene-related peptide from primary afferent nerve fibers in murine skin.

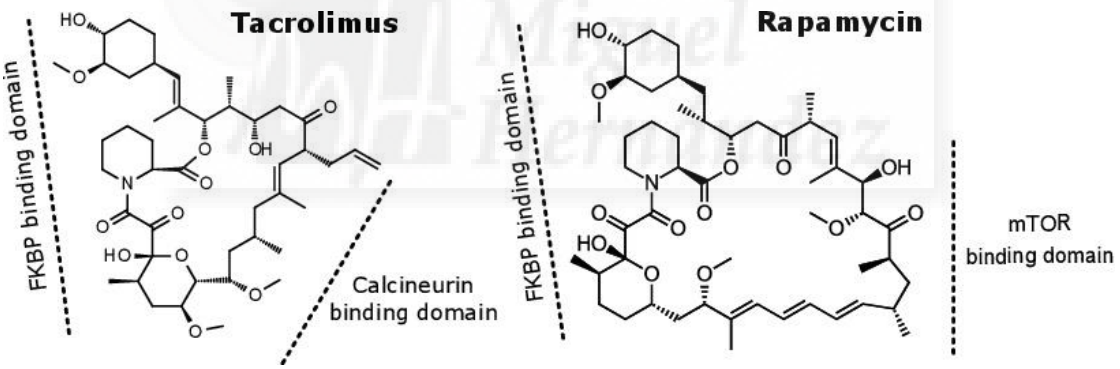

Figure 9. Molecular structure of Tacrolimus and Rapamycin. Both molecules share a common binding site for immunophilins (FKBP). After binding to FKBP protein tacrolimus inhibits calcineurin, a calcium dependent serine/threonine protein phosphatase. In contrast, the complex FKBP-rapamycin inhibits mTOR kinase.

Another study postulated the activation and subsequent desensitization of TRPV1 channels by TAC, however, no direct evidence were provided for an agonistic effect of TAC on TRPV1 channels (Pereira et al., 2010). Therefore, the mechanisms involved in TAC effectiveness in the treatment of cutaneous disorders and in DED, the sensory secondary symptoms after topical application and its molecular targets in these tissues are presently unclear.

Rapamycin, also called Sirolimus, is another natural macrolide originally isolated in 1972 from the bacterium *Streptomyces hygroscopicus* in Easter Island (also known as Rapa Nui). At first

identified as an antifungal, it was later shown to have immunosuppressive properties. Nowadays it has important clinical applications, including its use as immunosuppressant to prevent organ rejection. Since their discovery, rapamycin and derivatives have gained importance as an investigative tool and for the treatment of different disorders. Everolimus, a derivative of rapamycin, was approved by the FDA in 2011 for the treatment of different tumors. More recently, the discovery that rapamycin can extend the lifespan in numerous species (e.g. yeast, flies, mice) and improve age-related functional decline has generated great excitement in the field of aging biology (Cox & Mattison, 2009; Wilkinson et al., 2012; Bitto et al., 2016). Indeed, this is one of the first examples of a clinically approved drug capable of slowing the aging process in mammals. As in the case of TAC, rapamycin binds to the immunophilin FKBP12 to form a complex. Unlike TAC, which is a calcineurin inhibitor, the rapamycin-FKBP12 complex inhibits the mammalian target of rapamycin (mTOR) by directly binding to mTOR complex 1 (mTORC1), inhibiting its downstream signaling (Heitman et al., 1991). mTOR is a signal integrator, responding to multiple signals including growth factors, nutrients, energy and oxygen status to control processes that are required for cell growth and proliferation, including mRNA biogenesis, protein, lipid and nucleotide synthesis, energy metabolism and autophagy (Sabatini, 2017). Increased activation of mTOR is observed in numerous human cancers, which could be related with the antitumor activity of rapamycin.

Therefore, both TAC and rapamycin act through the binding to the immunophilin FKBP12, sharing a common binding structure to this immunophilin (Fig. 9). Immunophilins are protein chaperones with peptidyl-prolyl isomerase (PPIase) activity which catalyze the interconversion between the *cis* and *trans* isomers of peptide bonds containing the amino acid proline (Kang et al., 2008). They have been extensively studied as receptors for immunosuppressive drugs, however, the cellular role of this enzymatic function has not been clearly defined. Immunophilins are widely expressed and present at high levels in some tissues, as for example in the nervous system (Kang et al., 2008), where the endogenous cellular functions of PPIases and their substrates remain elusive. However, some studies have revealed a defined cellular role for immunophilins. For example, immunophilins have been shown to interact with different ion channels, modulating their biophysical properties. Specifically, FKBP12 was shown to physically interact with different types of calcium release channels like the ryanodine receptor (RyR) or the inositol 1,4,5-trisphosphate receptor (InsP3R) (Brillantes et al., 1994).

Immunophilins have also been shown to interact with different members of the TRP family. Goel et al. (2001) demonstrated that the *Drosophila* immunophilin dFKBP59 physically interacts with TRPL channels, which are involved in the phototransduction signaling cascade in flies. They showed that this interaction is specific, reversible, of high affinity and attenuated by TAC in a temperature-dependent manner. Remarkably, when TRPL channels and dFKBP59 were co-expressed in insect cells (Sf9), dFKBP59 produces an inhibition of Ca^{2+} influx via TRPL in calcium imaging assays. Additionally, mutagenesis studies suggest that the site of interaction of dFKBP59 on TRPL is a unique, highly conserved proline-rich region present in the COOH-terminal domain of TRPL. Moreover, FKBP12 and FKBP52 have been also shown to modulate TRPC1 channels

(Shim et al., 2009). TRPC1 co-immunoprecipitates with native FKBP52 in HEK293 cells, and when coexpressed in HEKs cells, both FKBP12 and FKBP52 significantly increase TRPC1 mediated currents. Point mutations of TRPC1 in the TRP box, including TRPC1-P645L, P646L, and F648R residues, disrupted the co-IP of TRPC1 with FKBP52. The dependence of binding upon P645 is consistent with the consensus binding site for the FKBP family PPIases that typically includes a hydrophobic amino acid (L644) followed by a proline (Schiene-Fischer & Yu, 2001).

In the somatosensory system, it has been reported that FKBP51, a different immunophilin, is crucial for the full development and maintenance of long-term pain states (Maiarù et al., 2016) and its silencing alleviates the mechanical pain threshold, inhibits DRG inflammatory factors and pain mediators through the NF-kappaB signaling pathway in a rat model of CCI (Yu et al., 2017). Also, inhibition of mTORC1 signaling pathway reduces itch behavior in mice (Obara et al., 2015).

UNIVERSITAS
Miguel
Hernández

2. Objectives

UNIVERSITAS
Miguel
Hernández

The objectives of this thesis are:

- To characterize the agonistic effect and the mechanism of action of the immunosupresant macrolides tacrolimus and rapamycin on recombinant TRPM8 channels and on primary sensory neurons.
- Study the GqPCR-mediated modulation of TRPM8 channels and identify the mechanism/s involved in this process.

UNIVERSITAS
Miguel
Hernández

3. Materials and methods

UNIVERSITAS
Miguel
Hernández

In the next section, I will describe the techniques used during this study. Mainly, I employed the patch-clamp and calcium imaging techniques in order to study the activity and the modulation of TRPM8 channels. Recordings were performed on heterologous expression systems transiently expressing different proteins of interest (ion channels, GqPCRs, imaging tools, etc) and on adult mice DRG sensory neurons in culture.

3.1 Animals

Adult mice (1-4 months) of either sex were used for DRG sensory neuron cultures and for behavioral experiments. Mice were kept in a barrier facility under 12/12 hours light dark cycle. The genotype of transgenic mice was established by PCR. All experimental procedures were performed according to the Spanish Royal Decree 1201/2005 and the European Community Council directive 2010/63/EU, regulating the use of animals in research.

Two transgenic mouse lines were used for calcium imaging experiments and electrophysiological recordings of DRG neuronal cultures. The TRPM8^{BAC}-EYFP transgenic line was generated previously in our laboratory (Morenilla-Palao et al., 2014) by Bacterial Artificial Chromosome (BAC) transgenesis to genetically label neurons expressing TRPM8. The modified BAC contained the EYFP coding sequence under the direction of regulatory elements from mouse TRPM8 and, therefore, EYFP expression occurs on those neurons in which endogenous TRPM8 is expressed. For the experiments with TRPM8-KO, I used a transgenic knockin line, TRPM8^{EGFPf} (Dhaka et al., 2007). Briefly, amino acid residues 2–29 following start codon of TRPM8 were disrupted by generating homologous recombination in embryonic stem cells using a BAC-based targeting approach and a farnesilated enhanced green fluorescent protein (EGFPf) was inserted in frame with the TRPM8 start codon. From this transgenic mice line, hemizygous (TRPM8$^{EGFPf/+}$) mice express EGFPf and one functional copy of TRPM8 and homozygous (TRPM8$^{EGFPf/EGFPf}$) mice totally lack TRPM8 expression. Both transgenic lines allowed us to identify TRPM8 expressing cells by EYFP or EGFPf fluorescence (TRPM8^{BAC}-EYFP and TRPM8$^{EGFPf/+}$) and the identification of putative TRPM8-expressing neurons in the TRPM8-null mice (TRPM8$^{EGFPf/EGFPf}$). As previously described, to enhance EGFPf expression the lox-P-flanked neomycin selection cassette introduced into the Trpm8 locus during the generation of the transgene was excised (Dhaka et al., 2008).

3.2 Culture and transfection of HEK293 cells

I used Human Embryonic Kidney 293 cells (HEK293) as a heterologous expression system, which constitute a powerful tool for the study of our protein of interest almost in isolation, allowing the investigation of its functional properties and regulation. HEK293 cells were derived in 1973 from the kidney of an aborted human embryo and have been used widely in cell biology and biotechnology because of their reliable growth and propensity for transfection (Russell et al., 1977).

HEK293 cells (ECACC, Salisbury, UK) were maintained in Dulbecco's Modified Eagle Medium (DMEM)+Glutamax (Thermo Fisher Scientific) plus 10% fetal bovine serum and 1% penicillin/streptomycin, incubated at 37 ºC in 5% CO_2 atmosphere. Cell passage number was monitored, limiting the use up to passage number 30, when a new batch of cells was thawed with low passage number. Once per month, cells were tested for the lack of mycoplasma infection.

Transient transfection is a technique commonly used to introduce foreign nucleic acids into cells (Kim & Eberwine, 2010). Among the different transfection methods, I used lipofection, which consist in the delivery of the nucleic acids into the cells by lipidic vesicles which merge with the cell membrane. I introduced mammalian expression cDNA vectors encoding the different proteins of interest (see table 3). Once in the cell, these expression vectors drive the expression of the inserted sequence without integration into the genome of the host cells (plasmids). The protocol of transient transfection consisted of the following steps:

HEK293 cells were plated in 24-well dishes at $2x10^5$ cells/well, and transiently transfected with Lipofectamine 2000 (Thermo Fisher Scientific). Depending on the experiments I (co)transfected 1, 2 or 3 plasmids simultaneously, maintaining the total amount of cDNA at 1.5 µg. GFP (0.3 µg) was cotransfected with those plasmids which do not include a fluorescence protein for posterior identification of successfully transfected cells. For the transfection, 2 µl of Lipofectamine 2000 were mixed with the DNA in 100 µl of OptiMem (Thermo Fisher Scientific), a reduced serum media, incubated for 20 minutes and added to the well. After 4-6 hours, the medium was replaced with fresh complete medium. Electrophysiological and calcium imaging recordings took place 24 hours after transfection. The evening before the experiment, cells were trypsinized (0.25% trypsin-EGTA) and reseeded at lower density in 12 mm diameter glass coverslips (Thermo Scientific) previously treated with poly-L lysine 0.01% (Sigma).

I also used a HEK293 cell line stably expressing rat TRPM8 channels (CR#1 cells) (Brauchi et al., 2004). Originally, a genomic vector with an antibiotic resistance gene for selection was transfected and integrated into the host genome of HEK293 cells. CR#1 cells were cultured in DMEM containing 10% of fetal bovine serum, 1% penicillin/ streptomycin, and 450 µg/ml geneticin (G418) for the selection of cells.

Plasmid	Vector	Plasmid	Vector
mTRPM8*	pcDNA5	**mTRPM3-myc**	pIRES2-GFP
mTRPM8-myc**	pcDNA3.1/myc	**hKv7.2 (KCNQ2)**	pcDNA3
mTRPM8-Y745H	pcDNA5	**hKv7.3-YFP (KCNQ3)**	pcDNA3
mTRPM8-N799A	pcDNA5	**mKir1.2**	pcDNA1-GFP
mTRPM8-P1012Q	pcDNA5	**hM1R**	pIRES2
hTRPM8	pcDNA3.1	**hH1R**	pcDNA3.1
cTRPM8	pcDNA3.1	**mMelanopsin**	pcDNA3.1
hTRPA1	pCMV6-AC-GFP	**Dr-VSP**	pIRES2-GFP
hTRPC3-GFP	pcDNA3	**PH-GFP**	pEGFP-C1
rTRPV1	pcDNA3	**GFP**	pGREEN LANTERN

Table 3. List of plasmids transiently transfected in HEK293 cells. The letter at the beginning of the construct indicates de species (m, mouse; r, rat; h, human; c, chicken). *mTRPM8 in pcDNA5 was used for experiments involving the study of immunosuppressant agonism. **mTRPM8-myc was used in experiments studying the effect of GqPCR activation.

3.3 Point mutagenesis

Single point mutations were obtained by site-directed mutagenesis from WT mouse TRPM8 in pcDNA5 and confirmed by whole sequencing of the plasmids and posterior analysis with DNAStar LaserGene software. Briefly, primers incorporating the mutation were designed and a PCR using the PfuTurbo DNA polymerase (Stratagene) was performed with the full-length cDNA encoding mouse TRPM8. The menthol-insensitive mutant (Y745H) and an icilin-insensitive mutant (N799A) were previously generated in our laboratory (Mälkiä et al., 2009). The following primers were used for the generation of the mutants:

TRPM8-L1009R; (for) 5´-AGTACTGCAACCGCCGAAACATCCCCTTCCC-3´; (rev) 5´-GGGAAGGGGATGTTTCGGCGGTTGCAGTACT-3´.

TRPM8-P1012Q; (for) 5´-GCAACCGCCTAAACATCCAGTTCCCCTTCGTTGTCTTC-3´; (rev) 5´-GAAGACAACGAAGGGGAACTGGATGTTTAGGCGGTTGC-3´.

3.4 Dorsal root ganglia primary sensory neurons culture

To study peripheral sensory neurons, I used primary cultures of DRG from adult mice, which were first isolated, enzymatically digested and mechanically dissociated in order to obtain a cell suspension of sensory neurons and a mix of non-neuronal cells that were plated on glass

coverslips. After plating them, DRG neurons show round- or ovoid-shaped soma and start to develop processes after a few hours in culture. The soma of cultured sensory neurons has been used widely for the study of mechanisms involved in stimulus transduction due to the difficulty of studying those mechanisms in the terminal end because of their small size (<1 µm) (Heppelmann et al., 2001; Alcalde et al., 2018). The use of the cell body as a model is based on the assumption that membrane ion channels of peripheral endings are also present in the soma. However, we have to take into account that with this technique we are applying the stimuli to the soma of neurons and therefore, we are in a different experimental situation than in the *in vivo* system, where the stimuli arrived to sensory nerve terminals.

The protocol for the DRG culture consisted of the following steps:

Adult animals of either sex (1-4 months) were anesthetized with isoflurane and decapitated. The spinal cord was isolated and the DRGs were dissected out from all spinal segments using a stereo microscope and maintained in ice-cold Hank's Balanced Salt Solution (HBSS) during the isolation. After isolation, DRG were cleaned of spinal nerves and roots and were incubated with collagenase type XI (1800 U/ml, Sigma) and dispase II (5 U/ml, GIBCO) for 30-45 min in Ca^{2+}- and Mg^{2+}-free HBSS at 37 ºC in 5% CO_2 atmosphere. Thereafter, DRG ganglia were mechanically dissociated by passing the suspension 15-20 times through a 1 ml pipette tip and filtered through a 70 µm nylon cell strainer (Falcon). Neurons were harvested by centrifugation at 1200 rpm during 5 minutes. The resultant pellet was resuspended in Minimum Essential Medium (MEM) supplemented with 10% FBS, 1% MEM-vit (Thermo Fisher Scientific) and 1% penicillin/ streptomycin. The same medium was used to maintain the neuronal culture. Neurons were plated on poly-L-lysine 0.01% (Sigma) treated glass coverslips (Thermo Scientific). No growth factors were added to the culture medium. Electrophysiological and calcium imaging recordings were performed after 12-36 hours in culture.

3.5 Fluorescence calcium imaging

The calcium imaging technique is based on the use of fluorescence calcium indicators to monitor the dynamics of intracellular calcium levels inside cells. I used the calcium indicator Fura-2 AM (Invitrogen), a membrane permeant probe that diffuses into the cells during incubation. Once inside the cell, esterases remove the acetoxymethyl ester (AM) group allowing the Fura-2 to be trapped inside the cell. Fura-2 is a fluorescence molecule which changes its excitation peak upon binding to calcium (Grynkiewicz et al., 1985). Unbound Fura-2 has an excitation peak at 362 nm, which shifts to 335 nm upon binding of calcium while the emission spectrum of the bound and unbound forms remains constant. Therefore, by exciting the probe at two different wavelengths (340 nm and 380 nm) one can obtain a ratio between the intensity of fluorescence emitted at these two wavelengths (F340/380), which is directly proportional to the concentration of free intracellular calcium.

The basic set-up to perform calcium imaging experiments includes a camera attached to a microscope and a regulated, properly filtered, light source to excite the fluorescent calcium

indicator. During this work, two different cameras and two different light sources were used, forced by the mandatory replacement of some equipment parts due to technical reasons. Fluorescence measurements were made with a Leica DMIRES-2 upright microscope equipped with a 20x objective (Leica HI Plan 20x/0.30na Ph1, working distance 2.4mm) and fitted with an Imago-QE Sensicam camera (PCO) or with a Retiga R3 CCD Camera (Qimaging). Fura-2 was excited at 340 and 380 nm with a rapid switching monochromator (TILL Photonics) or with a LED light source Lambda 421 (Sutter instruments). Mean fluorescence intensity ratios (F340/F380) were displayed online with TillVision software (TILL Photonics) or Metafluor software (Molecular Devices). Images were acquired at intervals of 2-3 seconds.

For calcium imaging experiments a physiological extracellular solution based on NaCl was used, from here on referred to as control solution (Table 4). Before each experiment, DRG neurons or HEK293 cells were incubated with 5 µM Fura-2 AM and 0.02% Pluronic for 45 min at 37 ºC in control solution and then transferred to the microscope chamber. Before starting the timed acquisition, images with transmitted light illumination and with 460 nm excitation wavelength were taken in order to posteriorly identify EYPF/EGFPf fluorescence cells. Thereafter, the acquisition of fluorescence images started and the different stimuli/drugs were applied.

3.6 Electrophysiological patch clamp recordings in cultured cells

The patch-clamp technique was developed by Neher and Sakmann in the late 1970s (Neher & Sakmann, 1976; Neher et al., 1978; Hamill et al., 1981) and is recognized as a critical development for the study of ion channels in excitable and non-excitable cells, providing a method to perform high-resolution electrophysiological recordings from cell-free membrane patches as well as whole-cell recordings. During this study, the patch-clamp technique was used in different configurations (e.g. whole-cell voltage- and current-clamp, cell-attached and inside-out modes). For current measurements, a glass micropipette (borosilicate glass patch-pipettes, Sutter Instruments) filled with a solution resembling the ionic conditions of the cytosol (Table 5) and connected to an Axopatch 200B patch-clamp amplifier (Molecular Devices) was used. These micropipettes had a small diameter, correlated with a higher electrical resistance, which was measured once in the bath by applying a square pulse of current. We used pipettes with resistance around 3-8 MΩ. The pipette was brought into contact with the cell membrane and, spontaneously or by applying negative pressure, a seal of high resistance (<1 GΩ) was formed between the pipette and the membrane. At this point we would be in the so called cell-attached configuration, in which extracellular recordings of the action potential currents of the neurons were obtained. The cell-attached configuration is the precursor to all other variants of the patch-clamp technique. The whole-cell configuration was attained by breaking the membrane patch at the tip of the pipette by application of a pulse of suction (i.e. negative pressure) through the patch pipette. After this maneuver, we have access to the intracellular environment of the cell and large transient capacitative currents appear during the square current pulse, due to the membrane electrical

properties that behaves as a capacitator in parallel with a resistor. These capacitative transients were electronically compensated by manually setting the whole cell capacitance and series resistance adjustments of the amplifier until the transient was minimized. From the capacitative current compensation readout we obtained an estimate of the whole-cell capacitance, indicative of the plasma membrane surface area, which allowed us to normalize the current amplitude to the area of the membrane (i.e. current density). By withdrawing the pipette from the cells during the cell-attached configuration, we obtained a patch of the membrane detached from the rest of the cell, resulting in the inside-out configuration, whit the internal side of the membrane facing the bath solution.

Currents and voltages were amplified and digitized with a Digidata 1322A AD converter (Molecular Devices). Stimulus delivery and data acquisition were performed using pCLAMP9 software (Molecular Devices). Voltage clamp (VC) recordings, in which the membrane voltage is controlled by current injection through the pipette, were performed on DRG neurons and on transiently transfected HEK293 cells. For VC recordings the amplifier gain was set at x1, acquisition rate was set to 10 KHz and the signal was filtered at 2 KHz (lowpass 4-pole Bessel filter). After the whole-cell configuration was stablished, cells were voltage-clamped at a potential of -60 mV and different voltage protocols were applied (explained in the text). Additionally, current-clamp (IC) recordings, in which membrane voltage is measured, were performed on DRG neurons. For IC recordings the amplifier gain was set at x10, the signal was filtered at 10 KHz and the acquisition rate was increased to 50 KHz in order to adequately sample a fast waveform such as an action potential and to avoid aliasing effects. In neurons that fired action potentials at rest, a small DC current was injected to bring the membrane potential to around -55 mV.

Recordings on DRG neurons were performed at a basal temperature of 32-34 ºC in the standard control solution (Table 4). To avoid high intracellular chloride concentrations, a K-gluconate based intracellular solution (Table 5) was used.

Electrophysiological recordings on HEK293 cells were performed at a temperature between 32 and 34 ºC, or between 22 and 24 ºC (specified in the text). Two different extracellular solutions were used for recordings in HEK293 cells. In experiments studying the agonistic effect of macrolide immunosuppressant, to avoid desensitization of the channel during consecutive application of different agonist, I used a calcium free extracellular solution (Table 4). In experiments studying the modulation of TRPM8 channels by GqPCRs I used the standard control solution because calcium has an important role in the signaling pathways studied (Table 4). Different intracellular solutions were used for HEK293 cells recordings, depending on the expressed channel (Table 5). For recordings on HEK293 cells expressing TRPM8, a CsCl based intracellular solution was used (Table 5). Cesium was used, instead of potassium as a major cation, because it blocks potassium currents flowing through endogenous K^+ channels expressed in HEK293. For recordings on HEK293 cells expressing K^+ channels (KCNQ2/3 and Kir2.1) a KCl based solution was used (Table 5).

For inside-out recordings, a simplified pipette solution was used (in mM): 150 NaCl, 1 Mg_2Cl, 10 HEPES and as bath solution 150 NaCl, 5 $MgCl_2$, 5 EGTA, 10 HEPES. The recording started once the gigaseal was obtained and the pipette was removed from the cell. The protocol consisted of a 100 ms pulse from 0 mV to +120 mV. Current values were measured at the end of the voltage pulse (5 ms). Ligands were included in the flowing bath solution.

Extracellular solutions			
Control solution		**Ca^{2+}-free solution**	
Compound	Concentration (mM)	Compound	Concentration (mM)
NaCl	140	NaCl	144.8
KCl*	3	KCl	3
$CaCl_2$	2.4	$MgCl_2$	1.3
$MgCl_2$	1.3	Glucose	10
Glucose	10	HEPES	10
HEPES	10	EGTA	1
pH= 7.4 adjusted with NaOH Osmolarity= 290-300 mOsm/L			

Table 4. Extracellular solutions used for calcium imaging and electrophysiological recordings.
*Increased to 10 mM for Kir2.1 channel recordings.

Intracellular solutions					
Neurons		**TRPM8 channels**		**K^+ channels**	
Compound	Concentration (mM)	Compound	Concentration (mM)	Compound	Concentration (mM)
K-gluconate	115	CsCl	135	KCl	140
KCl	25	$MgCl_2$	2	$MgCl_2$	0.6
NaCl	9	HEPES	10	HEPES	10
$MgCl_2$	1	EGTA	1	EGTA	1
EGTA	0.2	Na_2-ATP	5	Na_2-ATP	5
HEPES	10	Na-GTP	0.1	Na-GTP	0.1
K_2-ATP	3				
Na-GTP	1				
pH= 7.3 adjusted with NaOH Osmolarity= 284 mOsm/L		pH= 7.3 adjusted with CsOH Osmolarity= 282 mOsm/L		pH= 7.3 adjusted with KOH Osmolarity= 286 mOsm/L	

Table 5. Intracellular solutions used for electrophysiological recordings.

3.7 Perfusion system, temperature stimulation and light stimulation

Coverslip pieces with cultured cells were placed inside the microscope chamber (2 x 1.5 cm) and continuously perfused by a gravity fed perfusion system with solutions warmed at 32–34 ºC (except when indicated in the text). Six independent lines were connected to the chamber by a perfusion manifold (Warner Instruments) which allowed rapid solution changes. The volume of solution in the chamber was approximately 0.5 ml and the perfusion flow was around 0.8-1 ml/min,

obtaining a complete solution exchange in the camera in about 30 seconds. The inlet tube of the perfusion was placed slightly above the cells.

The temperature of the solution was adjusted with a Peltier device (CoolSolutions, Cork, Ireland) placed at the inlet of the chamber, and controlled by a feedback device. Cold sensitivity was investigated with a temperature drop to approximately 18°C (rate of change ~ -1.2 ºC/s). During calcium imaging experiments and patch-clamp recordings bath temperature was recorded simultaneously with an IT-18 T-thermocouple connected to a Physitemp BAT-12 micro- probe thermometer (Physitemp Instruments) and digitized with an Axon Digidata 1322A converter running pCLAMP9 software (Molecular Devices).

To activate melanopsin, a fiber-coupled LED light source of 460 nm connected to a BLCC-04 controller was used (Prizmatix, Israel). The controller was under the control of pCLAMP9 software. The fiber optic (1 mm diameter, NA 0.63, 2 mm protrusion) was placed above the cells. The light intensity was 140 mW/cm^2 measured with a light power meter model 843-R mounted with a 818-ST2 detector (Newport).

3.8 Confocal imaging of PH-GFP

Confocal images of HEK293 cells expressing PH-GFP were obtained with a Leica TCS SP2 RS confocal system mounted on a Leica DM LFSA upright microscope and equipped with a 63x water immersion objective (HCX APO L U-V-I 63x/W NA 0.9, working distance 2.2 mm). A 488 nm argon laser (Lasos, Germany) was used to excite the cells and images were obtained every 5 seconds and displayed using Leica confocal software. The fluorescence changes of a small cytosol region were measured and represented over time (PH-GFP F_{cyto}) and the baseline subtracted fluorescence values of this region were used to measure the translocation of PH-GFP (Δ PH-GFP F_{cyto}). A petri dish (35 mm diameter) was used as the microscope chamber and a similar perfusion system to this described previously was used. Vacuum suction was used to maintain a constant volume in the chamber.

3.9 Behavioral assessment of blinking

Adult male C57BL/6J or TRPM8$^{EGFPf/EGFPf}$ (Dhaka et al., 2008) mice were lightly restrained and 5 µl of either saline, vehicle (8% ethanol, 2% Cremophor in saline), TAC (1%) or a hyperosmolar (785 mOsm/kg) solution of saline supplemented with NaCl, was applied to one eye from the tip of a graduated micropipette (Gilson Pipetman P20). The blinking of that particular eye was recorded using a Logitech HD webcam camera at 30 frames per second. The solutions were then removed and the mice returned to their home cages and left undisturbed for at least 5 hours between each experiment. Each animal was tested in morning and afternoon sessions, alternating the left and right eyes. Recordings were replayed at slow motion on a computer screen and the number of blinks was counted over a 2 minute period. Counting started 3 seconds after the drop application, as there were always some blinks associated to the application of the drop.

Quantification of the number of blinks was performed independently by two observers on 100 videos. The correlation coefficient (r) for both measurements was 0.996.

3.10 Data analysis

3.10.1 Calcium measurements

Responses during calcium imaging experiments are expressed as the increment of Fura2 ratio fluorescence (ΔFura2), which was calculated by subtracting the mean baseline fluorescence (15 seconds previous to the agonist application) to the peak fluorescence during the agonist application. When specified, ΔFura2 ratio was normalized to the first cold response in control conditions. Traces of the Fura2 ratio time course were studied individually. A value of ΔFura2 ratio > 0.08 was established as a threshold criterion to consider a change in Fura2 ratio as a positive response. When studying DRG neurons, a pulse of KCl (30 mM) was applied at the end of the protocol in order to identify viable excitable cells (i.e. neurons). Cells with a Fura2 baseline fluorescence higher than 0.8 at the beginning of the recording were removed from the analysis, as well as those cells which did not show a calcium increase during high KCl application. The threshold temperature was estimated as the first point at which the measured signal (F340/F380 or current) deviated by at least four times the SD of its baseline.

3.10.2 Electrophysiological recordings

For recordings in VC configuration in which voltage ramps were applied, TRPM8 currents were quantified at -100 and +100 mV, KCNQ2/3 currents at +80 mV and Kir2.1 currents at -120 mV. The voltage ramps were analyzed using WinAscd software (Prof. G. Droogmans, Laboratory of Physiology, KU Leuven). Current values are expressed as current density values (pA/pF).

The effect of GqCPRs or Dr-VSP activation on TRPM8, KCNQ2/3 and Kir2.1 currents was expressed as the percentage of inhibition, calculated from the baseline subtracted density current values. The fraction of current inhibited was calculated by subtracting the remaining current at the end of GqPCR agonist application, or at the end of the depolarizing pulse, from the current value measured before agonist or voltage application: voltage-gated basal current (KCNQ2/3 and Kir2.1) or the menthol-evoked current (TRPM8). The inhibited current value was convert to a percentage with respect to total current (Fig. 10).

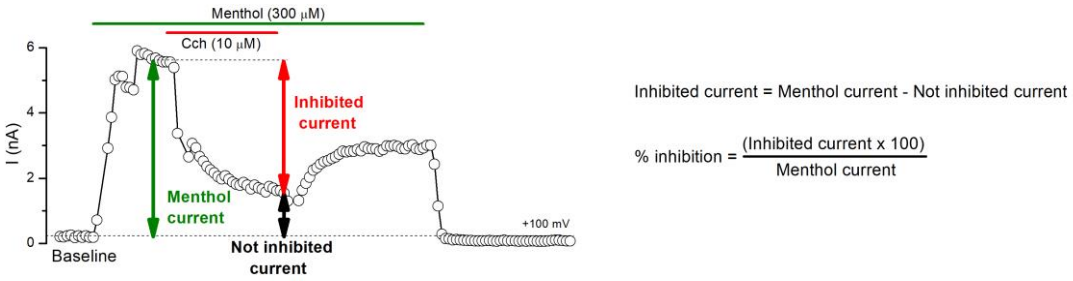

Figure 10. Illustration of the calculations used to obtain the value of current inhibition. A representative recording of TRPM8 menthol-evoked current and its inhibition by M1R activation at 33 ºC is shown.

To estimate shifts in the voltage dependence of TRPM8 activation, current-voltage (I-V) relationships obtained from repetitive (0.33 Hz) voltage ramps (-100 to +150 mV, 400 ms duration) were fitted with a function that combines a linear conductance multiplied by a Boltzmann activation term:

$I = G \times (V-E_{rev})/(1+\exp((V_{1/2}-V)/dx))$

where G is the whole-cell conductance, E_{rev} is the reversal potential of the current, $V_{1/2}$ is the potential for half-maximal activation and dx is the slope factor. The G value obtained for a high menthol concentration (800 μM) was taken as G_{max} and was used for the representation of G/G_{max} curves.

For the fitting of G/G_{max} curves extracted from the variable voltage pulse protocol a Boltzmann equation was used,

$G/G_{max} = A2 + (A1-A2)/(1 + \exp((V_m-V_{1/2})/dx))$

where A2 is de maximal normalized conductance, A1 is the minimal normalized conductance, V_m is the test potential, $V_{1/2}$ is the potential for half-maximal activation and dx is the slope factor

Conductance–voltage (G–V) curves were constructed from the I–V curves of individual cells by dividing the evoked current by the driving force, according to the following equation:

$G=I/(V_m-V_{rev})$

where V_m is the testing potential and V_{rev} is the reversal potential of the current.

All fittings were carried out with the Levenberg-Marquardt method implemented in the Origin 8.0 software.

3.10.3 Software and statistics

Origin 8.0 (OriginLab) was used for the analysis of calcium traces and electrophysiological recordings and for preparing the figures. Clampfit 10.2 (Molecular Devices) was used for the analysis of patch-clamp recordings in HEK293 cells and DRG neurons.

Data are reported as mean ± standard error of the mean (SEM). Statistical analysis of the data was performed using GraphPad Prism version 4.00 for Windows (GraphPad Software). When comparing two means, statistical significance ($p<0.05$) was assessed by Student's two-tailed t-test. For multiple comparisons of means, one-way or two-way ANOVAs were performed.

3.11 Chemicals

Tacrolimus, rapamycin and cyclosporine A (LC laboratories) were prepared in DMSO (50 mM) and were dissolved in pre-warmed (50 ˚C) control solution. When added to the control solution a white cloud of precipitation appears and gentle shaking was applied until a uniform solution was obtained. Due to their poor solubility in water, a final solution of 30 µM was the highest concentration tested for these compounds. Menthol (Scharlau, Spain), BCTC (4-(3-Chloro-2-pyridinyl)-N-[4-(1,1-dimethylethyl)phenyl]-1-piperazinecarboxamide; Tocris), AMTB (N-(3-Aminopropyl)-2-[(3-methylphenyl)methoxy]-N-(2-thienylmethyl)benzamide hydrochloride; Tocris), SKF-96365 (Sigma), pregnenolone sulfate (Tocris), AITC (Allyl isocyanate; Sigma), Capsaicin (8-Methyl-N-vanillyl-trans-6-nonenamide; Sigma), carbachol (Carbamoylcholine chloride, Sigma), histamine (Sigma), Serotonin (Sigma), bradykinin (Sigma), prostaglandin E_2 (Sigma), ATP (Sigma), UTP (Sigma), XE-991 (Sigma), U73122 (Tocris), U73343 (Tocris), Edelfosine (Tocris) were prepared as stocks and stored at -20 ºC. For in vivo experiments, a 10% (100 mg/ml) stock of TAC was prepared in 80% ethanol, 20% Cremophor in PEG-60 Hydrogenated Castor Oil (BASF, Germany) and diluted to 1% in saline on the day of the experiment. The final solution had a homogenous milky white color without precipitations.

UNIVERSITAS
Miguel
Hernández

4. Results

UNIVERSITAS
Miguel
Hernández

4.1 The immunosuppressant macrolide tacrolimus activates cold-sensing TRPM8 channels

In this block of experiments, tacrolimus (TAC), a widely used immunosuppressant, is presented as a novel TRPM8 agonist. The effect of TAC is characterized in heterologous expression systems and in sensory neurons in culture. Additionally, I explored the effect of TAC on the blinking reflex in mice. The results presented here are included in the publication accompanying this thesis (see annex). Additionally, other supplementary results not included in the publication are also presented.

4.1.1 Tacrolimus activates recombinant TRPM8 channels

To evaluate the agonist effect of TAC on TRPM8, I performed intracellular Ca^{2+} imaging experiments on HEK293 cells stably expressing rat TRPM8 channels. As shown in Figure 11A and 11B, TAC produced a dose-dependent activation of TRPM8, with an estimated EC50 of 14.1 ± 25.9 μM (n = 105 cells). Due to its poor solubility in aqueous solutions, it was not possible to test TAC at higher concentrations. At low concentrations, the calcium response evoked by TAC was sustained, while at higher concentrations there was some desensitization during agonist application, similar to the results observed with other chemical agonists of TRPM8 (e.g. menthol) (Rohacs et al., 2005). No changes in Ca^{2+} levels were observed when TAC was applied in the absence of external Ca^{2+} (not shown), indicating that Ca^{2+} influx rather than Ca^{2+} release from stores is responsible for TAC-induced elevation in cytosolic Ca^{2+}.

TRPM8 is activated by cold temperature (McKemy et al., 2002; Peier et al., 2002), and menthol potentiates responses to cold (Voets et al., 2004; Mälkiä et al., 2007). Similarly, TAC produced a dose-dependent potentiation of cold-evoked responses in mouse TRPM8, with effects evident at 1 μM and saturation at around 10 μM (Fig. 11C-D). At 10 μM, peak amplitude of cold-evoked responses increased about 4-fold with respect to responses in control ($p< 0.005$) (Fig. 11D). A closer inspection of TRPM8-evoked $[Ca^{2+}]_i$ responses during cooling pulses revealed that TAC, at concentrations of 10-30 μM, produced a marked shift in the threshold for cold-evoked responses towards warmer temperatures. The average shift was ~7 ºC for the highest concentration tested, changing from 21.9 ± 0.9 ºC in control solution to 29.1 ± 0.5 ºC in 30 μM TAC ($n = 15$, $p<0.005$).

I also explored the sensitivity of human TRPM8 to TAC. As shown in Figure 11E, TAC (30 μM) produced $[Ca^{2+}]_i$ elevations in HEK293 cells transiently expressing hTRPM8 and this activation was not observed in non-transfected cells (Fig. 11E). A summary of the effects of TAC, menthol and cold on hTRPM8 is shown in Figure 11F.

In contrast to the effects of TAC, cyclosporine (30 μM), a structurally unrelated calcineurin inhibitor, had no effect on HEK293 cells stably expressing rat TRPM8 channels (Fig. 11G-H).

Altogether, these results indicate that the immunosuppressant TAC acts like a potent cold-mimetic compound on TRPM8 channels of different mammalian species by a mechanism independent of its canonical signaling pathway.

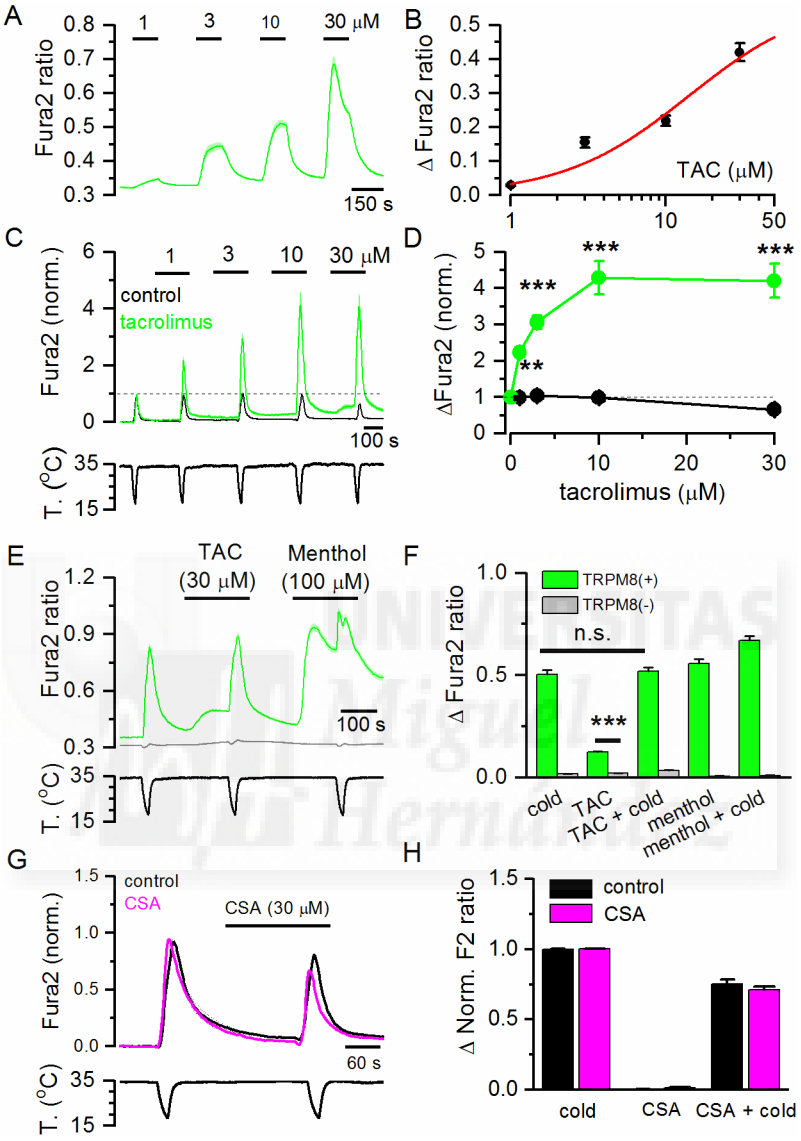

Figure 11. Tacrolimus activates recombinant TRPM8 channels and potentiates cold-evoked responses. *A*, Average ± SEM Fura2 ratio changes in HEK293 cells stably expressing rat TRPM8 during sequential application of TAC at different concentrations (n = 105). ***B*,** Dose-response curve of TAC effects on TRPM8-expressing cells. Data have been fitted with a logistic function (EC_{50} = 14.1 ± 25.9 μM). ***C*,** Average ± SEM time course of Fura2 ratio in HEK293 expressing mouse TRPM8 during consecutive application of cold pulses in control solution (black trace, n = 15) or in the presence of increasing TAC concentrations (green trace, n = 16). The bottom trace shows the time course of the corresponding temperature ramps. In the absence of TAC the response to cold was relatively stable, while in the presence of TAC the response to cold was strongly sensitized. Responses in individual cells have been normalized to their response to the first cooling pulse. ***D*,** Summary plot of the effect of different doses of TAC on the amplitude of cold-evoked responses in mTRPM8 cells. Statistical significance was assessed

by an ANOVA test in combination with Bonferroni's post-hoc test ** p < 0.01, *** p < 0.001. ***E*,** Average ± SEM Fura2 ratio responses to cold, TAC (30 μM) and menthol (100 μM) in HEK293 cells transiently transfected with human TRPM8 and GFP. GFP(+) cells (n = 132) are shown in green while GFP(-) cells (n = 87) are shown in grey. ***F*,** Summary of mean responses in cells transfected with hTRPM8 (green bars) to the different agonists. The responses of untransfected, GFP(-) cells, are shown in grey. TAC produced a significant activation of hTRPM8 (p<0.001; unpaired Student t-test). ***G,*** Average ± SEM Fura2 ratio changes in HEK293 cells stably expressing rat TRPM8 during application of two cooling ramps. For the black traces (n = 25), cooling ramps were delivered in control solution. For the pink traces (n = 107), the second cooling ramp was applied in the presence of 30 μM cyclosporine (CSA). ***H*,** Histogram summarizing the effects of cyclosporine on cold-evoked calcium responses during the protocol shown in G. No significant differences were found between the cells perfused with control solution or cyclosporine (unpaired Student t-test).

4.1.2 TAC activates TRPM8 currents

In whole-cell patch-clamp recordings, application of 30 μM TAC activated robust whole-cell currents in HEK293 cells expressing mouse TRPM8 (Fig. 12A). The current–voltage relationship of the TAC-activated current showed strong outward rectification and a reversal potential close to 0 mV, in line with the previously described properties of TRPM8 (Fig. 12B) (Voets et al., 2004; Mälkiä et al., 2007). Confirming the results obtained in calcium imaging experiments, cold-evoked inward and outward currents were strongly potentiated in the presence of TAC (Fig. 12A-B), leading to large inward (-8.3 ± 1.7 pA/pF cold *vs* -101.2 ± 30.9 pA/pF TAC + cold) and outward currents (437 ± 47 pA/pF cold *vs* 597 ± 59 pA/pF TAC + cold) (n = 7, p<0.01) (Fig. 12C). Similar results were observed in HEK293 cells transfected with human TRPM8. In cells expressing hTRPM8, TAC (30 μM) activated a rectifying non-selective current and cold-evoked currents were strongly potentiated by TAC: -78.7 ± 13.4 pA/pF *vs* -121.9 ± 18.3 pA/pF at -100 mV (n = 8, p<0.001) and 493 ± 26.2 pA/pF *vs* 594.3 55.5 pA/pF at +100 mV (n = 8, p = 0.0159) (Fig. 12D-F).

To confirm the agonism of TAC on TRPM8 channels, I tested the effect of AMTB, a selective TRPM8 antagonist. As shown in Figure 12G, the responses to TAC were fully suppressed by 10 μM AMTB (352 ± 55 pA/pF in TAC *vs* 16 ± 3 pA/pF in TAC + AMTB) (n= 6, p< 0.01). Note that AMTB also reduced the voltage-dependent activation of TRPM8 at the baseline temperature of 33 ºC. During combined application of cooling and TAC, the blocking effect of AMTB was only partial (Fig. 12G-I).

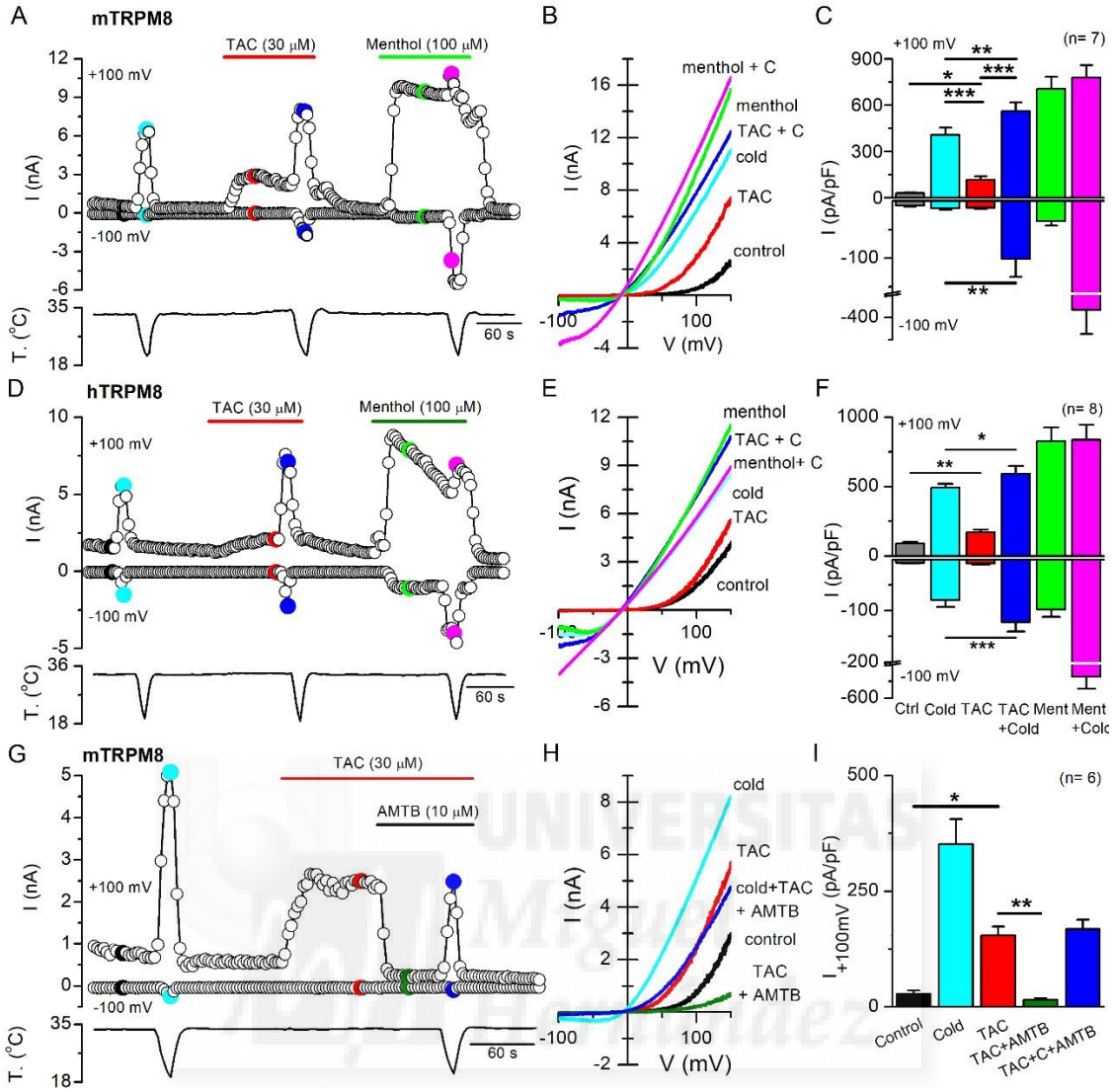

Figure 12. Tacrolimus activates mTRPM8- and hTRPM8-mediated whole-cell currents in HEK293 cells. ***A,*** Representative time course of whole-cell currents at -100 and +100 mV in HEK293 cell transiently transfected with mTRPM8 during application of agonists. The bottom trace shows the simultaneous recording of the bath temperature during the experiment. ***B,*** Current-voltage (I-V) relationship of responses shown in A, obtained with a 400 ms voltage ramp from -100 to +150 mV. The color of individual traces matches the color at each particular time point in A. TAC evokes a non-selective cationic current with typical TRPM8 features and potentiates the cold-evoked response. ***C,*** Bar histogram summarizing the mean ± SEM current density values at +100 and -100 mV to the different stimuli shown in A, with the same color code. Statistical differences were evaluated by a one-way ANOVA, followed by Bonferroni's post-hoc test. ***D*****,** Representative whole-cell recording of TRPM8 currents at +100 and -100 mV in a HEK293 cell transiently transfected with hTRPM8. At the bottom, simultaneous recording of bath temperature. ***E*****,** Current-voltage (I-V) relationships of hTRPM8 corresponding to points colored in D. I-V curves were obtained with a 400 ms voltage ramp from -100 to +150 mV. ***F*****,** Bar histogram representing the mean ± SEM values of maximal current density at +100 and -100 mV under the different conditions tested in experiments like D. Statistical significance was assessed by a paired t-test (*, p<0.05; **, p<0.01; ***, p<0.001). ***G,*** Representative time course of whole-cell currents at -100 mV and +100 mV during a

protocol in which the effect of AMTB was studied. AMTB 10 μM totally abolish TAC-evoked currents. Bottom trace represents the simultaneous recording of the bath temperature during the experiment. ***H*,** Current-voltage (I-V) relationship of responses shown in G. The color of the I-V curves matches the colored time points in G. Note that AMTB also blocks the voltage-dependent activation of TRPM8 at basal temperature. ***I,*** Bar histogram summarizing the mean ± SEM current density values at +100 mV to the different stimuli applied in G. Statistical differences were evaluated by a one-way ANOVA, followed by Bonferroni´s post-hoc test.

4.1.3 Biophysical characterization of TAC effects on TRPM8 gating

Previous studies showed that low temperature and menthol activate TRPM8 channels by producing a shift in the voltage-dependence of activation towards more negative potentials (Brauchi et al., 2004; Voets et al., 2004) while antagonists have the opposite effect (Mälkiä et al., 2007). Recently, Janssens et al. (2016) applied kinetic analysis to describe the mechanisms whereby chemical ligands impact on TRPM8 channel gating, and differentiated between two types of agonists, those stabilizing the open channel (e.g. menthol) and those which cause a destabilization of the closed state (e.g. AITC). I used mouse TRPM8 heterologously expressed in HEK293 to characterize the effects of TAC (30 μM) on voltage-dependence and channel gating and compared the effects of TAC, menthol and AITC. Whole-cell recordings during steps from -80 to +240 mV were obtained at room temperature (23 ± 1 ºC), leading to substantial baseline activation of TRPM8. Menthol was applied at 10 μM, TAC at 30 μM and AITC at 10 mM, concentrations that gave rise to similar steady-state TRPM8 current amplitudes. Following the sequential application of the three agonists, the voltage protocol was repeated in the presence of 800 μM menthol, a saturating concentration, in order to obtain a Gmax value for TRPM8 activity.

Figure 13A shows a representative example of a family of currents recorded in a cell expressing mTRPM8 during 100 ms voltage steps ranging from -80 to +240 mV. The average steady-state current-voltage (I-V) and conductance-voltage (G-V) curves for the different conditions are shown in Figures 13B and 13C respectively. Analysis of these curves revealed a strong leftward shift of the activation curve in the presence of the three agonists, with a change in the voltage for half-maximal activation ($V_{1/2}$) from 153 ± 7 mV in control to 106 ± 10 mV in the presence of TAC (calculated from G-V) (Fig. 13D). The shift in $V_{1/2}$ with respect to control conditions was highly significant ($p< 0.0001$). Menthol (10 μM) and AITC (10 mM) had similar effects on $V_{1/2}$ (Fig. 13D).

To characterize the effect of the different agonists on TRPM8 gating kinetics, I studied the changes in the time course of current activation during voltage steps to +120 mV (Fig. 13E) and their relaxation upon return to -80 mV (Fig. 13F). For a better comparison, currents were normalized to their steady state values. Both menthol and TAC produced a clear slowing of the gating kinetics during depolarization to +120 mV and after the return to -80 mV. In contrast, AITC clearly accelerates the activation kinetics (Fig. 13E), without affecting the current relaxation kinetics upon repolarization to -80 mV (Fig. 13F). Currents in control or during AITC application were adequately fitted with a single exponential (not shown). In contrast, the currents in TAC or menthol required a double exponential. To quantify the differences in kinetics produced by the

three chemical agonists in more detail, I compared the rise time to 95% of the initial value. These results are shown in Figures 13G and 13H for the activation and deactivation time course respectively.

These results show that the mechanism of action of TAC on TRPM8 gating resemble those of menthol and are different of the AITC gating mechanism (Janssens et al., 2016).

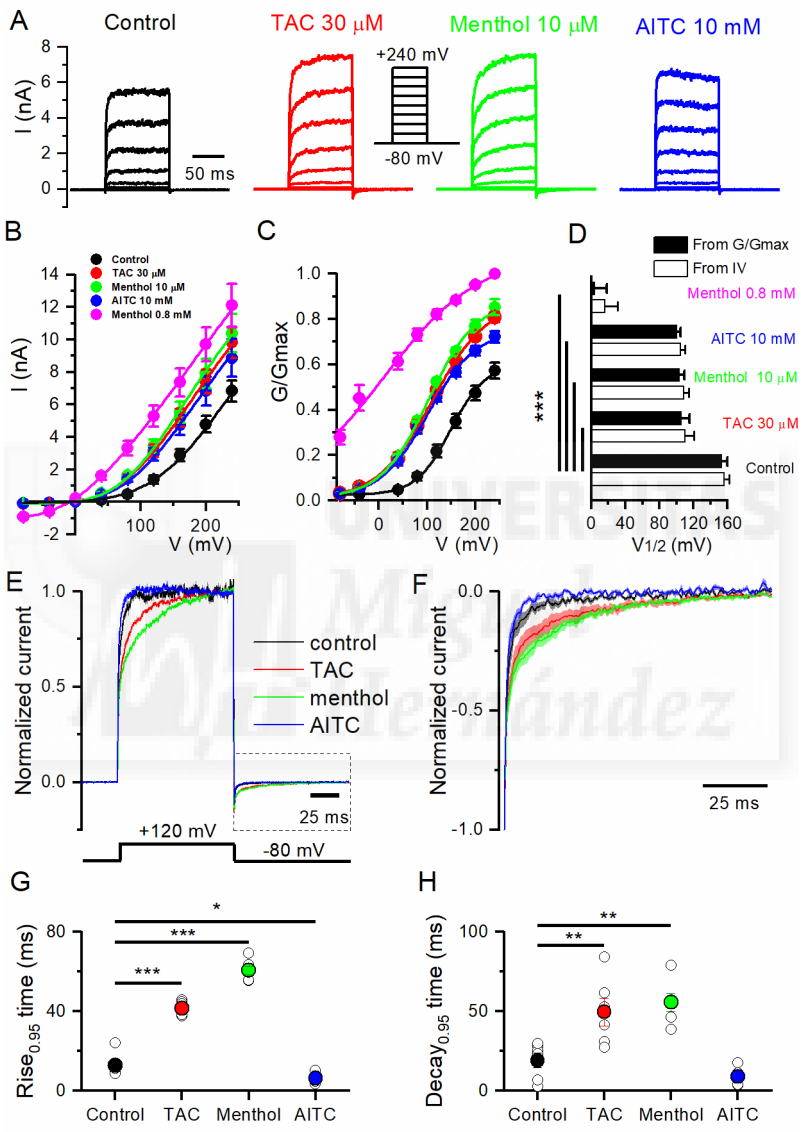

Figure 13. Biophysical characterization of tacrolimus effects on TRPM8 gating. ***A,*** Whole-cell TRPM8 currents in response to the indicated voltage step protocol (from -80 to 240 mV, Δv= 40 mV) in control conditions and in the presence of TAC (30 μM), menthol (10 μM) and AITC (10 mM) at 24 ºC. Note the variable effect of agonists on activation kinetics. ***B,*** Averaged (n = 6) steady-state I-V curves extracted from individual cells after application of protocol A. The lines represent the fitting to a linearized Boltzmann equation (see Methods). ***C,*** Averaged (n = 6) voltage-dependence activation curves in control conditions and in the presence of the different agonists. Conductance (G) was calculated as the steady-state current divided by the driving force (Driving force= V_{test} - E_{rev}), and normalized to the estimated maximal conductance (Gmax) which was the G value at +240 mV in the presence of 0.8 mM menthol. ***D,***

Mean (n = 6) $V_{1/2}$ values calculated from fitting the individual I-V curves to the linearized Boltzmann equation (white bars) or the individual G/G_{max}-V curves fitted to the Boltzmann equation (black bars). Note that all the three agonists produced similar shifts in $V_{1/2}$ values at the indicated concentrations. Statistical differences were evaluated by a one-way ANOVA, followed by Bonferroni's post-hoc test. ***E,*** Averaged TRPM8 current during a voltage step from -80 to +120 mV, in control condition and in the presence of the different agonists. Currents were normalized to their steady-state amplitude after baseline subtraction. ***F,*** Averaged ± SEM TRPM8 deactivation kinetics at -80 mV obtained from current tails after a voltage step to +120 mV (box bounded by dotted line in E), in control condition and in the presence of the different agonists. The current was normalized to the maximum value and baseline was subtracted. ***G,*** Mean values of the current activation time course, measured from baseline to 95% amplitude, for voltage steps to +120 mV. ***H,*** Mean values of current deactivation time course at -80 mV, measured from baseline to 95% amplitude, following a voltage step to +120 mV. Statistical differences in G and F were evaluated with a one-way ANOVA, followed by Bonferroni's post-hoc test.

4.1.4 Tacrolimus activates TRPM8 current in membrane delimited inside-out patches

To test the possible direct action of TAC on TRPM8 gating, I evaluated channel activity in cell-free inside-out patches from mouse TRPM8-expressing HEK293 cells. With this configuration, one can isolate channels in the patch of membrane under the pipette from the cytoplasmic factors which could participate in an indirect signaling route of activation. Rapid and reversible current responses to TAC were observed in cell-free inside-out patches, indicating that the effect of TAC on TRPM8 is membrane-delimited (Figure 14A-C). Comparable current activation was measured in 5 out of 5 patches. Menthol also evoked membrane-delimited TRPM8-medited currents (Figure 14A-C).

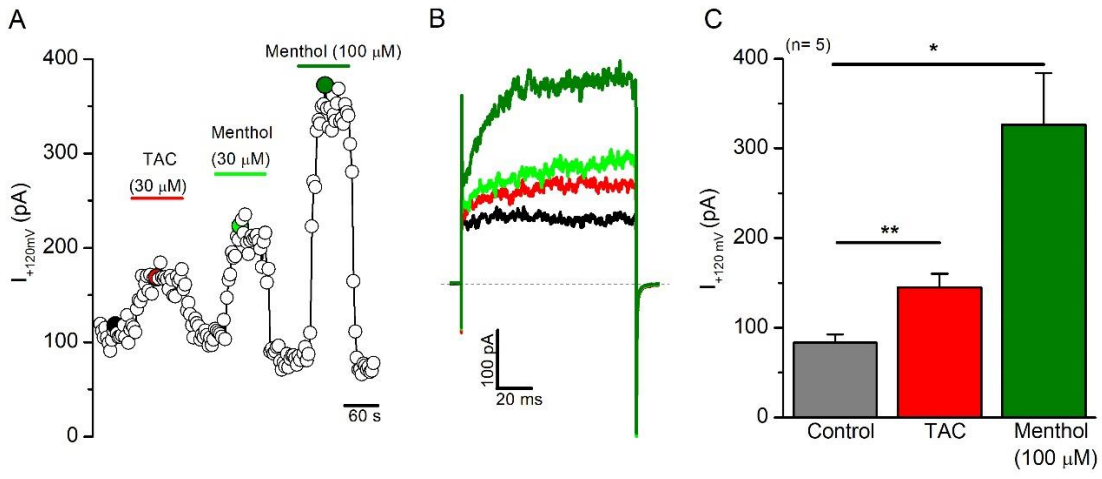

Figure 14. TAC activates mTRPM8 in cell-free inside-out patches. ***A,*** Time course of current elicited by repetitive 100 ms voltage steps (0.33 Hz) to +120 mV in a cell-free inside-out patch from a HEK293 cell expressing mTRPM8 at 23 ºC. Ligands were included in the bath solution. ***B****,* Average current traces recorded from 5 time points centered on each colored point in A. Dotted line represents the 0 pA value. Current values were measured during the last 5 ms of the voltage pulse. ***C,*** Bar histogram summarizing

the amplitude of currents during control conditions, during application of TAC (30 µM), and during application of menthol (100 µM). Statistical significance between control and TAC and control and menthol currents was calculated by a paired t-test (*, p<0.05; **, p<0. 01).

4.1.5 Tacrolimus effect is independent of menthol and icilin binding sites and is reduced in cTRPM8

A single tyrosine residue (Y745), located on transmembrane segment 1 according to recent cryo-EM structural analysis (Yin et al., 2018), is essential for the activating actions of menthol on TRPM8 channels (Bandell et al., 2006; Mälkiä et al., 2009). These mutant channels are completely insensitive to menthol but retain the normal responsiveness to cold and voltage exhibited by wildtype channels. At the same time, the Y745 residue is critical for inhibition mediated by SKF96365 of cold- and voltage-activated TRPM8 currents (Mälkiä et al., 2009). I explored the sensitivity of the TRPM8-Y745H mutant to TAC in order to find whether TAC shares the mechanism of action with menthol and I also compared the inhibitory effects of SKF96365 on TAC responses between WT TRPM8 and TRPM8-Y745H.

Using calcium imaging, I found that TAC activates mouse TRPM8-Y745H in a similar manner to WT channels (Fig. 15A-D). On average, the amplitude of the $[Ca^{2+}]_i$ elevation after application of 30 µM TAC, normalized to the response to a cold ramp in control conditions, was 0.20 ± 0.008 in wildtype channels (n= 66) compared to 0.17 ± 0.007 in TRPM8-Y745H (n= 38, p<0.05) (Fig. 15A-D). Remarkably, despite a normal response to cold or TAC, the TRPM8-Y745H mutant showed no potentiation of the cold-evoked response by TAC (ratio of TAC + cold/cold= 1.09 ± 0.05) (Fig. 15C-D). In contrast, the wildtype channel showed a strong potentiation (1.4 ± 0.08) (Fig. 15A-B, p<0.01).

SKF96365 strongly blocked WT TRPM8 responses to cold (cold + SKF96365/cold= 0,1 ± 0.007) and TAC responses, being the responses to TAC (normalized to cold) 0.22 ± 0.01 in the presence of vehicle and 0.06 ± 0.004 in the presence of SKF96365 (p<0.001) (Fig. 15A-B). SFK96365 also reduced the response of WT TRPM8 channels to cold in the presence of TAC (Fig. 15A-B). According to the critical role of Y745 residue in the SKF96365-mediated inhibition of TRPM8, SKF96365 fails to inhibit cold (cold + SKF96365/cold= 0.98 ± 0.03) and TAC responses, being the responses to TAC (normalized to cold) 0.19 ± 0.01 in the presence of the vehicle and 0.18 ± 0.01 in the presence of SKF96365 (Fig. 15C-D).

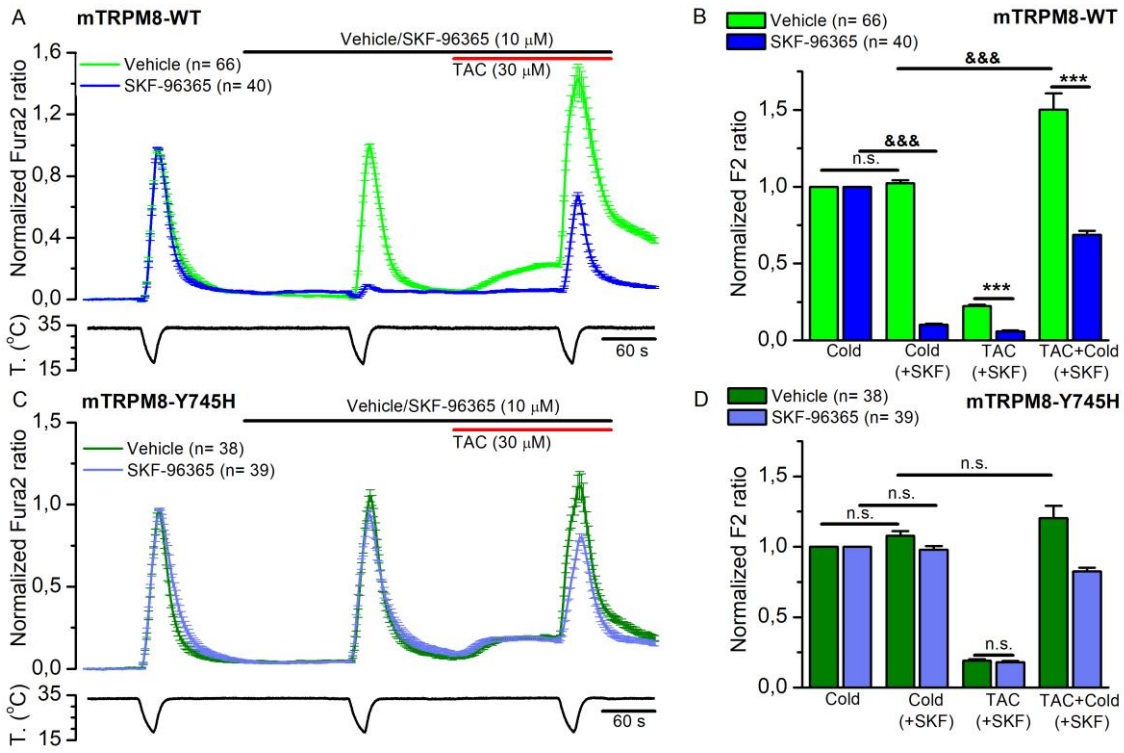

Figure 15. Tacrolimus activates the menthol- and SKF96365-insensitive mTRPM8-Y745H mutant. ***A*****,** Normalized average traces ± SEM of Fura2 fluorescence from HEK293 cells transfected with mTRPM8-WT channel. Fluorescence values were normalized to the peak fluorescence value during the first cold ramp and baseline subtracted. Green trace corresponds to control experiments in which vehicle was applied (control) whereas the blue trace corresponds to experiments in which SKF-96365 was applied. Bottom trace corresponds to a representative simultaneous recording of bath temperature during these experiments. ***B*****,** Bar histogram summarizing the normalized responses of mTRPM8-WT to the agonists applied in control cells (vehicle, green) and in cells perfused with SKF-96365 (blue). Statistical significance was assessed by an unpaired t-test when comparing Control vs SKF-96365 responses (***, $p<0.001$) and by an ANOVA test followed by a Bonferroni post-hoc when comparing responses within the same group (&&&, $p<0.001$). ***C*****,** Normalized average traces of Fura2 fluorescence from HEK293 cells transfected with mTRPM8-Y745H mutant channels. Fluorescence values were normalized to the peak fluorescence value during the first cold ramp and baseline subtracted. The protocol was the same than in A. ***D*****,** Bar histogram summarizing the normalized responses of mTRPM8-Y745H to the agonists applied in control cells (vehicle, green) and in cells perfused with SKF-96365 (blue). Statistical significance was assessed by an unpaired t-test when comparing Control vs SKF-96365 responses and by an ANOVA followed by a Bonferroni post-hoc when comparing responses within the same group.

To confirm these differences, I examined the effects of TAC on whole-cell currents in wildtype and TRPM8-Y745H mutant channels (Fig. 16A). The current generated by TAC was normalized to the cold response evoked in control conditions in the same cell, at a potential of +100 mV. On average, TAC current was 0.27 ± 0.04 in wildtype channels and 0.30 ± 0.04 in the Y745H mutant, confirming that the TRPM8-Y745H mutants retains their normal sensitivity to TAC. In the same cells, menthol (100 μM) had no effect and did not affect the cold response, as expected for the Y745H mutant (Fig. 16B). Moreover, whole-cell recordings confirmed that the potentiation of the cold-evoked response by TAC was absent in the Y745H mutant (WT Normalized TAC + cold=

1.39 ± 0.05 *vs* TRPM8-Y745H Normalized TAC + cold= 0.83 ± 0.09) (Fig. 16A-B). Additionally, I also explored the sensitivity for TAC of the mutant TRPM8-L1009R, which carries a mutation in the residue L1009, also critical for menthol sensitivity (Bandell et al., 2006). The TRPM8-L1009R mutant showed similar responses to TAC than WT channels (Normalized TAC= 0.29 ± 0.06) (Fig. 16A-B). However, as in the case of the TRPM8-Y745H mutant, the potentiation of the cold-evoked response by TAC was absent (Normalized TAC + cold= 1.08 ± 0.04) and the sensitivity for menthol was strongly reduced (Fig. 16A-B).

Next, I explored TAC sensitivity in the TRPM8-N799A mutant. This residue was shown to mediate responses to icilin, a different TRPM8 agonist (Chuang et al., 2004). TRPM8-N799A mutants behaved like TRPM8 wildtype channels, with normal responses to TAC (Normalized TAC= 0.26 ± 0.02) and the potentiation of the cold response in the presence of TAC (Normalized TAC + cold= 1.62 ± 0.13) (Fig. 16A-B), suggesting that the effects of TAC on TRPM8 do not involve the icilin-binding site.

Moreover, I also explored a TRPM8 mutant with a single point mutation in the TRP box, specifically, the mutation P1012Q. This proline residue is conserved in TRPC1 and has been involved in the binding of the immunophilins FKBP12 and FKBP52 to TRPC1 (Shim et al., 2009). The mutant mTRPM8-P1012Q showed reduced responses to cold and lost the sensitivity to TAC and to menthol, suggesting that this mutation affects the gating of TRPM8 to different chemical agonists and not exclusively to TAC (Fig. 16A-B). Noteworthy, the potentiation of the cold response in the presence of TAC was also lost in this mutant (Normalized TAC + cold= 1.06 ± 0.07), although menthol was still able to potentiate the cold response (Normalized Menthol + cold response= 2.01 ± 0.33) (Fig.16A-B).

I also tested the chicken TRPM8 orthologue, which shares an identity of 79.9% with mTRPM8 but displays different thermosensitivity (smaller responses to cold) and chemosensitivity (higher sensitivity to menthol and no icilin sensitivity) phenotypes (Pertusa et al., 2018). I found that TAC-activated currents were strongly reduced in cTRPM8, despite a normalization to a small cold response (Normalized TAC= 0.1 ± 0.02) and that the potentiation of the cold responses in the presence of TAC was lost (Normalized TAC + cold= 0.87 ± 0.06) (Fig. 16A-B). As previously described, menthol responses in cTRPM8 were significantly higher than in mTRPM8 (Fig. 16B).

These results suggest a mode of action of TAC independent of the putative menthol (Y745 and L1009) and icilin (N799) binding sites and unveil the importance of the Y745 residue in the allosteric coupling between cold and TAC activation of TRPM8. Moreover, the point mutation P1012Q affects the gating of the channel for all the chemical agonists tested. Additionally, I found that cTRPM8 showed reduced sensitivity to TAC and strong sensitivity to menthol.

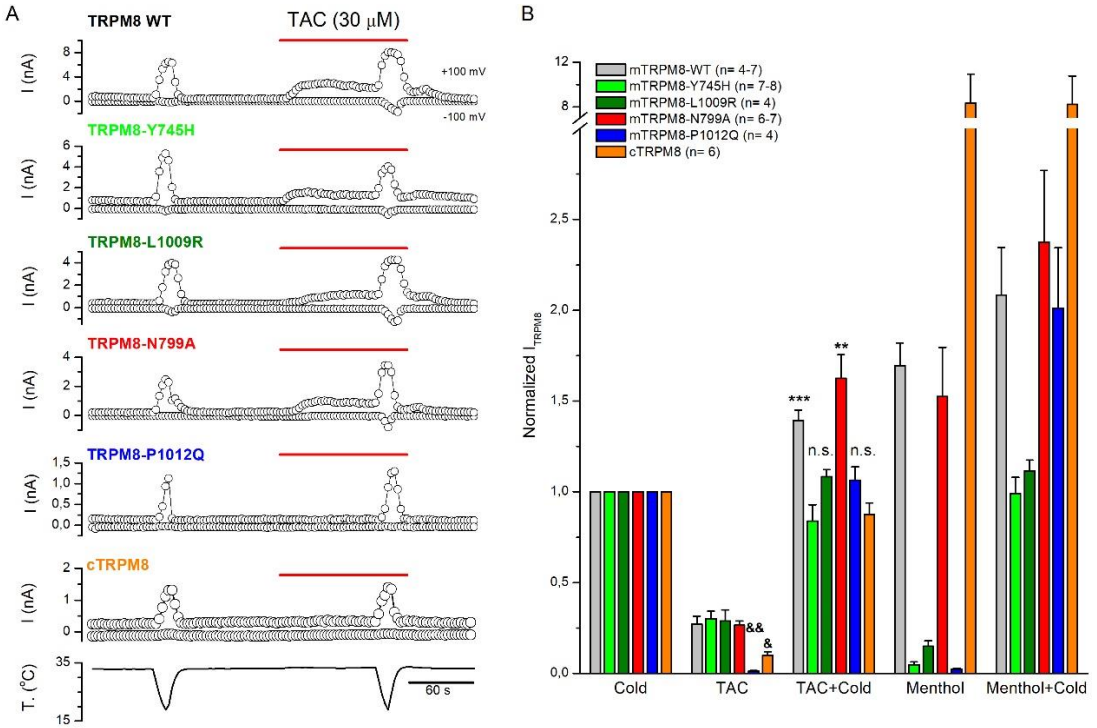

Figure 16. TAC effect varies on different TRPM8 single-residue mutants and in the cTRPM8 orthologue. ***A,*** Time course of whole cell current recordings at +100 and -100 mV obtained from HEK293 cells expressing (from bottom to the top); mTRPM8-WT, mTRPM8-Y745H, mTRPM8-L1009R, mTRPM8-N799A, mTRPM8-P1012Q, and the orthologue chicken TRPM8. At the bottom, a representative trace of bath temperature during the recordings, in which a cold ramp in control conditions and second cold ramp in the presence of TAC were applied. The recordings continued with menthol (100 μM) application and a third cold ramp in the presence of menthol (not shown). Recordings were obtained by applying consecutive voltage ramps from -100 to +100 mV. ***B,*** Bar histogram summarizing the normalized response of the different channels tested to the different agonists applied. Baseline subtracted currents were normalized to the baseline subtracted peak current value during the cold ramp in control conditions**.** Statistical significance for the potentiation of the cold response by TAC (Cold vs TAC + cold) was calculated by a paired t-test (**< 0.01; ***< 0.001). Statistical significance between TAC responses was calculated by a one-way ANOVA followed by Bonferroni's post-hoc test (&< 0.05; &&< 0.01).

4.1.6 Effects of tacrolimus on other thermoTRP channels

Next, I tested the effects of TAC on other thermally sensitive TRP channels (Dhaka et al., 2006). As shown in Figure 17A, TAC (30 μM) had no activating effect on rat TRPV1 or mouse TRPM3 channels. In contrast, the same concentration of TAC activated human TRPA1, with a slowly rising $[Ca^{2+}]_i$ response. The activating effects of TAC on hTRPA1 were more modest than those produced by its canonical agonist AITC (Fig. 17B). I noticed that application of TAC produced a modest inhibition of basal calcium levels in cells expressing TRPV1 or TRPM3, suggesting some inhibitory effect on background activity at this temperature (i.e. 33 ºC). The effects of TAC on recombinant TRPM8 and TRPA1 channels motivated a deeper characterization of its action on primary sensory neurons.

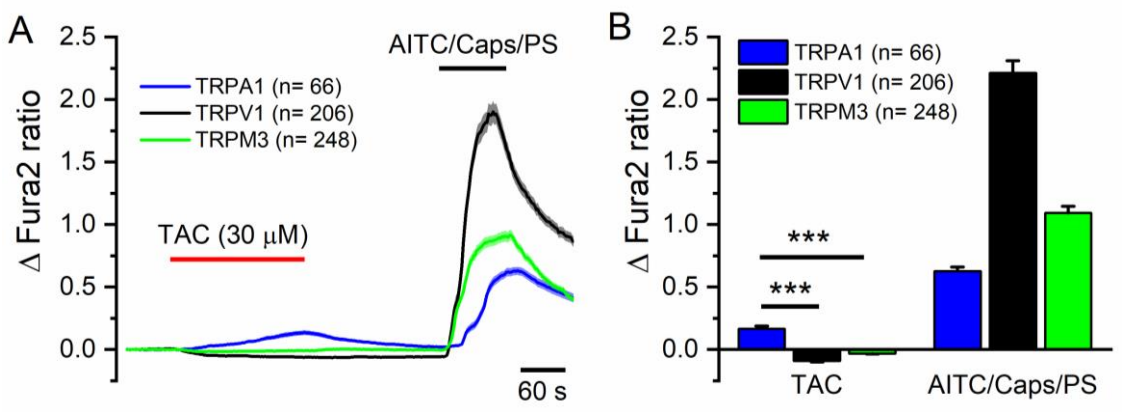

Figure 17. Tacrolimus activates human TRPA1 channels. ***A,*** Averaged ± SEM Fura2 fluorescence ratio of HEK292 cells transfected with human TRPA1 (blue trace), rat TRPV1 (black trace), or mouse TRPM3 (green trace) during applications of TAC (30 μM) and their canonical agonists capsaicin (100 nM), AITC (50 μM) and pregnenolone sulfate (PS, 50 μM). ***B***, Bar histogram summarizing the effect of TAC or the canonical agonists, capsaicin, AITC or PS, on Fura2 fluorescence ratio. Individual records have been baseline-subtracted. TAC produced a significant elevation in $[Ca^{2+}]_i$ in TRPA1-transfected cells compared to TRPV1- or TRPM3-transfected cells ($p<0.001$, one-way ANOVA followed by Bonferroni's post-hoc test).

4.1.7 Tacrolimus activates TRPM8-expressing cold-sensitive neurons and potentiates their cold response

TRPM8-expressing neurons represent only a small fraction of all DRG neurons (McKemy et al., 2002; Takashima et al., 2007; Dhaka et al., 2008). I used a BAC-transgenic mouse expressing enhanced YFP under the TRPM8 promoter, TRPM8BAC-EYFP, (Morenilla-Palao et al., 2014) and intracellular Ca^{2+} imaging to identify TRPM8-expressing neurons in DRG cultures. Confirming previous findings in this transgenic mouse line (Morenilla-Palao et al., 2014), most YFP(+) neurons were activated by cold (36 of 37) but only 1 in 130 YFP(-) was cold-sensitive, suggesting a very good correspondence between YFP fluorescence and TRPM8 expression (Fig. 18B-C).

Application of 30 μM TAC activated the majority of TRPM8-expressing thermoreceptor neurons (31 of 36), identified by the expression of YFP and by their response to a cold temperature ramp (Fig. 18A, 18C). In the presence of 30 μM TAC, the amplitude of cold-evoked responses also increased significantly in YFP(+) neurons (Fig. 18D). TAC and cold produced a similar activation of individual neurons, and the amplitude of both responses were strongly correlated (r^2= 0.42) (Fig. 18E). In contrast, none (0 out of 130) of the YFP(-) neurons (i.e. those not expressing TRPM8) were activated by 30 μM TAC, although they showed normal responses to 30 mM KCl (not shown).

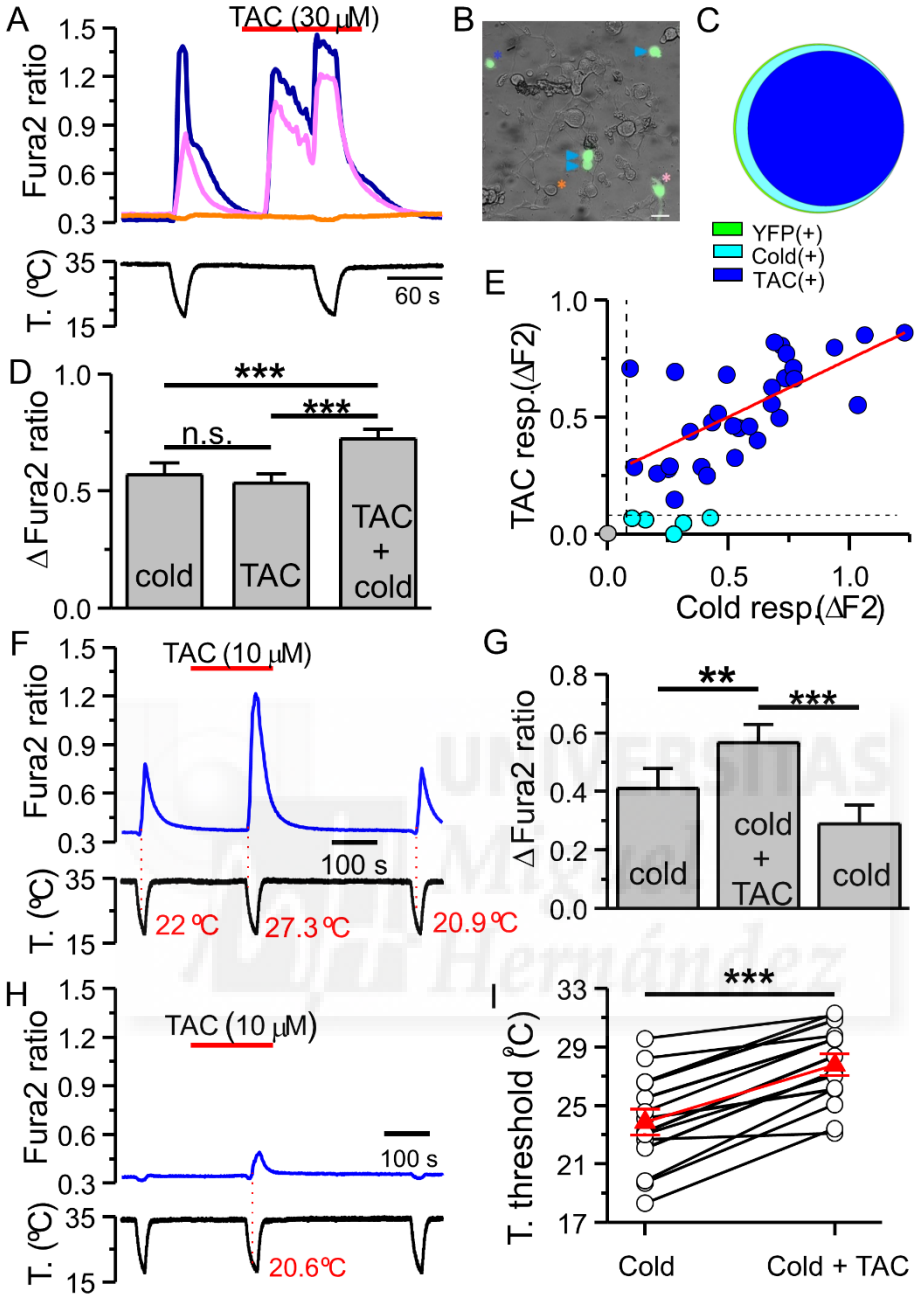

Figure 18. Tacrolimus activates cold-sensitive neurons selectively. ***A,*** Ratiometric [Ca^{2+}] measurement from Fura2-AM loaded cultured DRG neurons in $TRPM8^{BAC\text{-}EYFP}$ mice. Two cold-sensitive neurons (blue and magenta traces) increased their [Ca^{2+}] level during the cooling ramp. The same neurons also responded to 30 µM TAC and their response to cold was potentiated. The cold-insensitive neuron (orange trace) did not respond to any of these stimuli. ***B,*** Representative image of a DRG culture from a $TRPM8^{BAC\text{-}EYFP}$ mouse. The traces shown in A correspond to the neurons marked with the same colored asterisk: orange for YFP(-), blue and magenta for YFP(+). Three additional YFP(+) neurons, marked with blue arrowheads, also responded to cold and TAC. The calibration bar is 20 µm. ***C,*** Venn diagram showing the strong overlap between YFP(+) neurons (green, n= 37), the response to cooling

(cyan, n= 36) and the response to TAC (blue, n= 31). In this sample, none of the YFP(-) neurons (n = 130) responded to TAC. ***D,*** Bar histogram showing the average amplitude of the responses to cold, to TAC and to cold in the presence of TAC. Amplitudes were similar for cold and TAC while the responses to cold was significantly higher in the presence of TAC. One-way ANOVA for repeated measures followed by Bonferroni's post-hoc test. ***E,*** Correlation between amplitude of cold- and TAC-evoked responses in individual DRG neurons. Black dotted lines indicate the threshold amplitude established for considering a positive response. Blue points represent the neurons which responded to cold and TAC (n = 31) and cyan points represent the neurons which responded to cold but did not respond to TAC (n= 5). Note the small cold-evoked response in neurons unresponsive to TAC. The grey point represents the single YFP(+) neuron that did not respond to cold or TAC. The linear fit to the blue points (red line) yielded a correlation coefficient (r^2) of 0.42. ***F,*** Representative trace of Fura2 ratio fluorescence in a DRG neuron during three consecutive cooling ramps. Note the strong, reversible, potentiation of the cold-evoked response in the presence of 10 μM TAC. The numbers in red, mark the temperature at which the measured signal (F340/F380) deviated by at least four times the SD of its baseline (i.e. temperature threshold). ***G,*** Bar histogram summarizing the effect of 10 μM TAC on the amplitude of the cold-evoked response. One-way ANOVA for repeated measures followed by Bonferroni's post-hoc test. ***H,*** Time course of Fura2 ratio in a YFP(+) which was not activated in control conditions (i.e. cold insensitive) but was recruited in the presence of 10 μM TAC. ***I,*** Temperature threshold of individual YFP(+) neurons to cold or cold plus 10 μM TAC. The mean temperature threshold (red triangles) shifted from 23.9 ± 0.9 ºC in control solution to 27.8 ± 0.8 ºC the presence of 10 μM TAC ($p<0.001$, n = 14, paired Student t-test).

I also examined the effects of lower concentration of TAC on DRG neurons. As shown in Figure 18F, at 10 μM, the effects of TAC on $[Ca^{2+}]_i$ levels on a YFP(+) neuron were negligible. However, I found that this concentration of TAC sensitized the response of TRPM8-expressing neurons to cold in a reversible manner. This is a similar effect to that described for other chemical agonists of TRPM8 (McKemy et al., 2002; Voets et al., 2004). On average, the $[Ca^{2+}]_i$ response to cold increased from 0.41 ± 0.07 during the first cold ramp to 0.57 ± 0.06 during a second cold ramp, in the presence of TAC ($p <0.01$, n = 14) (Fig. 18G). The larger amplitude in the cold-evoked response was accompanied by a shift in the response threshold of individual neurons towards warmer temperatures (Fig. 18F and 18I). On average, the threshold shifted by ~4 ºC, from a mean of 23.8 ºC ± 0.9 in control to 27.8 ºC ± 0.7 in the presence of 10 μM TAC ($p<0.001$, n =14). In addition, one YFP(+) neuron initially insensitive to cold became cold sensitive during the application of this TAC concentration, and this activation was reversible (Fig. 18H).

Collectively, these results indicate that TAC excites cold-sensitive neurons that express TRPM8, and potentiates their cold response by shifting the threshold temperature to warmer temperatures.

In agreement with the observations obtained in TRPM8-transfected HEK293 cells, cyclosporine (30 μM) failed to activate YFP(+) DRG neurons (0 of 37), or sensitize their responses to cold: the increase in cold-evoked Fura2 ratio was 0.72 ± 0.13 in the presence of vehicle (n = 16), compared to 0.63 ± 0.06 in the presence of cyclosporine (n = 37) ($p=0.40$, unpaired Student t-test) (Fig. 19A-B).

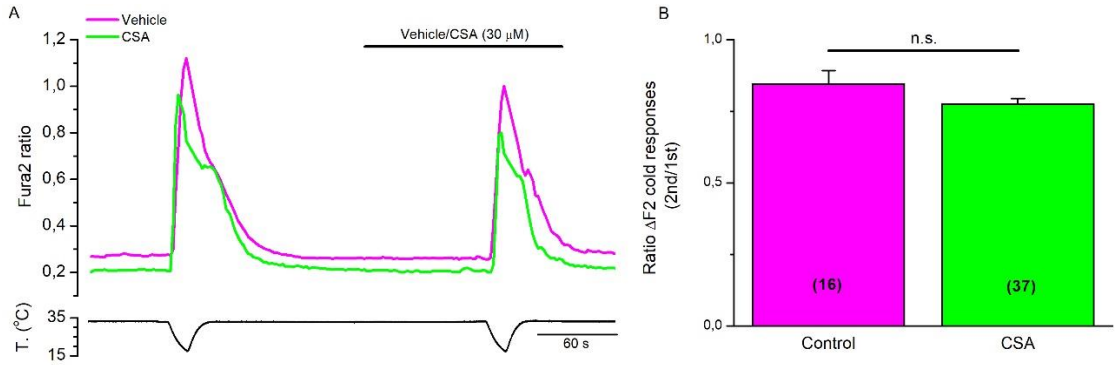

Figure 19. Cyclosporine does not have an effect on cold-sensitive DRG neurons. ***A***, Representative trace of Fura2 fluorescence in two cold-sensitive neurons during a protocol exploring the effect of CSA. After an initial cold ramp in control conditions vehicle (pink trace) or CSA (green trace) was perfused and a second cold ramp was applied. Bottom trace represents the simultaneous recording of bath temperature during the protocol. ***B,*** Bar histograms summarizing the effect of CSA on cold-evoked responses in cold-sensitive DRG neurons. Statistical differences were evaluated with an unpaired t-test (p= 0.40).

4.1.8 TRPM8 mediates tacrolimus responses in DRG neurons

Next, I explored whether TAC responses in cold-sensitive DRG neurons were mediated by TRPM8 activation. To this end, I combined two experimental strategies, a pharmacological approach using two different TRPM8 blockers, and a genetic approximation, characterizing responses in TRPM8 KO mice. If TAC responses were mediated by TRPM8 activation, they should be sensitive to TRPM8 antagonists. As shown in Figures 20A and 20B, this prediction was fulfilled; the responses to TAC in cold-sensitive DRG neurons were completely blocked by AMTB (10 µM) and BCTC (50 µM), two structurally unrelated TRPM8 antagonists (Almaraz et al., 2014). A summary of these results is shown in Figures 20C-D. Moreover, the $[Ca^{2+}]_i$ elevation during cold ramps in the presence of TAC were also greatly reduced by these two antagonists ($p<0.001$).

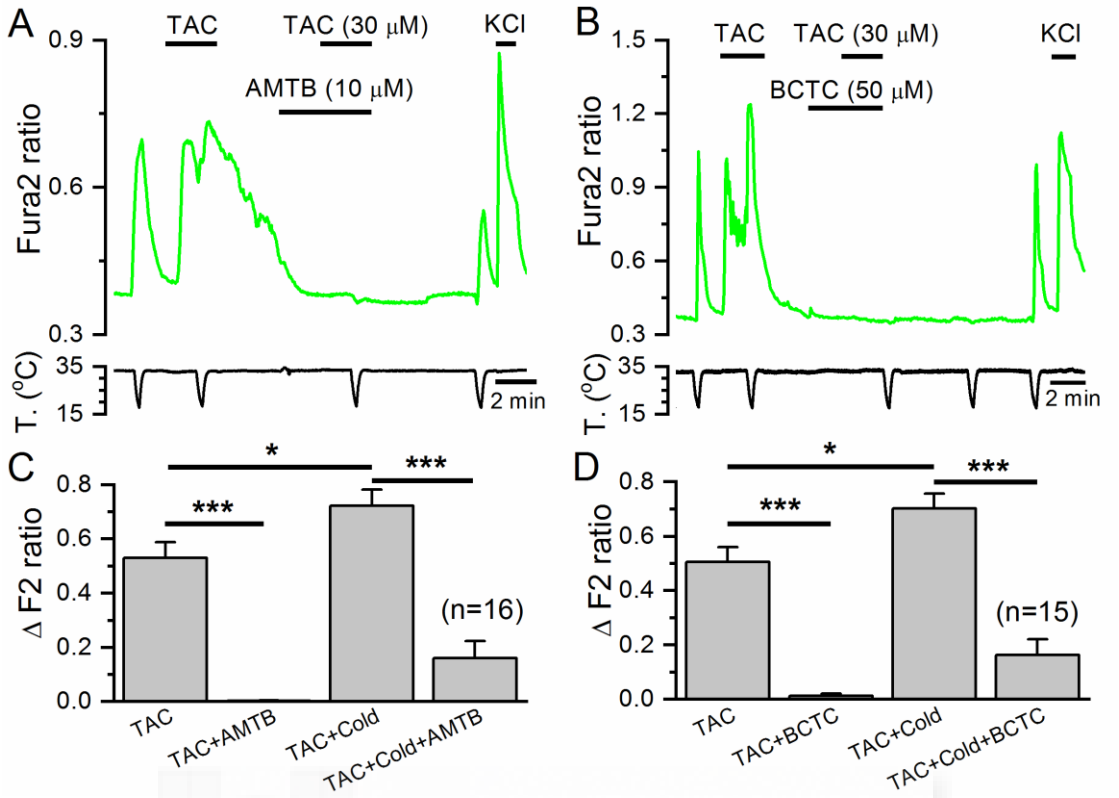

Figure 20. TRPM8 antagonists block the excitatory effects of tacrolimus on mice DRG neurons. *A,* Ratiometric [Ca^{2+}] levels in a Fura2-loaded cultured DRG neuron from a $TRPM8^{BAC\text{-}EYFP}$ mouse, showing the response to cold and TAC in control conditions and in the presence of the TRPM8 blocker AMTB (10 μM). ***B,*** A similar protocol in the presence of BCTC (50 μM), a different, structurally unrelated, TRPM8 blocker. ***C,*** Bar histograms summarizing the effects of AMTB (n = 16), and (**D**) BCTC (n = 15) on cold- and TAC-evoked responses. Statistical differences evaluated with one-way ANOVA followed by Bonferroni post-hoc test.

To confirm the effects of TAC on native TRPM8 channels, I examined responses to TAC in DRG cultures from a transgenic mouse line in which a farnesylated EGFP is expressed from the TRPM8 locus (*$TRPM8^{EGFPf}$*) in replacement of TRPM8, allowing the identification of putative TRPM8-expressing neurons (Dhaka et al. 2007). I compared responses in cultures from *$TRPM8^{EGFPf/+}$* mice, which maintain one copy of TRPM8, with those in *$TRPM8^{EGFPf/EGFPf}$* animals, thus null for TRPM8.

In *$TRPM8^{EGFPf/+}$* DRG cultures, 13% (67 out of 515) of the neurons were fluorescent and practically all of them (66 out of 67) were activated by cold or menthol, consistent with their expression of TRPM8 (Fig. 21A). Moreover, about half of the green fluorescent neurons were activated by TAC (35 out of 67). In the presence of TAC, or menthol, cold responses were potentiated (Fig. 21A, green trace), consistent with an effect on TRPM8. The phenotype of GFP(-) neurons was very different: very few (2.4%) were cold-sensitive and only 2.7% (12 out of 448) were activated by TAC (Figure 21A, red trace) a significantly lower percentage ($p<0.001$, Z test). A Venn diagram of these results is shown in Figure 21B. In summary, in agreement with the results observed in

TRPM8$^{BAC\text{-}EYFP}$ mice, there is a high correlation between expression of TRPM8 and responses to TAC.

The responses to TAC in *TRPM8$^{EGFPf/EGFPf}$* (i.e. TRPM8 KO) mice were very infrequent, albeit detectable in some neurons (Figure 21C, pink trace). In total, only 13 out of 516 (2.9%) DRG neurons respond to 30 µM TAC in TRPM8 KO animals (4 were GFP(+) and 9 were GFP(-)). The main reduction occurred in GFP(+) neurons, in parallel with a near suppression of their responses to cold or menthol (Figure 21C, green trace). As summarized in Figure 21D, out of 70 GFP(+) neurons tested, only 4 (5.7%) responded to TAC, a drastic reduction from the responses observed in GFP(+) neurons in *TRPM8$^{EGFPf/+}$* mice ($p<0.001$, Z test). Figure 21E summarizes the responses to TAC and cold in fluorescent and non-fluorescent cells of the two transgenic mouse lines. It is evident that expression of TRPM8 is highly correlated with responses to TAC.

Finally, in GFP(-) neurons of *TRPM8$^{EGFPf/EGFPf}$* mice only 2% (9 out of 446) responded to TAC, a very similar percentage to that observed in GFP(-) neurons of *TRPM8$^{EGFPf/+}$* mice. The responses to TAC in GFP(-) neurons had some distinct characteristics: since the results were similar in *TRPM8$^{EGFPf/+}$* and *TRPM8$^{EGFPf/EGFPf}$* animals, I pooled them together. In GFP(-) neurons, the amplitude of TAC responses were smaller ($p<0.001$) when compared to responses in fluorescent neurons of *TRPM8$^{EGFPf/+}$* mice or TRPM8$^{BAC\text{-}EYFP}$ mice (Fig. 21F) and they were nearly abolished during the cooling ramp (Fig. 21A, 21C). None of these neurons was cold-sensitive (Figure 21A, red trace). Interestingly, of the 21 GFP(-) neurons activated by TAC, 18 also responded to capsaicin (100 nM) and 11 responded to AITC (50 µM). These characteristics are consistent with a possible effect of TAC on TRPV1. However, I note that in these cultures 43.8% (452/1031) of the neurons responded to capsaicin but only 22 out these 452 (4.9%) responded to TAC.

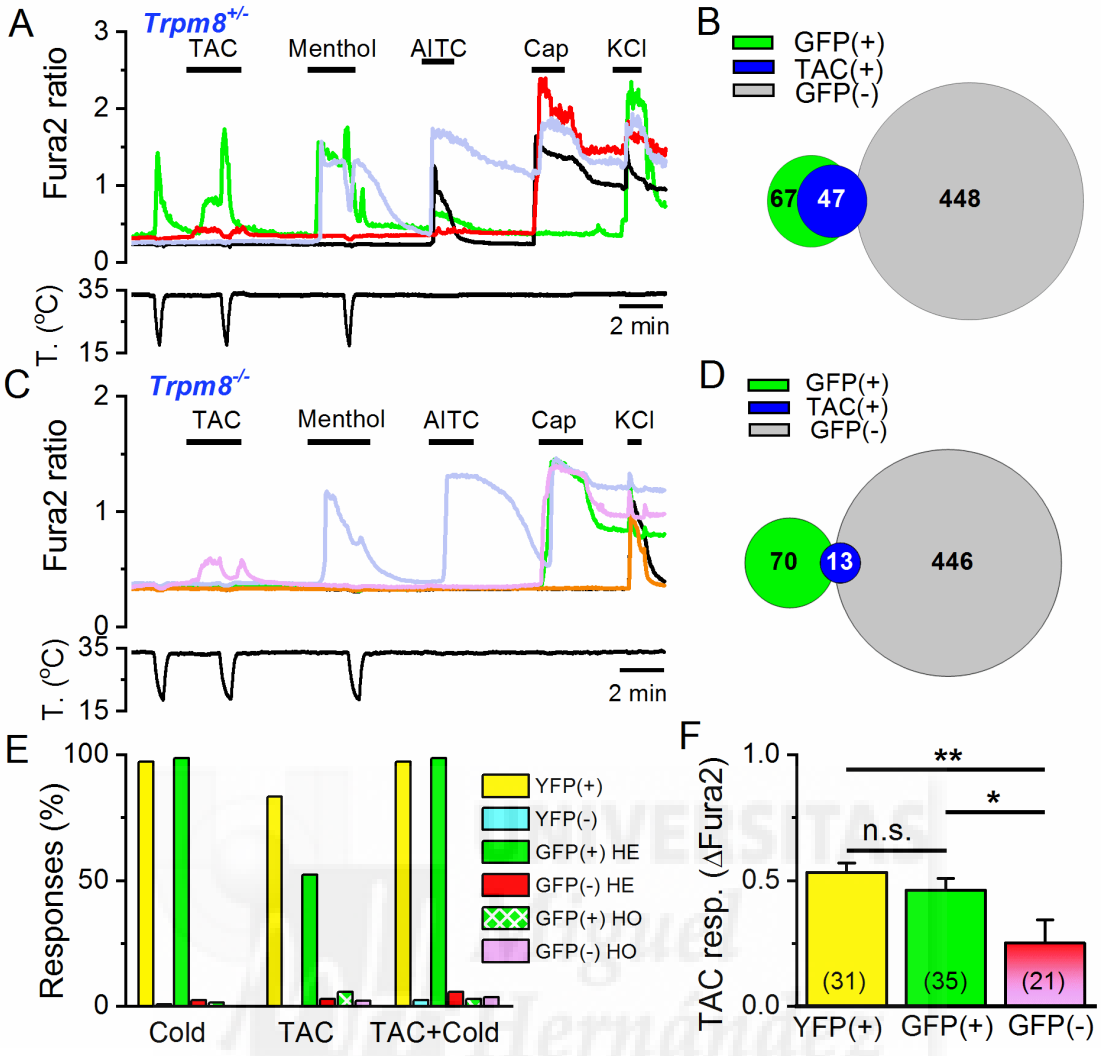

Figure 21. TRPM8 is the principal mediator of the excitatory effects of tacrolimus on DRG neurons. ***A,*** Representative traces of Fura-2 ratio fluorescence in a TRPM8$^{EGFPf/+}$ DRG culture. Consecutive applications of cold, TAC (30 μM), menthol (100 μM), AITC (100 μM), capsaicin (100 nM) and high K^+ (30 mM) were used to define the phenotype of each neuron. The GFP(+) neuron (green trace) is activated by cold, TAC and menthol. A GFP(-) neuron (red trace) is not activated by cold or menthol but shows a small response to TAC; typically these neurons are activated by capsaicin. ***B,*** Venn diagram summarizing the responses to TAC in GFP(+) and GFP(-) neurons in TRPM8$^{EGFPf/+}$ mice. ***C,*** Representative traces of Fura-2 ratio fluorescence in cultured DRG neurons from a TRPM8 KO mouse. Same protocol as in A. Note the inhibition of the small TAC response by cooling in a GFP(-) neuron (pink trace). A GFP(+) neuron (green trace) does not respond to cold or menthol but responds to capsaicin. ***D,*** Venn diagram summarizing the responses to TAC in GFP(+) and GFP(-) neurons in TRPM8 KO mice. ***E,*** Summary of responses (in percentage of total neurons) to cold, TAC and TAC plus cold in TRPM8$^{BAC\text{-}EYFP}$, *TRPM8*$^{EGFPf/+}$ and *TRPM8*$^{EGFPf/EGFPf}$ mice. For each mouse line, neurons have been separated as fluorescent or non-fluorescent. ***F,*** Mean amplitude of TAC responses in fluorescent (TRPM8$^{BAC\text{-}EYFP}$ and *TRPM8*$^{EGFPf/+}$) and non-fluorescent neurons (*TRPM8*$^{EGFPf/+}$ and *TRPM8*$^{EGFPf/EGFPf}$). Differences in amplitude between fluorescent and non-fluorescent neurons were statistically significant (one-way ANOVA).

Taken together, the results obtained with pharmacological blockers and after genetic inactivation of TRPM8 indicate that the main excitatory action of TAC in DRG neurons is mediated by activation of TRPM8 channels in cold-sensitive neurons, with some weaker effects on capsaicin-sensitive neurons, presumably though TRPV1.

4.1.9 Tacrolimus activates inward currents and elicits action potential firing in cold thermoreceptors

The effect of TAC on the excitability of cold thermoreceptors was further evaluated by performing electrophysiological recordings in cultured DRG neurons from TRPM8$^{BAC\text{-}EYFP}$ mice. As shown in Figure 22A, in whole-cell patch-clamp recordings, TAC (30 μM) activated an inward current and potentiated the currents evoked by cold temperature in all the YFP(+) neurons tested. This potentiation was accompanied by a clear shift in the activation of cold-evoked currents to warmer temperatures (Fig. 22B). In the same neurons, application of menthol (30 μM) produced similar effects to TAC, although its potentiating effect on cold-evoked currents was stronger. A summary of these results is shown in Figure 22C.

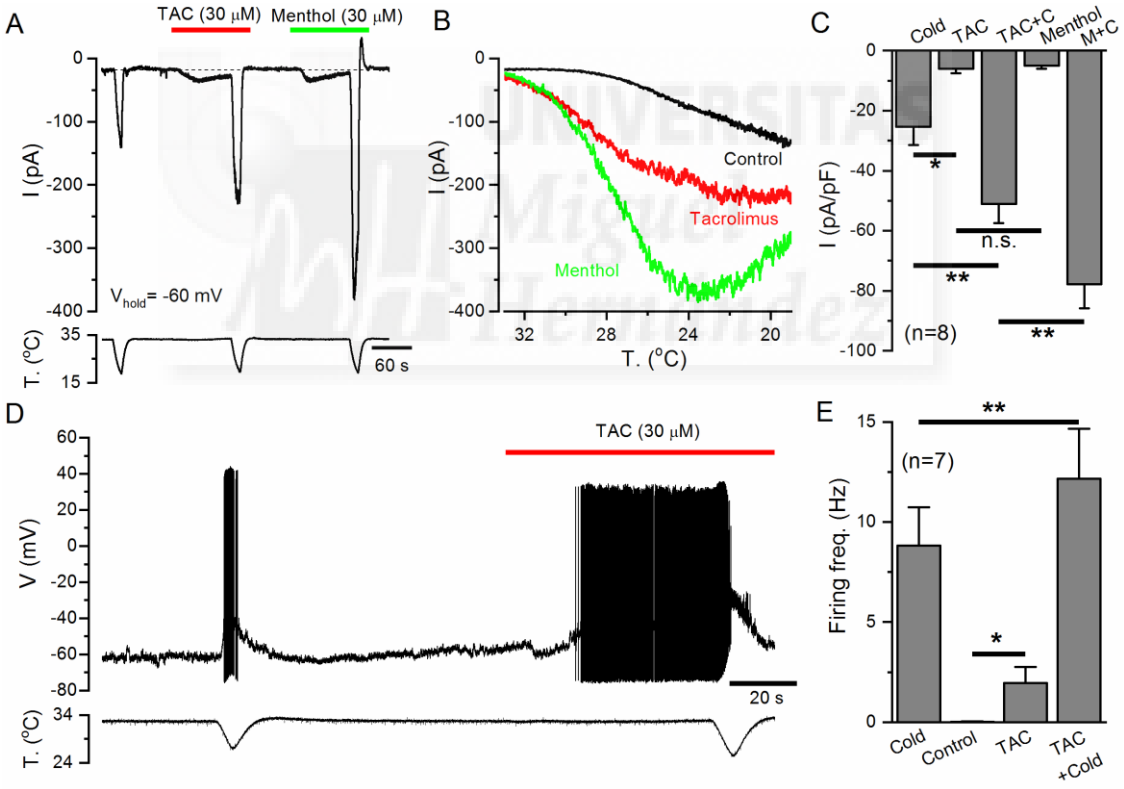

Figure 22. Tacrolimus increases the excitability of cold-sensitive DRG neurons. *A,* Representative whole-cell recording in the voltage-clamp configuration (V_{hold}= -60 mV) of a TRPM8-expressing, cold-sensitive DRG neuron identified by the expression of EYFP. TAC (30 μM) evoked an inward current similar in amplitude to that elicited by menthol (30 μM). Both, TAC and menthol strongly potentiate the response to cold. Bottom trace correspond to the simultaneous recording of bath temperature during the recording. ***B,*** Current–temperature relationships for the same neuron in control (black trace) and in the presence of 30 μM TAC (red trace) or 30 μM menthol (green trace). Note the marked shift in temperature

threshold. ***C,*** Bar histogram summarizing the effects of agonists on the amplitude of inward currents during the protocol shown in A. The statistical analysis consisted on a one-way ANOVA followed by Bonferroni's post-hoc test. **D,** Representative recording of a cold-sensitive DRG neuron in the whole-cell current-clamp configuration showing responses to cold and to the application of TAC (30 μM). TAC evoked AP firing at 33 ºC and greatly enhanced the firing frequency during a cold ramp. Bottom trace corresponds to the simultaneous recording of bath temperature. ***E,*** Bar histogram summarizing the mean responses, measured as average firing frequency, during the different stimuli applied. Firing frequency for cold was averaged from the first to the last spike during the cooling ramp. Firing frequency in control condition was calculated during the minute preceding TAC application (only 3 out of 7 neurons fired action potentials in control conditions). TAC-evoked firing was calculated from the first spike during TAC application to the start of the cold ramp. The analysis consisted of a paired t-test for cold vs TAC plus cold ($p = 0.009$) and control vs TAC ($p= 0.048$).

Recordings in the current-clamp configuration of TRPM8-expressing cold thermoreceptors, at a holding temperature of 33 ºC, showed that TAC application induced the firing of action potentials and strongly potentiated cold-evoked firing (Fig. 22D). These results are summarized in Figure 22E.

These data confirm that TAC activates a depolarizing inward current similar to the TRPM8-dependent I_{Cold} current, increasing the excitability of cold-sensitive neurons.

4.1.10 Tacrolimus triggers tearing and blinking

A previous study identified the critical role of TRPM8 channels on eye blinking in mice following application of hyperosmolar solutions (Quallo et al., 2015). Thus, I decided to investigate the effects of TAC solutions applied to the corneal surface. I was assisted by Katharina Gers-Barlag in these experiments. We counted the number of blinks observed after unilateral application of solutions with 1% TAC to the eyes of wild type (n = 8) and *Trpm8*$^{-/-}$ mice (n = 17). Application of saline (315 mOsm/kg) or vehicle had only a small effect on blinking. In contrast, as shown in Figure 23 (left panel), 1% TAC triggered a large increase in the number of blinks in wild type mice. In agreement with previous findings (Quallo et al., 2015), hyperosmotic solutions (785 mOsm/kg) also triggered a marked increase in eye blinking, similar to that observed with TAC.

Repeating the tests in TRPM8 KO mice confirmed a reduction in blinking, compared to wild type ($p<0.01$, unpaired t-test), produced by hyperosmolar solutions reported previously. In contrast, the blinks produced by 1% TAC in TRPM8 KO mice were very variable but they were not different from those observed in wild type mice (Fig. 23, right panel). These results suggest that 1% TAC has effects on blinking that are in independent of TRPM8 activity.

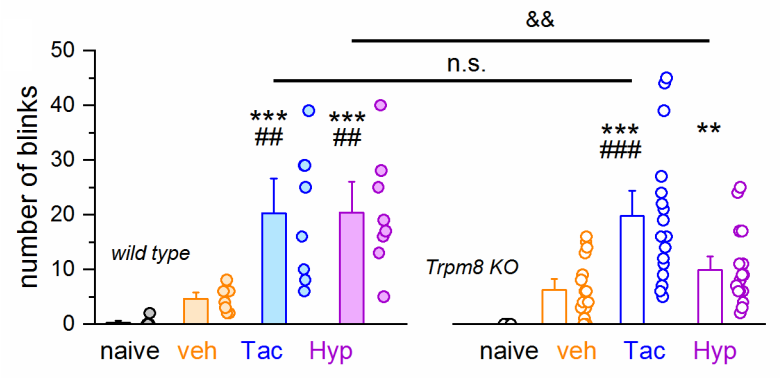

Figure 23. Tacrolimus triggers blinking in a TRPM8-independent manner. Effects of different topical solutions (5 µl) on eye blinking, monitored over a 2 minute period, in wild type mice (filled bars; n = 8). Compared to saline (*) and vehicle (#) (see above), 1% TAC and hyperosmotic (785 mOsm/kg) solution increased the number of blinks. In TRPM8 KO mice (open bars; n = 17), TAC increased the number of blinks with respect to saline ($p<0.001$, ***) or the TAC vehicle ($p<0.001$, ###) and Hyp increased the blinks with respect to saline ($p<0.001$) (one-way ANOVA followed by Bonferroni's post-hoc test). Note that the number of blinks to Hyp were significantly reduced in TRPM8 KO mice compared to wild type (&&$p<0.01$, unpaired Student t-test).

4.2 The immunosuppressant macrolide rapamycin activates TRPM8 channels

In this block of experiments rapamycin, a molecule structurally related to TAC, is presented as a novel TRPM8 agonist. I characterized the effect of rapamycin on recombinant TRPM8 channels and on native TRPM8 channels expressed in mouse DRG cold-sensitive neurons.

4.2.1 Rapamycin activates recombinant TRPM8 channels

To investigate the effect of rapamycin on TRPM8 channels, I performed intracellular Ca^{2+} imaging experiments on HEK293 cells stably expressing rat TRPM8 channels. Rapamycin was applied in independent experiments at four different concentrations (1, 3, 10 and 30 µM) during 150 s. As shown in Figure 24A and 24B, rapamycin produced a dose-dependent activation of TRPM8. Similar to TAC, rapamycin had poor solubility in aqueous solutions, limiting the maximum concentration I could test. At low concentrations the calcium response evoked by rapamycin had a slow rise and was sustained, while at higher concentrations rapamycin evoked faster responses that desensitized partially during the time of application (Fig. 24A). Rapamycin has been shown to interact with Ca^{2+} channels present in the endoplasmatic reticulum, such as ryanodine receptors (Brillantes et al., 1994; Lombardi et al., 2017). In order to corroborate that calcium responses evoked by rapamycin were due to a calcium influx from the outside (presumably through TRPM8 channels) and not by calcium release from intracellular stores, the effect of rapamycin was explored using the extracellular control solution (2.4 mM Ca^{2+}) and an extracellular solution without calcium. In calcium imaging experiments, rapamycin (30 µM) evoked clear responses in the presence of extracellular calcium, whereas when calcium was removed, rapamycin-evoked responses were totally absent (Fig. 24C-D).

Next, I studied the sensitivity of other TRPM8 orthologues to rapamycin. HEK293 cells expressing mouse TRPM8 were activated by a cooling ramp, by subsequent application of rapamycin (30 µM) and by menthol (30 µM) (Fig. 24E, blue trace). Rapamycin- and menthol-evoked responses were similar in amplitude and significantly smaller in amplitude compared to cold-evoked responses (Cold= 0.96 ± 0.08 *vs* Rapamycin= 0.4 ± 0.03 *vs* Menthol= 0.47 ± 0.03, n= 97) (Fig. 24F). TRPM8 agonists potentiate responses to cold (Voets et al., 2004; Mälkiä et al., 2007). In the presence of rapamycin, cold-evoked responses were strongly potentiated, a significantly more potent effect than that induced by menthol (Cold= 0.96 ± 0.08 *vs* Rapamycin + Cold= 2.96 ± 0.13 *vs* Menthol + Cold= 2.43 ± 0.12) (Fig. 24F). Additionally, there was a subset of cells which did not respond to cold in control conditions but responded to cold in the presence of rapamycin or menthol (Fig. 24E, green trace). Cells not expressing mTRPM8 (i.e. those not responding to cold in the presence of an agonist) did not show changes in intracellular Ca^{2+} levels in the presence of rapamycin (Fig. 24E, black trace).

I also explored the sensitivity of human TRPM8 to rapamycin. In HEK293 cells expressing hTRPM8, rapamycin (30 µM) evoked a robust response which was similar in amplitude to the

cold-evoked response and significantly higher than the menthol-induced response at the same concentration (Cold= 0.88 ± 0.06 *vs* Rapamycin= 0.93 ± 0.05 *vs* Menthol= 0.57 ± 0.04, n= 115) (Fig. 24G-H, red trace). hTRPM8-mediated cold responses were also strongly potentiated by rapamycin, and, remarkably, this effect was stronger than the menthol-evoked potentiation (Cold= 0.88 ± 0.06 *vs* Rapamycin + Cold= 2.52 ± 0.12 *vs* Menthol + Cold= 1.88 ± 0.1, n= 115) (Fig. 24G-H red trace). As in the case of mTRPM8, a subset of cold-insensitive cells in control conditions responded to cold in the presence of rapamycin and menthol (Fig. 24G green trace). Cells not expressing hTRPM8 did not showed changes in intracellular Ca^{2+} levels in the presence of rapamycin (Fig. 24G, black trace).

In conclusion, rapamycin acts as an agonist of rat, mouse and human TRPM8 channels. As in the case of other agonists, rapamycin potentiates the response to cold. I observed that this effect was more potent for rapamycin than for menthol, the canonical TRPM8 agonist.

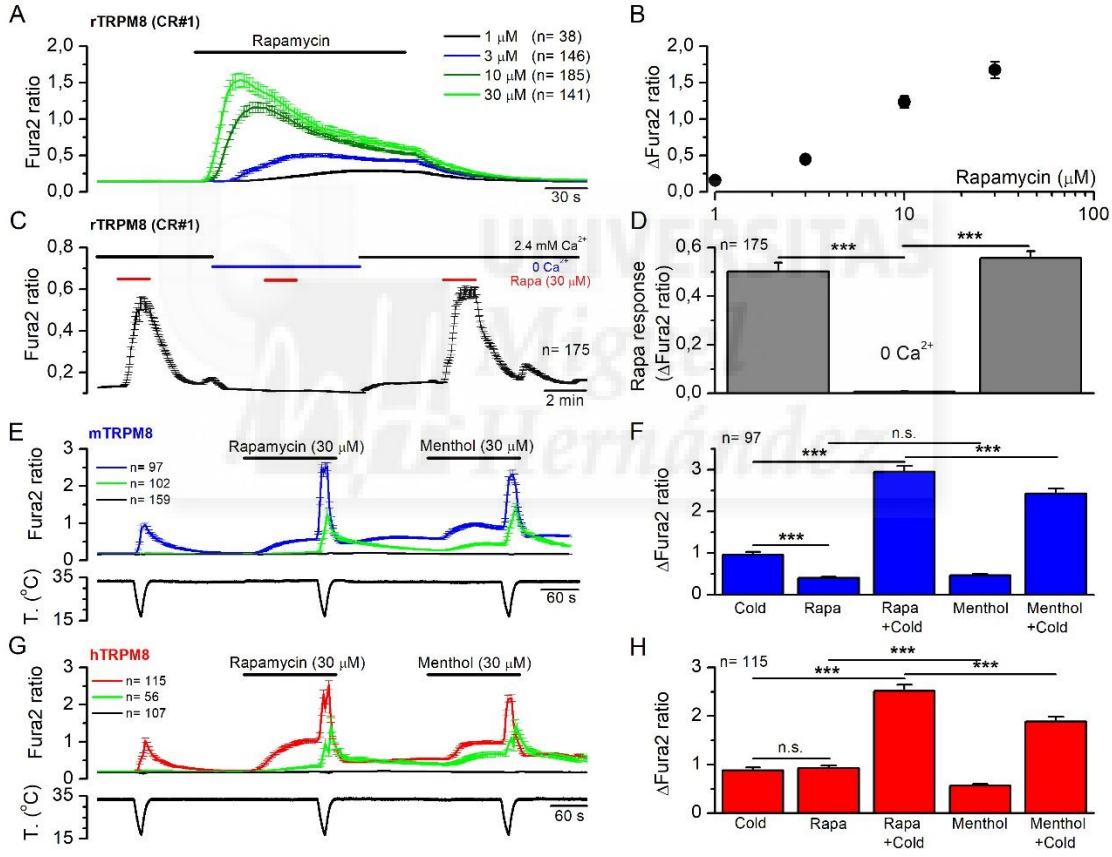

Figure 24. Rapamycin activates recombinant TRPM8 channels and potentiates cold-evoked responses. ***A,*** Average ± SEM Fura2 ratio time course in HEK293 cells stably expressing rat TRPM8 during rapamycin application at different concentrations. A single dose was applied in individual experiments. ***B,*** Dose-response curve of rapamycin effects. Averaged values were obtained from individual peak amplitudes from experiments shown in A. ***C,*** Average ± SEM Fura2 ratio time course in HEK293 cells stably expressing rat TRPM8 during a protocol in which rapamycin responses were explored in the presence (2.4 mM Ca^{2+}) and in the absence (0 Ca^{2+}) of extracellular calcium (n= 175). ***D,*** Bar histogram summarizing the amplitude of rapamycin responses in the experiment showed in C.

Statistical significance was calculated by a one-way ANOVA for repeated measures followed by Bonferroni post-hoc test. ***E,*** Average ± SEM fura2 ratio time course in HEK293 cells expressing mouse TRPM8. Three different behaviors were observed; cells which responded to a first cold ramp in control conditions (blue trace), cells which did not respond to a first cold ramp in control conditions but responded to cold in the presence of rapamycin or menthol (green trace), and cells which did not show any response to the applied stimuli (black trace). ***F,*** Bar histogram summarizing the responses of the cold-sensitive HEK293 cells transfected with mouse TRPM8 to different agonists. Statistical significance was calculated by a one-way ANOVA followed by Bonferroni post-hoc test. ***G,*** Average ± SEM Fura2 ratio time course in HEK293 cells expressing human TRPM8. The different traces represented the three behaviors described in E. ***H,*** Bar histogram summarizing the responses of the cold-sensitive HEK293 cells transfected with human TRPM8. Statistical significance was calculated by a one-way ANOVA followed by Bonferroni post-test.

4.2.2 Rapamycin activates TRPM8 currents

Next, I studied the effect of rapamycin on TRPM8 channels by electrophysiological techniques. In whole-cell patch-clamp recordings, application of 30 µM rapamycin activated robust whole-cell currents in HEK293 cells expressing mouse TRPM8 (Fig. 25A). The current-voltage relationship of the rapamycin-activated current showed strong outward rectification and a reversal potential close to 0 mV, in line with the known properties of TRPM8 channels (Voets et al., 2004) (Fig. 25B). These results confirmed the findings obtained in calcium imaging experiments. Cold-evoked inward currents, measured at -100 mV, were strongly potentiated in the presence of TAC, a similar effect than that produced by menthol at the same concentration (Cold= -10.2 ± 1.3 pA/pF *vs* Rapamycin + Cold= -497.32 ± 87.1 pA/pF *vs* Menthol + Cold= -384.26 ± 66 pA/pF, n= 9); similar effect was observed for outward currents, measured at +100 mV (Cold= 381.5 ± 49.5 pA/pF *vs* Rapamycin + Cold= 758.49 ± 134.5 pA/pF *vs* Menthol + Cold= 726.72 ± 80.2 pA/pF, n= 9). Moreover, rapamycin and menthol at the same concentration (30 µM) evoked outward currents of similar amplitude (Rapamycin= 253.64 ± 34.9 pA/pF *vs* Menthol= 326.76 ± 44 pA/pF, n= 9) suggesting that the potency of both compounds as TRPM8 agonist is similar. A summary of these results is shown in Figure 25C. Additionally, I estimated the $V_{1/2}$ values in the presence of cold, rapamycin and menthol by fitting the traces derived from the voltage ramps with a Boltzmann-linear function (see Material and methods) and compared them to the $V_{1/2}$ value in control conditions (Fig. 25D). Rapamycin causes a strong shift of $V_{1/2}$ toward more negative membrane potentials ($\Delta V_{1/2}$= -102.6 ± 4.7 mV) (Fig. 25D). Menthol has a similar effect ($\Delta V_{1/2}$= -109.3 ± 5.9 mV), while cold led to a more pronounced shift ($\Delta V_{1/2}$= -154.6 ± 5.4 mV) (Fig. 25D). This result corroborated that rapamycin, as other TRPM8 agonists, activates TRPM8 by a shift in the voltage activation curve toward physiologically relevant membrane potentials.

To confirm the agonism of rapamycin on TRPM8 channels, I tested the effect of AMTB, a selective antagonist of TRPM8 channels (Lashinger et al., 2008). As shown in Figure 25E, AMTB fully suppressed TRPM8 currents evoked by rapamycin (Rapamycin= 171.64 ± 26.2 pA/pF *vs* Rapamycin + AMTB= 19.84 ± 4.9 pA/pF) (n= 6, $p< 0.01$). AMTB at the concentration used (10 µM) also blocked the voltage-dependent activation of TRPM8 at the baseline temperature of 33

ºC, although it did not block totally the response to cold in the presence of rapamycin (Fig. 25E-G).

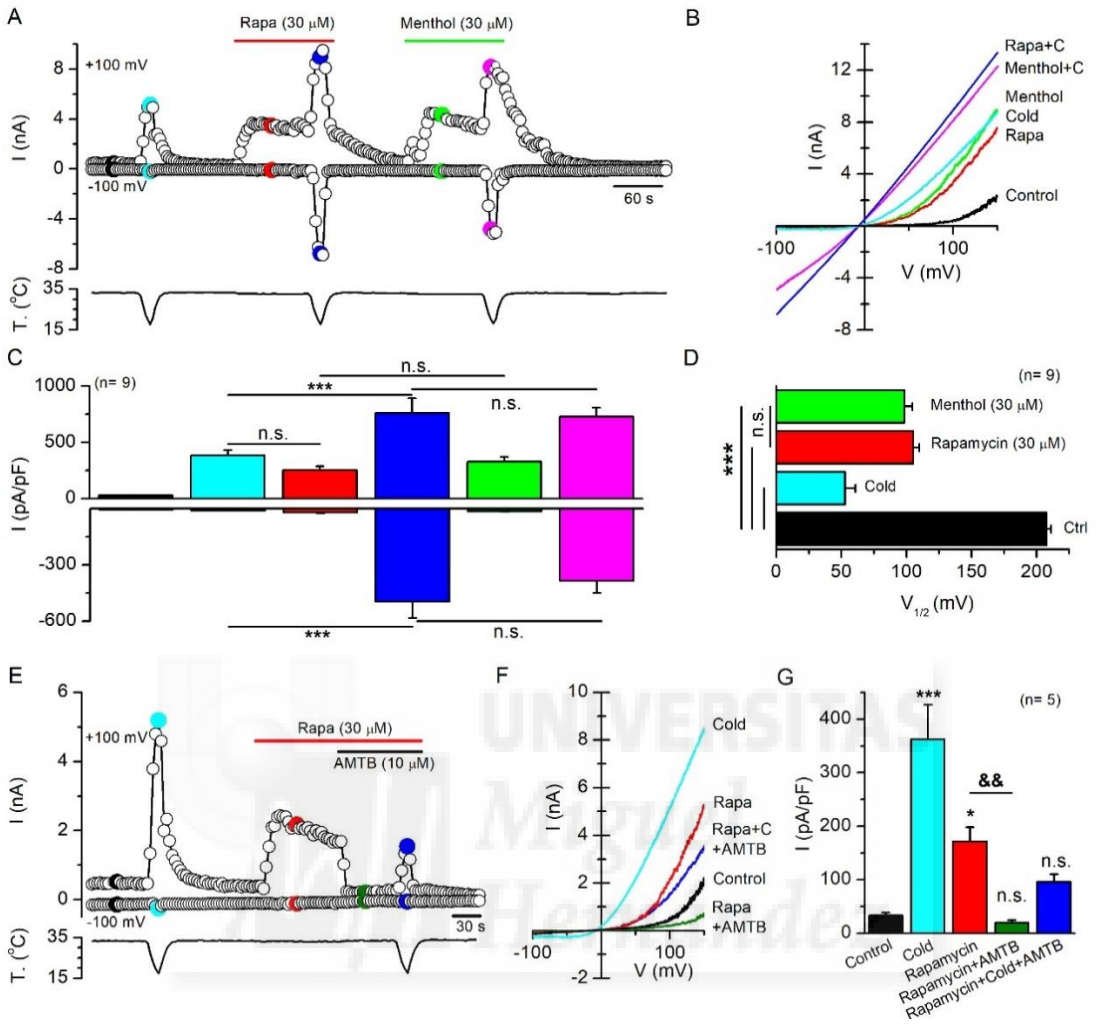

Figure 25. Rapamycin activates TRPM8 currents. ***A,*** Representative time course of whole-cell current at -100 and +100 mV in a HEK293 transiently transfected with mTRPM8 during the application of different agonists. The bottom trace shows the simultaneous recording of the bath temperature during the experiment. ***B,*** Current-voltage (I-V) relationship obtained by a 400 ms voltage ramp from -100 to +150 mV during the experiment shown in A. The color of individual traces matches the color at each particular time point in A. ***C,*** Bar histogram summarizing the mean current density at -100 and +100 mV evoked by the different stimuli shown in A, with the same color code. Statistical differences were evaluated by a one-way ANOVA, followed by Bonferroni's post-hoc test. ***D,*** Mean (n= 9) $V_{1/2}$ values calculated from fitting individual I-V curves to a linearized Boltzmann equation. Statistical differences were evaluated by a one-way ANOVA, followed by a Bonferroni´s post-hoc test. ***E,*** Representative whole-cell current at -100 and +100 mV in a HEK293 cell transiently transfected with mTRPM8 during a protocol in which the effect of AMTB on rapamycin response was explored. Bottom trace corresponds to the simultaneous recording of bath temperature during the experiment. ***F,*** Current-voltage relationship (I-V) obtained with a 400 ms voltage ramp from -100 to +150 mV of the responses plotted in E. The color of the I-V curves matches the colored time points in D. ***G,*** Bar histogram summarizing the mean current density at +100 mV evoked by the different stimuli shown in D. Statistical differences were evaluated by a one-way ANOVA, followed

by Bonferroni's post-hoc test. Asterisks are used for comparing the effect of the different stimuli with respect to control (*, p-value< 0.05; ***, p-value< 0.001) whereas the & symbol is used for the comparison of two different stimuli (&&, p-value< 0.01).

4.2.3 Rapamycin activates TRPM8-expressing cold-sensitive neurons in a TRPM8-dependent manner and potentiates their cold response

To study the effects of rapamycin on TRPM8-expressing sensory neurons, I performed calcium imaging experiments in DRG cultures from TRPM8$^{BAC\text{-}EYFP}$ mice. TRPM8-expressing neurons were identified by their response to a cold ramp and EYFP expression (Fig. 26A-B). Nearly all EYFP(+) neurons, 97% (33 out of 34), responded to a cooling ramp and 94.1% (32 out of 34) also responded to rapamycin (30 μM) application (Fig. 26C). In contrast, only a small percentage of EYFP(-) neurons were activated by 30 μM rapamycin (2 out of 236), although they showed normal responses to 30 mM KCl (data not shown). Rapamycin-evoked responses were comparable in amplitude to cold-evoked responses (Cold= 0.89 ± 0.07 *vs* Rapamycin= 0.69 ± 0.06) (n= 32, p< 0.05) and strongly correlated in individual neurons (r^2= 0.76) (Fig. 26D-E). Co-application of a cooling stimulus in the presence of rapamycin strongly potentiates the amplitude of the cold-evoked response (Cold= 0.89 ± 0.07 *vs* Rapamycin + Cold= 1.31 ± 0.09) (n= 32, p<0.001) (Fig. 26D). To explore the TRPM8-dependence of these responses, I studied a second rapamycin response in the presence of AMTB (10 μM), a specific blocker of TRPM8 channels. Rapamycin responses were totally abolished in the presence of AMTB (Rapamycin= 0.69 ± 0.06 *vs* Rapamycin + AMTB= 0.01 ± 0.005) (n= 32, p<0.001), confirming the absolute TRPM8 dependence of rapamycin responses in cold-sensitive neurons (Fig. 26A, 26D). The cold response in the presence of rapamycin was also strongly reduced in the presence of this antagonist, and cold-sensitivity was recovered after AMTB wash out (Fig. 26A, 26D).

Next, I examined the effect of a lower concentration of rapamycin (1 μM) on the thermal sensitivity of TRPM8 neurons (Fig. 26F). Rapamycin 1 μM activated 67% (10 out of 15) of the cold-sensitive and EYFP(+) neurons. Moreover, at this lower concentration, rapamycin significantly potentiates the cold-evoked response in a reversible manner (Cold= 0.87 ± 0.09 *vs* Rapamycin + Cold= 1.0 ± 0.1) (n= 15, p<0.01) (Fig. 26F-G).

Collectively, these results indicated that rapamycin activates cold-sensitive TRPM8-expressing neurons in a highly specific manner. Rapamycin, even at low concentrations, strongly potentiates de cold response of these neurons.

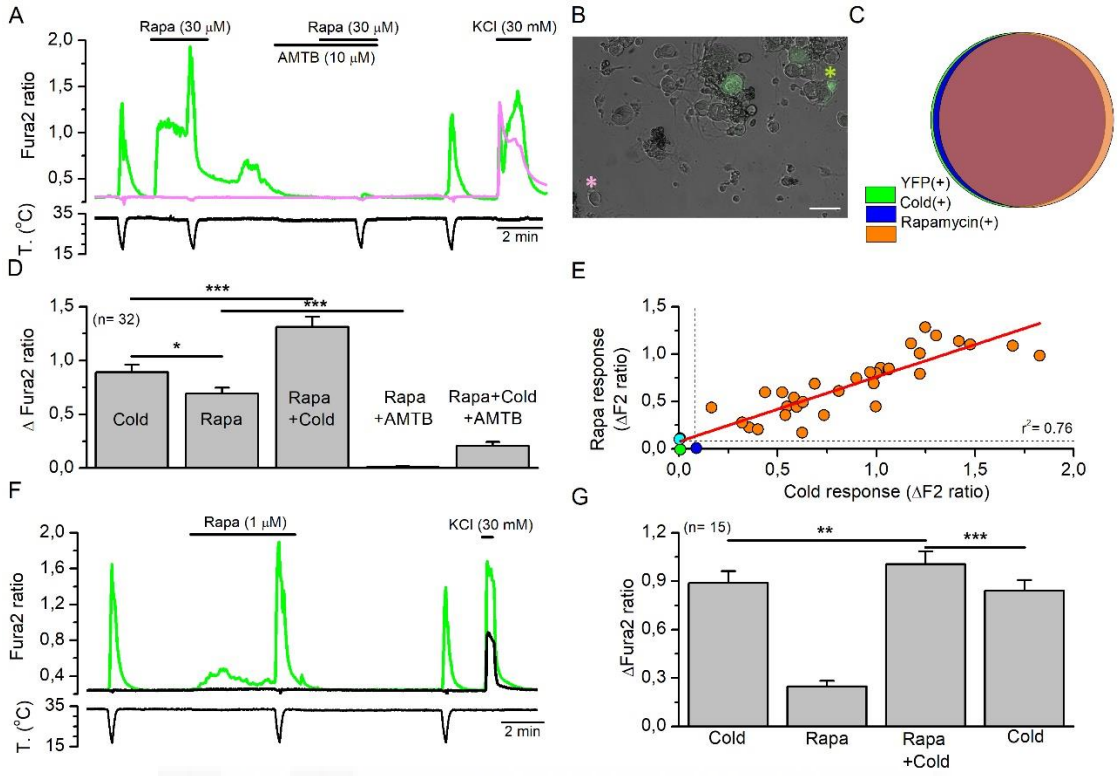

Figure 26. Rapamycin activates cold-sensitive neurons and potentiates their cold response. *A*, Representative Fura2 fluorescence measurement from cultured DRG neurons of TRPM8$^{BAC\text{-}EYFP}$ mice. A cold-sensitive and EYFP(+) neuron (green trace) and a EYFP(-) neuron (pink trace) are represented. Bottom trace corresponds to the simultaneous recording of bath temperature. ***B,*** Superimposed transmitted and EYFP fluorescence images from DRG cultured neurons of a TRPM8$^{BAC\text{-}EYFP}$ mouse. Asterisks correspond to the neurons whose traces are shown in A. The other two fluorescent neurons in the field had a baseline calcium level higher than 0.8 and were removed from the analysis. The calibration bar is 100 μm. ***C,*** Venn diagram showing the very strong overlap between EYFP(+) neurons (n= 34), cold-sensitive neurons (n= 33) and rapamycin-sensitive neurons (n= 32). Only 2 out of 236 EYFP(-) neurons were rapamycin-sensitive. ***D,*** Bar histogram showing the averaged amplitude of the responses observed in EYFP(+) rapamycin-sensitive neurons. Statistical significance was assessed by a one-way ANOVA for repeated measures followed by a Bonferroni's post-hoc test. ***E,*** Correlation between amplitude of cold- and rapamycin-evoked responses in individual EYFP(+) DRG neurons (n= 34). Orange circles represent neurons that responded to rapamycin and cold, dark blue point represents the neuron which responded to cold but not to rapamycin (note the very small response to cold), the green point represents the single EYFP(+) neuron which did not respond to either stimulus and the light blue points represent the only two EYFP(-) neurons which respond to rapamycin (overlapped). Dotted lines delimited the threshold that was considered as a response (ΔF2 ratio= 0.08). ***F,*** Time course of Fura2 fluorescence of a cold-sensitive EYFP(+) neuron (green trace) in which rapamycin (1 μM) evoked a substantially increase in intracellular calcium levels, and a cold-insensitive EYFP(-) neuron (black trace). Bottom trace corresponds to the simultaneous recording of bath temperature. ***G,*** Bar histogram summarizing the effect of rapamycin (1 μM) on cold-sensitive neurons. Statistical significance was assessed by a one-way ANOVA for repeated measures followed by a Bonferroni's post-hoc test.

4.2.4 Rapamycin responses are almost absent in TRPM8 KO mice

To investigate the dependence of rapamycin responses on TRPM8, I took advantage of a transgenic mouse line ($TRPM8^{EGFPf}$) expressing EGFPf from the TRPM8 locus (Dhaka et al., 2007). The heterozygous mice ($TRPM8^{EGFPf/+}$) express one functional copy of TRPM8 and one copy of EGFPf, while the homozygous littermates ($TRPM8^{EGFPf/EGFPf}$) are KO for TRPM8. In $TRPM8^{EGFPf/+}$ DRG cultures, all EGFPf(+) neurons (18 out of 18) responded to a control cold ramp in control conditions and to menthol (100 µM), confirming the expression of TRPM8. They represented 16% of all the neurons in the culture. The majority of these TRPM8-expressing neurons, 83.3% (15 out of 18), also responded to rapamycin (30 µM) (Fig. 27A-B). In contrast, only 3 neurons of the 112 EGFPf(-) neurons showed a response to rapamycin (Fig. 27B), a significant lower fraction compared to the EGFPf(+) population ($p<0.001$, Z test). Cold- and rapamycin-induced responses were similar in amplitude (Cold= 0.98 ± 0.12 *vs* Rapamycin= 0.73 ± 0.09) (n= 15, n.s.) and their size were strongly correlated in individual neurons ($r^2= 0.56$) (Fig. 27C-D). Rapamycin was also effective in potentiating the cold-evoked response (Cold= 0.98 ± 0.12 *vs* Rapamycin + Cold= 1.8 ± 0.2) (n= 15, $p<0.001$) (Fig. 27C). This effect was even more potent for rapamycin at 30 µM than for menthol at 100 µM (Menthol + Cold= 1.53 ± 0.16) (n= 15, n.s.) (Fig. 27A and 27C).

Confirming previous findings (Dhaka et al., 2007), in DRGs from homozygous mice ($TRPM8^{EGFPf/EGFPf}$) the responses to menthol and cold were abrogated; none of the 36 EGFPf(+) recorded neurons responded to menthol and only 2 of them responded to cold. Rapamycin responses were also very infrequent in these cultures. Only 5 out of 257 (1.9%) neurons responded to rapamycin, 3 were EGFPf(+) and 2 were EGFPf(-) (Fig. 27F). The most significant decreased of rapamycin responses occurred on EGFPf(+) neurons ($p<0.001$, Z test). Remarkably, the rapamycin responses in these three EGFPf(+) neurons were mantained during the time of application and decreased during the cooling ramp (Fig. 27E), while the responses of EGFPf(-) neurons were transient and smaller in amplitude. Two of these EGFPf(+) rapamycin sensitive neurons responded to capsaicin while the other was capsaicin-insensitive, AITC-insensitive, but was activated by cold and cold in the presence of menthol (not shown).

Altogether, the results obtained in TRPM8 KO mice suggest that the main excitatory action of rapamycin is mediated by TRPM8 channels in cold-sensitive neurons.

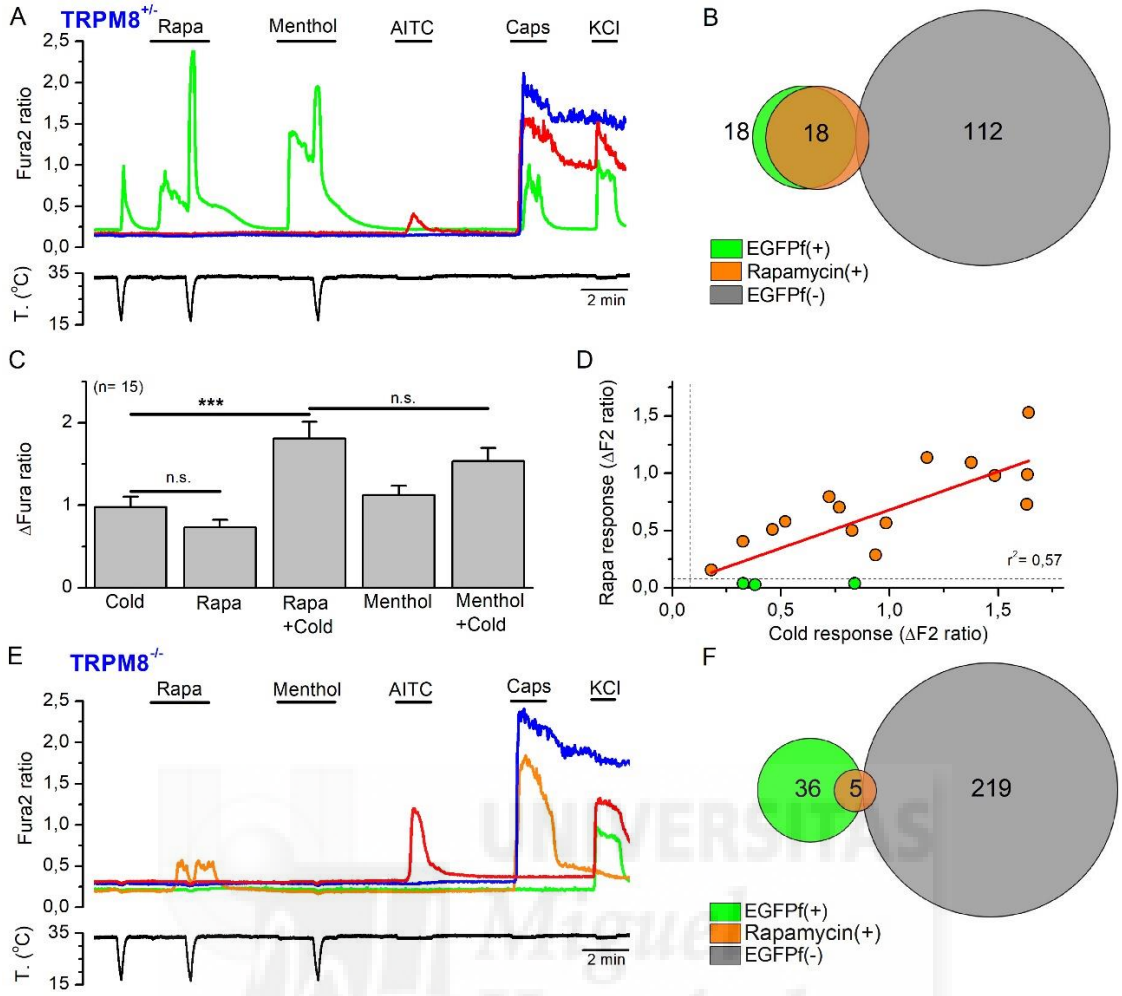

Figure 27. TRPM8 is the principal determinat of rapamycin responses in DRG neurons. *A,* Representative traces of Fura-ratio fluorescence in a TRPM8$^{EGFPf/+}$ DRG culture. Consecutive applications of cold, rapamycin, menthol (100 µM), AITC (100 µM), capsaicin (100 nM) and high K^+ (30 mM) were used to phenotype each neuron. The green trace corresponds to a EGFPf(+) neurons which responds to cold, rapamycin, menthol and capsaicin. The other two traces (blue and red) correspond to EGFP(-) neurons. Bottom trace shows the simultaneous recording of bath temperature. ***B,*** Venn diagram summarizing the responses to rapamycin in EGFPf(+) and EGFPf(-) neurons in TRPM8$^{EGFPf/+}$ DRG cultures. ***C*****,** Bar histogram summarizing the amplitude of the responses to different agonists in EGFPf(+) rapamycin-sensitive neurons. Statistical significance was analyzed by a one-way ANOVA for repeated measures followed by a Bonferroni's post-hoc test. ***D*****,** Correlation between the amplitude of the cold-evoked response and the rapamycin response (n= 15). Green points represent the EGFPf(+), cold-sensitive, rapamycin-insensitive neurons. ***E*****,** Representative traces of Fura2 fluorescence in cultured neurons from TRPM8 KO mouse. The protocol was the same as in A. Orange trace corresponds to a EGFPf(+) neuron that was rapamycin-sensitive. Green trace represent a EGFPf(+) neuron which was not sensitive to any agonist tested. Red trace corresponds to a EGFP(-) neuron. Bottom trace corresponds to the simultaneous recording of the bath temperature during the experiment. ***F*****,** Venn diagram summarizing the responses to rapamycin in EGFPf(+) and EGFPf(-) neurons in TRPM8$^{EGFPf/\ EGFPf}$ DRG cultures.

4.2.5 Rapamycin activates inward currents and elicits AP firing in cold thermoreceptors

Finally, I evaluated the effects of rapamycin on cold-sensitive neurons by patch-clamp recordings in cultured DRG neurons from TRPM8$^{BAC\text{-}EYFP}$ mice. In the whole-cell, voltage-clamp configuration, a cooling ramp in control conditions activated a small inward current (Fig. 28A). Application of rapamycin also activated a small inward current and strongly potentiated the cold-evoked response (Cold= -13.96 ± 5.9 pA/pF *vs* Rapamycin + Cold= -65.59 ± 7.7 pA/pF) (n= 7, p<0.001) (Fig. 28A-B). In the current-clamp configuration, rapamycin induced the firing of action potentials in cold-sensitive neurons at a basal temperature of 33 ºC in all the neurons tested (6 out of 6) (Fig. 28C). The cold- and rapamycin-evoked firing frequency was similar (Cold= 10.63 ± 1.9 Hz *vs* Rapamycin= 9.89 ± 3 Hz). In these neurons, rapamycin also increased the firing frequency during cold stimulation (Cold= 10.63 ± 1.9 Hz *vs* Rapamycin + Cold= 15.18 ± 2.9 Hz) (n= 6, p= 0.06; Fig. 28D).

These results corroborate that rapamycin is able to activate a depolarizing current in DRG cold-sensitive neurons increasing their excitability to cold.

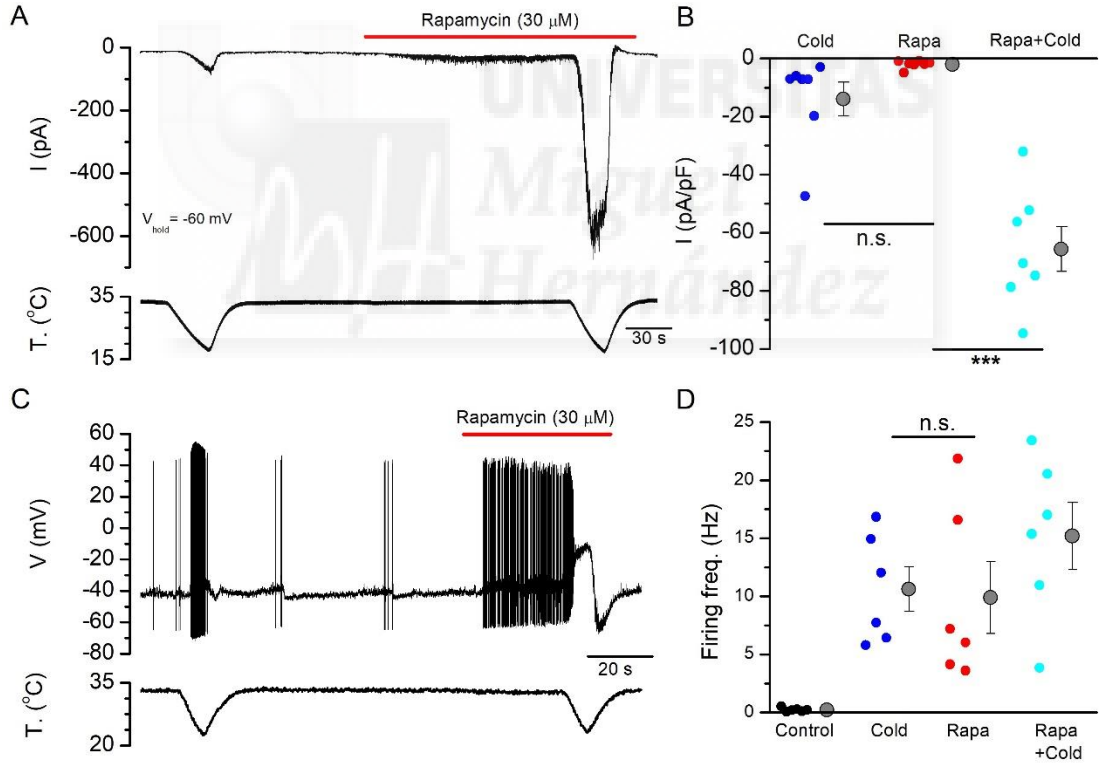

Figure 28. Rapamycin increases the excitability of cold-sensitive DRG neurons. *A*, Representative whole-cell recording in the voltage-clamp configuration (V_{hold}= -60 mV) of a TRPM8-expressing, cold-sensitive DRG neurons identified by EYFP expression. Bottom trace corresponds to the simultaneous recording of bath temperature during the experiment. ***B*,** Bar histogram summarizing the mean peak inward current density evoked by cold, rapamycin and cold in the presence of rapamycin of the recorded cells. The statistical analysis consisted on a one-way ANOVA for repeated measures followed by Bonferroni's post-hoc test. ***C,*** Representative recording of a cold-sensitive neuron in the whole-cell current-clamp configuration. Cold and rapamycin elicited the firing of action potentials. The combined

application of cold and rapamycin led to faster firing, followed by large depolarization and the blockade of spikes. ***D,*** Bar histogram summarizing the mean responses, measured as average firing frequency, during the different stimuli applied (n= 6). Firing frequency for cold was average from the first to the last spike during the cooling ramp. Firing frequency in control conditions was calculated during the 60 s previous to rapamycin application. Rapamycin-evoked firing was calculated from the first spike during rapamycin application to the start of the cold ramp. Statistical differences were calculated by a one-way ANOVA for repeated measures followed by a Bonferroni's post-hoc test.

4.3 TRPM8 modulation by GqPCR

The goal of this project was to investigate the mechanisms underlying TRPM8 channel modulation after GqPCR activation and examine the physiological effects of this modulation on cold-sensitive neurons.

To study the effect of GqPCRs activation on TRPM8 activity, and to dissect the role of the different secondary messengers involved in TRPM8 modulation, I used HEK293 cells transiently transfected with different plasmids encoding ion channels and GqPCRs receptors. Additionally, I used different pharmacological and molecular tools which allowed us to manipulate and image PI(4,5)P2, a main effector in the modulation of TRPM8 by GqPCRs (Rohacs et al., 2005). As a control of the tools effectiveness, I used KCNQ2/3 and Kir2.1 channels whose modulation by PI(4,5)P2 is well-stablished (Suh and Hille, 2002; Du et al., 2004). I also interrogated cold-sensitive DRG neurons for the expression of different GqPCRs involved in inflammatory conditions in and the effect of their activity on cold sensitivity.

4.3.1. GqPCR-mediated inhibition of TRPM8

GqPCR-mediated inhibition of TRPM8 channels was studied by activation of overexpressed muscarinic M1 receptor (M1R), which usually couples via the Gαq subunit and directly activates PLC, triggering the secondary messenger cascade in which PI(4,5)P2 is depleted from the plasma membrane. TRPM8 was expressed in HEK293 cells, either alone or co-expressed with the M1R, and TRPM8 currents were monitored by patch-clamp recordings in the whole cell voltage-clamp configuration, by applying consecutive voltage ramps (0.33 Hz) from -100 to +150 mV. During the protocol, TRPM8 was activated by menthol (300 µM) and subsequently carbachol (Cch), a specific agonist of M1R, was applied (Fig. 29A). Furthermore, inhibition was studied at two different temperatures: 33 ºC, similar to physiological temperatures at the skin surface, and at 23 ºC.

At 33 ºC, menthol evoked characteristic outwardly rectifying TRPM8 currents in cells overexpressing exclusively TRPM8 channels ($I_{density+100mV}$ = 458.6 ± 54.8 pA/pF, $I_{density-100mV}$ = -12.3 ± 2.7 pA/pF) (Fig. 29A, 29D). When M1R was coexpressed with TRPM8, menthol-evoked currents were identical in amplitude at positive potentials ($I_{density+100mV}$ = 440.2 ± 72.4 pA/pF), however they showed a tendency to be smaller at negative potentials ($I_{density-100mV}$ = -7 ± 1.7 pA/pF, p= 0.1388) (Fig. 29B, 29D). At 23 ºC, TRPM8 currents were similar in amplitude at positive

potentials but larger at negative potentials ($I_{density+100mV}$ = 431 ± 47.6 pA/pF, $I_{density-100mV}$ = -30.1 ± 9.2 pA/pF) (Fig. 29C, 29D). In experiments at 33 ºC, application of 10 µM Cch had almost no effect on TRPM8 currents when M1R was not overexpressed ($Inhibition_{+100mV}$ = 9.1 ± 2.8%, $Inhibition_{-100mV}$ = 14.9 ± 7.3%) (Fig. 29A). However, in cells overexpressing M1R, menthol-evoked currents at 33 ºC were completely inhibited by application of 10 µM Cch at negative or positive potentials ($Inhibition_{+100mV}$ = 97.2 ± 1.9%, $Inhibition_{-100mV}$ = 96.9 ± 1.7%) (Fig. 29B). When the same experiment was performed at 23 ºC, Cch application inhibited TRPM8 menthol-evoked currents partially at positive potentials and completely at negative potentials ($Inhibition_{+100mV}$ = 66.95 ± 3.1%, $Inhibition_{-100mV}$ = 99.16 ± 0.39%) (Fig. 29C). A summary of these results is shown in Figure 29E.

Two minutes after the removal of Cch, and in the continuous presence of menthol, TRPM8 outward currents recovered partially from M1R suppression (33 ºC, $I_{recovery+100mV}$= 53.6 ± 4.9%; 23 ºC, $I_{recovery+100mV}$= 60.1 ± 5.6%), while the recovery of inward currents was smaller (33 ºC, $I_{recovery-100mV}$= 9.1 ± 5.3%; 23 ºC, $I_{recovery-100mV}$= 23.3 ± 9%) (Fig. 2B-C).

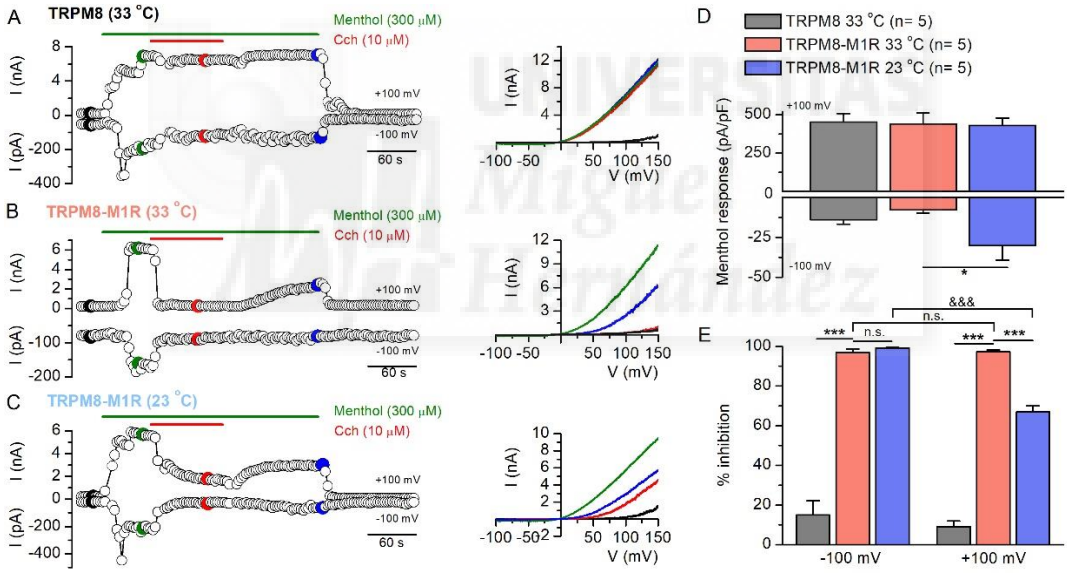

Figure 29. Activation of overexpressed M1R inhibits menthol-activated TRPM8 currents. Representative time course of whole-cell currents at -100 and +100 mV in a HEK293 cell transiently transfected with mTRPM8 alone (***A***), mTRPM8 with M1R at 33 ºC (***B***) and mTRPM8 with M1R at 23 ºC (***C***). On the right-hand side, current-voltage relationship of responses, obtained with a 500 ms voltage ramp from -100 to +150 mV. The color of individual traces matches the color at each particular time point in the current time course. ***D*****,** Bar histogram summarizing the mean current density values at +100 and -100 mV in response to menthol application in the different conditions tested. Statistical differences were calculated by a one-way ANOVA followed by a Bonferroni's post-test. ***E*****,** Bar histogram summarizing the inhibition evoked by M1R activation at negative (-100 mV) and positive (+100 mV) potentials. The legend is shared with D. The procedure used for calculate the percentage of inhibition are explained in detail on the material and methods section. Bars represent mean ± SEM for n= 5 for each group. Statistical significance was evaluated by a one-way ANOVA followed by a Bonferroni post-test for control and the

different temperatures (***, p-value< 0.001) and by a paired t-test for the different voltages (&&&, p-value< 0.001).

Next, I studied the effect of M1R activation on TRPM8 currents evoked by cold, the physiological activator of TRPM8 channels. The protocol consisted on a first cold temperature ramp from 32-34 ºC to 18 ºC in control conditions, followed by a second identical temperature ramp, in control conditions or in the presence of Cch (10 µM) (Fig. 30A). In the absence of Cch (Fig. 30A, black open circles) the second cold-evoked response was almost identical in amplitude to the first cold response ($Inhibition_{+100mV}$= 6.5 ± 3.5%) (Fig. 30A-C). However, when Cch was applied 30 seconds before the second cold ramp (Fig. 30A, red open circles), TRPM8 current at +100 mV was almost totally abolished ($Inhibition_{+100mV}$= 95.26 ± 3.8%) (Fig. 30A-C). Cold-evoked currents at -100 mV were almost negligible and were not analyzed.

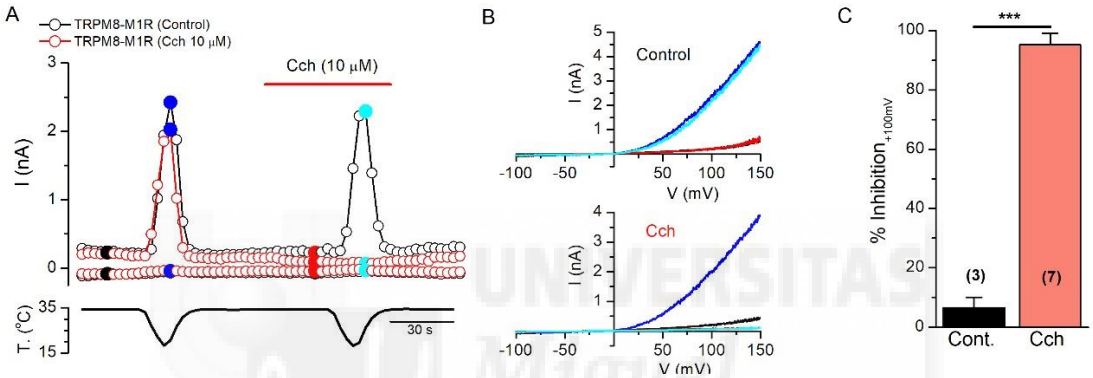

Figure 30. Activation of overexpressed M1R completely abolishes cold-activated TRPM8 currents. ***A*,** Representative time course of whole-cell currents at -100 and +100 mV in HEK293 cell transiently transfected with mTRPM8 and hM1R during the protocol exploring the effect of M1R activation on TRPM8 cold-evoked currents. Bottom trace corresponds to the simultaneous recording of bath temperature. ***B*,** Current-voltage relationship of TRPM8 channels obtained by a 500 ms voltage ramp from -100 to +150 mV corresponding to the colored points in A. ***C*,** Bar histogram summarizing the mean ± SEM inhibition values of the second cold-evoked response (+100 mV) in control conditions and when M1R was activated. The inhibition was calculated with respect to the current amplitude evoked by the first cold ramp. Statistical significance was calculated by an unpaired t-test (***, p-value< 0.001).

Additionally, I also studied the effect of Histamine 1 Receptor (H1R) activation, a different GqPCR, on menthol-evoked TRPM8 currents at 33 ºC. Histamine, physiological agonists of H1R, did not affect TRPM8 currents when H1R were not co-expressed (Fig. 31A). In contrast, in HEK293 cells co-transfected with TRPM8 and H1R, application of 10 µM histamine at 33 ºC evoked a partial inhibition of menthol-evoked currents at +100 mV ($Inhibition_{+100mV}$= 32.3 ± 2.1%), whereas at -100 mV the inhibition was significantly stronger ($Inhibition_{-100mV}$= 80.5 ± 1.2%) (p-value= 0.0046) (Fig. 31B). Higher concentration of histamine (100 µM) further increased the percentage of inhibition at +100 mV ($Inhibition_{+100mV}$= 63.7 ± 10.5%) and slightly increased the inhibition at -100 mV ($Inhibition_{-100mV}$= 87.1 ± 6.9%) (Fig. 31C). Thus, H1R activation also caused an inhibition of TRPM8 currents, although the magnitude of this inhibition was smaller than that observed after

M1R activation. In addition, inhibition at -100 mV was almost maximal with histamine 10 µM while at positive voltages histamine 100 µM doubled the inhibition evoked by 10 µM histamine, suggesting different sensitivity of TRPM8 currents to H1R activation at the different voltages studied.

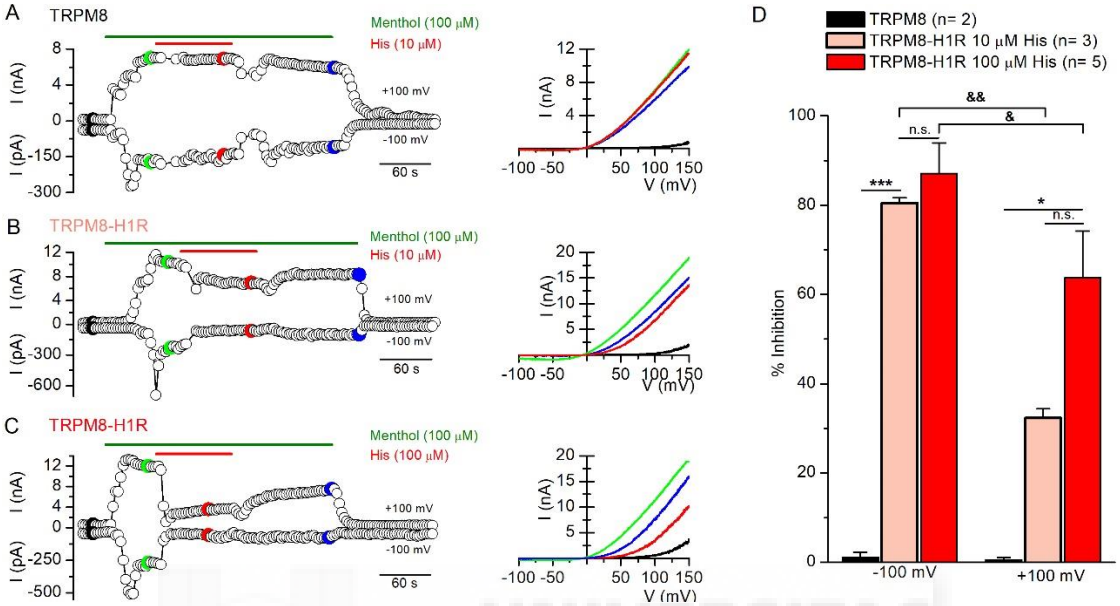

Figure 31. Activation of overexpressed H1R partially inhibits menthol-activated TRPM8 currents. ***A*****,** Representative time course of whole-cell currents at -100 and +100 mV in a HEK293 cell transiently transfected with mTRPM8 (control). Right panel, current-voltage relationship of TRPM8 currents obtained with a 500 ms voltage ramp from -100 to +150 mV corresponding to the colored points in the current time course. ***B*****,** Representative time course of whole-cell currents at -100 and +100 mV in a cell transfected with mTRPM8 and H1R. During the sustained phase of the menthol-evoked responses 10 µM or ***C*****,** 100 µM histamine (His) was applied. At right, current-voltage relationship of TRPM8 channels obtained with a 400 ms voltage ramp from -100 to +150 mV corresponding to the colored points in the current time course. ***D*****,** Bar histogram summarizing the inhibitory effect of H1R activation on TRPM8 currents at positive and negative membrane potentials during the different conditions tested. Statistical significance was calculated by a paired t-test between different voltages (&, p<0.05; &&, p<0. 01) and by a one-way ANOVA for the control and the different His concentrations (*, p<0.05; ***, p<0. 001)

In order to have a more precise temporal control of GqPCR activation, I tested the effects of melanopsin, a GqPCR which is activated by blue light (460 nm) (Provencio et al., 1998). Previously, different studies demonstrated the coupling between melanopsin and the receptor-operated channel TRPC3 (Qiu et al., 2005). In experiments co-expressing hTRPC3 and melanopsin in HEK293 cells, I confirmed that melanopsin coupled effectively to Gq and that illumination of the cells (460 nm) induced hTRPC3-mediated outward (I_{basal}= 27.23 ± 7.08 pA/pF vs I_{light}= 136.3 ± 21.32 pA/pF; n= 4, p= 0.012) and inward currents (I_{basal}= -8.79 ± 1.85 pA/pF vs I_{light}= -20.97 ± 3.43 pA/pF; n= 4, p= 0.018) (Fig. 32A). I next studied the effect of melanopsin activation on TRPM8 currents. In the presence of menthol (300 µM), activation of melanopsin by a 460 nm light pulse (15 s) evoked a partial inhibition of TRPM8 currents (+100 mV) at 33 ºC

(Inhibition$_{+100mV}$= 39 ± 4.2%) (Fig. 32B). In this set of experiments, menthol-evoked inward currents at 33 ºC were almost negligible, which may be explained by a basal activation of melanopsin by ambient light. During the menthol response, bath temperature was decreased to 23 ºC and a second pulse of light was applied. The effect of melanopsin activation at this temperature was almost negligible (Fig. 32B-C).

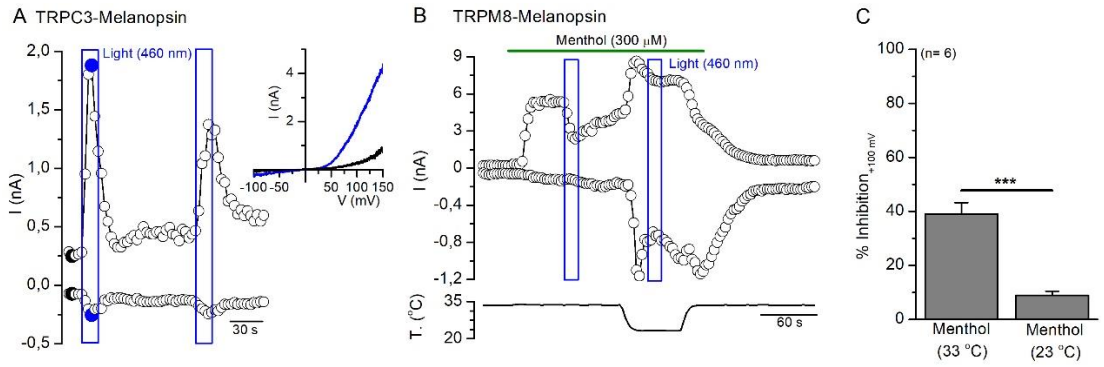

Figure 32. Melanopsin activation by light modulates TRP channels. *A*, Time course of a representative whole-cell recording from a HEK293 cell expressing hTRPC3 and mouse melanopsin. At right, current-voltage relationship from points colored in the current time course. ***B*,** Representative time course of a whole-cell recording from a HEK293 cell expressing mTRPM8 and melanopsin. Bottom trace corresponds to the simultaneous recording of bath temperature, which was decreased from 33 ˚C to 23 ˚C in order to explore the inhibitory effect of melanopsin activation at these two temperatures. ***C*,** Histogram summarizing the inhibition evoked by light-mediated melanopsin activation on menthol-evoked currents (+100 mV) at 33 ˚C and at 23 ˚C. Statistical significance was calculated with a paired t-test (***, p-value< 0.001).

Our results confirm that activation of different mammalian overexpressed GqPCRs modulate menthol- and cold-evoked TRPM8 currents in a fast and reversible manner. The inhibitory effect was stronger at negative potentials than at positive potentials and higher at 33 ºC that at 23 ºC. When comparing the inhibition exerted by different GqPCRs, I found that M1R activation evoked a stronger inhibition than H1R or the photopigment melanopsin.

The precise intracellular signaling events underlying TRPM8 inhibition by GqPCR activation are explored in the next set of experiments.

4.3.2 Dr-VSP-mediated inhibition of TRPM8

To assess the involvement of PI(4,5)P2 depletion on GqPCR mediated inhibition, I explored the effect on TRPM8 activity of *Danio rerio* Voltage-Sensitive Phosphatase (Dr-VSP) activation, a voltage-sensitive lipid 5-phosphatase which dephosphorylates PI(4,5)P2 on the 5 position to give PI(4)P during depolarization periods (Okamura et al., 2009). With this tool, I was able to bypass the PLC pathway and perturb the endogenous plasma membrane PI(4,5)P2 levels without producing other secondary messengers involved in the cascade triggered after GqPCR activation. I recorded HEK293 cells co-expressing TRPM8 and Dr-VSP in whole-cell voltage-clamp

configuration at -60 mV and at a basal temperature of 33 ºC. TRPM8 currents were activated by menthol (300 µM) application and, during the sustained phase of the response, 3 pulses of different duration (0.3, 1 and 3 seconds) to +100 mV were applied in order to activate Dr-VSP, with an interval between pulses of 10 seconds. This protocol allows the continuous measure of I_{TRPM8} at -60 mV and also monitor the I_{TRPM8} and its inhibition at +100 mV during the depolarizing pulses (Fig. 33A, 33B). At the end of the protocol AMTB, a specific TRPM8 blocker was applied to obtain a value of whole-cell current in the absence of I_{TRPM8}.

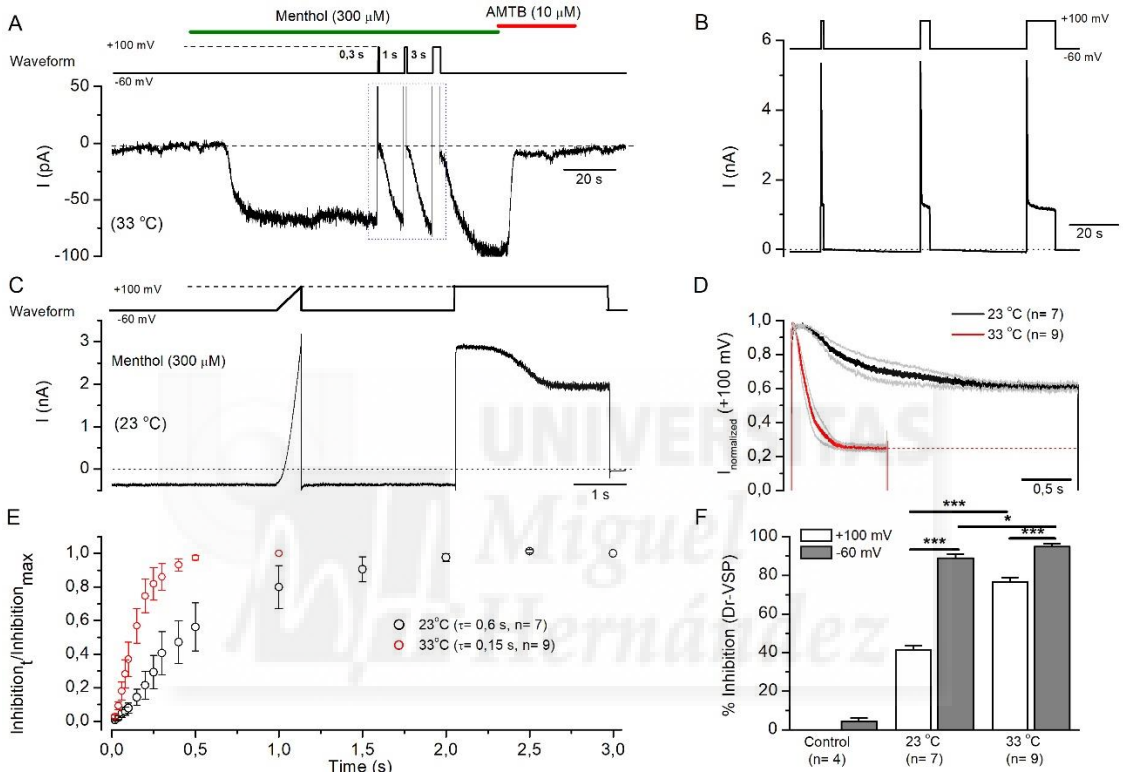

Figure 33. Dephosphorylation of PI(4,5)P2 by Dr-VSP inhibits TRPM8 channels. *A*, Representative whole cell recording from a HEK293 cell expressing mTRPM8 and Dr-VSP during a protocol exploring the effect of Dr-VSP activation on TRPM8 currents at 33 ˚C. The waveform trace corresponds to the voltage protocol applied during the recording; currents were measured at -60 mV and three consecutive depolarizing pulses to +100 mV of different duration were applied. ***B*,** Box in A is shown with the full range of current. Note the incomplete inhibition of the TRPM8 current at +100 mV. ***C*,** Whole cell recording of a HEK293 cell expressing TRPM8 and Dr-VSP during a protocol exploring the effect of Dr-VSP activation on TRPM8 current at 23 ºC. The waveform corresponds to the voltage protocol during the recording; current was measured at -60 mV, a first voltage ramp to +100 mV (400 ms) was applied and thereafter a hyperpolarizing pulse of 3 seconds was applied to activate the Dr-VSP. ***D*,** Averaged time course of TRPM8 currents at 23 ºC and 33 ºC during the depolarizing pulse (+100 mV) applied to activate Dr-VSP. Currents values were normalized to the menthol peak current at the beginning of the depolarizing pulse. ***E*,** Time course of Dr-VSP evoked inhibition of TRPM8 for experiments performed at 23 ºC and 33 ºC. The inhibition at different time points was normalized to the maximal inhibition at the end of the pulse. The time constant (τ) was calculated by fitting an exponential curve to the current decline. ***F*,** Summary of mean TRPM8 inhibition obtained at positive (+100 mV) and at negative (-60 mV) potentials after Dr-

VSP activation at the two temperatures tested. Statistical significance was calculated by a paired t-test between the values at the same temperature and by an unpaired t-test between the values at the same voltage (*< 0.05, ***< 0.001).

Activation of Dr-VSP led to an immediate inhibition of TRPM8 current. At both potentials, -60 and +100 mV, the inhibitory effect was maximal even with the shortest pulse (0.3 s), and I_{TRPM8} recovered fully during the interpulse period (Fig. 33A). For the rest of the analysis, the 1 second duration pulse was used. I found marked differences between the behavior of I_{TRPM8} at positive and negative potentials after Dr-VSP activation; the inhibition was almost complete at -60 mV ($Inhibition_{-60mV}$ = 94.8 ± 1.4%) while at +100 mV the inhibition was pronounced but only partial ($Inhibition_{+100mV}$ = 77.2 ± 1.7%) (n= 9, p<0.001) (Fig. 33A-B). Cells transfected only with TRPM8 did not show inhibition, neither at positive nor at negative potentials following the depolarizing pulse ($Inhibition_{-60mV}$ = 4.3 ± 1.8%, $Inhibition_{+100mV}$= -8 ± 3.2%, n= 4) (data not shown).

Similar experiments were performed at 23 ºC, although a slightly different protocol was used (Fig. 33C). At this temperature, a standing inward current was observable at 23 ºC. A control ramp to +100 mV (400 ms) was applied to measure TRPM8 current and, since the inhibition kinetics was slower at this lower temperature, only the 3 s +100 mV pulse was applied. The Dr-VSP evoked inhibition of TRPM8 current was significantly smaller than at 33 ºC; at +100 mV the inhibition was 41.4 ± 2.3% while at -60 mV the inhibitory effect accounted for 88.9 ± 2.1% of the initial current (n= 7, p<0.001) (Fig. 33C-F).

The kinetics of I_{TRPM8} decline during the depolarizing pulse were slower at 23 ºC than at 33º C, which was clearly reflected by representing the decline in normalized I_{TRPM8} during the depolarizing pulse (Fig. 33D). By exponential curve fitting of the normalized inhibition during the hyperpolarizing pulses, I obtained an averaged tau of inactivation of 150 ms (n= 9) at 33 ºC, reflecting the fast rate of the inhibition (Fig. 33E). At 23 ºC the time constant of the process was about 4 times slower (Fig. 33D- E).

Figure 34 summarizes the mean inhibitory values observed after M1R and Dr-VSP activation on menthol-evoked TRPM8 currents, at positive and negative voltages and at the two temperatures tested. The results show that activation of GqPCRs signaling cascade (M1R) or direct depletion of PI(4,5)P2 by Dr-VSP activation led to a full degree of TRPM8 current inhibition at negative membrane potentials. In contrast, at positive potentials, M1R activation had a stronger effect. These data suggest that selective PI(4,5)P2 depletion is sufficient to almost completely inhibit TRPM8 inward currents however, a percentage of the outward current still remains, meaning that additional mechanisms of the GqCPRs signaling cascade may participate in TRPM8 inhibition.

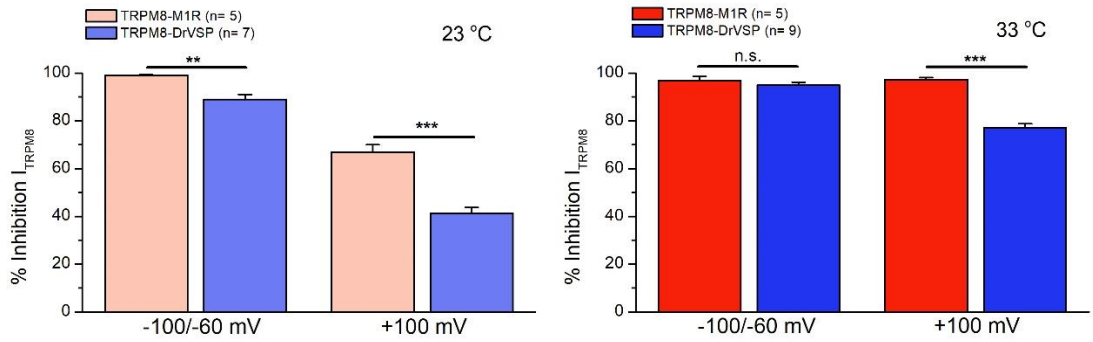

Figure 34. M1R- and Dr-VSP-mediated TRPM8 inhibition at the different voltages and temperatures tested. Comparison of the inhibition values obtained with the two different methods used (Dr-VSP and M1R) at positive (+100 mV) and negative potentials (-60 mV for Dr-VSP and -100 mV for M1R) at the two tested temperatures (23 ºC and 33 ºC). The statistical analysis was done using a two-way ANOVA test followed by Bonferroni post-hoc multiple-comparisons test: **, p<0.01; ***, p<0.001; n.s., p>0.05.

4.3.3 Melanopsin activation does not increase Dr-VSP evoked TRPM8 inhibition

Next, I studied the possibility that activation of a GqPCR increases the incomplete inhibition evoked by Dr-VSP activation at +100 mV by adding an additional modulatory mechanism to PI(4,5) modulation. To test this hypothesis, Dr-VSP, melanopsin and TRPM8 were co-transfected in HEK293 cells. Whole-cell recordings were performed at 33 ºC using the following protocol: TRPM8 currents were activated by menthol (300 µM) and, in the presence of menthol, a first voltage ramp to +100 mV (400 ms) was applied to measure I_{TRPM8} and afterwards Dr-VSP was activated by a sustained depolarization to +100 mV during 5 seconds. During the Dr-VSP inhibitory plateau, melanopsin was activated by a 3 second duration blue light pulse (Fig. 35A-B).

In cells transfected with TRPM8 and melanopsin (not Dr-VSP), TRPM8 currents decreased slightly during the first two seconds of the depolarizing pulse to +100 mV ($I_{pre\text{-}light}$= 7.43 ± 1.5), probably reflecting desensitization. Activation of melanopsin by blue light during the final three seconds of depolarization produced a substantial inhibition of TRPM8 currents ($I_{post\text{-}light}$= 49.2 ± 7.7, Δ% inhibition= 41.78 ± 6.7%) (p= 0.0016, n= 6) (Fig. 35A, 35C). When both, Dr-VSP and melanopsin were expressed simultaneously, Dr-VSP activation during the first two seconds evoked a strong but incomplete inhibition of TRPM8 currents ($I_{pre\text{-}light}$= 83.45 ± 2.8%) which was not affected by subsequent activation of melanopsin during the last 3 seconds of the pulse ($I_{post\text{-}light}$= 85.1 ± 3.5%, Δ% inhibition= 1.6 ± 0.9%) (p=0.11, n= 8) (Fig. 35B, 35D). Therefore, the inhibition of TRPM8 currents by Dr-VSP was not increased by melanopsin activation, suggesting that activation of a GqPCR does not increase inhibition evoked by exclusive PI(4,5)P2 depletion.

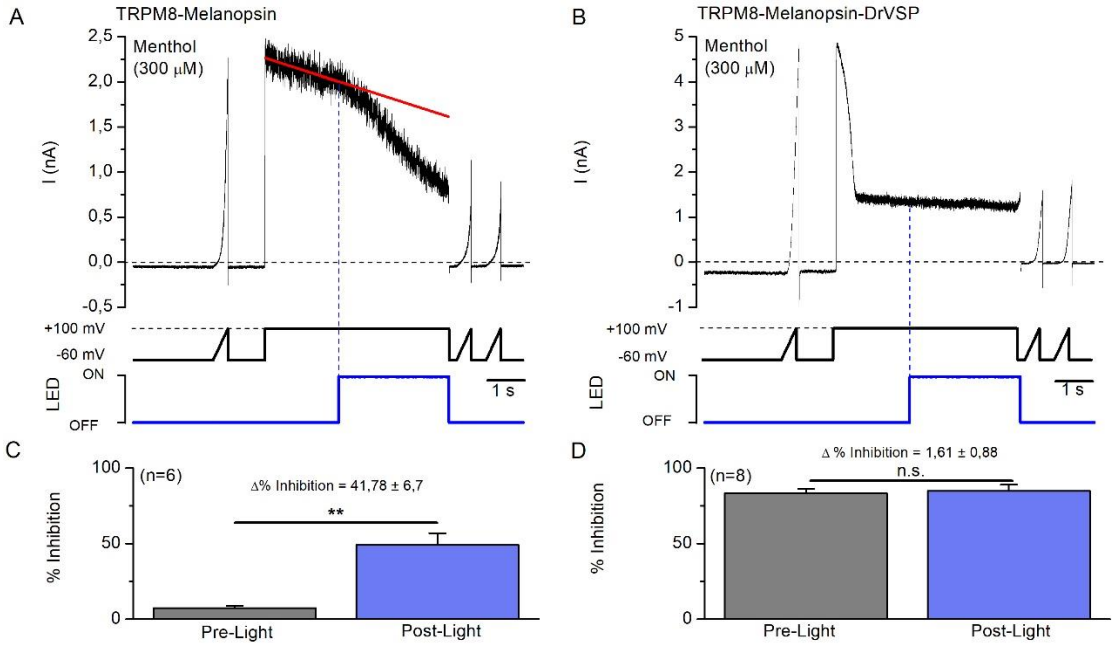

Figure 35. Melanopsin activation does not increase Dr-VSP inhibition of TRPM8. *A*, Whole-cell recording of a HEK293 cell expressing mTRPM8 and melanopsin and ***B*,** a HEK293 cell expressing TRPM8, melanopsin and Dr-VSP. The voltage protocol used and the LED activation (460 nm) are represented below. TRPM8 was activated by menthol (300 μM) application. Red line represents a linear fitting of TRPM8 current decline during the 2 first seconds of the voltage pulse. ***C*,** Histogram summarizing the percentage of inhibition at +100 mV after the first two seconds of the depolarizing pulse (Pre-Light) and after light application (Post-Light) in cells expressing TRPM8 and melanopsin and ***D*,** in cells expressing TRPM8, melanopsin, and Dr-VSP. Statistical significance was calculated by a paired t-test (**, $p<0.01$).

4.3.4 Exploring receptor- and Dr-VSP-mediated inhibition of KCNQ2/3 and Kir2.1 channels

In order to verify the effectiveness of our tools in manipulating PI(4,5)P2 levels, I tested their effects on two potassium channels already known to be PI(4,5)P2 sensitive.

First, I studied KCNQ2 (Kv7.2)/KCNQ3 (Kv7.3) channel currents, which have a strong PI(4,5)P2 requirement for their activity, reflected in the strong inhibition observed following PI(4,5)P2 depletion (Suh and Hille, 2002; Zhang et al., 2003; Winks et al., 2005; Falkenburger et al., 2010). Co-transfection of the plasmids for the two channel subunits KCNQ2 and KCNQ3 in HEK293 cells yielded robust outwardly rectifying potassium currents with a reversal potential of -36.5 ± 2.3 mV and an amplitude of 657.9 ± 166.2 pA/pF at +80 mV (23 ºC) (Fig. 36A). Current was activated by consecutive voltage ramps (0.33 Hz) from -60 to +100 mV (Fig. 36A). At the end of the protocol XE-991 (10 μM), a specific blocker of KCNQ2/3 channels, was applied in order to obtain a current value corresponding to the fully blocked KCNQ2/3 channel condition ($I_{KCNQ2/3}= 0$).

As expected, KCNQ2/3 current was almost fully abolished when overexpressed M1Rs were activated by 10 μM Cch ($Inhibition_{+80mV}= 91 \pm 3.9\%$) (Fig. 36A, 36B). The inhibition time course had a tau of 17.74 ± 3.7 seconds and after 2 min of Cch wash out, KCNQ2/3 current recovered

to 68.5 ± 5.4% of control values. When KCNQ2/3 was co-expressed with Dr-VSP, depolarizing pulses delivered at 23 ˚C evoked a strong inhibition of KCNQ2/3 currents ($Inhibition_{+100mV}$= 87.8 ± 2.5%, n= 5) (Fig. 36C). Therefore, KCNQ2/3 currents were strongly inhibited by the two methods tested, M1R activation and Dr-VSP activation (p= 0.57), confirming the ability of our tools in depleting PI(4,5)P2 (Fig. 36D). Notably, the inhibition of KCNQ2/3 currents was higher with the two methods than the inhibition of TRPM8 at the same temperature (23 ºC), suggesting a lower affinity of KCNQ channels for PI(4,5)P2.

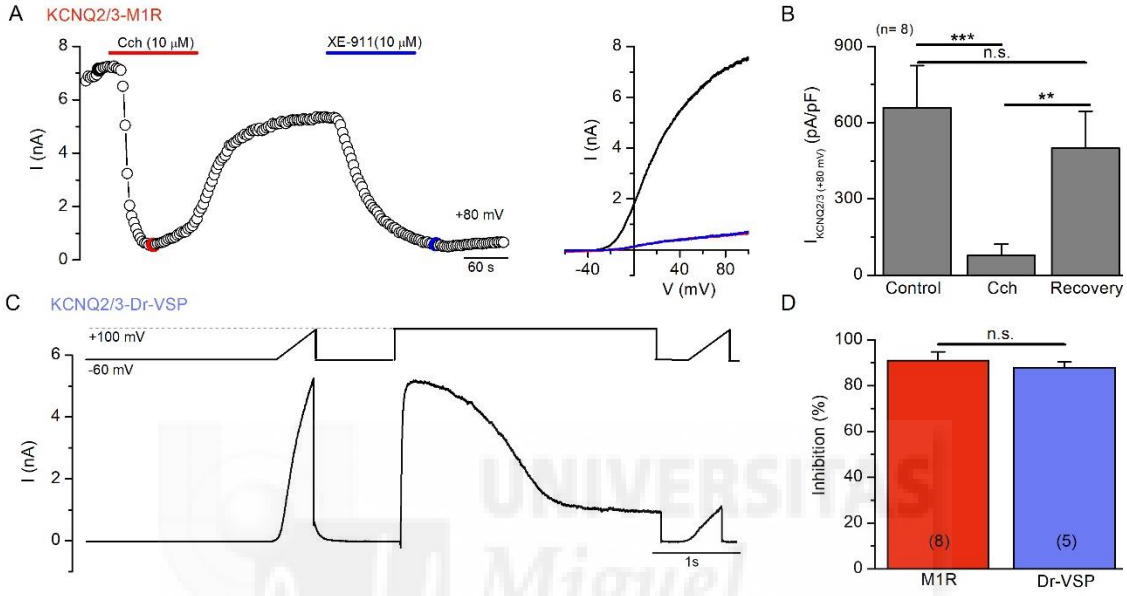

Figure 36. M1R and Dr-VSP activation strongly inhibit KCNQ2/3 currents. *A*, Time course of KCNQ2/3 currents recorded in the whole-cell configuration at +80 mV during a protocol exploring the effect of overexpressed M1R activation. At right, current-voltage relationship of KCNQ2/3 current during voltage ramps from -60 to +100 mV. Traces correspond to the colored points in the current time plot. ***B*,** Histogram of current density at +80 mV in control conditions, in the presence of Cch (10 µM) and two minutes after Cch wash out. Statistical difference was assessed by a one-way ANOVA for repeated measures followed by a Bonferroni post-test. ***C*,** Whole-cell recording of a HEK293 cell expressing KCNQ2/3 channels and Dr-VSP during the voltage protocol represented above. An initial control ramp to +100 mV was followed by a 3 second depolarizing pulse (+100 mV) to activate Dr-VSP, and a second voltage ramp. ***D*,** Histogram summarizing the percentage of KCNQ2/3 inhibition evoked by M1R activation and by Dr-VSP activation. Statistical significance was calculated by an unpaired t-test (p= 0.52).

Additionally, I tested these tools on the inwardly rectifying Kir2.1 channel, which have a particularly high affinity for PI(4,5)P2 and, therefore, its inhibition requires a substantial decrease in PI(4,5)P2 levels (Du et al., 2004). Can our methods deplete enough PI(4,5)P2 to turn off such a high-affinity channel?

In order to test this hypothesis, Kir2.1 channels were co-transfected with M1R in HEK293 cells and recorded in whole-cell voltage clamp configuration using a protocol consisting of repetitive voltage ramps (0.33 Hz) from -140 to +50 mV. Potassium concentration was increased in the extracellular solution to 10 mM in order to obtain robust Kir2.1 currents. Under this protocol,

HEK293 cells transfected with Kir2.1 channels showed a constitutive inwardly rectifying current with a reversal potential of -66.1 ± 1 mV and an amplitude of -813.6 ± 152.9 pA/pF at -120 mV (Fig. 37A). Application of Cch 10 µM during two minutes did not have any effect on Kir2.1 current amplitude (Inhibition$_{-120mV}$= 7.2 ± 1.9%) (Fig. 37A). In the same cells, a higher concentration of Cch (100 µM) was applied in order to saturate the activation of M1R. However, Cch 100 µM did not affect Kir2.1 channels activity (Inhibition$_{-120mV}$= 6.4 ± 1.2%). This result suggests that the high affinity of Kir2.1 channels for PI(4,5)P2 accounts for their resistance to modulation by receptor-mediated PI(4,5)P2 depletion (Kruse et al., 2012).

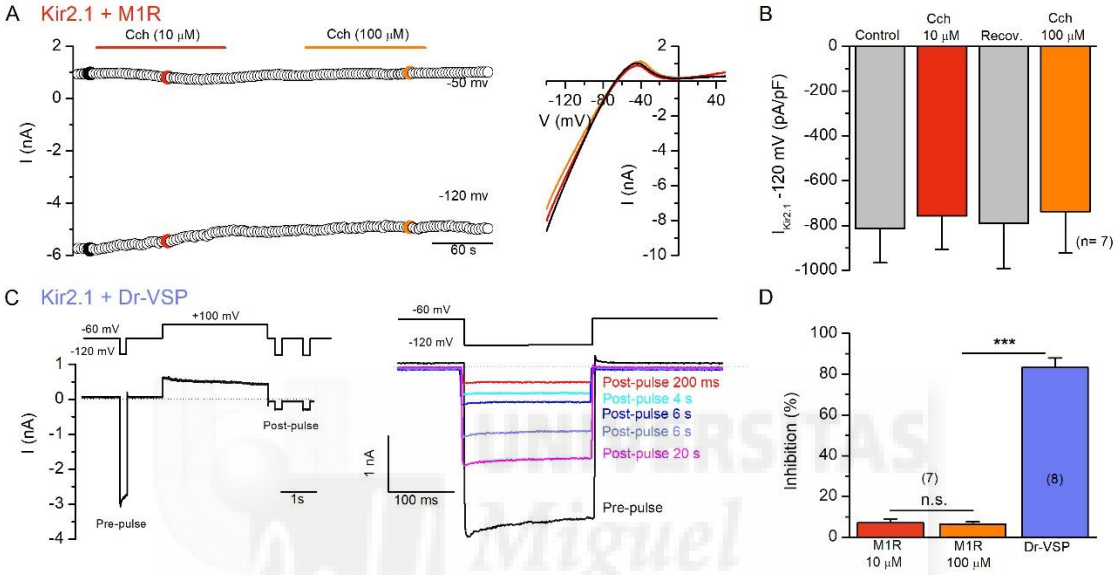

Figure 37. M1R activation has no effect on Kir2.1 channels whereas Dr-VSP activation strongly inhibits Kir2.1 currents. *A*, Representative whole-cell recording of Kir2.1 current at -50 and -120 mV recorded from a HEK293 cells expressing Kir2.1 channels and M1R**.** Current values were extracted from consecutive voltage ramps from -140 to +50 mV. The current-voltage relationship of points colored in the time course of the current are represented at right. ***B*,** Histogram of mean ± SEM current density at -120 mV in control conditions, in the presence of Cch (10 µM), two minutes after Cch (10 µM) wash out and during the presence of Cch (100 µM). No statistical differences were found (ANOVA test + Bonferroni's post-hoc test). ***C*,** Left panel; representative whole-cell recording of a HEK293 cell expressing Kir2.1 and Dr-VSP during the voltage protocol showed above. Right panel; superimposed Kir2.1 currents evoked by the hyperpolarizing pulses applied during the protocol. Pre-pulse trace (black) correspond to the current evoked by the hyperpolarizing pulse before activation of Dr-VSP, and post-pulse traces indicates currents to the same pulse at different times following activation of Dr-VSP. ***D*,** Mean percentage inhibition of Kir2.1-mediated currents evoked by activation of M1R and by Dr-VSP activation. Statistical significance was calculated by a one-way ANOVA followed by a Bonferroni post-test.

Next, I studied the inhibition of Kir2.1 by Dr-VSP activation. In cells expressing Kir2.1 and Dr-VSP, Kir2.1 current was measured by applying 200 ms hyperpolarizing voltage pulses to -120 mV before (Pre-pulse) and after (Post-pulse) Dr-VSP activation by a 3 seconds pulse to +100 mV (Fig. 37C). Kir2.1 current was largely inhibited after the activation of Dr-VSP (Inhibition$_{-120mV}$= 83.3

± 4.7%) (Fig. 37C). In the case of HEK293 cells expressing only Kir2.1 (i.e. whithout Dr-VSP), current measured at -120 mV did not change after the depolarizing pulse (data not shown).

In conclusion, I show that Dr-VSP activation by voltage depletes enough PI(4,5)P2 to modulate KCNQ2/3 channels and also the high-affinity channel Kir2.1. In contrast, M1R mediated depletion of PI(4,5)P2 seems to be less efficient: although it modulated KCNQ2/3 channels, it was not able to affect Kir2.1 channels.

4.3.5 PI(4,5)P2 depletion and TRPM8 current decay after M1R activation follow similar kinetics

In order to study the PI(4,5)P2 dependence of TRPM8 inhibition after GqPCR activation, I used a strategy in which whole-cell recordings and PI(4,5)P2 optical imaging were performed simultaneously. I co-expressed TRPM8 channels, M1R and the PI(4,5)P2 optical sensor PH-GFP in HEK293 cells. This construct consists of a fluorescent protein (GFP) fused to the pleckstrin homology (PH) domain of PLCδ1, which binds to PI(4,5)P2 and therefore, allows to spatially monitor PI(4,5)P2 localization by 460 nm excitation light (Várnai et al., 1999). I monitored translocation of PH-GFP by measuring the fluorescence in a region of the cytoplasm and recorded TRPM8 currents simultaneously in the whole-cell configuration (Fig. 38A). TRPM8 currents were activated by menthol (300 µM) at 33 ºC and during the menthol response Cch (10 µM) was applied. At basal conditions, the majority of PH-GFP fluorescence was localized to the plasma membrane. The stimulation of PLC by M1R activation caused the rapid translocation of fluorescence from the membrane to the cytosol, reflecting the cleavage of PI(4,5)P2 (Fig. 38A-B). The translocation of PH-GFP was accompanied by a complete inhibition of TRPM8 currents (Fig. 38A). I studied the kinetics of both processes at 33 ºC and found that TRPM8 current decay mirrored the time course of PI(4,5)P2 depletion: the time constant (τ) of the current decay at +100 mV averaged 18.8 ± 4.5 seconds, 17.05 ± 2.5 seconds for the current at -100 mV and 16.8 ± 2.6 seconds for the translocation of the PH-GFP probe (n= 7, p>0.05) (Fig. 38C). The similar time course of both processes suggest that TRPM8 current inhibition and PI(4,5)P2 depletion from the plasma membrane are related.

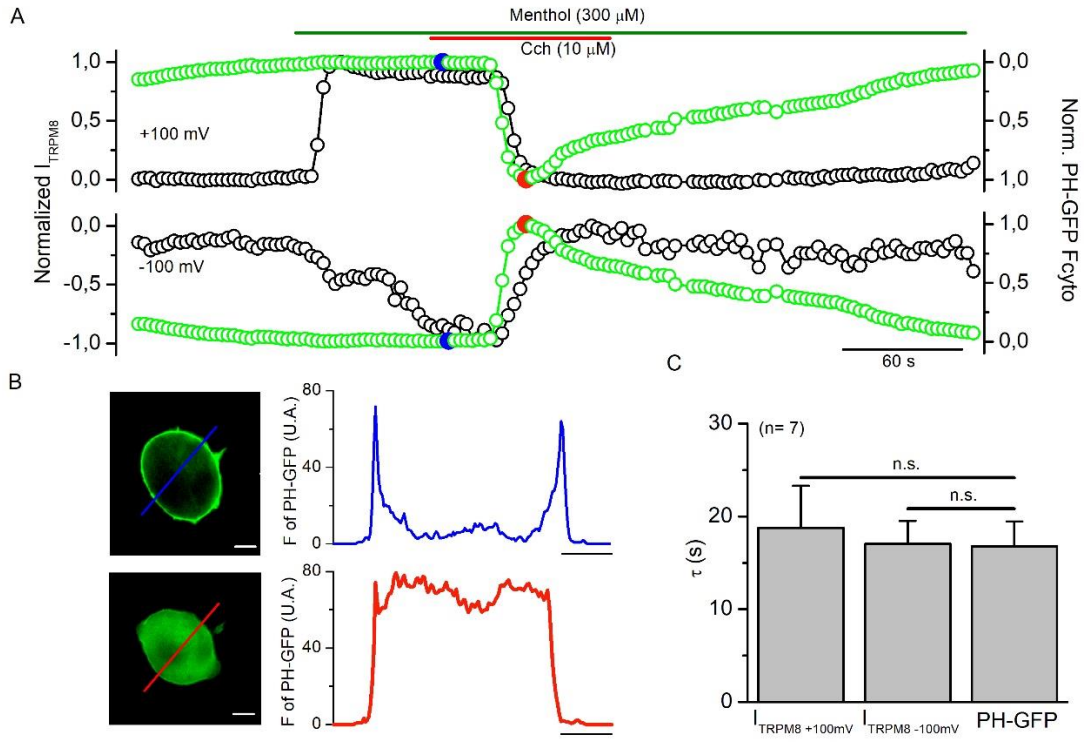

Figure 38. PH-GFP and TRPM8 current decay after M1R activation follow similar kinetics. *A*, Simultaneous whole-cell recording of TRPM8 current and PH-GFP fluorescence in a HEK293 cell expressing TRPM8, PH-GFP and M1R. Normalized currents at +100 and -100 mV (black trace, left axis) and the normalized fluorescence in a region of the cytoplasm are represented (green trace, right axis). The PH-GFP fluorescence is a unique signal, inverted in order to match the polarity of both currents. ***B*,** Fluorescence images corresponding to the colored points in A and the fluorescence profile across the segment (red and blue line) represented in the picture. At basal conditions (top) the GFP fluorescence followed a membrane pattern while stimulation with Cch (10 μM) triggered the translocation of the PH-GFP to the cytosol. The calibration bar is 10 μm. ***C*,** Histogram showing the averaged ± SEM time constant of TRPM8 current decay at +100 mV, -100 mV and the PH-GFP decay. Statistical significance was assessed by an ANOVA test followed by a Bonferroni post-test.

4.3.6 The PLC inhibitor edelfosine prevents M1R-mediated TRPM8 inhibition

In order to explore the possibility that events previous to the PLC activation modulate TRPM8, I used a pharmacological strategy based on the blockade of PLC. In this way, one can prevent PI(4,5)P2 depletion, which is downstream of PLC activation, while maintaining the activation and dissociation of the Gαq subunit from the heterotrimeric complex. The efficacy of two PLC inhibitors was first evaluated by confocal imaging of the translocation of the PI(4,5)P2 optical probe PH-GFP during agonist stimulation.

In HEK293 cells expressing M1R and PH-GFP, translocation of PH-GFP evoked by Cch application was reversible upon wash out and reproducible during a second application (Fig. 39A black circles). I first explored the inhibitory effect of U73122, an aminosteroid compound known

to block PLC (Bleasdale et al., 1989). As shown in Figure 39A, HEK293 cells expressing M1R and PH-GFP were incubated, during 5 minutes between the first and the second application of Cch, with U73122 (red circles) or its inactive analog U73343 (blue circles). As expected, U73122 strongly uncoupled activation of PLC by receptors, inhibiting almost completely the translocation of PH-GFP induced by Cch application (Fig. 39A-B). Unexpectedly, the control "inactive" compound U73343 also abolished the translocation of PH-GFP, with an effect similar to U73122 (Fig. 39A-B). The effect of both compounds on PH-GFP translocation was dose-dependent (Fig. 39B).

To confirm the inhibitory activity of the supposedly inactive compound U73343 on PLC, I studied its effect on the inhibition of KCNQ2/3 currents evoked by M1R activation. When HEK293 cells expressing KCNQ2/3 and M1R were pre-incubated with U73343 (2.5 µM) during 5-10 minutes the inhibitory effect of M1R activation was greatly reduced (Control= 87.2 ± 5.7% *vs* U73343= 13.8 ± 3.8%) ($p<0.001$, n= 6 for each condition) (Fig 39C-D). This data confirmed that U73343 was also active in inhibiting PLC (two different batches were tested with similar results). The only structural difference between U73122 and U73343 is one double bond that makes U73122 chemically reactive. However, in this set of experiments both compounds were equally effective, making the interpretation of the results somewhat more difficult. The actions of U73122 were sufficiently complex that I wanted to test a different PLC inhibitor.

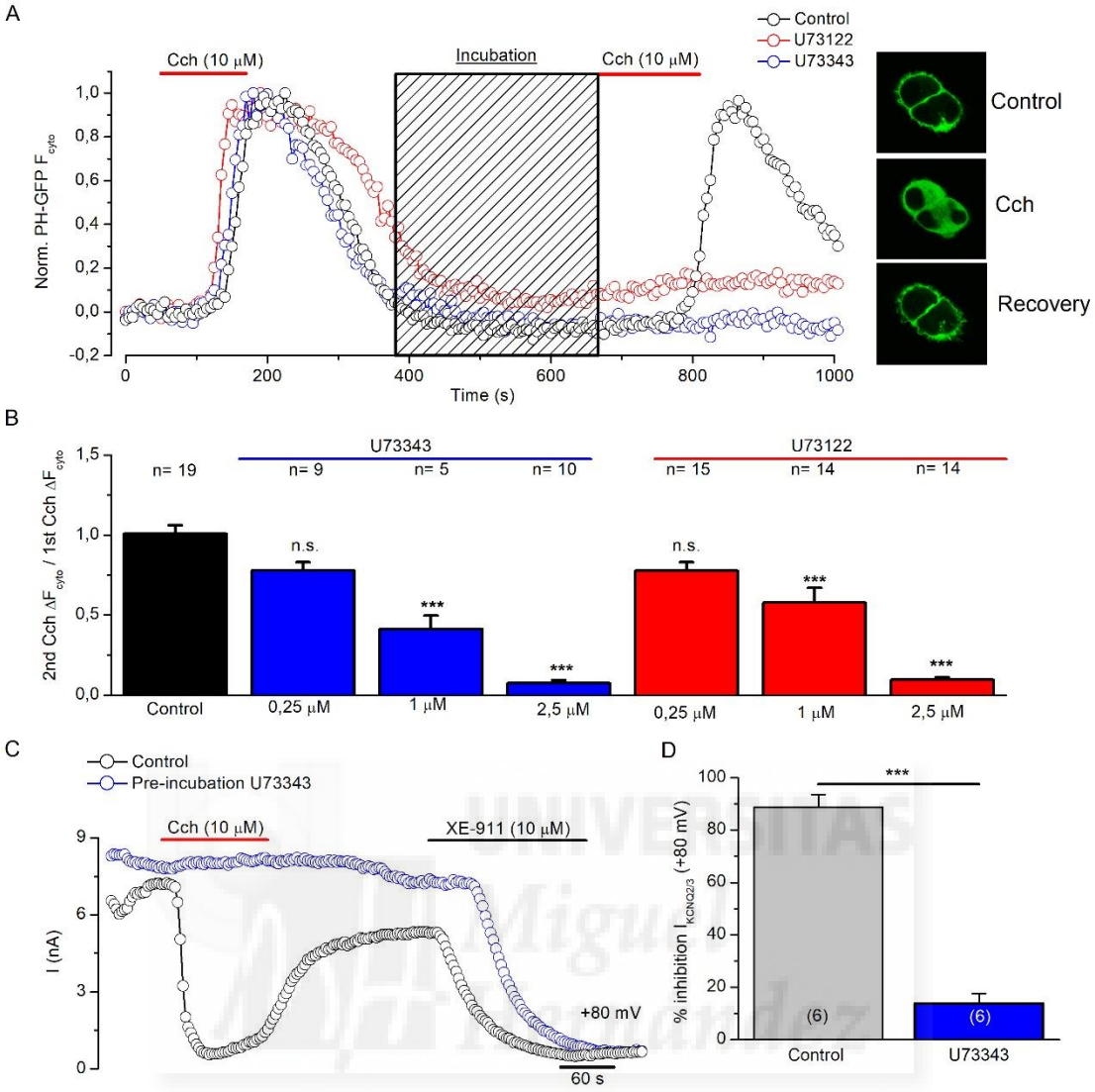

Figure 39. U73122 and U73343 block PLC-mediated PI(4,5)P2 hydrolysis. *A*, Representative time course of normalized PH-GFP fluorescence of a control cell (black trace, not incubated), a cell incubated with U73122 (red trace) and a cell incubated with U73343 (blue trace) at 23 ºC. At right, representative confocal fluorescence images of HEK293 cells expressing PH-GFP in control conditions, during application of 10 µM Cch and during the recovery following the first Cch application. ***B*,** Histogram summarizing the effects of incubation with U73122 and U73343 on the translocation of PH-GFP. Three different doses of each compound were tested, the inhibition of PH-GPF translocation was dose-dependent. Statistical significance with respect to control cells was calculated by one-way ANOVA followed by a Bonferoni post-test. ***C*,** Whole cell recording of a HEK293 cell expressing KCNQ2/3 channels and M1R in control conditions (black open circles) and in a cell pre-incubated during 10-15 minutes with U73343 (2.5 µM) (blue open circles). ***D*,** Histogram summarizing the effect of M1R activation on KCNQ2/3 currents on control cells and cells incubated with U73343. Statistical significance was calculated by using the unpaired t-test (***, p<0.001).

I performed similar experiments with another PLC inhibitor, the lipid-like, anti-neoplastic agent edelfosine (ET-18- OCH3). HEK293 cells overexpressing M1R and PH-GFP were pre-incubated with edelfosine (10 µM) during 10-15 minutes and, subsequently, PH-GFP fluorescence was

monitored. In control cells, Cch (10 µM) evoked the translocation of the PH-GFP probe to the cytosol due to PLC-mediated PI(4,5)P2 cleavage from the membrane. In contrast, Cch did not affect the distribution of PH-GFP in cells pre-incubated with edelfosine (Fig. 40A-B). Moreover, pre-incubation with edelfosine (10 µM) during 10-15 minutes totally abolished the M1R-mediated inhibition of KCNQ2/3 channels (Control= 87.2 ± 5.7% *vs* Edelfosine= -4.3 ± 2.8%) ($p<0.001$, n= 4-6), confirming the effective blockade of PLC by this drug (Fig. 40C-D).

Next, I explored the effect of edelfosine incubation on HEK293 cells expressing TRPM8 and M1R. Whole-cell recordings were performed at 23 ºC in control conditions and after incubation of cells with edelfosine during 10-15 minutes. After edelfosine incubation, recordings at 33 ºC were very difficult to maintain, probably due to some unspecific effect of incubation on the membrane state. Thus, I performed experiments at 23 ºC. Remarkably, cells incubated with edelfosine showed significantly higher basal outward currents at the beginning of the recording than non-incubated cells (Control; I_{basal}= 25.8 ± 4.4 pA/pF *vs* Edelfosine; I_{basal}= 125.7 ± 25.3 pA/pF) (p-value= 0.0046, n= 5) presumably because the PLC blockade prevented the PLC-dependent desensitization of the TRPM8 current at 23 ºC (Fig. 40E). However, the menthol-evoked current density was not significantly different (Control; I_{+100}= 431 ± 47.6 pA/pF, I_{-100}= -30.1 ± 9.2 pA/pF vs Edelfosine; I_{+100}= 371.6 ± 68.7 pA/pF, I_{-100}= -43.97 ± 7 pA/pF). In control cells, application of Cch (10 µM) partially inhibited TRPM8 menthol-evoked currents at positive potentials and completely at negative potentials ($Inhibition_{+100mV}$ = 66.95 ± 3.1%, $Inhibition_{-100mV}$ = 99.16 ± 0.39%) (Fig. 40E-F). However, when cells were pretreated with edelfosine (10 µM), the inhibition evoked by Cch application was drastically reduced ($Inhibition_{+100mV}$ = 7.2 ± 3.9%, $Inhibition_{-100mV}$ = 36.4 ± 12.9%) (Fig. 40E-F). The residual percentage of inhibition observed at -100 mV in edelfosine-treated cells is more likely due to the desensitization of the current during the prolonged response to menthol.

Therefore, when PLC activity was pharmacologically blocked and PIP(4,5)2 membrane levels are not altered, the inhibitory effect on TRPM8 currents evoked by GqPCR activation is fully prevented.

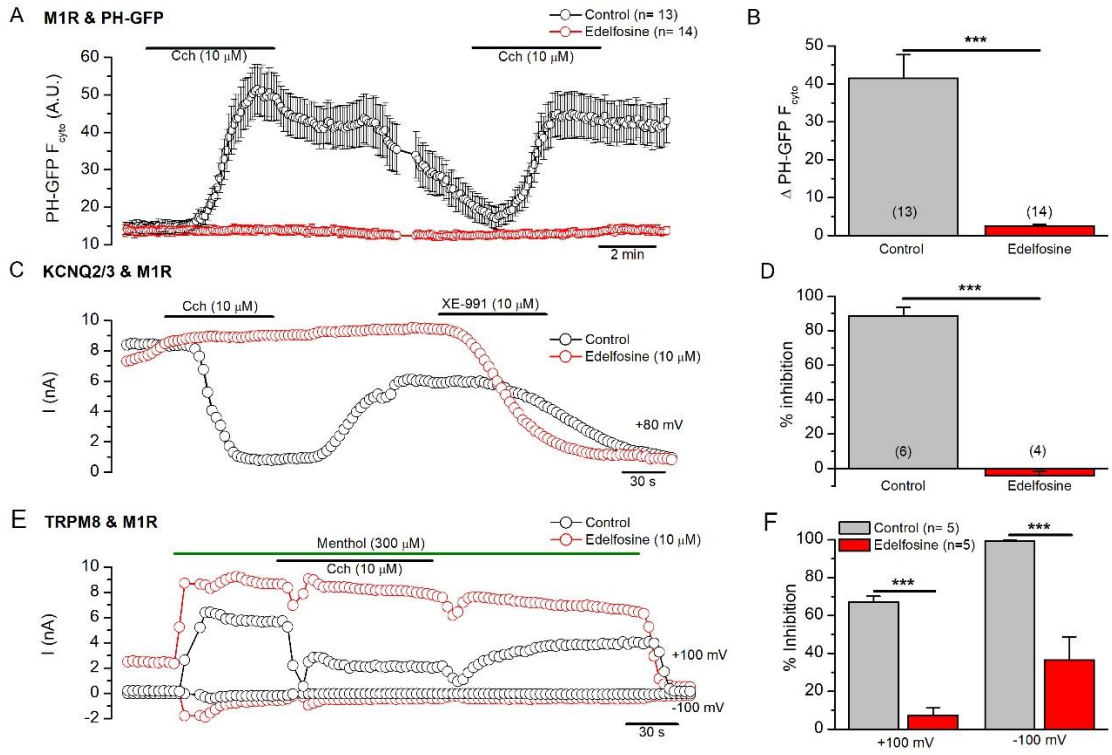

Figure 40. PLC blockade by edelfosine prevents GqPCR-mediated inhibition of TRPM8 channels. ***A*****,** Average time course of PH-GFP fluorescence in HEK293 cells transfected with PH-GFP and M1R. Experiments were performed at 23 ºC. The short gap in the recording corresponds to the transient movement of cells during one of the experiments by an air bubble. Control cells are represented in black while cells pre-incubated with edelfosine (10 μM) are represented in red. ***B*****,** Histogram summarizing the increase of fluorescence in the cytosol due to the translocation of PH-GFP in control cells and cells pre-incubated with edelfosine. Statistical significance was assessed by an unpaired t-test (***, p<0.001). ***C*****,** Representative whole-cell recordings of HEK293 cells expressing KCNQ2/3 and M1R in control conditions (black trace) and following incubation with edelfosine (red trace). ***D*****,** Histogram summarizing the percentage of KCNQ2/3 current inhibition produced by M1R activation in control cells and in cells pretreated with edelfosine. Statistical significance was assessed by an unpaired t-test (***, p<0.001). **E,** Representative whole-cell recordings of HEK293 cells expressing TRPM8 and M1R in control conditions (black trace) and incubated with edelfosine (red trace). **F,** Histogram summarizing the percentage of TRPM8 current inhibition by M1R activation in control cells and cells pretreated with edelfosine. Statistical significance was assessed by an unpaired t-test (***, p<0.001).

4.3.7 GqPCR activation on DRG cold-sensitive neurons have modest effects on cold-evoked responses

Mouse DRG neurons express different GPCRs (Thakur et al., 2014). I explored the effect of GqPCR activation on cold-evoked responses of DRG neurons from TRPM8^{BAC}-EYFP mice by calcium imaging experiments with a protocol consisting of three consecutive cooling ramps; a control cooling ramp, followed by a second cooling ramp in the presence of a GqPCR agonis and finishing with a third ramp in control solution. Thereafter a capsaicin (100 nM) was applied for 60 s, finishing with a pulse of high K^+ (Fig. 41A). Responses to bradykinin (BK), which its most

abundant receptor B2 coupled to Gq/11 and PLC activation, were first explored (Couture et al., 2001).

Out of 81 cold-sensitive neurons recorded, only 7.4% (6 of 81) showed a transient calcium response when BK (10 μM) was applied, suggesting that BK receptors are poorly expressed in TRPM8-expressing neurons (Fig. 41A-B, orange trace). For comparison, 36% (124 out of 344) of those activated by capsaicin, thus expressing TRPV1, were activated by BK ($p< 0.001$, Z test). Remarkably, the six neurons which responded to BK also responded to capsaicin, while among the rest (i.e. BK-insensitive) of cold-sensitive neurons, 25.3% (19 out of 75) responded to capsaicin. The effect of BK on cold-evoked response in these 6 neurons was variable (Fig. 41A-C). The amplitude of cold-evoked responses was drastically reduced in the presence of BK in two neurons, the two neurons with the smallest initial response to cold and the largest amplitude in response to BK (ΔFura2 ratio; Cold= 0.22 ± 0.06; BK= 1.23 ± 0.22) (Fig. 41C). Two other neurons with similar cold responses (0.36 ± 0.06) but smaller BK response (0.2 ± 0.02) showed a reversible increase in the amplitude of the calcium response to the cooling ramp in the presence of BK (Fig. 41C). In the remaining cold-sensitive BK-insensitive neurons (n=75), the cold response in the presence of BK was reduced, however, this reduction did not recover after wash out and was more likely due to desensitization of the response (Fig. 41D). The percentage of BK-sensitive neurons in the cold-insensitive neuronal population was higher (19.9%, 140 out of 704) ($p= 0.006$, Z test) (Fig. 41B). Notably, the percentage of capsaicin responses in BK-sensitive neurons was 88.6% (124 of 140) whereas in the BK-insensitive population the percentage of capsaicin responses was 39% (220 out of 564). It is well known that TRPV1 is sensitized by PKC phosphorylation after GqPCR activation (Prekumar et al., 2000). I compared the amplitude of the capsaicin response of cold-insensitive BK(+) and BK(-) neurons and found that capsaicin-evoked responses in BK(+) neurons were significantly higher than in BK(-) neurons, consistent with a potentiating effect of BK receptor activation on TRPV1 channels (Fig. 41A and 41E).

Next, I tried the GqPCR agonist prostaglandin E_2 (PGE2) and the results were similar (data not shown). Only 8.7% (2 out of 23) of cold-sensitive neurons responded to PGE2 (10 μM). The percentage of PGE2-sensitive neurons in the cold-insensitive population was similar, 11.4% (23 out of 202).

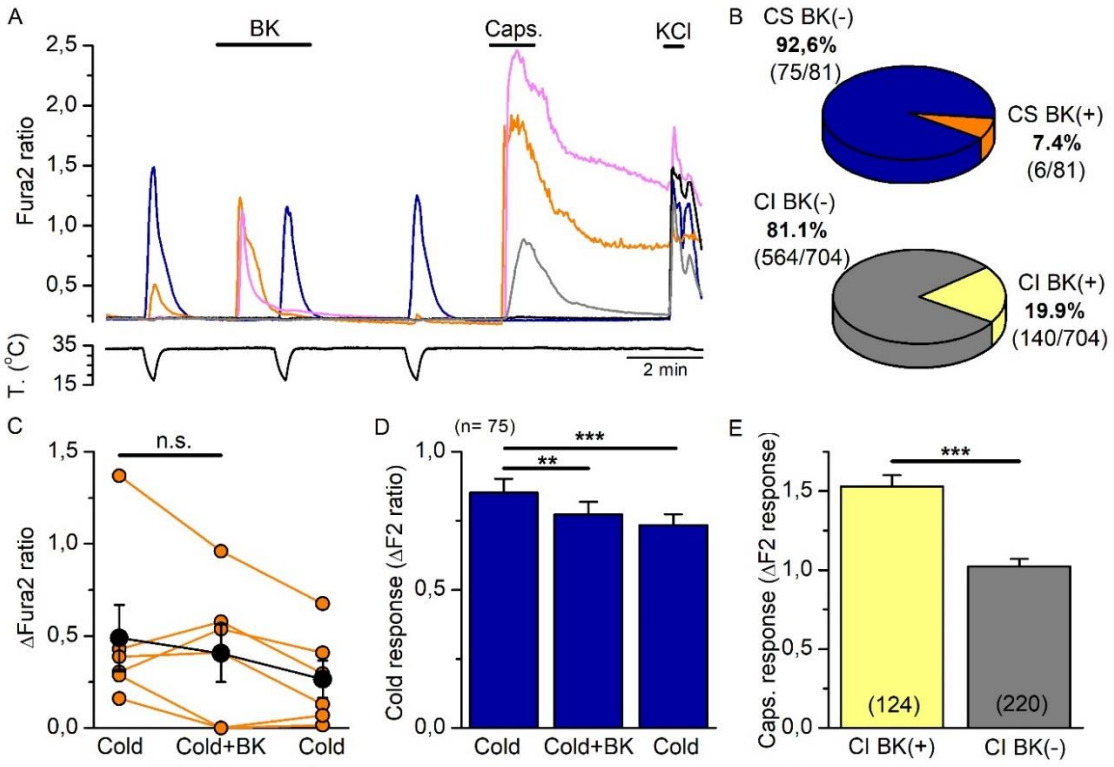

Figure 41. BK activates a small subset of cold-sensitive neurons and its activation has distinct effects on cold-evoked responses. ***A,*** Representative Fura2 traces of DRG neurons in culture during a protocol in which the effect of Bradykinin receptor activation by BK (10 µM) on cold-evoked responses was studied. Three consecutive cooling ramps, capsaicin (100 nM) and high K^+ solution (30 mM KCl) were applied. BK application evokes a transient calcium increase in a subset of neurons (orange and pink traces). Bottom trace correspond to the simultaneous recording of bath temperature. ***B,*** Pie charts showing the percentage of responses to BK observed in cold-sensitive (CS) (top) and cold-insensitive (CI) (bottom) neurons. ***C,*** Amplitude of cold-evoked responses in the cold-sensitive neurons which respond to BK. Statistical significance was assessed by an ANOVA test for repeated measures followed by a Bonferroni´s post-test. ***D,*** Bar histogram representing the mean ± SEM of the response amplitude evoked by cold in cold-sensitive BK-insensitive neurons. Statistical significance was assessed by an ANOVA test for repeated measures followed by a Bonferroni´s post-test (**, p< 0.01; ***, p<0.001). ***E,*** Bar histogram representing the mean ± SEM of the response amplitude evoked by capsaicin in BK(+) and BK(-) cold-insensitive neurons. Statistical significance was calculated by an unpaired t-test (***, p<0.001).

Therefore, I concluded that BK and PGE2 receptors are expressed in a low percentage of cold-sensitive neurons. In order to increase the probability of GqPCR activation on cold-sensitive neurons, I decided to apply an inflammatory cocktail that contained different agonists involved in inflammation (i.e. inflammatory soup): 100 µM serotonin, 100 µM histamine, 500 nM BK, 10 µM PGE2, 100 µM ATP and 100 µM UTP.

From the total number of DRG neurons recorded in calcium imaging experiments in $TRPM8^{BAC\text{-}EYFP}$ mice, 55.4% (206 out of 372) responded to the application of the inflammatory cocktail, showing robust intracellular calcium increases (Fig. 42A). Within the cold-sensitive population, 30% (18 out of 60) of the neurons showed a transient calcium increase when the inflammatory

cocktail was applied, while the percentage of responses to the inflammatory cocktail was significantly higher in the cold-insensitive population, 60.3% (188 out of 312) ($p<0.001$, Z test) (Fig. 42B). The higher percentage of responses was accompanied by larger amplitude responses to the inflammatory cocktail in the cold-insensitive population (CS= 0.38 ± 0.15 *vs* CI= 1.47 ± 0.07) ($p< 0.001$) (Fig. 42A). Moreover, in the cold-insensitive population, 77.1% (145 out of 188) of neurons that respond to the inflammatory cocktail also responded to capsaicin, while only 24.2% (30 out of 124) of the neurons which did not response to the inflammatory cocktail responded to capsaicin. Of those neurons activated by capsaicin, 82.8% (145 out of 175) were activated by BK ($p< 0.001$, Z test). Additionally, the amplitude of capsaicin response was higher in the neurons which responded to the inflammatory cocktail (1.47 ± 0.07) than the neurons which did not response to the inflammatory cocktail (0.98 ± 0.11) ($p= 0,0017$).

Next, I evaluated the effect of the inflammatory soup on cold-evoked responses in cold-sensitive neurons. The amplitude of the cold response in neurons which were sensitive to the inflammatory cocktail was reduced in the presence of the inflammatory cocktail and partially recovered after the inflammatory cocktail wash out (Cold= 0.55 ± 0.08 *vs* Cold + Inflammatory cocktail= 0.42 ± 0.07 *vs* Cold= 0.47 ± 0.08) (Fig. 42C). Notably, this effect was also observed in cold-sensitive neurons which did not respond directly to the inflammatory cocktail (Cold= 0.78 ± 0.06 *vs* Cold + Inflammatory cocktail= 0.59 ± 0.05 *vs* Cold= 0.64 ± 0.04) (Fig. 42D). The percentage of capsaicin response was higher in the cold-sensitive neurons which responded to the inflammatory cocktail (50%, 9 out of 18) than in the cold-sensitive neurons which did not showed a response to the inflammatory cocktail (30.9%, 13 out of 42), although the amplitude of capsaicin responses was not significantly different (Cold-sensitive Inflammatory cocktail-sensitive= 1.29 ± 0.7 *vs* Cold-sensitive Inflammatory cocktail-insensitive= 0.97 ± 0.23) ($p= 0.62$).

Next, I studied the changes in excitability of cold-sensitive neurons in the presence of the inflammatory cocktail in response to a cooling ramp by performing cell-attached electrophysiological recordings and simultaneous calcium imaging (Fig. 42E). I recorded 6 neurons which showed a calcium increase in response to the inflammatory cocktail (Fig. 42E). The amplitude of the cold-induced increase in intracellular calcium levels showed a tendency to be reduced in the presence of the inflammatory cocktail when compared to control responses (Cold= 0.93 ± 0.21 *vs* Cold + Inflammatory cocktail= 0.62 ± 0.12) ($n= 6$, $p= 0.064$) (Fig. 42F). The presence of the inflammatory cocktail did not affect drastically the excitability of the neurons during a cold ramp: neither the temperature threshold of activation (Cold= 27.36 ± 1.38 ºC *vs* Inflammatory cocktail= 25.02 ± 1.95) ($n= 6$, $p= 0.072$) nor the firing frequency during the cold stimuli (Cold= 14.19 ± 3.38 Hz *vs* Inflammatory cocktail= 14.81 ± 3.9 Hz) ($n= 6$, $p= 0.56$) (Fig. 23G-H).

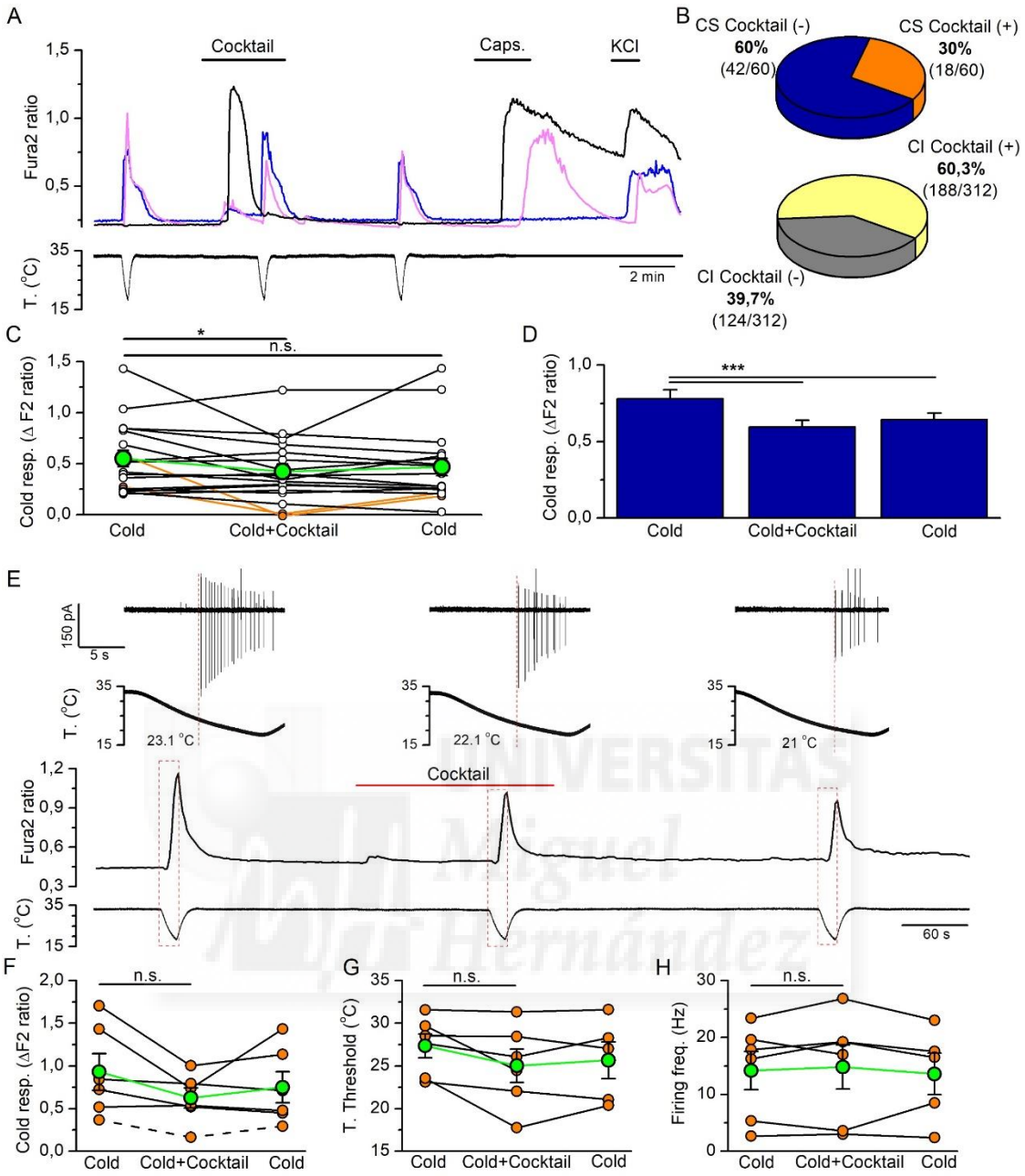

Figure 42. An inflammatory cocktail does not affect the cold-evoked response drastically. *A,* Time course of Fura2 fluorescence during a protocol exploring the effect of an inflammatory cocktail on cold-evoked responses. Two cold-sensitive neurons (blue and pink trace) are displayed together with a cold-insensitive neuron (black trace); the three neurons had an intracellular calcium increase in response to the inflammatory cocktail. Bottom trace represents the simultaneous recording of bath temperature. ***B,*** Summary of the percentage of responses to the inflammatory cocktail observed in cold-sensitive (CS) (top) and cold-insensitive (CI) (bottom) neurons. ***C,*** Amplitude of individual and averaged (green) cold-induced responses in cold-sensitive neurons that respond to the inflammatory cocktail. In orange, the two neurons in which the inflammatory cocktail had a notable, reversible effect. Statistical differences were calculated by an ANOVA test for repeated measures followed by a Bonferroni's post-test (*, $p< 0.05$). ***D,*** Averaged amplitude of cold-evoked responses in cold-sensitive neurons that showed no sensitivity to the inflammatory cocktail. Statistical differences were calculated by an ANOVA test for repeated measures followed by a Bonferroni's post-test (n= 42) (***, $p< 0.001$). ***E,*** Calcium imaging and simultaneous

electrophysiological recording of a cold-sensitive neuron. Displayed from top to bottom are action currents recorded in the cell-attached configuration evoked by three cooling ramps applied during the protocol (fragment of the recording corresponding to the time delimited by the red box in the calcium recording trace), simultaneous recording of bath temperature in which the temperature threshold of AP firing is indicated, Fura2 fluorescence time course and the simultaneous recording of the bath temperature. **F,** Individual and averaged (green) Fura2 amplitude response, ***G,*** temperature thresholds, ***H,*** and firing frequency during the three cooling ramps as in protocol E. Statistical significance was calculated by a paired t-test.

In conclusion, I found that the expression of GqPCR for the inflammatory mediators tested is lower in cold-sensitive neurons compared to the rest of DRG neuronal subpopulations. Calcium imaging and electrophysiological recordings show that GqPCR activation leads to somewhat smaller cold-evoked responses, although it does not affect drastically the cold sensitivity of these neurons.

5. Discussion

UNIVERSITAS
Miguel
Hernández

5.1 Agonism of macrolide immunosuppressants

In this thesis, I report that tacrolimus (TAC) and rapamycin, two clinically relevant macrolide immunosuppressants produced by soil microorganisms, are novel agonists of TRPM8 channels. Using calcium imaging and patch-clamp recordings, I demonstrate the agonistic effect of these two compounds on heterologously-expressed and on native TRPM8 ion channels.

5.1.1 Biophysical and molecular aspects of tacrolimus and rapamycin agonism on TRPM8

I found that TAC and rapamycin activate robust TRPM8 currents and evoke calcium influx in HEK293 cells expressing rat, mouse and human TRPM8. The effect of both compounds is dose-dependent although a complete dose-response curve could not be obtained and a reliable EC_{50} value was not calculated due to the poor solubility of these compounds in aqueous solutions that prevented testing concentrations higher than 30 µM *in vitro*. Nevertheless, at this concentration rapamycin evokes responses that are similar to those obtained with the same concentration of menthol, suggesting similar potency as a TRPM8 agonist. In the case of TAC, the potency, compared to menthol, was slightly lower. TAC and rapamycin activate TRPM8 channels by shifting the voltage dependence of channel activation towards physiological membrane potentials. Similar to menthol, TAC and rapamycin potentiate cold-evoked responses by shifting the TRPM8 temperature threshold of activation in a dose-dependent manner, with an obvious effect at low concentrations. The effects of TAC on TRPM8 gating also resemble those of menthol; TAC slows the activation kinetics, stabilizing the open channel conformation. The effects on channel gating fit with the description of TRPM8 type I agonists introduced by Janssens et al. (2016), which include menthol, thymol, icilin, and linalool.

I present multiple evidences demonstrating that TAC and rapamycin responses are mediated by TRPM8 channel activation. First, TAC- and rapamycin-evoked calcium increases were absent in HEK293 cells not expressing TRPM8, or when calcium was removed from the extracellular solution, denoting that calcium signals are due to calcium influx from the extracellular medium. In HEK293 cells expressing TRPM8 and in cold-sensitive DRG neurons, TAC- and rapamycin-evoked currents were fully blocked by BCTC (50 µM) and AMTB (10 µM), two structurally unrelated TRPM8 antagonists. Moreover, TAC responses observed in HEK293 cells were blocked by the unspecific Ca^{2+} channel blocker SKF-96365 (10 µM).

I exclude a possible activation of TRPM8 by downstream signaling pathways triggered by TAC by different approximations. First, cyclosporine A, a cyclic undecapeptide also targeting calcineurin signaling, had no effect on TRPM8 expressed heterologously or in cold-sensitive DRG neurons in culture. These results exclude the calcineurin pathway as the one involved in the effects of TAC. Moreover, the rapid and reversible current responses to TAC, observed in cell-free inside-out patches, conclusively demonstrate that the interaction of TAC with the channel is direct and does not require signaling cascades. This conclusion is further supported by

experiments of TAC effects on purified TRPM8 channels in planar lipid bilayers that are presented in the accompanying publication.

The next question I tried to address was to determine the region or residues of the TRPM8 channel involved in TAC activation. By using single residue mutants, I discarded the involvement of two critical residues for menthol activation, Y745 and L1009, and the residue critical for icilin activation, N799. Remarkably, although the mutants Y745H and L1009R had normal responses to TAC, they did not show potentiation of the cold-evoked response. Additionally, I studied the effect of a mutation on the conserved TRP box, specifically, the residue P1012, a conserved residue in TRPC1 which has been shown to participate in the binding of the immunophilin FKBP12, the molecular ligand of tacrolimus, to TRPC1 (Shim et al., 2009). The mutant mTRPM8-P1012Q showed reduced responses to cold and lost its sensitivity to TAC and to menthol, suggesting that this mutation affects the gating of TRPM8 to different agonist and not exclusively to TAC. Noteworthy, the potentiation of the cold response in the presence of TAC was also lost in this mutant, although menthol was still able to potentiate the cold response. In addition, I also tested the chicken TRPM8 orthologue, which share an identity of 79.9% with mTRPM8 but displays different thermosensitivity (smaller responses to cold) and chemosensitivity (higher sensitivity to menthol) (Pertusa et al., 2018). I found that TAC-activated currents were strongly reduced in cTRPM8 and that the potentiation of the cold responses in the presence of TAC were lost.

In conclusion, I demonstrate that TAC and rapamycin activate TRPM8 channels directly and exclude the interaction of TAC with the icilin and menthol binding sites. The identification of the critical residues for TAC effects should be addressed in the future. Taking advantage of the different TAC sensitivities of cTRPM8 and mTRPM8 channels one could design experiments that involve the design of chimeras between these two orthologs (Pertusa et al., 2018). The similar structure of some motifs on TAC and rapamycin suggest that both compounds may share a mechanism of action on TRPM8. Future experiments could analyze different analogs to resolve the part of the molecules interacting with TRPM8.

5.1.2 Specificity of tacrolimus and rapamycin effects

Based on a detailed pharmacological characterization of wildtype, hemizygous and TRPM8 KO mice, I conclude that TAC and rapamycin activate TRPM8-expressing sensory neurons, an effect which is highly selective at the concentrations tested.

In TRPM8^{BAC}-EYFP mice, TAC and rapamycin activated the majority of TRPM8-expressing cold-sensitive neurons, identified by EYFP fluorescence and by their response to a cold ramp from 32-34 to 18 ^{o}C. In contrast, only a minority of the EYFP(-) neurons (i.e. those not expressing TRPM8) were activated by TAC or rapamycin, suggesting a highly specific effect on TRPM8-expressing neurons. Moreover, low concentrations of TAC and rapamycin (10 µM and 1 µM respectively) sensitized the response to cold of these neurons in a reversible manner, an effect that was

accompanied by a shift in the temperature response threshold of individual neurons towards warmer temperatures.

The results in TRPM8$^{EGFPf/+}$ mice were very similar to those obtained in TRPM8^{BAC}-EYFP and supported our previous observation: a very strong correlation between TRPM8 expression and sensitivity to TAC and rapamycin. TAC had direct excitatory effects on more that 50% of TRPM8-expressing neurons in TRPM8$^{EGFPf/+}$ mice. This value is somewhat lower than in TRPM8^{BAC}-EYFP. This is not unexpected, considering that these animals only have one functional copy of the *Trpm8* gene. A similar gene dosage was found previously when characterizing cold-evoked activity in corneal endings using this transgenic mouse line (Parra et al., 2010).

In agreement with a critical role of TRPM8 in mediating responses to these two macrolide molecules, in DRG cultures from TRPM8-KO mice, TAC and rapamycin responses were almost absent in putative cold-thermorreceptors (identified by EGFPf fluorescence), in parallel with a near suppression of their responses to cold or menthol.

In cultured neurons of TRPM8$^{EGFPf/+}$ and TRPM8$^{EGFPf/EGFPf}$ mice residual responses to TAC and rapamycin were observed on EGFPf(-) neurons. A detailed analysis of these responses showed that they had some distinct characteristics; the amplitude was smaller, compared to responses in fluorescent neurons of TRPM8$^{EGFPf/+}$ mice or TRPM8^{BAC}-EYFP mice and they were nearly abolished during the cooling ramp. Additionally, the majority of these TAC-sensitive EGFPf(-) neurons express TRPV1 channels as they were activated by capsaicin. These characteristics suggest that residual responses to TAC could be mediated by TRPV1, although TAC-sensitive EGFPf(-) neurons constitute a small percentage from the total of capsaicin-sensitive neuronal population. Somewhat surprisingly TAC has no effect on recombinant TRPV1 channels at the concentration tested (30 µM), suggesting that TRPV1 does not mediate residual TAC responses in DRG neurons in culture. A previous study found that TAC activated a small percentage (3.1%) of rat DRG neurons and many of these neurons were also activated by capsaicin (Senba et al., 2004). As in our case, and consistent with a weak effect, the total percentage of capsaicin-positive neurons was much higher than those responding to TAC. Taking into account that they did not studied the response to TRPM8 agonists in these neurons, and considering our results, it is probable that a high percentage of TAC responses observed in the study of Senba and colleagues were mediated by TRPM8. Another study suggested that TAC modulates TRPV1 channels, although they propose an indirect mechanism involving calcineurin inhibition and TRPV1 phosphorilation, and not a direct effect (Pereira et al., 2010). Despite the clear effects on TRPM8(+) neurons, since the TRPV1(+) population is much larger than the TRPM8(+) one in the DRG, these “residual” responses could still be functionally significant.

I found that TAC activated TRPA1 channels expressed heterologously, albeit less effectively than TRPM8. In contrast, the indication that TAC or rapamycin were acting on native TRPA1 in DRG sensory neurons was only circumstantial. The large majority of AITC-sensitive neurons (i.e. those expressing TRPA1) showed no responses to TAC, indicating that the agonism was weak or absent. Moreover, only half of the TAC-sensitive EGFPf(-) neurons responded to AITC.

Nevertheless, consistent with a possible activation of TRPA1, in a murine model of chronic contact hypersensitivity, TAC increased the number of scratch bouts and these were significantly reduced by topical application of a TRPA1 antagonist (Wong et al., 2018). Future studies, analyzing the responses to TAC and rapamycin in TRPA1 and TRPV1 KO animals should clarify the mechanism underlying these responses.

During this study, I showed that topical applications of 1% TAC solutions on the corneal surface of mice triggered eye blinking. However, these effects were not reduced in TRPM8 KO mice, suggesting that this solution has irritant effects that are independent of TRPM8 activation. The residual responses observed in TRPM8(-) neurons in culture could provide an explanation for these irritant actions. Because the solution tested *in vivo* had a much higher concentration of the drug (12 mM) than I could test in solution *in vitro*, it could lead to more efficient activation of other nociceptive TRP channels expressed on corneal terminals, explaining the TRPM8-independent irritant effect. This effect could also explain the most common sensory side effects reported upon topical application of TAC to the eye and the skin, like the transient burning sensation (Fukushima et al., 2014; Abud et al., 2016).

In conclusion, I find that TAC and rapamycin have a highly selective effect on TRPM8-expressing DRG neurons in culture. However, these selectivity was not absolute at the highest concentration tested, with some weak effects remaining that are TRPM8-independent. TAC related side effects such as burning skin or irritation could be mediated by activation of other TRP channels expressed on nociceptors. Alternatively, since a subpopulation of TRPM8-expressing primary sensory neurons have a nociceptive phenotype (Xing et al., 2006; Alcalde et al., 2018), and many also express TRPV1, their activation may contribute to the transient discomfort produced by TAC.

5.1.3 Therapeutic implications and clinical relevance

The identification of TAC and rapamycin as effective and relatively selective TRPM8 agonists has several implications from the experimental and clinical point of view.

First, it expands the current arsenal of drugs targeting TRPM8, which can be used experimentally in basic research. The number of chemical agonists reported for TRPM8 channels is increasing slowly but, nevertheless is still very modest. I demonstrate that TAC and rapamycin can be used to identify and modulate the subpopulation of TRPM8-expressing neurons. Moreover, residues involved in TRPM8 activation by TAC are different from the residues involved in the activation of TRPM8 by other known agonists. Thus, the elucidation of these residues could provide new clues about the molecular mechanisms of TRPM8 activation.

From the clinical point of view, these macrolides provide a useful experimental tool for the modulation of TRPM8 expressing fibers. Menthol is widely included in topical cream formulations for the relief of pain; however, there are no available drugs for the selective modulation of TRPM8 channels in humans. As already mentioned in the introduction, TRPM8 plays important roles in different physiological processes and in diverse pathological conditions. On one hand, it appears to participate in the mechanisms of cold hyperalgesia and allodynia (Knowlton et al., 2013). At

the same time, it is the principal mechanism of menthol-induced analgesia (Liu et al., 2013), and also plays a significant role in cooling-mediated analgesia (Proudfoot et al., 2006; Knowlton et al., 2013). Activation of TRPM8 sensory pathways also relief the sensation of itch (Palkar et al., 2018). Moreover, TRPM8 activation has a potent anti-inflammatory role in the gut (Ramachandran et al., 2013). Therefore, TRPM8 modulators (agonists and antagonists) may offer multiple possibilities in the relief of pain and visceral inflammation and consequently, it has led to a strong interest in the pursuit of novel modulators of TRPM8 channels (Moran & Szallasi, 2018). TAC could be used experimentally to explore the effect of TRPM8 activation in different human pathological conditions, as for example chronic itch, a pathology in which TRPM8 agonists have been shown to be effective (Ständer et al., 2017).

Because activation of TRPM8 regulates basal tearing and blinking (Parra et al., 2010; Quallo et al., 2015), TRPM8 agonists have been proposed as a possible therapy for DED and the effectiveness of different TRPM8 agonist in improving DED symptoms have been reported (Belmonte and Gallar, 2011; Yang et al., 2017). Besides its use as a systemic immunosuppressant in the prevention of organ rejection, TAC is also used topically in the treatment of DED symptoms (Jones et al., 2017). In clinical ophthalmology, TAC has been used in solutions at concentrations up to 0.1%. This is equivalent to 1.2 mM, suggesting that it should readily activate TRPM8 channels at corneal endings. I observed a clear effect of 1% TAC solutions on basal tearing and eye blinking, suggesting that some of the beneficial effects reported for TAC in dry-eye conditions (Abud et al., 2016) may involve activation of TRPM8 channels in trigeminal cold thermoreceptor endings. However, the fact that blinking was not reduced in TRPM8 KO animals clearly indicates that other mechanisms are involved at this concentration and with this particular formulation. The possible activation of TRPA1 or TRPV1, at these high concentrations of TAC could also explain the burning sensation reported by some patients. Knowledge of the agonistic effect of TAC on TRPM8 channels and possibly in other TRP channels expressed in nociceptors may form the basis for the development of new TAC preparations with reduced sensory side effects.

Whether activation of TRPM8 by TAC is relevant for the treatment of atopic dermatitis is currently unclear. However, the effect of TAC on cutaneous cold thermoreceptor endings also suggest relevant consequences for topical use in the skin (see additional experiments in the publication accompanying this thesis). The apparent potency was lower than for corneal endings. This however may reflect a poor accessibility of the drug in the in vitro preparation used to test the compound, which lacks vascularization and requires application of substances through the corium. It is becoming well established that electrical activity in peripheral sensory endings can have potent immunomodulatory effects (Chavan et al., 2017), suggesting that modulation of TRPM8 channels by TAC may play a role in its anti-inflammatory actions. At this point, this is just a hypothesis but with important implications.

Rapamycin (Sirolimus) and analogs (Everolimus and Temsirolimus) are widely used in humans, mainly as immunosuppressants following kidney and liver transplants, but they have also been

used to treat certain types of cancers and trialed for many different pathologies (Arriola Apelo & Lamming, 2016). However, diverse and severe negative side effects have been described for these drugs, probably because its canonical target, mTOR, participates in many vital cellular functions (Kim & Blenis, 2014).

The results presented here imply that TAC and rapamycin, already approved compounds for clinical use, could be repurposed for another target/disease (i.e. TRPM8 modulation), a concept that is called “drug repositioning” (Doan et al., 2011). Drug repositioning is a promising strategy in drug discovery, with some important advantages compared to the *de novo* identification and development of active compounds. Because the safety and pharmacokinetic profiles of the repositioned candidates are already established, it allows a dramatic reduction in development time and expense.

5.2 TRPM8 modulation by GqPCRs

The main goal of this set of experiments was to elucidate the mechanism involved in TRPM8 modulation by GqPCRs: different mechanisms have been proposed to be involved in this process. PI(4,5)P2-dependence of TRPM8 activity is well-stablished and therefore PLC-mediated hydrolysis of PI(4,5)P2 downstream of GqPCR activation has been proposed as the main effector participating in the inhibition of TRPM8 by GqPCR activation (Rohacs et al., 2005; Liu and Qin, 2005; Daniels et al. 2009; Zakharian et al., 2010). PKC-mediated dephosphorylation of the channel has also been proposed to be the principal mechanism by which GqPCR activation inhibits TRPM8 channels, in a similar manner than TRPV1 is sensitized (Premkumar et al., 2005; Abe et al., 2006; Linte et al., 2007). A different research group supports the hypothesis that modulation of TRPM8 is exerted by a direct interaction of TRPM8 with activated Gαq subunits and, therefore, independent of cell signaling pathways downstream of GqPCRs (Zhang et al., 2012; Li & Zhang, 2013). Specifically, this last hypothesis based its conclusions on the following arguments; direct interaction of Gαq subunit to TRPM8 was demonstrated by co-immunoprecipitation, Gαq mutant subunits constitutively active inhibited TRPM8 activity in inside-out patches and a chimeric Gαq subunit unable to active PLC was still able to inhibit TRPM8. Additionally, Zhang et al. (2012) proposed that depletion of membrane PI(4,5)P2 is not crucial for TRPM8 downregulation after GqPCRs activation based on the following results; histamine 1 receptor activation inhibited TRPM8 in the presence of the PLC inhibitor U73122 and different “PI(4,5)P2 insensitive” TRPM8 mutants were inhibited by GqPCR activation.

Here I revisited this question, and demonstrate by different strategies that PI(4,5)P2 depletion is crucial for TRPM8 inhibition after GqPCRs activation. I also explored the effects of GqPCRs activation on sensory neurons in culture and their responses to cold temperature.

5.2.1 TRPM8 modulation by GqPCR in an heterologous expression system

G protein-coupled receptors (GPCRs) form the largest class of membrane proteins in the human genome and are the targets of most drugs in the clinic. I studied GqPCR-mediated inhibition of

TRPM8 activity by overexpressing TRPM8 channels and the Muscarinic 1 receptor (M1R) in HEK293 cells. Activation of M1R is known to activate PLC, leading to PI(4,5)P2 hydrolysis. In my hands, activation of M1R by Cch totally suppressed inward and outward TRPM8-mediated currents evoked by menthol at 33 ºC. The same experiment performed at 23 ºC showed different results; inward currents were fully suppressed while outward currents were only partially reduced. Importantly, I demonstrated that responses to cold, the physiological stimulus of TRPM8, were also fully suppressed in the presence of the M1R agonist Cch. The effect of Histamine 1 Receptor (H1R) activation on TRPM8 currents were weaker. The differences observed between M1R and H1R could reflect quantitative differences in the efficiency of coupling of these two membrane receptors to their intracellular effectors. Additionally, I also used melanopsin, a GqPCR that is activated by light (Provencio et al., 1998; Qiu et al., 2005). By using light activation, I achieved a more precise temporal control of GqPCR activation, and I demonstrated that it may become a powerful tool in the study of GqPCR signaling. Our results demonstrate that melanopsin activation has an inhibitory action on TRPM8 channels, although the effect was more modest than that produced by M1R or H1R activation.

Previous studies reported a similar receptor-mediated inhibition of TRPM8 activity. However, an important difference with my work is the fact that only inhibition of menthol-evoked responses was characterized at non-physiological temperatures (Rohacs et al., 2005; Liu & Qin et al., 2005; Zhang et al., 2012). Indeed, I found important temperature- and voltage-dependent differences in GqPCR-mediated inhibition of TRPM8 channels; the inhibitory effect was weaker at 23 ºC than at 33 ºC and also weaker at positive voltages than at negative voltages. These differences could be explained by the results described by Rohacs et al. (2005). By performing dose-response curves with a water-soluble analog of PI(4,5)P2 (1,2-dioctanoyl PI(4,5)P2), they demonstrated that cold, menthol and voltage increase the apparent affinity of TRPM8 for PI(4,5)P2. The apparent affinity of a channel for PI(4,5)P2 has key functional implications because it will determine the sensitivity of the channel to changes in PI(4,5)P2 levels; higher affinity for PI(4,5)P2 leads to a weaker effect on channel activity following a PI(4,5)P2 decrease. The higher affinity of TRPM8 for PI(4,5)P2 at lower temperatures could explain the weaker inhibitions observed at 23 ºC compared with those observed at 33 ºC. In the same way, the weaker inhibitions at positive potentials could be due to the higher affinity of TRPM8 for PI(4,5)P2 at higher voltages. I obtained the smallest value of M1R-evoked inhibition at +100 mV in experiments performed at 23 ºC, the experimental situation at which TRPM8 affinity for PI(4,5)P2 is maximal. Therefore, we can hypothesize that the magnitude of GqPCR-mediated inhibition of TRPM8 is directly related with the TRPM8 affinity for PI(4,5)P2, which at the same time is dependent on agonist concentration, temperature and voltage.

Establishing a causal relationship between PI(4,5)P2 depletion after GqPCR activation and TRPM8 channel inhibition requires the demonstration that the exclusive modulation of PI(4,5)P2 levels can recapitulate the effects evoked by GqPCR activation. For this purpose, I used a voltage-sensitive lipid 5-phosphatase (Dr-VSP) which allows the direct manipulation of PI(4,5)P2 levels without affecting other signaling cascades downstream of GqPCR activation (Hossain et

al., 2008). I found that exclusive PI(4,5)P2 depletion by Dr-VSP activation recapitulated the effects of GqPCR activation on TRPM8 inward currents; Dr-VSP activation completely inhibited inward menthol-evoked currents at 33 ºC. However, at positive potentials GqPCR activation led to a stronger inhibition than Dr-VSP activation, and the same situation was observed at 23 ºC. The differences observed in the degree of inhibition of outward currents between the two methods tested could have different explanations. First, a number of studies found that membrane voltage can modulate signal transduction and ligand binding in GPCRs, including muscarinic M1 receptors (Rinne et al., 2015). I have not explored this mechanism in my studies. In addition, it could be that GqCPR activation led to more profound PI(4,5)P2 decreases than Dr-VSP. In order to study the effectiveness of the two methods in depleting PI(4,5)P2, I performed experiments using two potassium channels whose PI(4,5)P2-dependence is well-established and can be used as biosensors of relative PI(4,5)P2 levels. KCNQ2/3 channels have a strong PI(4,5)P2 requirement and, in agreement with this characteristic, I found that both methods, the activation of M1R or the Dr-VSP, strongly suppress KCNQ2/3 currents. I also studied the inwardly rectifying potassium channel Kir2.1, which have a special high affinity for PI(4,5)P2 and therefore its inhibition requires a profound decrease of PI(4,5)P2. I observed that Dr-VSP activation strongly suppressed Kir2.1 current while M1R activation evoked no changes in Kir2.1 current even with Cch concentrations ten times higher than those used for inhibition of KCNQ2/3 or TRPM8. Therefore, these results reject the hypothesis that GqCPRs evoke stronger PI(4,5)P2 depletion than Dr-VSP and somehow demonstrate the opposite, Dr-VSP evoke larger PI(4,5)P2 decreases because it was able to inhibit Kir2.1 while M1R activation does not.

Another possible explanation for the higher inhibitory effect observed at positive potentials after GqPCR compared to Dr-VSP activation is that an alternative mechanism activated downstream of GqPCR (e.g. direct Gq subunit binding) participate in the inhibition of TRPM8 channels and account for the inhibition of the remaining outward current after PI(4,5)P2 depletion by Dr-VSP. If this explanation is correct, the effects of direct PI(4,5)P2 depletion and GqPCR activation should be additive. To test this hypothesis, I combined the two methods, depletion of PI(4,5)P2 and activation of a GqPCR in the same cell. I used melanopsin as the GqPCR for this experiment because its agonist (light) allows a precise activation during the depolarizing pulse of Dr-VSP. I found that activation of melanopsin during the plateau phase of Dr-VSP inhibition did not increase the percentage of inhibition and the remaining outward current was unchanged. Therefore, this result is inconsistent with the hypothesis of an additional mechanism of channel inhibition: the activation of a GqPCR did not increase the inhibition evoked by exclusive PI(4,5)P2 depletion. The most likely explanation for the percentage of current still remaining after PI(4,5)P2 depletion by Dr-VSP is based on the mechanism of action of this tool. Although both methods, GqPCR activation and Dr-VSP, reduce PI(4,5)P2 levels, their end products are different; GqCPR activates PLC which cleaves PI(4,5)P2 into DAG and IP3, while Dr-VSP removes the phosphate groups from PI(4,5)P2 and PI(3,4,5)P3 producing PI(4)P and PI. It has been demonstrated that, although with less efficiency, PI(4)P can also support TRPM8 activity. Therefore, the remaining TRPM8 current at positive potentials, after Dr-VSP activation, could be supported by the excess of PI(4)P

(Rohacs et al., 2005; Zakharian et al., 2010). This hypothesis could be tested by using a combined 5' and 4' phosphatase which depletes both PI(4,5)P2 and PI(4)P. The different products of both reactions could also explain the differences in TRPM8 current recovery after M1R and Dr-VSP activation; TRPM8 recovery after Dr-VSP-mediated inhibition was fast and almost complete. In contrast, recovery of TRPM8 after M1R activation was slower and only partial. This is in agreement with the results previously presented by Falkenburguer et al. (2010) which showed that recovery of KCNQ2/3 currents after Dr-VSP activation was much faster than after M1R stimulation. These differences could be attributed to the fact that PLC degrades PI(4,5)P2 and PI(4)P and therefore PIP5K and PI4K are needed to recover PI(4,5)P2 levels while Dr-VSP only degrades PI(4,5)P2 thus requiring only PIP5K to re-synthesize PI(4,5)P2.

In accordance with the dependence of TRPM8 current on PI(4,5)P2 levels, I found an excellent correlation between the time course of TRPM8 inhibition and the time course of PI(4,5)P2 translocation from the membrane to the cytosol after M1R activation (a reporter of PI(4,5)P2 depletion) measured by the PI(4,5)P2 fluorescent sensor PH-GFP.

Thus, all of our results point to PI(4,5)P2 depletion as a critical determinant of GqPCR inhibition of TRPM8. I also tried to replicate the experiments of Zhang et al. (2012) in which they use a PLC inhibitor as a crucial experimental strategy to distinguish between direct Gq subunit effects and PI(4,5)P2 depletion because PLC acts downstream of Gαq but upstream of PI(4,5)P2 concentration changes (Horowitz et al. 2005). I first investigated the effects of the PLC blocker U73122. In order to test its effectiveness in blocking PLC, I performed confocal imaging of the fluorescence PI(4,5)P2 reporter PH-GFP and studied its translocation before and after the incubation of cells with U73122 and its inactive analog U73343. I found that U73122 strongly uncoupled activation of PLC by receptors as expected. Unexpectedly, I also found that U73343, the presumed inactive analog, was also effective in blocking PLC activation at a concentration within the range of usage observed in the bibliography. Both compounds showed a dose-dependent effect on PH-GFP translocation. Moreover, I demonstrated that U73343 totally abolished the inhibitory effect of M1R activation on KCNQ2/3 currents. A large number of scientific articles have used the PLC inhibitor U73122 as a tool to verify that a certain signaling pathway requires PLC. However, the literature on U73122 contains additional suggestions about unexpected side effects, raising the question whether this agent can be used as a specific pharmacological tool. For example, it has been shown that U73122 acts as a nonspecific thiol reagent that can even stimulate some PLC isoforms (Horowitz et al., 2005; Klein et al., 2011). Moreover, recently it has been demonstrated that U73122 is a direct modulator of different members of the TRPM subfamily, being an agonist of TRPM4 channels by a mechanism which does not involve PLC and PI(4,5)P2, and an antagonist of TRPM3 channels (Leitner et al., 2016). However, there is no description on the bibliography of U73343 activity. Taking into account the described side effects of this drug and the fact that the control compound U73343 was not working as expected, I decided to test edelfosine, a theoretically cleaner PLC inhibitor. I explored the effectiveness of edelfosine by studying the effects of incubation in the translocation of PH-GFP; incubation with edelfosine totally prevented the translocation of PH-GFP to the cytosol. Moreover,

I studied the effect of edelfosine pre-incubation on M1R-mediated KCNQ2/3 inhibition and found that edelfosine was able to fully abrogate the effect of M1R activation on KCNQ2/3 currents. When cells expressing TPRM8 and M1R were incubated with edelfosine, the TRPM8 inhibition evoked by M1R activation was also lost, suggesting that the involvement of PLC and PI(4,5)P2 depletion is crucial for TRPM8 inhibition after GqPCR activation. Therefore, our experiments exclude that GqPCR-mediated TRPM8 inhibition can still occur without the activation of PLC. At present, I cannot explain the discrepant findings between our experiments and previous studies with PLC blockers reported by Zhang et al. (2012). When they incubated HEK293 cells with U73122, TRPM8 inhibition by H1R or B2R activation was little affected, obtaining similar degree of inhibition than in control cells. However, I demonstrated that by blocking PLC with edelfosine, the inhibitory effect of M1R activation totally disappears.

Collectively, my data support the conclusion that TRPM8 activity depends on PI(4,5)P2 levels and demonstrate that the principal mechanisms involved in GqPCRs modulation of TRPM8 channels is PI(4,5)P2 hydrolysis as a result of activation of PLC by activated Gq subunits. I also corroborate that TRPM8 affinity for PI(4,5)P2 varies with temperature and voltage, as previously demonstrated by Rohacs and colleagues (Rohacs et al., 2005).

5.2.2 TRPM8 modulation by GqPCR in cold-sensitive DRG neurons

An important, remaining aspect of discussion is the physiological relevance of GqPCR modulation on cold thermoreceptor activity. To test the effect of GqPCR activation on native TRPM8 channels, I stimulated GqPCRs expressed on sensory neurons by application of a single agonist or by application of an inflammatory cocktail. In general, I found that GqPCR of the agonists tested were expressed in a low percentage of cold-sensitive neurons. The frequency of responses to inflammatory mediators was higher in the rest of sensory neurons subpopulations. From all the neurons that responded to the inflammatory mediators, a high percentage was also sensitive to capsaicin, indicating the expression of TRPV1 and denoting a nociceptive phenotype. Moreover, responses to capsaicin were larger in amplitude in the neurons that were activated by GqPCRs agonists, which could be due to the already described potentiation effect of GqPCR activation on TRPV1 activity (Cesare and McNaughton, 1996; Caterina et al., 2000; Premkumar & Ahern, 2000). In general, TRPM8-mediated cold responses were not drastically affected in the presence of inflammatory mediators. However, I found a variable effect in individual neurons, probably reflecting different levels of GqPCR expression. For example, in the two neurons that showed the largest amplitude in response to BK, the cold response in the presence of BK was abolished. Cell-attached recordings of cold-sensitive neurons also reflect a mild effect of inflammatory mediators in the electrical activity during cold-evoked responses. As I have demonstrated, PI(4,5)P2 depletion is the main mechanisms by which GqPCRs modulate TRPM8 activity. However, the physiological situation in neurons is different than when GqPCR are overexpressed heterologously. Different studies have estimated the extent to which PI(4,5)P2 is decreased in sensory neurons when a GqPCR is activated. Liu et al. (2010) measured the translocation of a PI(4,5)P2 optical probe transiently transfected in rat DRG neurons in response to BK and found

that membrane PI(4,5)P2 levels do not drop to a significant enough degree to induce translocation of the probe. Using the same optical probe, Lukacs et al. (2013) showed that BK caused a moderate reduction in PI(4,5)P2 membrane levels of sensory neurons. These results could explain the modest effects observed in cold-responses of TRPM8-expressing neurons during the application of GqPCRs agonists. If activation of GqPCR does not have a drastic effect on the global PI(4,5)P2 levels in plasma membrane, TRPM8 would still be able to generate robust depolarizing currents that induce the firing of action potentials. Therefore, our results suggest that native TRPM8 activity is not significantly affected in the acute presence of inflammatory mediators. The higher responses to capsaicin observed in the neurons that responded to inflammatory mediators suggest that the molecular mechanism of TRPV1 upregulation after GqPCR activation is more effective than the mechanisms involved in TRPM8 modulation, and therefore it is more likely to participate in acute pathophysiological processes. However, it is still possible that under chronic inflammatory conditions, which lead to important changes in GqPCR signaling, the PI(4,5)P2 levels would experience changes compatible with a stronger modulatory efficiency.

UNIVERSITAS
Miguel
Hernández

6. Conclusions

UNIVERSITAS
Miguel
Hernández

1. Tacrolimus and rapamycin activate TRPM8 channels in different species, including humans, and sensitize their response to cold temperature.
2. The activating effects of tacrolimus and rapamycin on TRPM8 involve a leftward shift on the voltage-dependent activation curve.
3. The mechanism of action of TAC is direct and independent of the menthol- and icilin-binding sites of TRPM8 channels, suggesting an interaction with different residues.
4. In cultured mouse DRG neurons, tacrolimus and rapamycin activate almost exclusively cold-sensitive neurons, by a TRPM8-dependent mechanism.
5. PI(4,5)P2 depletion is crucial for TRPM8 inhibition after GqPCRs activation.
6. In cold-sensitive neurons, activation of GqPCRs by canonical agonists have a mild effect on cold evoked response, suggesting a limited capacity to reduce PI(4,5)P2 levels.

UNIVERSITAS
Miguel
Hernández

7. Bibliography

UNIVERSITAS
Miguel
Hernández

Abe, J., Hosokawa, H., Sawada, Y., Matsumura, K., & Kobayashi, S. (2006). Ca2+-dependent PKC activation mediates menthol-induced desensitization of transient receptor potential M8. *Neuroscience Letters*, *397*(1–2), 140–4. https://doi.org/10.1016/j.neulet.2005.12.005

Abud, T. B., Amparo, F., Saboo, U. S., Di Zazzo, A., Dohlman, T. H., Ciolino, J. B., … Dana, R. (2016). A Clinical Trial Comparing the Safety and Efficacy of Topical Tacrolimus versus Methylprednisolone in Ocular Graft-versus-Host Disease. *Ophthalmology*, *123*(7), 1449–57. https://doi.org/10.1016/j.ophtha.2016.02.044

Aguettaz, E., Bois, P., Cognard, C., & Sebille, S. (2017). Stretch-activated TRPV2 channels: Role in mediating cardiopathies. *Progress in Biophysics and Molecular Biology*, *130*(Pt B), 273–280. https://doi.org/10.1016/j.pbiomolbio.2017.05.007

Alcalde, I., Íñigo-Portugués, A., González-González, O., Almaraz, L., Artime, E., Morenilla-Palao, C., … Belmonte, C. (2018). Morphological and functional changes in TRPM8-expressing corneal cold thermoreceptor neurons during aging and their impact on tearing in mice. *Journal of Comparative Neurology*, *526*(11), 1859–1874. https://doi.org/10.1002/cne.24454

Almaraz, L., Manenschijn, J.-A., de la Peña, E., & Viana, F. (2014). TRPM8. In *Handbook of experimental pharmacology* (Vol. 222, pp. 547–579). https://doi.org/10.1007/978-3-642-54215-2_22

Almeida, M. C., Hew-Butler, T., Soriano, R. N., Rao, S., Wang, W., Wang, J., … Romanovsky, A. A. (2012). Pharmacological Blockade of the Cold Receptor TRPM8 Attenuates Autonomic and Behavioral Cold Defenses and Decreases Deep Body Temperature. *Journal of Neuroscience*, *32*(6), 2086–2099. https://doi.org/10.1523/JNEUROSCI.5606-11.2012

Andersson, D. A., Chase, H. W. N., & Bevan, S. (2004). TRPM8 Activation by Menthol, Icilin, and Cold Is Differentially Modulated by Intracellular pH. *Journal of Neuroscience*, *24*(23), 5364–5369. https://doi.org/10.1523/JNEUROSCI.0890-04.2004

Andersson, D. A., Nash, M., & Bevan, S. (2007). Modulation of the Cold-Activated Channel TRPM8 by Lysophospholipids and Polyunsaturated Fatty Acids. *Journal of Neuroscience*, *27*(12), 3347–3355. https://doi.org/10.1523/JNEUROSCI.4846-06.2007

Arriola Apelo, S. I., & Lamming, D. W. (2016). Rapamycin: An InhibiTOR of Aging Emerges From the Soil of Easter Island. *The Journals of Gerontology. Series A, Biological Sciences and Medical Sciences*, *71*(7), 841–9. https://doi.org/10.1093/gerona/glw090

Asuthkar, S., Velpula, K. K., Elustondo, P. A., Demirkhanyan, L., & Zakharian, E. (2015). TRPM8 channel as a novel molecular target in androgen-regulated prostate cancer cells. *Oncotarget*, *6*(19), 17221–36. https://doi.org/10.18632/oncotarget.3948

Babes, A., Zorzon, D., & Reid, G. (2004). Two populations of cold-sensitive neurons in rat dorsal root ganglia and their modulation by nerve growth factor. *The European Journal of Neuroscience*, *20*(9), 2276–82. https://doi.org/10.1111/j.1460-9568.2004.03695.x

Babes, A., Zorzon, D., & Reid, G. (2006). A novel type of cold-sensitive neuron in rat dorsal root ganglia with rapid adaptation to cooling stimuli. *European Journal of Neuroscience*, *24*(3), 691–698. https://doi.org/10.1111/j.1460-9568.2006.04941.x

Babes, R. M., Selescu, T., Domocos, D., & Babes, A. (2017). The anthelminthic drug praziquantel is a selective agonist of the sensory transient receptor potential melastatin type 8 channel. *Toxicology and Applied Pharmacology*, *336*(October), 55–65. https://doi.org/10.1016/j.taap.2017.10.012

Badheka, D., Borbiro, I., & Rohacs, T. (2015). Transient receptor potential melastatin 3 is a phosphoinositide-dependent ion channel. *The Journal of General Physiology*, *146*(1), 65–77. https://doi.org/10.1085/jgp.201411336

Badheka, D., Yudin, Y., Borbiro, I., Hartle, C. M., Yazici, A., Mirshahi, T., & Rohacs, T. (2017). Inhibition of Transient Receptor Potential Melastatin 3 ion channels by G-protein βγ

subunits. *eLife*, *6*, 1–21. https://doi.org/10.7554/eLife.26147

Bai, V. U., Murthy, S., Chinnakannu, K., Muhletaler, F., Tejwani, S., Barrack, E. R., … Veer Reddy, G. P. (2010). Androgen regulated TRPM8 expression: a potential mRNA marker for metastatic prostate cancer detection in body fluids. *International Journal of Oncology*, *36*(2), 443–50.

Bandell, M., Dubin, A. E., Petrus, M. J., Orth, A., Mathur, J., Sun, W. H., & Patapoutian, A. (2006). High-throughput random mutagenesis screen reveals TRPM8 residues specifically required for activation by menthol. *Nature Neuroscience*, *9*(4), 493–500. https://doi.org/10.1038/nn1665

Bandell, M., Story, G. M., Hwang, S. W., Viswanath, V., Eid, S. R., Petrus, M. J., … Patapoutian, A. (2004). Noxious cold ion channel TRPA1 is activated by pungent compounds and bradykinin. *Neuron*, *41*(6), 849–57.

Bautista, D. M., Jordt, S. E., Nikai, T., Tsuruda, P. R., Read, A. J., Poblete, J., … Julius, D. (2006). TRPA1 Mediates the Inflammatory Actions of Environmental Irritants and Proalgesic Agents. *Cell*, *124*(6), 1269–1282. https://doi.org/10.1016/j.cell.2006.02.023

Bautista, D. M., Siemens, J., Glazer, J. M., Tsuruda, P. R., Basbaum, A. I., Stucky, C. L., … Julius, D. (2007). The menthol receptor TRPM8 is the principal detector of environmental cold. *Nature*, *448*(7150), 204–208. https://doi.org/10.1038/nature05910

Bavencoffe, A., Gkika, D., Kondratskyi, A., Beck, B., Borowiec, A. S., Bidaux, G., … Prevarskaya, N. (2010). The transient receptor potential channel TRPM8 is inhibited via the α2A adrenoreceptor signaling pathway. *Journal of Biological Chemistry*, *285*(13), 9410–9419. https://doi.org/10.1074/jbc.M109.069377

Bavencoffe, A., Kondratskyi, A., Gkika, D., Mauroy, B., Shuba, Y., Prevarskaya, N., & Skryma, R. (2011). Complex regulation of the TRPM8 cold receptor channel: Role of arachidonic acid release following M3 muscarinic receptor stimulation. *Journal of Biological Chemistry*, *286*(11), 9849–9855. https://doi.org/10.1074/jbc.M110.162016

Beccari, A. R., Gemei, M., Monte, M. Lo, Menegatti, N., Fanton, M., Pedretti, A., … Vistoli, G. (2017). Novel selective, potent naphthyl TRPM8 antagonists identified through a combined ligand-and structure-based virtual screening approach. *Scientific Reports*, *7*(1), 1–15. https://doi.org/10.1038/s41598-017-11194-0

Beck, B., Bidaux, G., Bavencoffe, A., Lemonnier, L., Thebault, S., Shuba, Y., … Prevarskaya, N. (2007). Prospects for prostate cancer imaging and therapy using high-affinity TRPM8 activators. *Cell Calcium*, *41*(3), 285–294. https://doi.org/10.1016/j.ceca.2006.07.002

Beck, L. A. (2005). The efficacy and safety of tacrolimus ointment: A clinical review. *Journal of the American Academy of Dermatology*, *53*(2), S165–S170. https://doi.org/10.1016/j.jaad.2005.04.059

Behrendt, H. J., Germann, T., Gillen, C., Hatt, H., & Jostock, R. (2004). Characterization of the mouse cold-menthol receptor TRPM8 and vanilloid receptor type-1 VR1 using a fluorometric imaging plate reader (FLIPR) assay. *British Journal of Pharmacology*, *141*(4), 737–745. https://doi.org/10.1038/sj.bjp.0705652

Belmonte, C., Brock, J. a, & Viana, F. (2009). Converting cold into pain. *Experimental Brain Research*, *196*(1), 13–30. https://doi.org/10.1007/s00221-009-1797-2

Belmonte, C., & Gallar, J. (2011). Cold Thermoreceptors, Unexpected Players in Tear Production and Ocular Dryness Sensations. *Investigative Opthalmology & Visual Science*, *52*(6), 3888. https://doi.org/10.1167/iovs.09-5119

Belmonte, C., & Viana, F. (2008). Molecular and cellular limits to somatosensory specificity. *Molecular Pain*, *4*, 1–17. https://doi.org/10.1186/1744-8069-4-14

Berridge, M. J., & Irvine, R. F. (n.d.). Inositol trisphosphate, a novel second messenger in cellular signal transduction. *Nature*, *312*(5992), 315–21.

Bevan, S., Hothi, S., Hughes, G., James, I. F., Rang, H. P., Shah, K., … Yeats, J. C. (1992). Capsazepine: a competitive antagonist of the sensory neurone excitant capsaicin. *British Journal of Pharmacology*, *107*(2), 544–52.

Bhave, G., Hu, H.-J., Glauner, K. S., Zhu, W., Wang, H., Brasier, D. J., … Gereau, R. W. (2003). Protein kinase C phosphorylation sensitizes but does not activate the capsaicin receptor transient receptor potential vanilloid 1 (TRPV1). *Proceedings of the National Academy of Sciences*, *100*(21), 12480–12485. https://doi.org/10.1073/pnas.2032100100

Bista, P., Pawlowski, M., Cerina, M., Ehling, P., Leist, M., Meuth, P., … Budde, T. (2015). Differential phospholipase C-dependent modulation of TASK and TREK two-pore domain K+ channels in rat thalamocortical relay neurons. *The Journal of Physiology*, *593*(1), 127–44. https://doi.org/10.1113/jphysiol.2014.276527

Bitto, A., Ito, T. K., Pineda, V. V, LeTexier, N. J., Huang, H. Z., Sutlief, E., … Kaeberlein, M. (2016). Transient rapamycin treatment can increase lifespan and healthspan in middle-aged mice. *eLife*, *5*. https://doi.org/10.7554/eLife.16351

Bleasdale, J. E., Bundy, G. L., Bunting, S., Fitzpatrick, F. A., Huff, R. M., Sun, F. F., & Pike, J. E. (1989). Inhibition of phospholipase C dependent processes by U-73, 122. *Advances in Prostaglandin, Thromboxane, and Leukotriene Research*, *19*, 590–3. Retrieved from http://www.ncbi.nlm.nih.gov/pubmed/2526542

Bödding, M., Wissenbach, U., & Flockerzi, V. (2007). Characterisation of TRPM8 as a pharmacophore receptor. *Cell Calcium*, *42*(6), 618–628. https://doi.org/10.1016/j.ceca.2007.03.005

Borhani Haghighi, A., Motazedian, S., Rezaii, R., Mohammadi, F., Salarian, L., Pourmokhtari, M., … Miri, R. (2010). Cutaneous application of menthol 10% solution as an abortive treatment of migraine without aura: a randomised, double-blind, placebo-controlled, crossed-over study. *International Journal of Clinical Practice*, *64*(4), 451–6. https://doi.org/10.1111/j.1742-1241.2009.02215.x

Bowman, L. J., & Brennan, D. C. (2008). The role of tacrolimus in renal transplantation. *Expert Opinion on Pharmacotherapy*, *9*(4), 635–643. https://doi.org/10.1517/14656566.9.4.635

Brauchi, S. (2006). A Hot-Sensing Cold Receptor: C-Terminal Domain Determines Thermosensation in Transient Receptor Potential Channels. *Journal of Neuroscience*, *26*(18), 4835–4840. https://doi.org/10.1523/JNEUROSCI.5080-05.2006

Brauchi, S., Orio, P., & Latorre, R. (2004). Clues to understanding cold sensation: Thermodynamics and electrophysiological analysis of the cold receptor TRPM8. *Proceedings of the National Academy of Sciences*, *101*(43), 15494–15499. https://doi.org/10.1073/pnas.0406773101

Brillantes, A.-M. B., Ondrias, K., Scott, A., Kobrinsky, E., Ondriašová, E., Moschella, M. C., … Marks, A. R. (1994). Stabilization of calcium release channel (ryanodine receptor) function by FK506-binding protein. *Cell*, *77*(4), 513–523. https://doi.org/10.1016/0092-8674(94)90214-3

Brown, D. A., & Adams, P. R. (1980). Muscarinic suppression of a novel voltage-sensitive K+ current in a vertebrate neurone. *Nature*, *283*(5748), 673–6.

Burgos-Vega, C. C., Ahn, D. D.-U., Bischoff, C., Wang, W., Horne, D., Wang, J., … Dussor, G. (2016). Meningeal transient receptor potential channel M8 activation causes cutaneous facial and hindpaw allodynia in a preclinical rodent model of headache. *Cephalalgia*, *36*(2), 185–193. https://doi.org/10.1177/0333102415584313

Burstein, R., Yarnitsky, D., Goor-Aryeh, I., Ransil, B. J., & Bajwa, Z. H. (2000). An association between migraine and cutaneous allodynia. *Annals of Neurology*, *47*(5), 614–24.

Calvo, R. R., Meegalla, S. K., Parks, D. J., Parsons, W. H., Ballentine, S. K., Lubin, M. Lou, … Player, M. R. (2012). Discovery of vinylcycloalkyl-substituted benzimidazole TRPM8

antagonists effective in the treatment of cold allodynia. *Bioorganic and Medicinal Chemistry Letters*, *22*(5), 1903–1907. https://doi.org/10.1016/j.bmcl.2012.01.060

Carpenter, D. O. (1981). Ionic and metabolic bases of neuronal thermosensitivity. *Federation Proceedings*, *40*(14), 2808–13.

Carr, R. W., Pianova, S., Fernandez, J., Fallon, J. B., Belmonte, C., & Brock, J. A. (2003). Effects of Heating and Cooling on Nerve Terminal Impulses Recorded from Cold-sensitive Receptors in the Guinea-pig Cornea. *The Journal of General Physiology*, *121*(5), 427–439. https://doi.org/10.1085/jgp.200308814

Carrasquel-Ursulaez, W., Moldenhauer, H., Castillo, J. P., Latorre, R., & Alvarez, O. (2015). Biophysical analysis of thermosensitive TRP channels with a special focus on the cold receptor TRPM8. *Temperature*, *2*(2), 188–200. https://doi.org/10.1080/23328940.2015.1047558

Castillo, K., Diaz-Franulic, I., Canan, J., Gonzalez-Nilo, F., & Latorre, R. (2018). Thermally activated TRP channels: Molecular sensors for temperature detection. *Physical Biology*, *15*(2). https://doi.org/10.1088/1478-3975/aa9a6f

Caterina, M. J., Leffler, A., Malmberg, A. B., Martin, W. J., Trafton, J., Petersen-Zeitz, K. R., … Julius, D. (2000). Impaired Nocicieption and Pain Sensation in Mice Lacking the Capsaicin Receptor. *Science, Apr. 14*(288), 306–313. https://doi.org/10.1126/science.288.5464.306

Caterina, M. J., Rosen, T. A., Tominaga, M., Brake, A. J., & Julius, D. (1999). A capsaicin-receptor homologue with a high threshold for noxious heat. *Nature*, *398*(6726), 436–441. https://doi.org/10.1038/18906

Caterina, M. J., Schumacher, M. A., Tominaga, M., Rosen, T. A., Levine, J. D., & Julius, D. (1997). The capsaicin receptor: A heat-activated ion channel in the pain pathway. *Nature*, *389*(6653), 816–824. https://doi.org/10.1038/39807

Cesare, P., & McNaughton, P. (1996). A novel heat-activated current in nociceptive neurons and its sensitization by bradykinin. *Proceedings of the National Academy of Sciences of the United States of America*, *93*(26), 15435–15439.

Chasman, D. I., Schürks, M., Anttila, V., de Vries, B., Schminke, U., Launer, L. J., … Kurth, T. (2011). Genome-wide association study reveals three susceptibility loci for common migraine in the general population. *Nature Genetics*, *43*(7), 695–698. https://doi.org/10.1038/ng.856

Chavan, S. S., Pavlov, V. A., & Tracey, K. J. (2017). Mechanisms and Therapeutic Relevance of Neuro-immune Communication. *Immunity*, *46*(6), 927–942. https://doi.org/10.1016/j.immuni.2017.06.008

Chen, G. L., Lei, M., Zhou, L. P., Zeng, B., & Zou, F. (2016). Borneol is a TRPM8 agonist that increases ocular surface wetness. *PLoS ONE*, *11*(7), 1–15. https://doi.org/10.1371/journal.pone.0158868

Chen, J., & Hackos, D. H. (2015). TRPA1 as a drug target—promise and challenges. *Naunyn-Schmiedeberg's Archives of Pharmacology*, *388*(4), 451–463. https://doi.org/10.1007/s00210-015-1088-3

Chen, J., Kang, D., Xu, J., Lake, M., Hogan, J. O., Sun, C., … Kim, D. (2013). Species differences and molecular determinant of TRPA1 cold sensitivity. *Nature Communications*, *4*, 1–7. https://doi.org/10.1038/ncomms3501

Chen, X., Talley, E. M., Patel, N., Gomis, A., McIntire, W. E., Dong, B., … Bayliss, D. A. (2006). Inhibition of a background potassium channel by Gq protein -subunits. *Proceedings of the National Academy of Sciences*, *103*(9), 3422–3427. https://doi.org/10.1073/pnas.0507710103

Choi, Y., Yoon, Y. W., Na, H. S., Kim, S. H., & Chung, J. M. (1994). Behavioral signs of ongoing pain and cold allodynia in a rat model of neuropathic pain. *Pain*, *59*(3), 369–76. Retrieved

from http://www.ncbi.nlm.nih.gov/pubmed/7708411

Chuang, H. H., Neuhausser, W. M., & Julius, D. (2004). The super-cooling agent icilin reveals a mechanism of coincidence detection by a temperature-sensitive TRP channel. *Neuron*, *43*(6), 859–869. https://doi.org/10.1016/j.neuron.2004.08.038

Chukyo, A., Chiba, T., Kambe, T., Yamamoto, K., Kawakami, K., Taguchi, K., & Abe, K. (2018). Oxaliplatin-induced changes in expression of transient receptor potential channels in the dorsal root ganglion as a neuropathic mechanism for cold hypersensitivity. *Neuropeptides*, *67*, 95–101. https://doi.org/10.1016/j.npep.2017.12.002

Cohen, M. R., & Moiseenkova-Bell, V. Y. (2014). Structure of Thermally Activated TRP Channels. *Current Topics in Membranes*, *74*, 181–211. https://doi.org/10.1016/B978-0-12-800181-3.00007-5

Colburn, R. W., Lubin, M. Lou, Stone, D. J., Wang, Y., Lawrence, D., D'Andrea, M. R. R., … Qin, N. (2007). Attenuated Cold Sensitivity in TRPM8 Null Mice. *Neuron*, *54*(3), 379–386. https://doi.org/10.1016/j.neuron.2007.04.017

Cordero-Morales, J. F., Gracheva, E. O., & Julius, D. (2011). Cytoplasmic ankyrin repeats of transient receptor potential A1 (TRPA1) dictate sensitivity to thermal and chemical stimuli. *Proceedings of the National Academy of Sciences*, *108*(46), E1184–E1191. https://doi.org/10.1073/pnas.1114124108

Cosens, D. J., & Manning, A. (1969). Abnormal electroretinogram from a Drosophila mutant [30]. *Nature*, *224*(5216), 285–287. https://doi.org/10.1038/224285a0

Couture, R., Harrisson, M., Vianna, R. M., & Cloutier, F. (2001). Kinin receptors in pain and inflammation. *European Journal of Pharmacology*, *429*(1–3), 161–76. Retrieved from http://www.ncbi.nlm.nih.gov/pubmed/11698039

Cox, L. S., & Mattison, J. A. (2009). Increasing longevity through caloric restriction or rapamycin feeding in mammals: common mechanisms for common outcomes? *Aging Cell*, *8*(5), 607–613. https://doi.org/10.1111/j.1474-9726.2009.00509.x

Craig, A. D., & Dostrovsky, J. O. (2001). Differential projections of thermoreceptive and nociceptive lamina I trigeminothalamic and spinothalamic neurons in the cat. *Journal of Neurophysiology*, *86*(2), 856–70. https://doi.org/10.1152/jn.2001.86.2.856

Daniels, R. L., Takashima, Y., & McKemy, D. D. (2009). Activity of the neuronal cold sensor TRPM8 is regulated by phospholipase C via the phospholipid phosphoinositol 4,5-bisphosphate. *The Journal of Biological Chemistry*, *284*(3), 1570–82. https://doi.org/10.1074/jbc.M807270200

Davis, J. B., Gray, J., Gunthorpe, M. J., Hatcher, J. P., Davey, P. T., Overend, P., … Sheardown, S. A. (2000). Vanilloid receptor-1 is essential for in ¯ ammatory thermal hyperalgesia, 183–187.

Davis, K. D. (1998). Cold-induced pain and prickle in the glabrous and hairy skin. *Pain*, *75*(1), 47–57.

De Blas, G. A., Darszon, A., Ocampo, A. Y., Serrano, C. J., Castellano, L. E., Hernández-González, E. O., … Treviño, C. L. (2009). TRPM8, a versatile channel in human sperm. *PloS One*, *4*(6), e6095. https://doi.org/10.1371/journal.pone.0006095

De La Torre-Martínez, R., Bonache, M. A., Llabrés-Campaner, P. J., Balsera, B., Fernández-Carvajal, A., Fernández-Ballester, G., … González-Muñiz, R. (2017). Synthesis, high-throughput screening and pharmacological characterization of β-lactam derivatives as TRPM8 antagonists. *Scientific Reports*, *7*(1), 1–13. https://doi.org/10.1038/s41598-017-10913-x

DeFalco, J., Duncton, M. A. J., & Emerling, D. (2011). TRPM8 biology and medicinal chemistry. *Current Topics in Medicinal Chemistry*, *11*(17), 2237–52.

Dembla, S., Behrendt, M., Mohr, F., Goecke, C., Sondermann, J., Schneider, F. M., …

Oberwinkler, J. (2017). Anti-nociceptive action of peripheral mu- opioid receptors by G-beta-gamma protein-mediated inhibition of TRPM3 channels, 1–32.

Denis, V., & Cyert, M. S. (2002). Internal Ca $^{2+}$ release in yeast is triggered by hypertonic shock and mediated by a TRP channel homologue. *The Journal of Cell Biology*, *156*(1), 29–34. https://doi.org/10.1083/jcb.200111004

Descoeur, J., Pereira, V., Pizzoccaro, A., Francois, A., Ling, B., Maffre, V., … Bourinet, E. (2011). Oxaliplatin-induced cold hypersensitivity is due to remodelling of ion channel expression in nociceptors. *EMBO Molecular Medicine*, *3*(5), 266–278. https://doi.org/10.1002/emmm.201100134

Dhaka, A., Earley, T. J., Watson, J., & Patapoutian, A. (2008). Visualizing Cold Spots: TRPM8-Expressing Sensory Neurons and Their Projections. *Journal of Neuroscience*, *28*(3), 566–575. https://doi.org/10.1523/JNEUROSCI.3976-07.2008

Dhaka, A., Murray, A. N., Mathur, J., Earley, T. J., Petrus, M. J., & Patapoutian, A. (2007). TRPM8 is required for cold sensation in mice. *Neuron*, *54*(3), 371–8. https://doi.org/10.1016/j.neuron.2007.02.024

Di Paolo, G., & De Camilli, P. (2006). Phosphoinositides in cell regulation and membrane dynamics. *Nature*, *443*(7112), 651–7. https://doi.org/10.1038/nature05185

Doan, T. L., Pollastri, M., Walters, M. A., & Georg, G. I. (2011). The Future of Drug Repositioning: Old Drugs, New Opportunities. *Annual Reports in Medicinal Chemistry*, *46*, 385–401. https://doi.org/10.1016/B978-0-12-386009-5.00004-7

Dragoni, I., Guida, E., & McIntyre, P. (2006). The cold and menthol receptor TRPM8 contains a functionally important double cysteine motif. *The Journal of Biological Chemistry*, *281*(49), 37353–60. https://doi.org/10.1074/jbc.M607227200

Du, X., Zhang, H., Lopes, C., Mirshahi, T., Rohacs, T., & Logothetis, D. E. (2004). Characteristic interactions with phosphatidylinositol 4,5-bisphosphate determine regulation of kir channels by diverse modulators. *The Journal of Biological Chemistry*, *279*(36), 37271–81. https://doi.org/10.1074/jbc.M403413200

Eid, S. R. (2011). Therapeutic targeting of TRP channels--the TR(i)P to pain relief. *Current Topics in Medicinal Chemistry*, *11*(17), 2118–30.

El Karim, I. A., Linden, G. J., Curtis, T. M., About, I., McGahon, M. K., Irwin, C. R., & Lundy, F. T. (2011). Human odontoblasts express functional thermo-sensitive TRP channels: implications for dentin sensitivity. *Pain*, *152*(10), 2211–23. https://doi.org/10.1016/j.pain.2010.10.016

Erler, I., Al-Ansary, D. M. M., Wissenbach, U., Wagner, T. F. J., Flockerzi, V., & Niemeyer, B. A. (2006a). Trafficking and assembly of the cold-sensitive TRPM8 channel. *Journal of Biological Chemistry*, *281*(50), 38396–38404. https://doi.org/10.1074/jbc.M607756200

Esserlind, A.-L., Christensen, A. F., Le, H., Kirchmann, M., Hauge, A. W., Toyserkani, N. M., … Olesen, J. (2013). Replication and meta-analysis of common variants identifies a genome-wide significant locus in migraine. *European Journal of Neurology*, *20*(5), 765–72. https://doi.org/10.1111/ene.12055

Everaerts, W., Gees, M., Alpizar, Y. A., Farre, R., Leten, C., Apetrei, A., … Talavera, K. (2011). The capsaicin receptor TRPV1 is a crucial mediator of the noxious effects of mustard oil. *Current Biology*, *21*(4), 316–321. https://doi.org/10.1016/j.cub.2011.01.031

Fajardo, O., Meseguer, V., Belmonte, C., & Viana, F. (2008). TRPA1 Channels Mediate Cold Temperature Sensing in Mammalian Vagal Sensory Neurons: Pharmacological and Genetic Evidence. *Journal of Neuroscience*, *28*(31), 7863–7875. https://doi.org/10.1523/JNEUROSCI.1696-08.2008

Falkenburger, B. H., Jensen, J. B., Dickson, E. J., Suh, B. C., & Hille, B. (2010). Phosphoinositides: Lipid regulators of membrane proteins. *Journal of Physiology*, *588*(17),

3179–3185. https://doi.org/10.1113/jphysiol.2010.192153

Fan, Z., & Makielski, J. C. (1997). Anionic phospholipids activate ATP-sensitive potassium channels. *The Journal of Biological Chemistry*, *272*(9), 5388–95.

Feketa, V. V, Balasubramanian, A., Flores, C. M., Player, M. R., & Marrelli, S. P. (2013). Shivering and tachycardic responses to external cooling in mice are substantially suppressed by TRPV1 activation but not by TRPM8 inhibition. *American Journal of Physiology. Regulatory, Integrative and Comparative Physiology*, *305*(9), R1040-50. https://doi.org/10.1152/ajpregu.00296.2013

Finch, P. M., & Drummond, P. D. (2015). Topical treatment in pain medicine: from ancient remedies to modern usage. *Pain Management*, *5*(5), 359–71. https://doi.org/10.2217/pmt.15.23

Flegel, C., Schöbel, N., Altmüller, J., Becker, C., Tannapfel, A., Hatt, H., & Gisselmann, G. (2015). RNA-Seq Analysis of Human Trigeminal and Dorsal Root Ganglia with a Focus on Chemoreceptors. *PloS One*, *10*(6), e0128951. https://doi.org/10.1371/journal.pone.0128951

Fleig, A., & Penner, R. (2004). The TRPM ion channel subfamily: molecular, biophysical and functional features. *Trends in Pharmacological Sciences*, *25*(12), 633–639. https://doi.org/10.1016/j.tips.2004.10.004

Ford, C. P., Stemkowski, P. L., & Smith, P. A. (2004). Possible role of phosphatidylinositol 4,5 bisphosphate in luteinizing hormone releasing hormone-mediated M-current inhibition in bullfrog sympathetic neurons. *The European Journal of Neuroscience*, *20*(11), 2990–8. https://doi.org/10.1111/j.1460-9568.2004.03786.x

Frederick, J., Buck, M. E., Matson, D. J., & Cortright, D. N. (2007). Increased TRPA1, TRPM8, and TRPV2 expression in dorsal root ganglia by nerve injury. *Biochemical and Biophysical Research Communications*, *358*(4), 1058–64. https://doi.org/10.1016/j.bbrc.2007.05.029

Fujita, F., Uchida, K., Takaishi, M., Sokabe, T., & Tominaga, M. (2013). Ambient Temperature Affects the Temperature Threshold for TRPM8 Activation through Interaction of Phosphatidylinositol 4,5-Bisphosphate. *Journal of Neuroscience*, *33*(14), 6154–6159. https://doi.org/10.1523/JNEUROSCI.5672-12.2013

Fukushima, A., Ohashi, Y., Ebihara, N., Uchio, E., Okamoto, S., Kumagai, N., … Nakagawa, Y. (2014). Therapeutic effects of 0 . 1 % tacrolimus eye drops for refractory allergic ocular diseases with proliferative lesion or corneal involvement, 1–5. https://doi.org/10.1136/bjophthalmol-2013-304453

Gallar, J., Pozo, M. A., Tuckett, R. P., & Belmonte, C. (1993). Response of sensory units with unmyelinated fibres to mechanical, thermal and chemical stimulation of the cat's cornea. *The Journal of Physiology*, *468*, 609–22.

Gauchan, P., Andoh, T., Kato, A., & Kuraishi, Y. (2009). Involvement of increased expression of transient receptor potential melastatin 8 in oxaliplatin-induced cold allodynia in mice. *Neuroscience Letters*, *458*(2), 93–5. https://doi.org/10.1016/j.neulet.2009.04.029

Gaudioso, C., Hao, J., Martin-Eauclaire, M.-F., Gabriac, M., & Delmas, P. (2012). Menthol pain relief through cumulative inactivation of voltage-gated sodium channels. *Pain*, *153*(2), 473–484. https://doi.org/10.1016/j.pain.2011.11.014

Gavva, N. R., Davis, C., Lehto, S. G., Rao, S., Wang, W., & Zhu, D. X. (2012). Transient Receptor Potential Melastatin 8 (TRPM8) Channels are Involved in Body Temperature Regulation. *Molecular Pain*, *8*, 1744-8069-8–36. https://doi.org/10.1186/1744-8069-8-36

Gentry, C., Stoakley, N., Andersson, D. A., & Bevan, S. (2010). The roles of iPLA2, TRPM8 and TRPA1 in chemically induced cold hypersensitivity. *Molecular Pain*, *6*, 4. https://doi.org/10.1186/1744-8069-6-4

Ghosh, D., Pinto, S., Danglot, L., Vandewauw, I., Segal, A., Van Ranst, N., … Voets, T. (2016). VAMP7 regulates constitutive membrane incorporation of the cold-activated channel

TRPM8. *Nature Communications*, *7*, 1–15. https://doi.org/10.1038/ncomms10489

Gkika, D., Flourakis, M., Lemonnier, L., & Prevarskaya, N. (2010). PSA reduces prostate cancer cell motility by stimulating TRPM8 activity and plasma membrane expression. *Oncogene*, *29*(32), 4611–4616. https://doi.org/10.1038/onc.2010.210

Goel, M., Garcia, R., Estacion, M., & Schilling, W. P. (2001). Regulation of Drosophila TRPL Channels by Immunophilin FKBP59. *Journal of Biological Chemistry*, *276*(42), 38762–38773. https://doi.org/10.1074/jbc.M104125200

González, A., Ugarte, G., Restrepo, C., Herrera, G., Piña, R., Gómez-Sánchez, J. A., … Madrid, R. (2017). Role of the Excitability Brake Potassium Current I_{KD} in Cold Allodynia Induced by Chronic Peripheral Nerve Injury. *The Journal of Neuroscience*, *37*(12), 3109–3126. https://doi.org/10.1523/JNEUROSCI.3553-16.2017

Gracheva, E. O., Ingolia, N. T., Kelly, Y. M., Cordero-Morales, J. F., Hollopeter, G., Chesler, A. T., … Julius, D. (2010). Molecular basis of infrared detection by snakes. *Nature*, *464*(7291), 1006–11. https://doi.org/10.1038/nature08943

Grolez, G. P., & Gkika, D. (2016). TRPM8 Puts the Chill on Prostate Cancer. https://doi.org/10.3390/ph9030044

Grynkiewicz, G., Poenie, M., & Tsien, R. Y. (1985). A new generation of Ca2+ indicators with greatly improved fluorescence properties. *The Journal of Biological Chemistry*, *260*(6), 3440–50. Retrieved from http://www.ncbi.nlm.nih.gov/pubmed/3838314

Hamill, O. P., Marty, A., Neher, E., Sakmann, B., & Sigworth, F. J. (1981). Improved patch-clamp techniques for high-resolution current recording from cells and cell-free membrane patches. *Pflugers Archiv : European Journal of Physiology*, *391*(2), 85–100. Retrieved from http://www.ncbi.nlm.nih.gov/pubmed/6270629

Hansen, S. B. (2015). Lipid agonism: The PIP2paradigm of ligand-gated ion channels. *Biochimica et Biophysica Acta - Molecular and Cell Biology of Lipids*, *1851*(5), 620–628. https://doi.org/10.1016/j.bbalip.2015.01.011

Hardie, R. C., & Minke, B. (1992). The trp gene is essential for a light-activated Ca2+channel in Drosophila photoreceptors. *Neuron*, *8*(4), 643–651. https://doi.org/10.1016/0896-6273(92)90086-S

Hardie, R. C., & Raghu, P. (2001). Visual transduction in Drosophila. *Nature*, *413*(6852), 186–193. https://doi.org/10.1038/35093002

Harrington, A. M., Hughes, P. A., Martin, C. M., Yang, J., Castro, J., Isaacs, N. J., … Brierley, S. M. (2011a). A novel role for TRPM8 in visceral afferent function. *Pain*, *152*(7), 1459–1468. https://doi.org/10.1016/j.pain.2011.01.027

Harteneck, C., Frenzel, H., & Kraft, R. (2007). N-(p-Amylcinnamoyl)anthranilic Acid (ACA): A Phospholipase A2 Inhibitor and TRP Channel Blocker. *Cardiovascular Drug Reviews*, *25*(1), 61–75. https://doi.org/10.1111/j.1527-3466.2007.00005.x

Hayashi, T., Kondo, T., Ishimatsu, M., Yamada, S., Nakamura, K., Matsuoka, K., & Akasu, T. (2009). Expression of the TRPM8-immunoreactivity in dorsal root ganglion neurons innervating the rat urinary bladder. *Neuroscience Research*, *65*(3), 245–251. https://doi.org/10.1016/j.neures.2009.07.005

Heitman, J., Movva, N. R., & Hall, M. N. (1991). Targets for cell cycle arrest by the immunosuppressant rapamycin in yeast. *Science (New York, N.Y.)*, *253*(5022), 905–9.

HENSEL, H., & ZOTTERMAN, Y. (1951). The Effect of Menthol on the Thermoreceptors. *Acta Physiologica Scandinavica*, *24*(1), 27–34. https://doi.org/10.1111/j.1748-1716.1951.tb00824.x

HENSEL, H., & ZOTTERMAN, Y. (1951). The response of the cold receptors to constant cooling. *Acta Physiologica Scandinavica*, *22*(2–3), 96–105. https://doi.org/10.1111/j.1748-1716.1951.tb00758.x

Henshall, S. M., Afar, D. E. H., Hiller, J., Horvath, L. G., Quinn, D. I., Rasiah, K. K., … Sutherland, R. L. (2003). Survival analysis of genome-wide gene expression profiles of prostate cancers identifies new prognostic targets of disease relapse. *Cancer Research*, *63*(14), 4196–203.

Heppelmann, B., Gallar, J., Trost, B., Schmidt, R. F., & Belmonte, C. (2001). Three-dimensional reconstruction of scleral cold thermoreceptors of the cat eye. *The Journal of Comparative Neurology*, *441*(2), 148–54. Retrieved from http://www.ncbi.nlm.nih.gov/pubmed/11745641

Herlitze, S., Garcia, D. E., Mackie, K., Hille, B., Scheuer, T., & Catterall, W. A. (1996). Modulation of Ca2+ channels βγ G-protein py subunits. *Nature*, *380*(6571), 258–262. https://doi.org/10.1038/380258a0

Hilgemann, D. W., & Ball, R. (1996). Regulation of cardiac Na+,Ca2+ exchange and KATP potassium channels by PIP2. *Science (New York, N.Y.)*, *273*(5277), 956–9.

Hille, B. (2001). *Ion channels of excitable membranes*. Sinauer.

Hille, B., Dickson, E. J., Kruse, M., Vivas, O., & Suh, B. C. (2015). Phosphoinositides regulate ion channels. *Biochimica et Biophysica Acta - Molecular and Cell Biology of Lipids*, *1851*(6), 844–856. https://doi.org/10.1016/j.bbalip.2014.09.010

Hirata, H., & Meng, I. D. (2010). Cold-sensitive corneal afferents respond to a variety of ocular stimuli central to tear production: implications for dry eye disease. *Investigative Ophthalmology & Visual Science*, *51*(8), 3969–76. https://doi.org/10.1167/iovs.09-4744

Horowitz, L. F., Hirdes, W., Suh, B.-C., Hilgemann, D. W., Mackie, K., & Hille, B. (2005). Phospholipase C in living cells: activation, inhibition, Ca2+ requirement, and regulation of M current. *The Journal of General Physiology*, *126*(3), 243–62. https://doi.org/10.1085/jgp.200509309

Hossain, M. I., Iwasaki, H., Okochi, Y., Chahine, M., Higashijima, S., Nagayama, K., & Okamura, Y. (2008). Enzyme domain affects the movement of the voltage sensor in ascidian and zebrafish voltage-sensing phosphatases. *The Journal of Biological Chemistry*, *283*(26), 18248–59. https://doi.org/10.1074/jbc.M706184200

Hu, H. Z., Gu, Q., Wang, C., Colton, C. K., Tang, J., Kinoshita-Kawada, M., … Zhu, M. X. (2004). 2-Aminoethoxydiphenyl borate is a common activator of TRPV1, TRPV2, and TRPV3. *Journal of Biological Chemistry*, *279*(34), 35741–35748. https://doi.org/10.1074/jbc.M404164200

Huang, C. L., Feng, S., & Hilgemann, D. W. (1998). Direct activation of inward rectifier potassium channels by PIP2 and its stabilization by Gbetagamma. *Nature*, *391*(6669), 803–6. https://doi.org/10.1038/35882

Huang, D., Li, S., Dhaka, A., Story, G. M., & Cao, Y.-Q. (2012). Expression of the transient receptor potential channels TRPV1, TRPA1 and TRPM8 in mouse trigeminal primary afferent neurons innervating the dura. *Molecular Pain*, *8*(1), 66. https://doi.org/10.1186/1744-8069-8-66

Ito, H., Aizawa, N., Sugiyama, R., Watanabe, S., Takahashi, N., Tajimi, M., … Igawa, Y. (2016). Functional role of the transient receptor potential melastatin 8 (TRPM8) ion channel in the urinary bladder assessed by conscious cystometry and *ex vivo* measurements of single-unit mechanosensitive bladder afferent activities in the rat. *BJU International*, *117*(3), 484–494. https://doi.org/10.1111/bju.13225

Janssens, A., Gees, M., Toth, B. I., Ghosh, D., Mulier, M., Vennekens, R., … Voets, T. (2016). Definition of two agonist types at the mammalian cold-activated channel TRPM8. *eLife*, *5*(JULY), 1–21. https://doi.org/10.7554/eLife.17240

Johnson, C. D., Melanaphy, D., Purse, A., Stokesberry, S. A., Dickson, P., & Zholos, A. V. (2009). Transient receptor potential melastatin 8 channel involvement in the regulation of

vascular tone. *American Journal of Physiology. Heart and Circulatory Physiology*, *296*(6), H1868-77. https://doi.org/10.1152/ajpheart.01112.2008

Jones, L., Downie, L. E., Korb, D., Benitez-del-Castillo, J. M., Dana, R., Deng, S. X., … Craig, J. P. (2017). TFOS DEWS II Management and Therapy Report. *The Ocular Surface*, *15*(3), 575–628. https://doi.org/10.1016/j.jtos.2017.05.006

Jordt, S.-E., Bautista, D. M., Chuang, H., McKemy, D. D., Zygmunt, P. M., Högestätt, E. D., … Julius, D. (2004). Mustard oils and cannabinoids excite sensory nerve fibres through the TRP channel ANKTM1. *Nature*, *427*(6971), 260–265. https://doi.org/10.1038/nature02282

Jun, J. H., Kang, H. J., Jin, M. H., Lee, H. Y., Im, Y. J., Jung, H. J., & Han, S. W. (2012). Function of the Cold Receptor (TRPM8) Associated with Voiding Dysfunction in Bladder Outlet Obstruction in Rats. *International Neurourology Journal*, *16*(2), 69. https://doi.org/10.5213/inj.2012.16.2.69

Kamel, M., Kadian, M., Srinivas, T., Taber, D., & Salas, M. A. P. (2016). Tacrolimus confers lower acute rejection rates and better renal allograft survival compared to cyclosporine. *World Journal of Transplantation*, *6*(4), 697. https://doi.org/10.5500/wjt.v6.i4.697

Kanda, H., & Gu, J. G. (2017). Effects of cold temperatures on the excitability of rat trigeminal ganglion neurons that are not for cold sensing. *Journal of Neurochemistry*, *141*(4), 532–543. https://doi.org/10.1111/jnc.13511

Kandel, E. (2000). Principles of Neural Science, 1414.

Kang, C. B., Hong, Y., Dhe-Paganon, S., & Yoon, H. S. (2008). FKBP Family Proteins: Immunophilins with Versatile Biological Functions. *Neurosignals*, *16*(4), 318–325. https://doi.org/10.1159/000123041

Kang, K., Panzano, V. C., Chang, E. C., Ni, L., Dainis, A. M., Jenkins, A. M., … Garrity, P. A. (2012). Modulation of TRPA1 thermal sensitivity enables sensory discrimination in Drosophila. *Nature*, *481*(7379), 76–80. https://doi.org/10.1038/nature10715

Karashima, Y., Damann, N., Prenen, J., Talavera, K., Segal, A., Voets, T., & Nilius, B. (2007). Bimodal Action of Menthol on the Transient Receptor Potential Channel TRPA1. *Journal of Neuroscience*, *27*(37), 9874–9884. https://doi.org/10.1523/JNEUROSCI.2221-07.2007

Karashima, Y., Talavera, K., Everaerts, W., Janssens, A., Kwan, K. Y., Vennekens, R., … Voets, T. (2009). TRPA1 acts as a cold sensor in vitro and in vivo. *Proceedings of the National Academy of Sciences*, *106*(4), 1273–1278. https://doi.org/10.1073/pnas.0808487106

Kayama, Y., Shibata, M., Takizawa, T., Ibata, K., Nakahara, J., Shimizu, T., … Suzuki, N. (2017). Signaling Pathways Relevant to Nerve Growth Factor-induced Upregulation of Transient Receptor Potential M8 Expression. *Neuroscience*, *367*, 178–188. https://doi.org/10.1016/j.neuroscience.2017.10.037

Kayama, Y., Shibata, M., Takizawa, T., Ibata, K., Shimizu, T., Ebine, T., … Suzuki, N. (2018). Functional interactions between transient receptor potential M8 and transient receptor potential V1 in the trigeminal system: Relevance to migraine pathophysiology. *Cephalalgia*, *38*(5), 833–845. https://doi.org/10.1177/0333102417712719

Khalil, M., Babes, A., Lakra, R., Försch, S., Reeh, P. W., Wirtz, S., … Engel, M. A. (2016). Transient receptor potential melastatin 8 ion channel in macrophages modulates colitis through a balance-shift in TNF-alpha and interleukin-10 production. *Mucosal Immunology*, *9*(6), 1500–1513. https://doi.org/10.1038/mi.2016.16

Kim, T. K., & Eberwine, J. H. (2010). Mammalian cell transfection: the present and the future. *Analytical and Bioanalytical Chemistry*, *397*(8), 3173–3178. https://doi.org/10.1007/s00216-010-3821-6

Kirk, C. J., Bone, E. A., Palmer, S., & Michell, R. H. (1984). The role of phosphatidylinositol 4,5 bisphosphate breakdown in cell-surface receptor activation. *Journal of Receptor Research*, *4*(1–6), 489–504.

Klein, R. R., Bourdon, D. M., Costales, C. L., Wagner, C. D., White, W. L., Williams, J. D., … Thakker, D. R. (2011). Direct activation of human phospholipase C by its well known inhibitor u73122. *The Journal of Biological Chemistry*, *286*(14), 12407–16. https://doi.org/10.1074/jbc.M110.191783

Knowlton, W. M., Bifolck-Fisher, A., Bautista, D. M., & McKemy, D. D. (2010). TRPM8, but not TRPA1, is required for neural and behavioral responses to acute noxious cold temperatures and cold-mimetics in vivo. *Pain*, *150*(2), 340–50. https://doi.org/10.1016/j.pain.2010.05.021

Knowlton, W. M., Daniels, R. L., Palkar, R., McCoy, D. D., & McKemy, D. D. (2011). Pharmacological blockade of TRPM8 ion channels alters cold and cold pain responses in mice. *PLoS ONE*, *6*(9). https://doi.org/10.1371/journal.pone.0025894

Knowlton, W. M., Palkar, R., Lippoldt, E. K., McCoy, D. D., Baluch, F., Chen, J., & McKemy, D. D. (2013). A Sensory-Labeled Line for Cold: TRPM8-Expressing Sensory Neurons Define the Cellular Basis for Cold, Cold Pain, and Cooling-Mediated Analgesia. *Journal of Neuroscience*, *33*(7), 2837–2848. https://doi.org/10.1523/JNEUROSCI.1943-12.2013

Koch, S. E., Mann, A., Jones, S., Robbins, N., Alkhattabi, A., Worley, M. C., … Rubinstein, J. (2017). Transient receptor potential vanilloid 2 function regulates cardiac hypertrophy via stretch-induced activation. *Journal of Hypertension*, *35*(3), 602–611. https://doi.org/10.1097/HJH.0000000000001213

Kovács, I., Luna, C., Quirce, S., Mizerska, K., Callejo, G., Riestra, A., … Gallar, J. (2016). Abnormal activity of corneal cold thermoreceptors underlies the unpleasant sensations in dry eye disease. *PAIN*, *157*(2), 399–417. https://doi.org/10.1097/j.pain.0000000000000455

Kraft, R., Grimm, C., Frenzel, H., & Harteneck, C. (2006). Inhibition of TRPM2 cation channels by N-(p-amylcinnamoyl)anthranilic acid. *British Journal of Pharmacology*, *148*(3), 264–73. https://doi.org/10.1038/sj.bjp.0706739

Kruse, M., Hammond, G. R. V., & Hille, B. (2012). Regulation of voltage-gated potassium channels by PI(4,5)P $_2$. *The Journal of General Physiology*, *140*(2), 189–205. https://doi.org/10.1085/jgp.201210806

Kühn, F. J. P., Winking, M., Kühn, C., Hoffmann, D. C., & Lückhoff, A. (2013). Surface expression and channel function of TRPM8 are cooperatively controlled by transmembrane segments S3 and S4. *Pflügers Archiv - European Journal of Physiology*, *465*(11), 1599–1610. https://doi.org/10.1007/s00424-013-1302-4

Kunert-Keil, C., Bisping, F., Krüger, J., & Brinkmeier, H. (2006). Tissue-specific expression of TRP channel genes in the mouse and its variation in three different mouse strains. *BMC Genomics*, *7*(1), 159. https://doi.org/10.1186/1471-2164-7-159

Kwan, K. Y., Allchorne, A. J., Vollrath, M. A., Christensen, A. P., Zhang, D.-S., Woolf, C. J., & Corey, D. P. (2006). TRPA1 Contributes to Cold, Mechanical, and Chemical Nociception but Is Not Essential for Hair-Cell Transduction. *Neuron*, *50*(2), 277–289. https://doi.org/10.1016/j.neuron.2006.03.042

Kwan, K. Y., & Corey, D. P. (2009). Burning cold: involvement of TRPA1 in noxious cold sensation. *The Journal of General Physiology*, *133*(3), 251–6. https://doi.org/10.1085/jgp.200810146

Kwon, Y., Shim, H.-S., Wang, X., & Montell, C. (2008). Control of thermotactic behavior via coupling of a TRP channel to a phospholipase C signaling cascade. *Nature Neuroscience*, *11*(8), 871–873. https://doi.org/10.1038/nn.2170

Lai, H. C., & Jan, L. Y. (2006). The distribution and targeting of neuronal voltage-gated ion channels. *Nature Reviews. Neuroscience*, *7*(7), 548–62. https://doi.org/10.1038/nrn1938

Lashinger, E. S. R., Steiginga, M. S., Hieble, J. P., Leon, L. A., Gardner, S. D., Nagilla, R., … Su, X. (2008). AMTB, a TRPM8 channel blocker: evidence in rats for activity in overactive

bladder and painful bladder syndrome. *American Journal of Physiology-Renal Physiology*, *295*(3), F803–F810. https://doi.org/10.1152/ajprenal.90269.2008

LATORRE, R., BRAUCHI, S., ORTA, G., ZAELZER, C., & VARGAS, G. (2007). ThermoTRP channels as modular proteins with allosteric gating. *Cell Calcium*, *42*(4–5), 427–438. https://doi.org/10.1016/j.ceca.2007.04.004

Lau, C., Hunter, M. J., Stewart, A., Perozo, E., & Vandenberg, J. I. (2018). Never at rest: insights into the conformational dynamics of ion channels from cryo-electron microscopy. *Journal of Physiology*, *596*(7), 1107–1119. https://doi.org/10.1113/JP274888

Leffingwell, J., Rowsell, D., & Resources, C. (2014). Wilkinson Sword Cooling Compounds : From the Beginning to Now, (March 2014).

Leffler, A., Linte, R. M., Nau, C., Reeh, P., & Babes, A. (2007). A high-threshold heat-activated channel in cultured rat dorsal root ganglion neurons resembles TRPV2 and is blocked by gadolinium. *European Journal of Neuroscience*, *26*(1), 12–22. https://doi.org/10.1111/j.1460-9568.2007.05643.x

Lehto, S. G., Weyer, A. D., Zhang, M., Youngblood, B. D., Wang, J., Wang, W., … Gavva, N. R. (2015). AMG2850, a potent and selective TRPM8 antagonist, is not effective in rat models of inflammatory mechanical hypersensitivity and neuropathic tactile allodynia. *Naunyn-Schmiedeberg's Archives of Pharmacology*, *388*(4), 465–76. https://doi.org/10.1007/s00210-015-1090-9

Leitner, M. G., Michel, N., Behrendt, M., Dierich, M., Dembla, S., Wilke, B. U., … Oliver, D. (2016). Direct modulation of TRPM4 and TRPM3 channels by the phospholipase C inhibitor U73122. *British Journal of Pharmacology*, 2555–2569. https://doi.org/10.1111/bph.13538

Li, J., Kim, S. G., & Blenis, J. (2014). Rapamycin: one drug, many effects. *Cell Metabolism*, *19*(3), 373–9. https://doi.org/10.1016/j.cmet.2014.01.001

Li, L., & Zhang, X. (2013). Differential inhibition of the TRPM8 ion channel by $G\alpha_q$ and $G\alpha_{11}$. *Channels*, *7*(2), 115–118. https://doi.org/10.4161/chan.23466

Liao, M., Cao, E., Julius, D., & Cheng, Y. (2013). Structure of the TRPV1 ion channel determined by electron cryo-microscopy. *Nature*, *504*(7478), 107–112. https://doi.org/10.1038/nature12822

Light, A. R., Trevino, D. L., & Perl, E. R. (1979). Morphological features of functionally defined neurons in the marginal zone and substantia gelatinosa of the spinal dorsal horn. *The Journal of Comparative Neurology*, *186*(2), 151–71. https://doi.org/10.1002/cne.901860204

Lin, M. C., & Polse, K. A. (2015). Improving Care for Patients with Dry Eye Symptoms. *Optometry and Vision Science*, *92*(9), e342–e349. https://doi.org/10.1097/OPX.0000000000000651

Lindner, M., Leitner, M. G., Halaszovich, C. R., Hammond, G. R. V., & Oliver, D. (2011). Probing the regulation of TASK potassium channels by PI(4,5)P2with switchable phosphoinositide phosphatases. *Journal of Physiology*, *589*(13), 3149–3162. https://doi.org/10.1113/jphysiol.2011.208983

Ling, J., Erol, F., & Gu, J. G. (2018). Role of KCNQ2 channels in orofacial cold sensitivity: KCNQ2 upregulation in trigeminal ganglion neurons after infraorbital nerve chronic constrictive injury. *Neuroscience Letters*, *664*, 84–90. https://doi.org/10.1016/j.neulet.2017.11.026

Linte, R. M., Ciobanu, C., Reid, G., & Babes, A. (2007). Desensitization of cold- and menthol-sensitive rat dorsal root ganglion neurones by inflammatory mediators. *Experimental Brain Research*, *178*(1), 89–98. https://doi.org/10.1007/s00221-006-0712-3

Liu, B. (2005). Functional Control of Cold- and Menthol-Sensitive TRPM8 Ion Channels by Phosphatidylinositol 4,5-Bisphosphate. *Journal of Neuroscience*, *25*(7), 1674–1681.

https://doi.org/10.1523/JNEUROSCI.3632-04.2005

Liu, B., Fan, L., Balakrishna, S., Sui, A., Morris, J. B., & Jordt, S.-E. (2013). TRPM8 is the principal mediator of menthol-induced analgesia of acute and inflammatory pain. *Pain*, *154*(10), 2169–2177. https://doi.org/10.1016/j.pain.2013.06.043

Liu, B., Linley, J. E., Du, X., Zhang, X., Ooi, L., Zhang, H., & Gamper, N. (2010). The acute nociceptive signals induced by bradykinin in rat sensory neurons are mediated by inhibition of M-type K+ channels and activation of Ca2+-activated Cl– channels. *Journal of Clinical Investigation*, *120*(4), 1240–1252. https://doi.org/10.1172/JCI41084

Liu, D., & Liman, E. R. (2003). Intracellular Ca2+ and the phospholipid PIP2 regulate the taste transduction ion channel TRPM5. *Proceedings of the National Academy of Sciences*, *100*(25), 15160–15165. https://doi.org/10.1073/pnas.2334159100

LIU, T., FANG, Z., WANG, G., SHI, M., WANG, X., JIANG, K., … ZHOU, J. (2016). Anti-tumor activity of the TRPM8 inhibitor BCTC in prostate cancer DU145 cells. *Oncology Letters*, *11*(1), 182–188. https://doi.org/10.3892/ol.2015.3854

Liu, Y., & Qin, N. (2011). TRPM8 in Health and Disease: Cold Sensing and Beyond. In *Advances in experimental medicine and biology* (Vol. 704, pp. 185–208). https://doi.org/10.1007/978-94-007-0265-3_10

Logothetis, D. E., Kurachi, Y., Galper, J., Neer, E. J., & Clapham, D. E. (1987). The βγ subunits of GTP-binding proteins activate the muscarinic K+ channel in heart. *Nature*, *325*(6102), 321–326. https://doi.org/10.1038/325321a0

Lombardi, A., Gambardella, J., Du, X.-L., Sorriento, D., Mauro, M., Iaccarino, G., … Santulli, G. (2017). Sirolimus induces depletion of intracellular calcium stores and mitochondrial dysfunction in pancreatic beta cells. *Scientific Reports*, *7*(1), 15823. https://doi.org/10.1038/s41598-017-15283-y

Lukacs, V., Yudin, Y., Hammond, G. R., Sharma, E., Fukami, K., & Rohacs, T. (2013). Distinctive Changes in Plasma Membrane Phosphoinositides Underlie Differential Regulation of TRPV1 in Nociceptive Neurons. *Journal of Neuroscience*, *33*(28), 11451–11463. https://doi.org/10.1523/JNEUROSCI.5637-12.2013

Lumpkin, E. A., & Bautista, D. M. (2005). Feeling the pressure in mammalian somatosensation. *Current Opinion in Neurobiology*, *15*(4), 382–388. https://doi.org/10.1016/j.conb.2005.06.005

Lumpkin, E. A., & Caterina, M. J. (2007). Mechanisms of sensory transduction in the skin. *Nature*, *445*(7130), 858–865. https://doi.org/10.1038/nature05662

Ma, S., Yu, H., Zhao, Z., Luo, Z., Chen, J., Ni, Y., … Zhu, Z. (2012). Activation of the cold-sensing TRPM8 channel triggers UCP1-dependent thermogenesis and prevents obesity. *Journal of Molecular Cell Biology*, *4*(2), 88–96. https://doi.org/10.1093/jmcb/mjs001

Macpherson, L. J., Hwang, S. W., Miyamoto, T., Dubin, A. E., Patapoutian, A., & Story, G. M. (2006). More than cool: Promiscuous relationships of menthol and other sensory compounds. *Molecular and Cellular Neuroscience*, *32*(4), 335–343. https://doi.org/10.1016/j.mcn.2006.05.005

Madrid, R., de la Pena, E., Donovan-Rodriguez, T., Belmonte, C., & Viana, F. (2009). Variable Threshold of Trigeminal Cold-Thermosensitive Neurons Is Determined by a Balance between TRPM8 and Kv1 Potassium Channels. *Journal of Neuroscience*, *29*(10), 3120–3131. https://doi.org/10.1523/JNEUROSCI.4778-08.2009

Madrid, R., Donovan-Rodriguez, T., Meseguer, V., Acosta, M. C., Belmonte, C., & Viana, F. (2006). Contribution of TRPM8 Channels to Cold Transduction in Primary Sensory Neurons and Peripheral Nerve Terminals. *Journal of Neuroscience*, *26*(48), 12512–12525. https://doi.org/10.1523/JNEUROSCI.3752-06.2006

Madrid, R., & Pertusa, M. (2014). *Intimacies and Physiological Role of the Polymodal Cold-*

Sensitive Ion Channel TRPM8. *Current Topics in Membranes* (Vol. 74). Elsevier. https://doi.org/10.1016/B978-0-12-800181-3.00011-7

Mahieu, F., Janssens, A., Gees, M., Talavera, K., Nilius, B., & Voets, T. (2010). Modulation of the cold-activated cation channel TRPM8 by surface charge screening. *Journal of Physiology*, *588*(2), 315–324. https://doi.org/10.1113/jphysiol.2009.183582

Maiarù, M., Tochiki, K. K., Cox, M. B., Annan, L. V., Bell, C. G., Feng, X., … Géranton, S. M. (2016). The stress regulator FKBP51 drives chronic pain by modulating spinal glucocorticoid signaling. *Science Translational Medicine*, *8*(325), 325ra19-325ra19. https://doi.org/10.1126/scitranslmed.aab3376

Maingret, F., Lauritzen, I., Patel, A. J., Heurteaux, C., Reyes, R., Lesage, F., … Honoré, E. (2000). TREK-1 is a heat-activated background K+ channel. *The EMBO Journal*, *19*(11), 2483–2491. https://doi.org/10.1093/emboj/19.11.2483

Mälkiä, A., Madrid, R., Meseguer, V., de la Peña, E., Valero, M., Belmonte, C., & Viana, F. (2007). Bidirectional shifts of TRPM8 channel gating by temperature and chemical agents modulate the cold sensitivity of mammalian thermoreceptors. *The Journal of Physiology*, *581*(Pt 1), 155–174. https://doi.org/10.1113/jphysiol.2006.123059

Malkia, A., Pertusa, M., Fernández-Ballester, G., Ferrer-Montiel, A., & Viana, F. (2009). Differential role of the menthol-binding residue Y745 in the antagonism of thermally gated TRPM8 channels. *Molecular Pain*, *5*, 62. https://doi.org/10.1186/1744-8069-5-62

Manteniotis, S., Lehmann, R., Flegel, C., Vogel, F., Hofreuter, A., Schreiner, B. S. P., … Gisselmann, G. (2013). Comprehensive RNA-Seq expression analysis of sensory ganglia with a focus on ion channels and GPCRs in trigeminal ganglia. *PLoS ONE*, *8*(11), 1–30. https://doi.org/10.1371/journal.pone.0079523

Marshall, L. L., & Roach, J. M. (2016). Treatment of Dry Eye Disease. *The Consultant Pharmacist*, *31*(2), 96–106. https://doi.org/10.4140/TCP.n.2016.96

Martin, T. F. J. (2015). PI(4,5)P_2-binding effector proteins for vesicle exocytosis. *Biochimica et Biophysica Acta*, *1851*(6), 785–93. https://doi.org/10.1016/j.bbalip.2014.09.017

McKemy, D. D., Neuhausser, W. M., & Julius, D. (2002). Identification of a cold receptor reveals a general role for TRP channels in thermosensation. *Nature*, *416*(6876), 52–8. https://doi.org/10.1038/nature719

McMahon, S. B., & Abel, C. (1987). A model for the study of visceral pain states: chronic inflammation of the chronic decerebrate rat urinary bladder by irritant chemicals. *Pain*, *28*(1), 109–27. Retrieved from http://www.ncbi.nlm.nih.gov/pubmed/3822491

McNamara, C. R., Mandel-Brehm, J., Bautista, D. M., Siemens, J., Deranian, K. L., Zhao, M., … Fanger, C. M. (2007). TRPA1 mediates formalin-induced pain. *Proceedings of the National Academy of Sciences*, *104*(33), 13525–13530. https://doi.org/10.1073/pnas.0705924104

Melzack, R., & Wall, P. D. (1965). Pain mechanisms: a new theory. *Science (New York, N.Y.)*, *150*(3699), 971–9.

Memon, T., Chase, K., Leavitt, L. S., Olivera, B. M., & Teichert, R. W. (2017). TRPA1 expression levels and excitability brake by KVchannels influence cold sensitivity of TRPA1-expressing neurons. *Neuroscience*, *353*(April), 76–86. https://doi.org/10.1016/j.neuroscience.2017.04.001

Mergler, S., Mertens, C., Valtink, M., Reinach, P. S., Székely, V. C., Slavi, N., … Pleyer, U. (2013). Functional significance of thermosensitive transient receptor potential melastatin channel 8 (TRPM8) expression in immortalized human corneal endothelial cells. *Experimental Eye Research*, *116*, 337–49. https://doi.org/10.1016/j.exer.2013.10.003

Meseguer, V., Karashima, Y., Talavera, K., D'Hoedt, D., Donovan-Rodriguez, T., Viana, F., … Voets, T. (2008). Transient Receptor Potential Channels in Sensory Neurons Are Targets of the Antimycotic Agent Clotrimazole. *Journal of Neuroscience*, *28*(3), 576–586.

https://doi.org/10.1523/JNEUROSCI.4772-07.2008

Michael, G. J., & Priestley, J. V. (1999). Differential expression of the mRNA for the vanilloid receptor subtype 1 in cells of the adult rat dorsal root and nodose ganglia and its downregulation by axotomy. *The Journal of Neuroscience*, *19*(5), 19. Retrieved from http://www.ncbi.nlm.nih.gov/pubmed/10024368

Mishra, S. K., Tisel, S. M., Orestes, P., Bhangoo, S. K., & Hoon, M. a. (2011). TRPV1-lineage neurons are required for thermal sensation. *The EMBO Journal*, *30*(3), 582–93. https://doi.org/10.1038/emboj.2010.325

Mittag, J., Lyons, D. J., Sällström, J., Vujovic, M., Dudazy-Gralla, S., Warner, A., … Vennström, B. (2013). Thyroid hormone is required for hypothalamic neurons regulating cardiovascular functions. *The Journal of Clinical Investigation*, *123*(1), 509–16. https://doi.org/10.1172/JCI65252

Montell, C., Birnbaumer, L., Flockerzi, V., Bindels, R. J., Bruford, E. A., Caterina, M. J., … Zhu, M. X. (2002). A unified nomenclature for the superfamily of TRP cation channels. *Molecular Cell*, *9*(2), 229–31.

Montell, C., & Rubin, G. M. (1989). Molecular characterization of the Drosophila trp locus: a putative integral membrane protein required for phototransduction. *Neuron*, *2*(4), 1313–23.

Moparthi, L., Kichko, T. I., Eberhardt, M., Högestätt, E. D., Kjellbom, P., Johanson, U., … Zygmunt, P. M. (2016). Human TRPA1 is a heat sensor displaying intrinsic U-shaped thermosensitivity. *Scientific Reports*, *6*(June), 1–10. https://doi.org/10.1038/srep28763

Moran, M. M., & Szallasi, A. (2018). Targeting nociceptive transient receptor potential channels to treat chronic pain: current state of the field. *British Journal of Pharmacology*, *175*(12), 2185–2203. https://doi.org/10.1111/bph.14044

Morenilla-Palao, C., Luis, E., Fernández-Peña, C., Quintero, E., Weaver, J. L., Bayliss, D. A., & Viana, F. (2014). Ion Channel Profile of TRPM8 Cold Receptors Reveals a Role of TASK-3 Potassium Channels in Thermosensation. *Cell Reports*, *8*(5), 1571–1582. https://doi.org/10.1016/j.celrep.2014.08.003

Morenilla-Palao, C., Pertusa, M., Meseguer, V., Cabedo, H., & Viana, F. (2009). Lipid raft segregation modulates TRPM8 channel activity. *Journal of Biological Chemistry*, *284*(14), 9215–9224. https://doi.org/10.1074/jbc.M807228200

Morrison, S. F., & Nakamura, K. (2011). Central neural pathways for thermoregulation. *Frontiers in Bioscience (Landmark Edition)*, *16*, 74–104. Retrieved from http://www.ncbi.nlm.nih.gov/pubmed/21196160

Munns, C., AlQatari, M., & Koltzenburg, M. (2007). Many cold sensitive peripheral neurons of the mouse do not express TRPM8 or TRPA1. *Cell Calcium*, *41*(4), 331–42. https://doi.org/10.1016/j.ceca.2006.07.008

Muraki, K., Iwata, Y., Katanosaka, Y., Ito, T., Ohya, S., Shigekawa, M., & Imaizumi, Y. (2003). TRPV2 Is a Component of Osmotically Sensitive Cation Channels in Murine Aortic Myocytes. *Circulation Research*, *93*(9), 829–838. https://doi.org/10.1161/01.RES.0000097263.10220.0C

Murthy, S. E., Dubin, A. E., & Patapoutian, A. (2017). Piezos thrive under pressure: mechanically activated ion channels in health and disease. *Nature Reviews Molecular Cell Biology*, *18*(12), 771–783. https://doi.org/10.1038/nrm.2017.92

Nebbioso, M., Del Regno, P., Gharbiya, M., Sacchetti, M., Plateroti, R., & Lambiase, A. (2017). Analysis of the Pathogenic Factors and Management of Dry Eye in Ocular Surface Disorders. *International Journal of Molecular Sciences*, *18*(8). https://doi.org/10.3390/ijms18081764

Neher, E., & Sakmann, B. (1976). Single-channel currents recorded from membrane of denervated frog muscle fibres. *Nature*, *260*(5554), 799–802. Retrieved from

http://www.ncbi.nlm.nih.gov/pubmed/1083489

Neher, E., Sakmann, B., & Steinbach, J. H. (1978). The extracellular patch clamp: a method for resolving currents through individual open channels in biological membranes. *Pflugers Archiv : European Journal of Physiology*, *375*(2), 219–28. Retrieved from http://www.ncbi.nlm.nih.gov/pubmed/567789

Nilius, B., Mahieu, F., Prenen, J., Janssens, A., Owsianik, G., Vennekens, R., & Voets, T. (2006). The Ca2+-activated cation channel TRPM4 is regulated by phosphatidylinositol 4,5-biphosphate. *EMBO Journal*, *25*(3), 467–478. https://doi.org/10.1038/sj.emboj.7600963

Nilius, B., & Owsianik, G. (2011). The transient receptor potential family of ion channels. *Genome Biol*, *12*(3), 218. https://doi.org/10.1186/gb-2011-12-3-218

Nilius, B., & Szallasi, A. (2014). Transient Receptor Potential Channels as Drug Targets: From the Science of Basic Research to the Art of Medicine. *Pharmacological Reviews*, *66*(3), 676–814. https://doi.org/10.1124/pr.113.008268

Nomoto, Y., Yoshida, A., Ikeda, S., Kamikawa, Y., Harada, K., Ohwatashi, A., & Kawahira, K. (2008). Effect of menthol on detrusor smooth-muscle contraction and the micturition reflex in rats. *Urology*, *72*(3), 701–5. https://doi.org/10.1016/j.urology.2007.11.137

Norrsell, U., Finger, S., & Lajonchere, C. (1999). Cutaneous sensory spots and the "law of specific nerve energies": History and development of ideas. *Brain Research Bulletin*, *48*(5), 457–465. https://doi.org/10.1016/S0361-9230(98)00067-7

Obara, I., Medrano, M. C., Signoret-Genest, J., Jiménez-Díaz, L., Géranton, S. M., & Hunt, S. P. (2015). Inhibition of the mammalian target of rapamycin complex 1 signaling pathway reduces itch behaviour in mice. *Pain*, *156*(8), 1519–29. https://doi.org/10.1097/j.pain.0000000000000197

Ohmi, M., Shishido, Y., Inoue, T., Ando, K., Fujiuchi, A., Yamada, A., … Kawamura, K. (2014). Identification of a novel 2-pyridyl-benzensulfonamide derivative, RQ-00203078, as a selective and orally active TRPM8 antagonist. *Bioorganic and Medicinal Chemistry Letters*, *24*(23), 5364–5368. https://doi.org/10.1016/j.bmcl.2014.10.074

Okamura, Y., Murata, Y., & Iwasaki, H. (2009). Voltage-sensing phosphatase: actions and potentials. *The Journal of Physiology*, *587*(3), 513–20. https://doi.org/10.1113/jphysiol.2008.163097

Okazawa, M., Terauchi, T., Shiraki, T., Matsumura, K., & Kobayashi, S. (2000). l-Menthol-induced [Ca2+]i increase and impulses in cultured sensory neurons. *Neuroreport*, *11*(10), 2151–5.

Orio, P., Parra, A., Madrid, R., Gonzalez, O., Belmonte, C., & Viana, F. (2012). Role of Ih in the firing pattern of mammalian cold thermoreceptor endings. *Journal of Neurophysiology*, *108*(11), 3009–3023. https://doi.org/10.1152/jn.01033.2011

Ortar, G., Petrocellis, L. De, Morera, L., Moriello, A. S., Orlando, P., Morera, E., … Marzo, V. Di. (2010). (-)-Menthylamine derivatives as potent and selective antagonists of transient receptor potential melastatin type-8 (TRPM8) channels. *Bioorganic and Medicinal Chemistry Letters*, *20*(9), 2729–2732. https://doi.org/10.1016/j.bmcl.2010.03.076

Palkar, R., Ongun, S., Catich, E., Li, N., Borad, N., Sarkisian, A., & McKemy, D. D. (2018). Cooling Relief of Acute and Chronic Itch Requires TRPM8 Channels and Neurons. *Journal of Investigative Dermatology*. https://doi.org/10.1016/j.jid.2017.12.025

PALMER, C. P., AYDAR, E., & DJAMGOZ, M. B. A. (2005). A microbial TRP-like polycystic-kidney-disease-related ion channel gene. *Biochemical Journal*, *387*(1), 211–219. https://doi.org/10.1042/BJ20041710

Palmer, C. P., Zhou, X. L., Lin, J., Loukin, S. H., Kung, C., & Saimi, Y. (2001). A TRP homolog in Saccharomyces cerevisiae forms an intracellular Ca(2+)-permeable channel in the yeast vacuolar membrane. *Proceedings of the National Academy of Sciences of the United States*

of America, *98*(14), 7801–5. https://doi.org/10.1073/pnas.141036198

Pan, Y., Thapa, D., Baldissera, L., Argunhan, F., Aubdool, A. A., & Brain, S. D. (2018). Relevance of TRPA1 and TRPM8 channels as vascular sensors of cold in the cutaneous microvasculature. *Pflugers Archiv : European Journal of Physiology*, *470*(5), 779–786. https://doi.org/10.1007/s00424-017-2085-9

Park, U., Vastani, N., Guan, Y., Raja, S. N., Koltzenburg, M., & Caterina, M. J. (2011). TRP Vanilloid 2 Knock-Out Mice Are Susceptible to Perinatal Lethality But Display Normal Thermal and Mechanical Nociception. *Journal of Neuroscience*, *31*(32), 11425–11436. https://doi.org/10.1523/JNEUROSCI.1384-09.2011

Parra, A., Madrid, R., Echevarria, D., del Olmo, S., Morenilla-Palao, C., Acosta, M. C., … Belmonte, C. (2010). Ocular surface wetness is regulated by TRPM8-dependent cold thermoreceptors of the cornea. *Nature Medicine*, *16*(12), 1396–1399. https://doi.org/10.1038/nm.2264

Patel, R., Gonçalves, L., Leveridge, M., Mack, S. R., Hendrick, A., Brice, N. L., & Dickenson, A. H. (2014). Anti-hyperalgesic effects of a novel TRPM8 agonist in neuropathic rats: a comparison with topical menthol. *Pain*, *155*(10), 2097–107. https://doi.org/10.1016/j.pain.2014.07.022

Paulsen, C. E., Armache, J.-P., Gao, Y., Cheng, Y., & Julius, D. (2015). Structure of the TRPA1 ion channel suggests regulatory mechanisms. *Nature*, *520*(7548), 511–517. https://doi.org/10.1038/nature14367

Pawson, A. J., Sharman, J. L., Benson, H. E., Faccenda, E., Alexander, S. P. H., Buneman, O. P., … Harmar, A. J. (2014). The IUPHAR/BPS Guide to PHARMACOLOGY: an expert-driven knowledgebase of drug targets and their ligands. *Nucleic Acids Research*, *42*(D1), D1098–D1106. https://doi.org/10.1093/nar/gkt1143

Pearce, J. M. S. (2006). Von Frey's pain spots. *Journal of Neurology, Neurosurgery, and Psychiatry*, *77*(12), 1317. https://doi.org/10.1136/jnnp.2006.098970

Pedretti, A., Marconi, C., Bettinelli, I., & Vistoli, G. (2009). Comparative modeling of the quaternary structure for the human TRPM8 channel and analysis of its binding features. *Biochimica et Biophysica Acta*, *1788*(5), 973–82. https://doi.org/10.1016/j.bbamem.2009.02.007

Peier, A. M., Moqrich, A., Hergarden, A. C., Reeve, A. J., Andersson, D. a, Story, G. M., … Patapoutian, A. (2002). A TRP channel that senses cold stimuli and menthol. *Cell*, *108*(5), 705–15. Retrieved from http://www.ncbi.nlm.nih.gov/pubmed/11893340

Peier, A. M., Reeve, A. J., Andersson, D. A., Moqrich, A., Earley, T. J., Hergarden, A. C., … Patapoutian, A. (2002). A Heat-Sensitive TRP Channel Expressed in Keratinocytes. *Science*, *296*(5575), 2046–2049. https://doi.org/10.1126/science.1073140

Pereira, U., Boulais, N., Lebonvallet, N., Pennec, J. P., Dorange, G., & Misery, L. (2010). Mechanisms of the sensory effects of tacrolimus on the skin. *British Journal of Dermatology*, *163*(1), 70–77. https://doi.org/10.1111/j.1365-2133.2010.09757.x

Pérez De Vega, M. J., Gómez-Monterrey, I., Ferrer-Montiel, A., & González-Muñiz, R. (2016). Transient Receptor Potential Melastatin 8 Channel (TRPM8) Modulation: Cool Entryway for Treating Pain and Cancer. *Journal of Medicinal Chemistry*, *59*(22), 10006–10029. https://doi.org/10.1021/acs.jmedchem.6b00305

Pertusa, M., González, A., Hardy, P., Madrid, R., & Viana, F. (2014). Bidirectional modulation of thermal and chemical sensitivity of TRPM8 channels by the initial region of the N-terminal domain. *Journal of Biological Chemistry*, *289*(32), 21828–21843. https://doi.org/10.1074/jbc.M114.565994

Pertusa, M., Madrid, R., Morenilla-Palao, C., Belmonte, C., & Viana, F. (2012). N-glycosylation of TRPM8 ion channels modulates temperature sensitivity of cold thermoreceptor neurons.

Journal of Biological Chemistry, *287*(22), 18218–18229. https://doi.org/10.1074/jbc.M111.312645

Pertusa, M., Rivera, B., González, A., Ugarte, G., & Madrid, R. (2018). Critical role of the pore domain in the cold response of TRPM8 channels identified by ortholog functional comparison. *Journal of Biological Chemistry*, *293*(32), 12454–12471. https://doi.org/10.1074/jbc.RA118.002256

Phelps, C. B., & Gaudet, R. (2007). The role of the N terminus and transmembrane domain of TRPM8 in channel localization and tetramerization. *Journal of Biological Chemistry*, *282*(50), 36474–36480. https://doi.org/10.1074/jbc.M707205200

Pierau, F. K., Torrey, P., & Carpenter, D. (1975). Effect of ouabain and potassium-free solution on mammalian thermosensitive afferents in vitro. *Pflugers Archiv : European Journal of Physiology*, *359*(4), 349–56.

Posor, Y., Eichhorn-Grünig, M., & Haucke, V. (2015). Phosphoinositides in endocytosis. *Biochimica et Biophysica Acta (BBA) - Molecular and Cell Biology of Lipids*, *1851*(6), 794–804. https://doi.org/10.1016/j.bbalip.2014.09.014

Premkumar, L. S., & Abooj, M. (2013). TRP channels and analgesia. *Life Sciences*, *92*(8–9), 415–24. https://doi.org/10.1016/j.lfs.2012.08.010

Premkumar, L. S., & Ahern, G. P. (2000). Induction of vanilloid receptor channel activity by protein kinase C. *Nature*, *408*(6815), 985–90. https://doi.org/10.1038/35050121

Premkumar, L. S., Raisinghani, M., Pingle, S. C., Long, C., & Pimentel, F. (2005). Downregulation of transient receptor potential melastatin 8 by protein kinase C-mediated dephosphorylation. *The Journal of Neuroscience : The Official Journal of the Society for Neuroscience*, *25*(49), 11322–9. https://doi.org/10.1523/JNEUROSCI.3006-05.2005

Prince, P. B., Rapoport, A. M., Sheftell, F. D., Tepper, S. J., & Bigal, M. E. (2004). The Effect of Weather on Headache. *Headache: The Journal of Head and Face Pain*, *44*(6), 596–602. https://doi.org/10.1111/j.1526-4610.2004.446008.x

Proudfoot, C. J., Garry, E. M., Cottrell, D. F., Rosie, R., Anderson, H., Robertson, D. C., … Mitchell, R. (2006). Analgesia mediated by the TRPM8 cold receptor in chronic neuropathic pain. *Current Biology : CB*, *16*(16), 1591–605. https://doi.org/10.1016/j.cub.2006.07.061

Provencio, I., Jiang, G., De Grip, W. J., Hayes, W. P., & Rollag, M. D. (1998). Melanopsin: An opsin in melanophores, brain, and eye. *Proceedings of the National Academy of Sciences of the United States of America*, *95*(1), 340–5. Retrieved from http://www.ncbi.nlm.nih.gov/pubmed/9419377

Qiu, X., Kumbalasiri, T., Carlson, S. M., Wong, K. Y., Krishna, V., Provencio, I., & Berson, D. M. (2005). Induction of photosensitivity by heterologous expression of melanopsin. *Nature*, *433*(7027), 745–9. https://doi.org/10.1038/nature03345

Quallo, T., Alkhatib, O., Gentry, C., Andersson, D. A., & Bevan, S. (2017). G protein bg subunits inhibit TRPM3 ion channels in sensory neurons, 1–22. https://doi.org/10.7554/eLife.26138

Quallo, T., Vastani, N., Horridge, E., Gentry, C., Parra, A., Moss, S., … Bevan, S. (2015). TRPM8 is a neuronal osmosensor that regulates eye blinking in mice. *Nature Communications*, *6*(May), 7150. https://doi.org/10.1038/ncomms8150

Ramachandran, R., Hyun, E., Zhao, L., Lapointe, T. K., Chapman, K., Hirota, C. L., … Hollenberg, M. D. (2013). TRPM8 activation attenuates inflammatory responses in mouse models of colitis. *Proceedings of the National Academy of Sciences of the United States of America*, *110*(18), 7476–81. https://doi.org/10.1073/pnas.1217431110

Ray, P., Torck, A., Quigley, L., Wangzhou, A., Neiman, M., Rao, C., … Price, T. J. (2018). Comparative transcriptome profiling of the human and mouse dorsal root ganglia. *PAIN*, *159*(7), 1325–1345. https://doi.org/10.1097/j.pain.0000000000001217

Reid, G., Babes, A., & Pluteanu, F. (2002). A cold- and menthol-activated current in rat dorsal

root ganglion neurones: Properties and role in cold transduction. *Journal of Physiology*, *545*(2), 595–614. https://doi.org/10.1113/jphysiol.2002.024331

Reid, G., & Flonta, M.-L. (2001a). Cold current in thermoreceptive neurons. *Nature*, *413*(6855), 480–480. https://doi.org/10.1038/35097164

Reid, G., & Flonta, M. L. (2001b). Cold transduction by inhibition of a background potassium conductance in rat primary sensory neurones. *Neuroscience Letters*, *297*(3), 171–174. https://doi.org/10.1016/S0304-3940(00)01694-3

Reimúndez, A., Fernández-Peña, C., García, G., Fernández, R., Ordás, P., Gallego, R., … Señarís, R. (2018). Deletion of the cold thermoreceptor TRPM8 increases heat loss and food intake leading to reduced body temperature and obesity in mice. *The Journal of Neuroscience*, *38*(15), 3002–17. https://doi.org/10.1523/JNEUROSCI.3002-17.2018

Reitamo, S., Ortonne, J. P., Sand, C., Bos, J., Cambazard, F., Bieber, T., … Schuttelaar, M. (2007). Long-term treatment with 0.1% tacrolimus ointment in adults with atopic dermatitis: Results of a two-year, multicentre, non-comparative study. *Acta Dermato-Venereologica*, *87*(5), 406–412. https://doi.org/10.2340/00015555-0282

Ren, L., Dhaka, A., & Cao, Y.-Q. (2015). Function and postnatal changes of dural afferent fibers expressing TRPM8 channels. *Molecular Pain*, *11*, 37. https://doi.org/10.1186/s12990-015-0043-0

Rinne, A., Mobarec, J. C., Mahaut-Smith, M., Kolb, P., & Bünemann, M. (2015). The mode of agonist binding to a G protein-coupled receptor switches the effect that voltage changes have on signaling. *Science Signaling*, *8*(401), ra110. https://doi.org/10.1126/scisignal.aac7419

Robbins, A., Kurose, M., Winterson, B. J., & Meng, I. D. (2012). Menthol activation of corneal cool cells induces TRPM8- mediated lacrimation but not nociceptive responses in rodents. *Investigative Ophthalmology and Visual Science*, *53*(11), 7034–7042. https://doi.org/10.1167/iovs.12-10025

Rohács, T., Lopes, C. M. B., Michailidis, I., & Logothetis, D. E. (2005). PI(4,5)P2regulates the activation and desensitization of TRPM8 channels through the TRP domain. *Nature Neuroscience*, *8*(5), 626–634. https://doi.org/10.1038/nn1451

Rossato, M., Granzotto, M., Macchi, V., Porzionato, A., Petrelli, L., Calcagno, A., … Vettor, R. (2014). Human white adipocytes express the cold receptor TRPM8 which activation induces UCP1 expression, mitochondrial activation and heat production. *Molecular and Cellular Endocrinology*, *383*(1–2), 137–146. https://doi.org/10.1016/j.mce.2013.12.005

Runnels, L. W., Yue, L., & Clapham, D. E. (2002). The TRPM7 channel is inactivated by PIP2hydrolysis. *Nature Cell Biology*, *4*(5), 329–336. https://doi.org/10.1038/ncb781

Rusnak, F., & Mertz, P. (2000). Calcineurin: form and function. *Physiological Reviews*, *80*(4), 1483–521. https://doi.org/10.1152/physrev.2000.80.4.1483

Russell, W. C., Graham, F. L., Smiley, J., & Nairn, R. (1977). Characteristics of a Human Cell Line Transformed by DNA from Human Adenovirus Type 5. *Journal of General Virology*, *36*(1), 59–72. https://doi.org/10.1099/0022-1317-36-1-59

Saarikangas, J., Zhao, H., & Lappalainen, P. (2010). Regulation of the Actin Cytoskeleton-Plasma Membrane Interplay by Phosphoinositides. *Physiological Reviews*, *90*(1), 259–289. https://doi.org/10.1152/physrev.00036.2009

Sabatini, D. M. (2017). Twenty-five years of mTOR: Uncovering the link from nutrients to growth. *Proceedings of the National Academy of Sciences of the United States of America*, *114*(45), 11818–11825. https://doi.org/10.1073/pnas.1716173114

Sabnis, A. S., Shadid, M., Yost, G. S., & Reilly, C. A. (2008). Human lung epithelial cells express a functional cold-sensing TRPM8 variant. *American Journal of Respiratory Cell and Molecular Biology*, *39*(4), 466–74. https://doi.org/10.1165/rcmb.2007-0440OC

Sarria, I., Ling, J., & Gu, J. G. (2012). Thermal sensitivity of voltage-gated Na+ channels and A-type K+ channels contributes to somatosensory neuron excitability at cooling temperatures. *Journal of Neurochemistry*, *122*(6), 1145–1154. https://doi.org/10.1111/j.1471-4159.2012.07839.x

Sawada, Y., Hosokawa, H., Hori, A., Matsumura, K., & Kobayashi, S. (2007). Cold sensitivity of recombinant TRPA1 channels. *Brain Research*, *1160*, 39–46. https://doi.org/10.1016/j.brainres.2007.05.047

Schäfer, K., Braun, H. a, & Isenberg, C. (1986). Effect of menthol on cold receptor activity. Analysis of receptor processes. *The Journal of General Physiology*, *88*(6), 757–776. https://doi.org/10.1085/jgp.88.6.757

Schiene-Fischer, C., & Yu, C. (2001). Receptor accessory folding helper enzymes: the functional role of peptidyl prolyl cis/trans isomerases. *FEBS Letters*, *495*(1–2), 1–6.

Schmidt, M., Dubin, A. E., Petrus, M. J., Earley, T. J., & Patapoutian, A. (2009). Nociceptive Signals Induce Trafficking of TRPA1 to the Plasma Membrane. *Neuron*, *64*(4), 498–509. https://doi.org/10.1016/j.neuron.2009.09.030

Selescu, T., Ciobanu, A. C., Dobre, C., Reid, G., & Babes, A. (2013). Camphor activates and sensitizes transient receptor potential melastatin 8 (TRPM8) to cooling and icilin. *Chemical Senses*, *38*(7), 563–575. https://doi.org/10.1093/chemse/bjt027

Senba, E., Katanosaka, K., Yajima, H., & Mizumura, K. (2004). The immunosuppressant FK506 activates capsaicin- and bradykinin-sensitive DRG neurons and cutaneous C-fibers. *Neuroscience Research*, *50*(3), 257–62. https://doi.org/10.1016/j.neures.2004.07.005

Señarís, R., Ordás, P., Reimúndez, A., & Viana, F. (2018). Mammalian cold TRP channels: impact on thermoregulation and energy homeostasis. *Pflügers Archiv - European Journal of Physiology*. https://doi.org/10.1007/s00424-018-2145-9

Shapovalov, G., Gkika, D., Devilliers, M., Kondratskyi, A., Gordienko, D., Busserolles, J., … Prevarskaya, N. (2013). Opiates modulate thermosensation by internalizing cold receptor TRPM8. *Cell Reports*, *4*(3), 504–15. https://doi.org/10.1016/j.celrep.2013.07.002

Shen, Y., Rampino, M. A. F., Carroll, R. C., & Nawy, S. (2012). G-protein-mediated inhibition of the Trp channel TRPM1 requires the G dimer. *Proceedings of the National Academy of Sciences*, *109*(22), 8752–8757. https://doi.org/10.1073/pnas.1117433109

Sherkheli, M. A., Gisselmann, G., Vogt-Eisele, A. K., Doerner, J. F., & Hatt, H. (2008). Menthol derivative WS-12 selectively activates transient receptor potential melastatin-8 (TRPM8) ion channels. *Pakistan Journal of Pharmaceutical Sciences*, *21*(4), 370–378.

Sherrington, C. S. (1911). *The integrative action of the nervous system.* New Haven: Yale University Press. https://doi.org/10.1037/13798-000

Shim, S., Yuan, J. P., Kim, J. Y., Zeng, W., Huang, G., Milshteyn, A., … Worley, P. F. (2009). Peptidyl-Prolyl Isomerase FKBP52 Controls Chemotropic Guidance of Neuronal Growth Cones via Regulation of TRPC1 Channel Opening. *Neuron*, *64*(4), 471–483. https://doi.org/10.1016/j.neuron.2009.09.025

Sidell, N., Verity, M. A., & Nord, E. P. (1990). Menthol blocks dihydropyridine-insensitive Ca2+ channels and induces neurite outgrowth in human neuroblastoma cells. *Journal of Cellular Physiology*, *142*(2), 410–9. https://doi.org/10.1002/jcp.1041420226

Simons, K., & Ikonen, E. (1997). Functional rafts in cell membranes. *Nature*, *387*(6633), 569–572. https://doi.org/10.1038/42408

Smrcka, A. V, Hepler, J. R., Brown, K. O., & Sternweis, P. C. (1991). Regulation of polyphosphoinositide-specific phospholipase C activity by purified Gq. *Science (New York, N.Y.)*, *251*(4995), 804–7.

Sobhan, U., Sato, M., Shinomiya, T., Okubo, M., Tsumura, M., Muramatsu, T., … Shibukawa, Y. (2013). Immunolocalization and distribution of functional temperature-sensitive TRP

channels in salivary glands. *Cell and Tissue Research*, *354*(2), 507–519. https://doi.org/10.1007/s00441-013-1691-x

Song, K., Wang, H., Kamm, G. B., Pohle, J., De Castro Reis, F., Heppenstall, P., … Siemens, J. (2016). The TRPM2 channel is a hypothalamic heat sensor that limits fever and can drive hypothermia. *Science*, *353*(6306), 1393–1398. https://doi.org/10.1126/science.aaf7537

Spray, D. C. (1986). Cutaneous Temperature Receptors. *Annual Review of Physiology*, *48*(1), 625–638. https://doi.org/10.1146/annurev.ph.48.030186.003205

Ständer, S., Augustin, M., Roggenkamp, D., Blome, C., Heitkemper, T., Worthmann, A. C., & Neufang, G. (2017). Novel TRPM8 agonist cooling compound against chronic itch: results from a randomized, double-blind, controlled, pilot study in dry skin. *Journal of the European Academy of Dermatology and Venereology*, *31*(6), 1064–1068. https://doi.org/10.1111/jdv.14041

Ständer, S., Ständer, H., Seeliger, S., Luger, T. A., & Steinhoff, M. (2007). Topical pimecrolimus and tacrolimus transiently induce neuropeptide release and mast cell degranulation in murine skin. *British Journal of Dermatology*, *156*(5), 1020–1026. https://doi.org/10.1111/j.1365-2133.2007.07813.x

Stein, A. T., Ufret-Vincenty, C. A., Hua, L., Santana, L. F., & Gordon, S. E. (2006). Phosphoinositide 3-kinase binds to TRPV1 and mediates NGF-stimulated TRPV1 trafficking to the plasma membrane. *The Journal of General Physiology*, *128*(5), 509–22. https://doi.org/10.1085/jgp.200609576

Stein, R. J., Santos, S., Nagatomi, J., Hayashi, Y., Minnery, B. S., Xavier, M., … De Miguel, F. (2004). Cool (TRPM8) and hot (TRPV1) receptors in the bladder and male genital tract. *The Journal of Urology*, *172*(3), 1175–8. https://doi.org/10.1097/01.ju.0000134880.55119.cf

Stewart, A. P., Egressy, K., Lim, A., & Edwardson, J. M. (2010). AFM imaging reveals the tetrameric structure of the TRPM8 channel. *Biochemical and Biophysical Research Communications*, *394*(2), 383–6. https://doi.org/10.1016/j.bbrc.2010.03.027

Story, G. M., Peier, A. M., Reeve, A. J., Eid, S. R., Mosbacher, J., Hricik, T. R., … Patapoutian, A. (2003). ANKTM1, a TRP-like channel expressed in nociceptive neurons, is activated by cold temperatures. *Cell*, *112*(6), 819–29. Retrieved from http://www.ncbi.nlm.nih.gov/pubmed/12654248

Strassman, A. M., Raymond, S. A., & Burstein, R. (1996). Sensitization of meningeal sensory neurons and the origin of headaches. *Nature*, *384*(6609), 560–564. https://doi.org/10.1038/384560a0

Stull, C., Lavery, M. J., & Yosipovitch, G. (2016). Advances in therapeutic strategies for the treatment of pruritus. *Expert Opinion on Pharmacotherapy*, *17*(5), 671–687. https://doi.org/10.1517/14656566.2016.1127355

Su, L., Wang, C., Yu, Y., Ren, Y., Xie, K., & Wang, G. (2011). Role of TRPM8 in dorsal root ganglion in nerve injury-induced chronic pain. *BMC Neuroscience*, *12*(1), 120. https://doi.org/10.1186/1471-2202-12-120

Suh, B.-C., & Hille, B. (2008). PIP2 is a necessary cofactor for ion channel function: how and why? *Annual Review of Biophysics*, *37*(1), 175–95. https://doi.org/10.1146/annurev.biophys.37.032807.125859

Suh, B. C., & Hille, B. (2002). Recovery from muscarinic modulation of M current channels requires phosphatidylinositol 4,5-bisphosphate synthesis. *Neuron*, *35*(3), 507–520. https://doi.org/10.1016/S0896-6273(02)00790-0

Suh, B. C., Leal, K., & Hille, B. (2010). Modulation of high-voltage activated Ca2+ channels by membrane phosphatidylinositol 4,5-bisphosphate. *Neuron*, *67*(2), 224–238. https://doi.org/10.1016/j.neuron.2010.07.001

Swandulla, D., Carbone, E., Schäfer, K., & Lux, H. D. (1987). Effect of menthol on two types of

Ca currents in cultured sensory neurons of vertebrates. *Pflugers Archiv : European Journal of Physiology*, *409*(1–2), 52–9.

Tajino, K., Matsumura, K., Kosada, K., Shibakusa, T., Inoue, K., Fushiki, T., … Kobayashi, S. (2007). Application of menthol to the skin of whole trunk in mice induces autonomic and behavioral heat-gain responses. *American Journal of Physiology-Regulatory, Integrative and Comparative Physiology*, *293*(5), R2128–R2135. https://doi.org/10.1152/ajpregu.00377.2007

Takashima, Y., Daniels, R. L., Knowlton, W., Teng, J., Liman, E. R., & McKemy, D. D. (2007). Diversity in the neural circuitry of cold sensing revealed by genetic axonal labeling of transient receptor potential melastatin 8 neurons. *The Journal of Neuroscience : The Official Journal of the Society for Neuroscience*, *27*(51), 14147–57. https://doi.org/10.1523/JNEUROSCI.4578-07.2007

Talavera, K., Yasumatsu, K., Voets, T., Droogmans, G., Shigemura, N., Ninomiya, Y., … Nilius, B. (2005). Heat activation of TRPM5 underlies thermal sensitivity of sweet taste. *Nature*, *438*(7070), 1022–1025. https://doi.org/10.1038/nature04248

Tan, C.-H., & McNaughton, P. A. (2016). The TRPM2 ion channel is required for sensitivity to warmth. *Nature*, *536*(7617), 460–463. https://doi.org/10.1038/nature19074

Tang, Z., Kim, A., Masuch, T., Park, K., Weng, H., Wetzel, C., & Dong, X. (2013). Pirt functions as an endogenous regulator of TRPM8. *Nature Communications*, *4*(1), 2179. https://doi.org/10.1038/ncomms3179

Teichert, R. W., Memon, T., Aman, J. W., & Olivera, B. M. (2014). Using constellation pharmacology to define comprehensively a somatosensory neuronal subclass. *Proceedings of the National Academy of Sciences*, *111*(6), 2319–2324. https://doi.org/10.1073/pnas.1324019111

Thakur, M., Crow, M., Richards, N., Davey, G. I. J., Levine, E., Kelleher, J. H., … McMahon, S. B. (2014). Defining the nociceptor transcriptome. *Frontiers in Molecular Neuroscience*, *7*(November), 87. https://doi.org/10.3389/fnmol.2014.00087

Togashi, K., Hara, Y., Tominaga, T., Higashi, T., Konishi, Y., Mori, Y., & Tominaga, M. (2006). TRPM2 activation by cyclic ADP-ribose at body temperature is involved in insulin secretion. *The EMBO Journal*, *25*(9), 1804–15. https://doi.org/10.1038/sj.emboj.7601083

Tominaga, M., Caterina, M. J., Malmberg, A. B., Rosen, T. A., Gilbert, H., Skinner, K., … Julius, D. (1998). The cloned capsaicin receptor integrates multiple pain-producing stimuli. *Neuron*, *21*(3), 531–43.

Toro, C. A., Eger, S., Veliz, L., Sotelo-Hitschfeld, P., Cabezas, D., Castro, M. A., … Brauchi, S. (2015). Agonist-Dependent Modulation of Cell Surface Expression of the Cold Receptor TRPM8. *Journal of Neuroscience*, *35*(2), 571–582. https://doi.org/10.1523/JNEUROSCI.3820-13.2015

Tóth, B. I., Konrad, M., Ghosh, D., Mohr, F., Halaszovich, C. R., Leitner, M. G., … Voets, T. (2015). Regulation of the transient receptor potential channel TRPM3 by phosphoinositides. *The Journal of General Physiology*, *146*(1), 51–63. https://doi.org/10.1085/jgp.201411339

Tousova, K., Susankova, K., Teisinger, J., Vyklicky, L., & Vlachova, V. (2004). Oxidizing reagent copper-o-phenanthroline is an open channel blocker of the vanilloid receptor TRPV1. *Neuropharmacology*, *47*(2), 273–85. https://doi.org/10.1016/j.neuropharm.2004.04.001

Tsavaler, L., Shapero, M. H., Morkowski, S., & Laus, R. (2001). Trp-p8 , a Novel Prostate-specific Gene , Is Up-Regulated in Prostate Cancer and Other Malignancies and Shares High Homology with Transient Receptor Potential Calcium Channel Proteins Trp-p8 , a Novel Prostate-specific Gene , Is Up-Regulated in Prostate C.

Tsuruda, P. R., Julius, D., & Minor, D. L. (2006). Coiled coils direct assembly of a cold-activated

TRP channel. *Neuron*, *51*(2), 201–12. https://doi.org/10.1016/j.neuron.2006.06.023

Usoskin, D., Furlan, A., Islam, S., Abdo, H., Lönnerberg, P., Lou, D., … Ernfors, P. (2015). Unbiased classification of sensory neuron types by large-scale single-cell RNA sequencing. *Nature Neuroscience*, *18*(1), 145–153. https://doi.org/10.1038/nn.3881

Valente, P., García-Sanz, N., Gomis, A., Fernández-Carvajal, A., Fernández-Ballester, G., Viana, F., … Ferrer-Montiel, A. (2008). Identification of molecular determinants of channel gating in the transient receptor potential box of vanilloid receptor I. *The FASEB Journal*, *22*(9), 3298–3309. https://doi.org/10.1096/fj.08-107425

Valenzano, K. J., Grant, E. R., Wu, G., Hachicha, M., Schmid, L., Tafesse, L., … Hodges, D. (2003). N-(4-Tertiarybutylphenyl)-4-(3-chloropyridin-2-yl)tetrahydropyrazine -1(2H)-carbox-amide (BCTC), a Novel, Orally Effective Vanilloid Receptor 1 Antagonist with Analgesic Properties: I. In Vitro Characterization and Pharmacokinetic Properties. *Journal of Pharmacology and Experimental Therapeutics*, *306*(1), 377–386. https://doi.org/10.1124/jpet.102.045674

Valero, M. L., Mello de Queiroz, F., Stühmer, W., Viana, F., & Pardo, L. A. (2012). TRPM8 Ion Channels Differentially Modulate Proliferation and Cell Cycle Distribution of Normal and Cancer Prostate Cells. *PLoS ONE*, *7*(12), e51825. https://doi.org/10.1371/journal.pone.0051825

Valero, M., Morenilla-Palao, C., Belmonte, C., & Viana, F. (2011). Pharmacological and functional properties of TRPM8 channels in prostate tumor cells. *Pflugers Archiv European Journal of Physiology*, *461*(1), 99–114. https://doi.org/10.1007/s00424-010-0895-0

Vanden Abeele, F., Zholos, A., Bidaux, G., Shuba, Y., Thebault, S., Beck, B., … Prevarskaya, N. (2006). Ca2+-independent phospholipase A2-dependent gating of TRPM8 by lysophospholipids. *The Journal of Biological Chemistry*, *281*(52), 40174–82. https://doi.org/10.1074/jbc.M605779200

Vandewauw, I., De Clercq, K., Mulier, M., Held, K., Pinto, S., Van Ranst, N., … Voets, T. (2018). A TRP channel trio mediates acute noxious heat sensing. *Nature*, *555*(7698), 662–666. https://doi.org/10.1038/nature26137

Várnai, P., Rother, K. I., & Balla, T. (1999). Phosphatidylinositol 3-kinase-dependent membrane association of the Bruton's tyrosine kinase pleckstrin homology domain visualized in single living cells. *The Journal of Biological Chemistry*, *274*(16), 10983–9. Retrieved from http://www.ncbi.nlm.nih.gov/pubmed/10196179

Varnai, P., Thyagarajan, B., Rohacs, T., & Balla, T. (2006). Rapidly inducible changes in phosphatidylinositol 4,5-bisphosphate levels influence multiple regulatory functions of the lipid in intact living cells. *The Journal of Cell Biology*, *175*(3), 377–82. https://doi.org/10.1083/jcb.200607116

Veliz, L. A., Toro, C. A., Vivar, J. P., Arias, L. A., Villegas, J., Castro, M. A., & Brauchi, S. (2010). Near-membrane dynamics and capture of TRPM8 channels within transient confinement domains. *PLoS ONE*, *5*(10). https://doi.org/10.1371/journal.pone.0013290

Vetter, I., Hein, A., Sattler, S., Hessler, S., Touska, F., Bressan, E., … Zimmermann, K. (2013). Amplified Cold Transduction in Native Nociceptors by M-Channel Inhibition. *Journal of Neuroscience*, *33*(42), 16627–16641. https://doi.org/10.1523/JNEUROSCI.1473-13.2013

Viana, F. (2018). Nociceptors: thermal allodynia and thermal pain. In *Handbook of clinical neurology* (Vol. 156, pp. 103–119). https://doi.org/10.1016/B978-0-444-63912-7.00006-0

Viana, F., de la Peña, E., & Belmonte, C. (2002). Specificity of cold thermotransduction is determined by differential ionic channel expression. *Nature Neuroscience*, *5*(3), 254–60. https://doi.org/10.1038/nn809

Vissers, K., & Meert, T. (2005). A Behavioral and Pharmacological Validation of the Acetone Spray Test in Gerbils with a Chronic Constriction Injury. *Anesthesia & Analgesia*, *101*(2),

457–464. https://doi.org/10.1213/01.ANE.0000158471.41575.F0

Voets, T. (2012). Quantifying and modeling the temperature-dependent gating of TRP channels. *Reviews of Physiology, Biochemistry and Pharmacology*, *162*, 91–119. https://doi.org/10.1007/112_2011_5

Voets, T., Droogmans, G., Wissenbach, U., Janssens, A., Flockerzi, V., & Nilius, B. (2004). The principle of temperature-dependent gating in cold- and heat-sensitive TRP channels. *Nature*, *430*(7001), 748–754.

Voets, T., Owsianik, G., Janssens, A., Talavera, K., & Nilius, B. (2007). TRPM8 voltage sensor mutants reveal a mechanism for integrating thermal and chemical stimuli. *Nature Chemical Biology*, *3*(3), 174–182. https://doi.org/10.1038/nchembio862

Vriens, J., Owsianik, G., Hofmann, T., Philipp, S. E., Stab, J., Chen, X., … Voets, T. (2011). TRPM3 Is a Nociceptor Channel Involved in the Detection of Noxious Heat. *Neuron*, *70*(3), 482–494. https://doi.org/10.1016/j.neuron.2011.02.051

Wan, X. C., & Dimov, V. (2014). Pharmacokinetic evaluation of topical calcineurin inhibitors for treatment of allergic conjunctivitis. *Expert Opinion on Drug Metabolism & Toxicology*, *10*(4), 543–9. https://doi.org/10.1517/17425255.2014.884070

Wang, H. S., Pan, Z., Shi, W., Brown, B. S., Wymore, R. S., Cohen, I. S., … McKinnon, D. (1998). KCNQ2 and KCNQ3 potassium channel subunits: molecular correlates of the M-channel. *Science (New York, N.Y.)*, *282*(5395), 1890–3. Retrieved from http://www.ncbi.nlm.nih.gov/pubmed/9836639

Wang, S., Zhang, D., Hu, J., Jia, Q., Xu, W., Su, D., … Xiao, J. (2017). A clinical and mechanistic study of topical borneol-induced analgesia. *EMBO Molecular Medicine*, *9*(6), 802–815. https://doi.org/10.15252/emmm.201607300

Wang, X.-P., Yu, X., Yan, X.-J., Lei, F., Chai, Y.-S., Jiang, J.-F., … Du, L.-J. (2017). TRPM8 in the negative regulation of TNFα expression during cold stress. *Scientific Reports*, *7*(1), 45155. https://doi.org/10.1038/srep45155

Watanabe, H., Vriens, J., Suh, S. H., Benham, C. D., Droogmans, G., & Nilius, B. (2002). Heat-evoked Activation of TRPV4 Channels in a HEK293 Cell Expression System and in Native Mouse Aorta Endothelial Cells. *Journal of Biological Chemistry*, *277*(49), 47044–47051. https://doi.org/10.1074/jbc.M208277200

Watt, E. E., Betts, B. A., Kotey, F. O., Humbert, D. J., Griffith, T. N., Kelly, E. W., … Hall, A. C. (2008). Menthol shares general anesthetic activity and sites of action on the GABA(A) receptor with the intravenous agent, propofol. *European Journal of Pharmacology*, *590*(1–3), 120–6. https://doi.org/10.1016/j.ejphar.2008.06.003

Weil, A., Moore, S. E., Waite, N. J., Randall, A., & Gunthorpe, M. J. (2005). Conservation of functional and pharmacological properties in the distantly related temperature sensors TRVP1 and TRPM8. *Molecular Pharmacology*, *68*(2), 518–27. https://doi.org/10.1124/mol.105.012146

Wilke, B. U., Lindner, M., Greifenberg, L., Albus, A., Kronimus, Y., Bünemann, M., … Oliver, D. (2014). Diacylglycerol mediates regulation of TASK potassium channels by Gq-coupled receptors. *Nature Communications*, *5*(May), 5540. https://doi.org/10.1038/ncomms6540

Wilkinson, J. E., Burmeister, L., Brooks, S. V., Chan, C.-C., Friedline, S., Harrison, D. E., … Miller, R. A. (2012). Rapamycin slows aging in mice. *Aging Cell*, *11*(4), 675–682. https://doi.org/10.1111/j.1474-9726.2012.00832.x

Winchester, W. J., Gore, K., Glatt, S., Petit, W., Gardiner, J. C., Conlon, K., … Reynolds, D. S. (2014). Inhibition of TRPM8 Channels Reduces Pain in the Cold Pressor Test in Humans. *Journal of Pharmacology and Experimental Therapeutics*, *351*(2), 259–269. https://doi.org/10.1124/jpet.114.216010

Winkler, P. A., Huang, Y., Sun, W., Du, J., & Lü, W. (2017). Electron cryo-microscopy structure

of a human TRPM4 channel. *Nature*. https://doi.org/10.1038/nature24674

Winks, J. S., Hughes, S., Filippov, A. K., Tatulian, L., Abogadie, F. C., Brown, D. A., & Marsh, S. J. (2005). Relationship between membrane phosphatidylinositol-4,5-bisphosphate and receptor-mediated inhibition of native neuronal M channels. *The Journal of Neuroscience : The Official Journal of the Society for Neuroscience*, *25*(13), 3400–13. https://doi.org/10.1523/JNEUROSCI.3231-04.2005

Winter, Z., Gruschwitz, P., Eger, S., Touska, F., & Zimmermann, K. (2017). Cold Temperature Encoding by Cutaneous TRPA1 and TRPM8-Carrying Fibers in the Mouse. *Frontiers in Molecular Neuroscience*, *10*(June). https://doi.org/10.3389/fnmol.2017.00209

Wong, L. S., Otsuka, A., Yamamoto, Y., Nonomura, Y., Nakashima, C., Kitayama, N., … Kabashima, K. (2018). TRPA1 channel participates in tacrolimus-induced pruritus in a chronic contact hypersensitivity murine model. *Journal of Dermatological Science*, *89*(2), 207–209. https://doi.org/10.1016/j.jdermsci.2017.10.012

Woodbury, C. J., Zwick, M., Wang, S., Lawson, J. J., Caterina, M. J., Koltzenburg, M., … Davis, B. M. (2004). Nociceptors Lacking TRPV1 and TRPV2 Have Normal Heat Responses. *Journal of Neuroscience*, *24*(28), 6410–6415. https://doi.org/10.1523/JNEUROSCI.1421-04.2004

Xie, J., Sun, B., Du, J., Yang, W., Chen, H. C., Overton, J. D., … Yue, L. (2011). Phosphatidylinositol 4,5-bisphosphate (PIP 2) controls magnesium gatekeeper TRPM6 activity. *Scientific Reports*, *1*, 1–11. https://doi.org/10.1038/srep00146

Xing, H., Chen, M., Ling, J., Tan, W., & Gu, J. G. (2007). TRPM8 Mechanism of Cold Allodynia after Chronic Nerve Injury. *Journal of Neuroscience*, *27*(50), 13680–13690. https://doi.org/10.1523/JNEUROSCI.2203-07.2007

Xing, H., Ling, J., Chen, M., & Gu, J. G. (2006). Chemical and cold sensitivity of two distinct populations of TRPM8-expressing somatosensory neurons. *Journal of Neurophysiology*, *95*(2), 1221–30. https://doi.org/10.1152/jn.01035.2005

Xu, C., Watras, J., & Loew, L. M. (2003). Kinetic analysis of receptor-activated phosphoinositide turnover. *The Journal of Cell Biology*, *161*(4), 779–791. https://doi.org/10.1083/jcb.200301070

Yamamoto, A., Takahashi, K., Saito, S., Tominaga, M., & Ohta, T. (2016). Two different avian cold-sensitive sensory neurons: Transient receptor potential melastatin 8 (TRPM8)-dependent and -independent activation mechanisms. *Neuropharmacology*, *111*, 130–141. https://doi.org/10.1016/j.neuropharm.2016.08.039

Yang, J. M., Li, F., Liu, Q., Rüedi, M., Wei, E. T., Lentsman, M., … Yoon, K. C. (2017). A novel TRPM8 agonist relieves dry eye discomfort. *BMC Ophthalmology*, *17*(1), 101. https://doi.org/10.1186/s12886-017-0495-2

Yang, X.-R., Lin, M.-J., McIntosh, L. S., & Sham, J. S. K. (2006). Functional expression of transient receptor potential melastatin- and vanilloid-related channels in pulmonary arterial and aortic smooth muscle. *American Journal of Physiology. Lung Cellular and Molecular Physiology*, *290*(6), L1267-76. https://doi.org/10.1152/ajplung.00515.2005

Yao, J., Liu, B., & Qin, F. (2010). Kinetic and Energetic Analysis of Thermally Activated TRPV1 Channels. *Biophysical Journal*, *99*(6), 1743–1753. https://doi.org/10.1016/j.bpj.2010.07.022

Yapa, K. T. D. S., Deuis, J., Peters, A. A., Kenny, P. A., Roberts-Thomson, S. J., Vetter, I., & Monteith, G. R. (2018). Assessment of the TRPM8 inhibitor AMTB in breast cancer cells and its identification as an inhibitor of voltage gated sodium channels. *Life Sciences*, *198*, 128–135. https://doi.org/10.1016/j.lfs.2018.02.030

Yee, N. S. (2015). Roles of TRPM8 Ion Channels in Cancer : Proliferation , Survival , and Invasion, (June), 2134–2146. https://doi.org/10.3390/cancers7040882

Yee, N. S., Zhou, W., & Lee, M. (2010). Transient receptor potential channel TRPM8 is over-expressed and required for cellular proliferation in pancreatic adenocarcinoma. *Cancer Letters*, *297*(1), 49–55. https://doi.org/10.1016/j.canlet.2010.04.023

Yin, K., Zimmermann, K., Vetter, I., & Lewis, R. J. (2015). Therapeutic opportunities for targeting cold pain pathways. *Biochemical Pharmacology*, *93*(2), 125–40. https://doi.org/10.1016/j.bcp.2014.09.024

Yin, Y., Wu, M., Zubcevic, L., Borschel, W. F., Lander, G. C., & Lee, S.-Y. (2018). Structure of the cold- and menthol-sensing ion channel TRPM8. *Science (New York, N.Y.)*, *359*(6372), 237–241. https://doi.org/10.1126/science.aan4325

Yonemitsu, T., Kuroki, C., Takahashi, N., Mori, Y., Kanmura, Y., Kashiwadani, H., … Kuwaki, T. (2013). TRPA1 detects environmental chemicals and induces avoidance behavior and arousal from sleep. *Scientific Reports*, *3*(1), 3100. https://doi.org/10.1038/srep03100

Yoshida, A., Hayashi, H., Tanabe, K., & Fujita, A. (2017). Segregation of phosphatidylinositol 4-phosphate and phosphatidylinositol 4,5-bisphosphate into distinct microdomains on the endosome membrane. *Biochimica et Biophysica Acta (BBA) - Biomembranes*, *1859*(10), 1880–1890. https://doi.org/10.1016/j.bbamem.2017.06.014

Yu, H. M., Wang, Q., & Sun, W. B. (2017). Silencing of FKBP51 alleviates the mechanical pain threshold, inhibits DRG inflammatory factors and pain mediators through the NF-kappaB signaling pathway. *Gene*, *627*(16), 169–175. https://doi.org/10.1016/j.gene.2017.06.029

Yu, J., Asche, C. V, & Fairchild, C. J. (2011). The Economic Burden of Dry Eye Disease in the United States: A Decision Tree Analysis. *Cornea*, *30*(4), 379–387. https://doi.org/10.1097/ICO.0b013e3181f7f363

Yudin, Y., Lukacs, V., Cao, C., & Rohacs, T. (2011). Decrease in phosphatidylinositol 4,5-bisphosphate levels mediates desensitization of the cold sensor TRPM8 channels. *The Journal of Physiology*, *589*(Pt 24), 6007–27. https://doi.org/10.1113/jphysiol.2011.220228

Zakharian, E., Cao, C., & Rohacs, T. (2010). Gating of Transient Receptor Potential Melastatin 8 (TRPM8) Channels Activated by Cold and Chemical Agonists in Planar Lipid Bilayers. *Journal of Neuroscience*, *30*(37), 12526–12534. https://doi.org/10.1523/JNEUROSCI.3189-10.2010

Zhang, H., Craciun, L. C., Mirshahi, T., Rohács, T., Lopes, C. M. B., Jin, T., & Logothetis, D. E. (2003). PIP(2) activates KCNQ channels, and its hydrolysis underlies receptor-mediated inhibition of M currents. *Neuron*, *37*(6), 963–75.

Zhang, L., & Barritt, G. J. (2004). Evidence that TRPM8 Is an Androgen-Dependent Ca 2 ⁺ Channel Required for the Survival of Prostate Cancer Cells, 8365–8373.

Zhang, X., Huang, J., & McNaughton, P. A. (2005). NGF rapidly increases membrane expression of TRPV1 heat-gated ion channels. *The EMBO Journal*, *24*(24), 4211–23. https://doi.org/10.1038/sj.emboj.7600893

Zhang, X., Li, X., & Xu, H. (2012). Phosphoinositide isoforms determine compartment-specific ion channel activity. *Proceedings of the National Academy of Sciences*, *109*(28), 11384–11389. https://doi.org/10.1073/pnas.1202194109

Zhang, X., Mak, S., Li, L., Parra, A., Denlinger, B., Belmonte, C., & McNaughton, P. a. (2012). Direct inhibition of the cold-activated TRPM8 ion channel by Gαq. *Nature Cell Biology*, *14*(8), 851–8. https://doi.org/10.1038/ncb2529

Zhu, B., Xia, M., Xu, X., Ludovici, D. W., Tennakoon, M., Youngman, M. A., … MacIelag, M. J. (2013). Arylglycine derivatives as potent transient receptor potential melastatin 8 (TRPM8) antagonists. *Bioorganic and Medicinal Chemistry Letters*, *23*(7), 2234–2237. https://doi.org/10.1016/j.bmcl.2013.01.062

Zimmermann, K., Leffler, A., Babes, A., Cendan, C. M., Carr, R. W., Kobayashi, J., … Reeh, P. W. (2007). Sensory neuron sodium channel Nav1.8 is essential for pain at low temperatures.

Nature, *447*(7146), 856–859. https://doi.org/10.1038/nature05880

Zimmermann, K., Lennerz, J. K., Hein, A., Link, A. S., Kaczmarek, J. S., Delling, M., … Clapham, D. E. (2011). Transient receptor potential cation channel, subfamily C, member 5 (TRPC5) is a cold-transducer in the peripheral nervous system. *Proceedings of the National Academy of Sciences*, *108*(44), 18114–18119. https://doi.org/10.1073/pnas.1115387108

Zotterman, Y. (1935). Action potentials in the glossopharyngeal nerve and in the chorda tympani1. *Skandinavisches Archiv Für Physiologie*, *72*(2), 73–77. https://doi.org/10.1111/j.1748-1716.1935.tb00412.x

Zotterman, Y. (1936). Specific action potentials in the lingual nerve of cat. *Skandinavisches Archiv Für Physiologie*, *75*(3), 105–119. https://doi.org/10.1111/j.1748-1716.1936.tb01558.x

Zubcevic, L., Herzik, M. A., Chung, B. C., Liu, Z., Lander, G. C., & Lee, S.-Y. (2016). Cryo-electron microscopy structure of the TRPV2 ion channel. *Nature Structural & Molecular Biology*, *23*(2), 180–186. https://doi.org/10.1038/nsmb.3159

Zygmunt, P. M., & Högestätt, E. D. (2014). TRPA1 (pp. 583–630). https://doi.org/10.1007/978-3-642-54215-2_23

UNIVERSITAS
Miguel
Hernández

8. Annex: publication

UNIVERSITAS
Miguel
Hernández

UNIVERSITAS
Miguel
Hernández

UNIVERSITAS
Miguel
Hernández